Atlantic Marine Assessment Program for Protected Species: FY20 – FY25

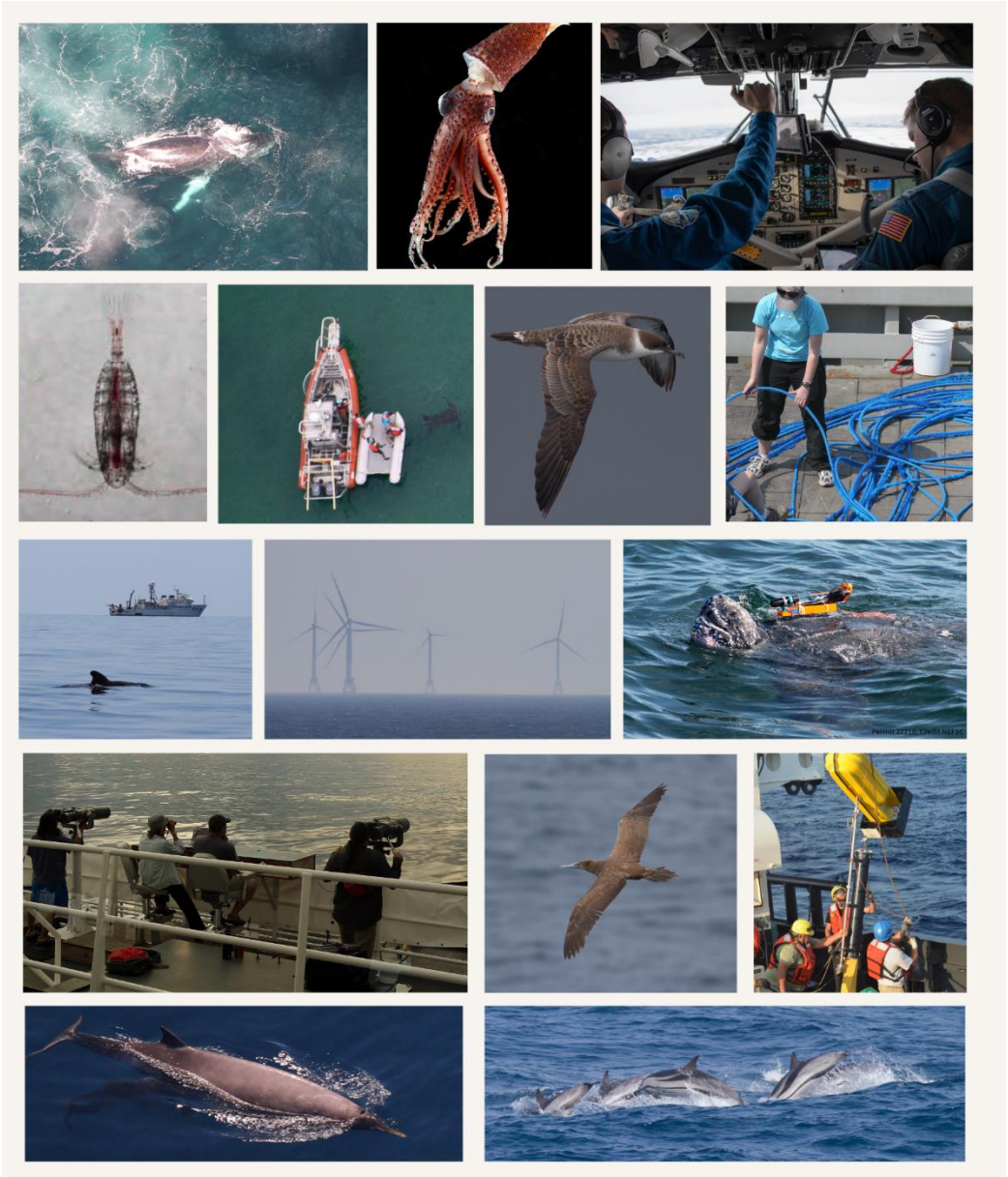

Atlantic Marine Assessment Program for Protected Species: FY19 – FY25

August 2026

Palka, Avens, Aichinger Dias, Chavez-Rosales, Choate, Cholewiak, DeAngelis, Garrison, Goetz, Haas, Hyde, Jech, Josephson, Khan, Patel, Sasso, Sigourney, Soldevilla, Walsh, Westell

By
National Oceanic Atmospheric Administration
National Marine Fisheries Service
Northeast Fisheries Science Center
166 Water Street
Woods Hole, MA 01543-1026

National Oceanic Atmospheric Administration
National Marine Fisheries Service
Southeast Fisheries Science Center
75 Virginia Beach Dr.
Key Biscayne, FL 33149

ABOUT THE COVER

The cover is a compilation of various work conducted as part of the AMAPPS III project including surveys of cetaceans, sea turtles, seals, seabirds, and general ecosystem conditions. The photos are courtesy of Dr. Debra Palka of the National Marine Fisheries Service. We conducted our surveys and collected pictures under U.S. Marine Mammal Protection Act permit numbers 17355, 21371, 21719, and 27066 issued to the Northeast Fisheries Science Center and Marine Mammal Protection Act permit numbers 779-1633, 14450-11, and 21938 issued to the Southeast Fisheries Science Center. Sea turtle animal studies were approved by the NOAA Fisheries Institutional Animal Care and Use Committee and conducted under Endangered Species Act permits (21233, 18526, 22218, 17225, 23639) issued to the NMFS Southeast Fisheries Science Center, NMFS Northeast Fisheries Science Center, or Coonamessett Farm Foundation.

ACKNOWLEDGMENTS

The AMAPPS I, II, and III studies were funded in part by two Interagency Agreements with the U.S. Department of the Commerce, National Oceanic and Atmospheric Administration (NOAA), National Marine Fisheries Service (NMFS), Northeast Fisheries Science Center (NEFSC): Interagency Agreements M10PG0075, M14G00005, and M19PG00007 with the U.S. Department of the Interior, Bureau of Ocean Energy Management, and Interagency Agreements NEC 11-009, NEC 15-004, NEC-16-011-01, and N4657923MP001WF with the Department of Defense, U.S. Navy. We also thank our many internal and external collaborators who made strong contributions to AMAPPS objectives.

Contents

List of Figures

List of Tables

List of Abbreviations and Acronyms

Abbreviation	Explanation
AIC	Akaike Information Criterion
AMAPPS	Atlantic marine assessment program for protected species
AMAR	Acoustic recorder
ASPE	Mean square prediction error
BHDMS	Bayesian hierarchical density surface model
BOEM	Bureau of Ocean Energy Management
CDS	Conventional distance sampling
CFF	Coonamessett Farm Foundation
CI	Confidence interval
CTD	Conductivity, temperature and depth sampling device
CV	Coefficient of variation
CvM	Cramer-von Mises goodness-of-fit test
DASBR	Drifting autonomous spar buoy recorder
DFO	Department of Fisheries and Oceans Canada
DOI	United States Department of the Interior
DS	Distance sampling
DTAG	Digital acoustic recording tag
EcoMon	Ecosystem Monitoring Program
EDF	Effective degrees of freedom
eDNA	Environmental deoxyribonucleic acid
ERDDAP	Environmental Research Division's Data Access Program
ESA	Endangered Species Act
ESPIS	Environmental Studies Program Information System
ESHW	Effective strip half width
GAIA	Geospatial Artificial Intelligence for Animals
GAM	Generalized additive statistical model
GE	Gas embolism
GLM	Generalized linear model
GoMex	Gulf of Mexico
GOMMAPPS	Gulf of Mexico marine assessment for protected species
GPS	Global positioning system
HARPs	High-frequency recording packages
HYCOM	Hybrid Coordinate Ocean Model
IFAW	International Fund for Animal Welfare
IPI	Inter-pulse interval
ITS.DEEP	Integrated Technologies for Deep Diving Cetaceans Program
kts	Knots, unit of speed equal to 1 nautical mile per hour
MAE	Mean absolute error goodness-of-fit test
MAPE	Mean absolute percentage error goodness-of-fit test
MARUs	Marine autonomous recording units
MIT	Massachusetts Institute of Technology
MMPA	Marine Mammal Protection Act
MODIS	Moderate Resolution Imaging Spectroradiometer
MR	Mark-recapture
MRDS	Mark-recapture distance sampling
mtDNA	Mitochondrial deoxyribonucleic acid
NAO	North Atlantic Oscillation index
NASA	National Aeronautics and Space Administration
NCEI	National Centers for Environmental Information
NE	Northeast
NEFSC	Northeast Fisheries Science Center

Abbreviation	Explanation
NEPA	National Environmental Policy Act
NMFS	National Marine Fisheries Service
NOAA	National Oceanic and Atmospheric Administration
OBIS-SEAMAP	Ocean Biodiversity Information System - Spatial Ecological Analysis of Megavertebrate Populations
OCS	Outer continental shelf
PAM	Passive acoustic monitoring
PBR	Potential biological removal
RHO	Spearman's rank correlation goodness-of-fit test
SDM	Spatial density-habitat model
SE	Southeast
SEFSC	Southeast Fisheries Science Center
SEUS	Southeastern United States
sp.	Species
SRE	Surface reflected echoes
SST	Sea surface temperature
U.S.	United States
UAS	Uncrewed aerial system
USFWS	US Fish and Wildlife Service
WEA	Wind energy area
VPR	Video Plankton Recorder
WHOI	Woods Hole Oceanographic Institution
XBT	Expendable bathythermograph

Executive Summary

The Atlantic Marine Assessment Program for Protected Species (AMAPPS) was a comprehensive multi-agency research program focusing on the U.S. Atlantic outer continental shelf, from Maine to the Florida Keys, covering waters from the coast to beyond the U.S. Exclusive Economic Zone. The overarching goal of AMAPPS is to assess the abundance, distribution, ecology, and behavior of marine mammals, sea turtles, and seabirds throughout the U.S. Atlantic outer continental shelf and to evaluate these data within an ecosystem context where the results are accessible to managers, scientists and the public. Because marine ecosystems are complex and involve dynamic assemblages of many coexisting species, to understand these marine ecosystem processes and achieve the AMAPPS objectives, our research integrated across taxonomic groups among multiple trophic levels, and we used a suite of data collection and analytical techniques.

The main agencies involved were the National Marine Fisheries Service (NMFS), Bureau of Ocean Energy Management (BOEM), the U.S. Navy and U.S. Fish and Wildlife Service. We also built collaborations with numerous other national and international organizations.

Our primary goal during AMAPPS I (1 Oct 2010 – 30 Sep 2014) and AMAPPS II (1 Oct 2014 – 30 Sep 2019) was to establish a baseline for evaluating trends in protected species (cetacean, sea turtle, and seabird) populations within their ecosystem (Palka et al. 2017; 2021). AMAPPS III (1 Oct 2019 – 30 Sep 2025) continued critical field survey work to monitor inter-annual variations in oceanographic conditions and protected species distribution and behavior, and we developed innovative methods to integrate the results from the suite of data collected. Our field work collected the following: visual observations from dedicated aerial and shipboard surveys; passive acoustic detections from towed and bottom-mounted hydrophones; active acoustic data from shipboard echosounders, fish and zooplankton samples using nets and trawls; location, dive patterns and biological samples from animals equipped with tags; and direct and indirect samples of the oceanic ecosystem's physical and biological components (refer to Chapter 10 for a summary of the data sources).

A key focus of AMAPPS III was to enhance methods for processing and analyzing these diverse data sources and integrating information from different data sources. These enhancements led to improved understanding of the distribution, abundance, ecology, and behavior of cetaceans (Chapters 4-6, 11), sea turtles (Chapters 4 and 7), seabirds (Chapter 8), and lower trophic levels, including tuna larvae, plankton, and fish (Chapter 9). Specific achievements included developing spatially explicit habitat-density models, estimating abundance, describing the shifting distribution patterns of the protected species, investigating dive behavior patterns of deep-diving cetaceans and sea turtles, enhancing our knowledge of the biology and ecology of sea turtles, connecting protected species to their ecosystem habitat characteristics, and investigating the possibilities of using very high- resolution commercial satellite imagery to monitor cetaceans.

The comprehensive data collected during AMAPPS III resulted in 60 published or in-review scientific papers and 34 presentations at various meetings and conferences (as detailed in Chapter 3). Here we present the key findings derived from these projects.

Key Findings in Chapter 4 - Distribution, Abundance and Trends Research

Our year-round AMAPPS shipboard and aerial line transect surveys provided pivotal visual and passive acoustic data, offering insights into the dynamic distribution and abundance of cetaceans and sea turtles in response to their evolving physical and biological ecosystems. Key findings included:

- **Updated Cetacean Stock Assessments:** The summer 2021 ship and plane surveys yielded visual line transect data that we utilized to calculate abundance estimates for 32 cetacean species or species groups (Section 4.6). We derived these estimates using a design-based multivariate distance sampling analysis, incorporating adjustments for perception and availability bias. We achieved a significant improvement over past practices through enhanced field training and new analysis methods: we were able to calculate abundance estimates for more individual species, rather than being required to pool several species together. The 32 updated abundance estimates subsequently allowed for a reassessment of the species' status, as reported in the Atlantic Marine Mammal Status of Stock report. The assessments of these 32 cetacean species indicated that the total U.S. annual mortalities and injuries exceeded the calculated Potential Biological Removal (PBR) level—which is determined by the abundance estimate—in only two cases: the short-finned pilot whale (*Globicephala macrorhynchus)* and the common bottlenose dolphin in the Northern North Carolina estuarine system (*Tursiops truncatus*). Both of these species are already the subject of a take reduction team; for more information see marine-mammal-take-reduction-plans-and-teams.

- **Analysis Innovations:** Our model-based analysis methods incorporated several innovative and improved techniques to enhance precision and reduce bias in abundance estimates. These advancements included:

    - New methods for separating ambiguous field species identifications into specific species for abundance estimates, utilizing environmental factors and passive acoustic detections (Section 4.4).
    - Improved acoustic classifiers for confirming species of passive acoustic detections, particularly for Kogiidae (Section 4.5).
    - Further developments of the hierarchical Bayesian multi-covariate method used to estimate abundance and estimate the probability the population size is above a user chosen threshold (Section 4.8).
    - Refinement of an innovative method to estimate the depth of passive acoustic detections (Section 6.1) used to estimate an appropriately corrected perpendicular distance for use in distance sampling abundance estimation methods.
    - New methods to estimate subsurface abundance estimates of sperm (*Physeter macrocephalus*; Section 4.9) and beaked whales (Ziphiidae; Section 4.10).
    - Development of a novel method to integrate passive acoustic and visual detections of sperm whales for abundance estimation (Section 4.11 and 4.12).

- **Spatiotemporal Abundance and Trends (2010-2023):** Utilizing year-round line transect data from 2010-2023 and the aforementioned innovations, we estimated spatial abundance (Sections 4.7 and 4.8) and trends (Section 4.14). These analyses incorporated adjustments for perception and availability bias (Section 4.3) and documented relationships with habitat characteristics using model-based multivariate distance sampling (Sections 4.7 and 5.4). The models, based on generalized additive (Section 4.7) and hierarchical Bayesian (Section 4.8) frameworks, revealed spatiotemporal shifts and trends both within and between years that were related to changes in their environment (Section 4.14). The most common environmental covariates associated with the animal's abundance included latitude and bottom temperature (that could reflect the annual seasonal migrations), and distance to the 1000 m depth contour, sea surface temperature, mixed layer thickness, primary productivity, and distance to the Gulf Stream (that could reflect the species-specific habitat preferences as related to their prey). Within this time period, the visual and passive acoustic detections have shown general shifts northeastwardly for many species, especially during winter.

Key Findings in Chapter 5 - Cetacean Ecology Research

Our AMAPPS surveys and collaborative fieldwork yielded significant insights into the ecology of cetaceans:

- **New Species Discovery:** We contributed data to identify and describe a new beaked whale species, *Mesoplodon eueu* (Section 5.1).
- **Deep-Water Habitat Survey:** In summer 2025, we conducted a multidisciplinary survey in the slope and offshore waters of Georges Bank to evaluate multispecies occurrence in deep-water habitats in relation to their physical and biological ecosystem (Section 5.2).
- **Killer Whale Ecology:** We contributed data to assess the spatial and temporal distribution, social structure, genetics, morphology, acoustics, and predatory behavior of Northern Gulf of Mexico and the Western North Atlantic killer whales (*Orcinus orca*; Section 5.3).
- **Cetacean-Habitat Relationships:** Using visual and passive acoustic detections, we described the relationships between cetacean distribution and their environmental habitats:
    - We defined habitat segregation among beaked whales (Section 5.4).
    - We identified key habitat variables (latitude, bottom and sea surface temperature, primary productivity, and distance to depth isobaths) that explain the year-round spatiotemporal distribution and abundance of migrating cetaceans (Section 5.4).
    - We contributed data to demonstrate the utility of prey distribution indices for defining cetacean spatiotemporal abundance when available (Section 5.5).
    - We contributed data to show the feasibility of short-term future habitat predictions using subseasonal forecasting techniques (Section 5.6).

Key Findings in Chapter 6 - Cetacean Behavior Research

We introduced an innovative approach to estimate the depth of passive acoustic detections using surface reflections (Section 6.2). This method allowed us to gain a deeper understanding of deep-diving animal habitat usage and behavior:

- **Subsurface Abundance:** We estimated the horizontal perpendicular distance of the acoustic detections (Section 6.2) to estimate the abundance of subsurface animals and abundance of animals throughout the water column (Sections 4.9 - 4.12).
- **Demographics of sperm whales:** We applied a new method to estimate the acoustic body length of an echolocating sperm whale as well as the sex and maturity stage. This method is currently undergoing testing and validation, but preliminary results from analyzing a quarter of the click trains during the 2021 northeast summer cruise indicated that most of the vocalizing sperm whales were adult females or juveniles (Section 6.3).
- **Diving Behavior of Sperm Whales:** We demonstrated the detectability of foraging buzzes using towed hydrophone arrays (Section 6.4). Furthermore, we showed that sperm whale clicks recorded on these arrays can establish the minimum and maximum depths for shallow, medium, and deep foraging dives (Section 6.5). This passive acoustic method offers an advantage over the more challenging and method of tagging sperm whales, yet yields comparable dive data. By documenting these foraging dive patterns, we integrated the passive acoustic dive profile estimations with EK60-collected prey layer backscatter data (Section 6.6) to enhance our understanding of sperm whale diet and foraging behavior.

- **Assessment of the EK60 acoustic footprint:** In collaboration with the Department of Fisheries and Oceans Canada, we examined the spatial extent the active acoustic multibeam EK60 echosounder is received by bottom mounted recorders stationed around 1100 m deep, which is analogous to the dive range of acoustically sensitive beaked whale species. We combine those results with *in situ* playbacks of the EK60 to foraging beaked whales to better understand their behavioral response to the EK60 echosounder (Section 6.7).

Key Findings in Chapter 7 - Sea Turtle Research

During fieldwork to tag loggerhead (*Caretta caretta*) and leatherback (*Dermochelys coriacea*) turtles, AMAPPS researchers and their collaborators collected various biological characteristics, offering new insights into sea turtle behavior and ecology:

- **Blood Biochemistry and Hematology:** By establishing baseline blood profiles for healthy loggerhead turtles, we observed differences in blood characteristics between migrating and resident turtles. This baseline can be used to assess turtles affected by anthropogenic or environmental disturbances like fisheries bycatch and climate change (Section 7.3.1).

- **Gas Embolism Risk:** AMAPPS data contributed in the development of a baseline model to estimate the risk of gas embolism formation in several sea turtle species. This formation can occur when a turtle makes an abnormally rapid ascent after a dive, potentially due to incidental capture in fishing gear or disturbance by acoustic sources (Section 7.3.2).

- **Trophic Positions:** AMAPPS investigators are currently collaborating with other investigators in an ongoing study that uses stable isotope techniques that appear to have demonstrated that sea turtles in southern New England exhibit similar trophic positions to each other (Section 7.3.3).

We gained insights into the distribution and dive patterns of loggerhead and leatherback turtles through the location and depth data collected on the animal-borne tags:

- **Loggerhead Turtle Responses to Environmental Changes:**
    - **Short-term:** We documented short-term responses to a hurricane, showing northward movement during the storm, followed by southward movement and/or deeper dives to cooler waters post-hurricane (Section 7.4.1).
    - **Long-term:** We predicted long-term northward movement responses to future environmental changes over the next 80 years, particularly during fall and spring (Section 7.4.2).

- **Leatherback Turtle Foraging Behaviors:**
    - We found evidence that leatherbacks may be foraging in the Southern and Mid-Atlantic Bights during summer, as revealed by differentiating searching behavior from transiting behaviors using time-depth information from tags (Section 7.4.3).

- **Estimating Abundance throughout the Water Column:**
    - We utilized average dive and surfacing times from animal-borne tags to predict monthly averages in 20x20 km grid cells for loggerhead turtles (Section 7.5.1) and monthly averaged percent time at the surface for leatherback turtles (Section 7.5.2).

    - We then used these predictions to develop monthly availability bias correction factors (Section 4.3), which we applied to at-surface abundance estimates to determine the abundance of both species throughout the water column (Section 4.7) and the spatiotemporal trends (Section 4.14).

- **Overlap with Human Activities:**
    - We used the location data from tagged loggerhead and leatherback turtles to study the overlap of loggerheads with the sea scallop fishery and leatherbacks with offshore wind areas in the Mid-Atlantic Bight and Southern New England (Section 7.6).

Key Findings in Chapter 8 - Seabird Research

From 2017 to 2025, we piggybacked visual surveys of seabirds, marine mammals, turtles, large pelagic fish, and marine debris on the Northeast Fisheries Science Center's Ecosystem Monitoring surveys and other opportunistic surveys. The concurrent collection of seabird and marine mammal data, alongside other biotic and abiotic data, enhances our understanding of species' spatiotemporal distributions and their relationships with other trophic levels within the evolving marine ecosystem.

We used standardized 300 m strip transect methodology across 42 surveys and 707 days of data collection, where we counted over 184,000 birds from more than 260 sea and land bird species. We found Great Shearwater (*Puffinus gravis*) and Wilson's Storm-petrel (*Oceanites oceanicus*) were the most frequently recorded seabirds on the Northeast U.S. shelf (>38%) and in the Slope Sea region (>52%).

Key Findings in Chapter 9 - Ecosystem Research

On AMAPPS shipboard surveys, we systematically collected a comprehensive suite of data to fulfill the program's multidisciplinary objectives. This included acquiring high-resolution active acoustic data, which is essential for mapping the distribution and abundance of organisms throughout the water column. Complementing this were detailed oceanographic measurements, encompassing parameters such as temperature, salinity, and water current profiles, which provided the environmental context for the biological findings. Furthermore, we collected a wide array of biological samples, including plankton (both zooplankton and phytoplankton), various life stages of fish, and cephalopods. These biological collections were instrumental in characterizing the lower and intermediate trophic levels of the marine ecosystem. These investigations provided foundational ecological data for regions of the marine environment that had been historically understudied, thereby closing key knowledge gaps and providing a more holistic and scientifically robust basis for marine resource management and conservation efforts. For example, we found the following:

Plankton: Concentrations (number of individuals per 100 m^{-3}) of zooplankton and ichthyoplankton are higher on the shelf than in the Slope Sea.

Tuna Spawning Ground: The tuna larval data collected on the AMAPPS surveys contributed to the conclusions that the Slope Sea waters within the AMAPPS study area is a major spawning ground for Atlantic bluefin tuna (*Thunnus thynnus*); and there are two weakly differentiated but demographically connected ancestral populations of Atlantic bluefin tuna that interbreed in the Slope Sea.

eDNA to Assess Fish Diversity: The midwater trawl data collected on the AMAPPS surveys contributed to the conclusion that eDNA and net samples often yielded different species, with eDNA detecting species missed by traditional methods.

Key Findings in Chapter 10 – Databases and Data Sharing

This chapter summarizes the data collected throughout AMAPPS I, II, and III. It provides details on the types of data gathered, the collection methodologies employed, and where these data can be accessed. Focusing on the AMAPPS III program we conducted extensive field efforts that involved:

- **Aerial and Shipboard Transect Abundance surveys:** Collecting data from approximately 84,320 km documenting a significant number of marine animals: 7,335 marine mammals, 1,771 sea turtles, and 22,252 seabirds.
- **Passive Acoustics:** Gathering data over roughly 7,000 km using towed hydrophone arrays during shipboard operations.
- **Animal Tagging:** Deploying 123 tags on loggerhead turtles and 116 on leatherback turtles to track location, time, and depth.
- **Water Column Sampling:** Conducting 218 conductivity, temperature and depth (CTD) casts to collect depth and temperature data.
- **Plankton Studies:** Collecting plankton data from 265 bongo tows, 33 visual plankton recorder deployments and 47 frame-net tows.

Key Findings in Chapter 11 – Initial AMAPPS Investment in GAIA: Catalyzing a National Framework for Satellite-Based Marine Mammal Monitoring

NOAA Fisheries launched the Geospatial Artificial Intelligence for Animals (GAIA) initiative to monitor marine mammals across their range using very high-resolution commercial satellite imagery, augmenting traditional surveys, especially in remote areas. The initial AMAPPS investment, despite limited scientific output, was crucial for shaping NOAA's strategy and providing the momentum to establish GAIA as a national marine mammal monitoring platform. GAIA's debut was monitoring North Atlantic right whale (*Eubalaena glacialis*) habitat in Cape Cod Bay, using aerial-survey-confirmed scenes to evaluate performance and create training data. It is now expanding to support priority species like belugas (*Delphinapterus leucas*), Hawaiian monk seals (*Monachus schauinslandi*), and Rice's whales (*Balaenoptera ricei*). Future efforts will focus on system robustness, performance, and securing sustained funding.

1 Introduction

The overarching goals of the Atlantic Marine Assessment Program for Protected Species (AMAPPS) is to assess the abundance, distribution, ecology, and behavior of marine mammals, sea turtles, and seabirds throughout the U.S. Atlantic state and outer continental shelf waters, and place them in an ecosystem context, and to provide these results in formats that are easily accessible and user-friendly for decision-makers and others. AMAPPS is a collaborative program involving the National Marine Fisheries Service (NMFS) of the National Oceanic and Atmospheric Administration, Department of Commerce, Bureau of Ocean Energy Management (BOEM) of the Department of the Interior, U.S. Navy, and U.S. Fish and Wildlife Service (USFWS) of the Department of the Interior. Other collaborators contributing to AMAPPS are noted in the appropriate sections.

All of the agencies involved in AMAPPS require information on protected species (marine mammals, sea turtles, and seabirds) to implement and support compliance with federal mandates. This includes the Marine Mammal Protection Act (MMPA; NOAA Fisheries 2021a), Endangered Species Act (ESA; NOAA Fisheries 2021b), National Environmental Policy Act (NEPA; NOAA Fisheries 2021c), Migratory Bird Treaty Act, and Executive Order 13186: Responsibilities of Federal Agencies to Protect Migratory Birds (USFWS 2021). In addition, up-to-date information on protected species enhances public outreach and education.

BOEM requires information on protected species to regulate energy and mineral resources associated with the Atlantic outer continental shelf (OCS), which includes all submerged lands lying seaward of state coastal waters (i.e., 3 miles offshore) to the Exclusive Economic Zone boundary approximately 200 nm from the coast (BOEM 2021). Areas of particular interest to BOEM relevant to AMAPPS include the areas related to development of offshore wind energy (**Figure 2-1**) and marine minerals, for example beach replenishment activities. The U.S. Navy requires information on protected species to support their environmental compliance documentation for their activities in U.S. waters that include at-sea training and testing, low-, medium-, and high-frequency sonar and explosives, and in-water construction projects involving pile driving at Navy installations. Areas of particular interest to the Navy are all waters within the U.S. Exclusive Economic Zone and beyond. Furthermore, NMFS requires information on protected species to develop Stock Assessment Reports, monitor and evaluate Take Reduction Plans, develop Section 7 consultations (Biological Opinions), and Section 10 incidental take permits. Areas of particular interest to NMFS are waters within the U.S. Atlantic Exclusive Economic Zone.

AMAPPS III was in place during Fiscal Years (FY) 2019 to FY2025 (October 2018 through September 2025). It was an extension of AMAPPS I (FY2010 to FY2014; October 2009 through September 2014) and AMAPPS II (FY2014 to FY2019; October 2013 through September 2019). USFWS and BOEM developed its own inter-agency agreement in FY17, so in this document we will only report on results from data collected by NMFS.

AMAPPS III updated marine ecosystem data for marine mammals, sea turtles, and seabirds (**Appendix A**), filling information gaps in their assessments, and provided needed information on the animals' ecology and behavior. AMAPPS research adopted an integrated approach, acknowledging the intricate nature of marine ecosystems and their ever-changing species compositions. This involved spanning various taxonomic groups and trophic levels, utilizing a wide array of data collection and analysis methods. A key component of this research was also the development of new field and analysis techniques, aimed at enhancing our comprehension of the target species and their surrounding ecosystem. The program primarily focuses on the U.S. Atlantic Exclusive Economic Zone waters. While primary

researchers are from the Northeast Fisheries Science Center (NEFSC) in Woods Hole, MA, and the Southeast Fisheries Science Center (SEFSC) in Miami, FL, nearly all projects are collaborative. Numerous other organizations, beyond those in inter-agency agreements, participated in data collection and analysis, and also funded the research detailed in Chapters 4–10.

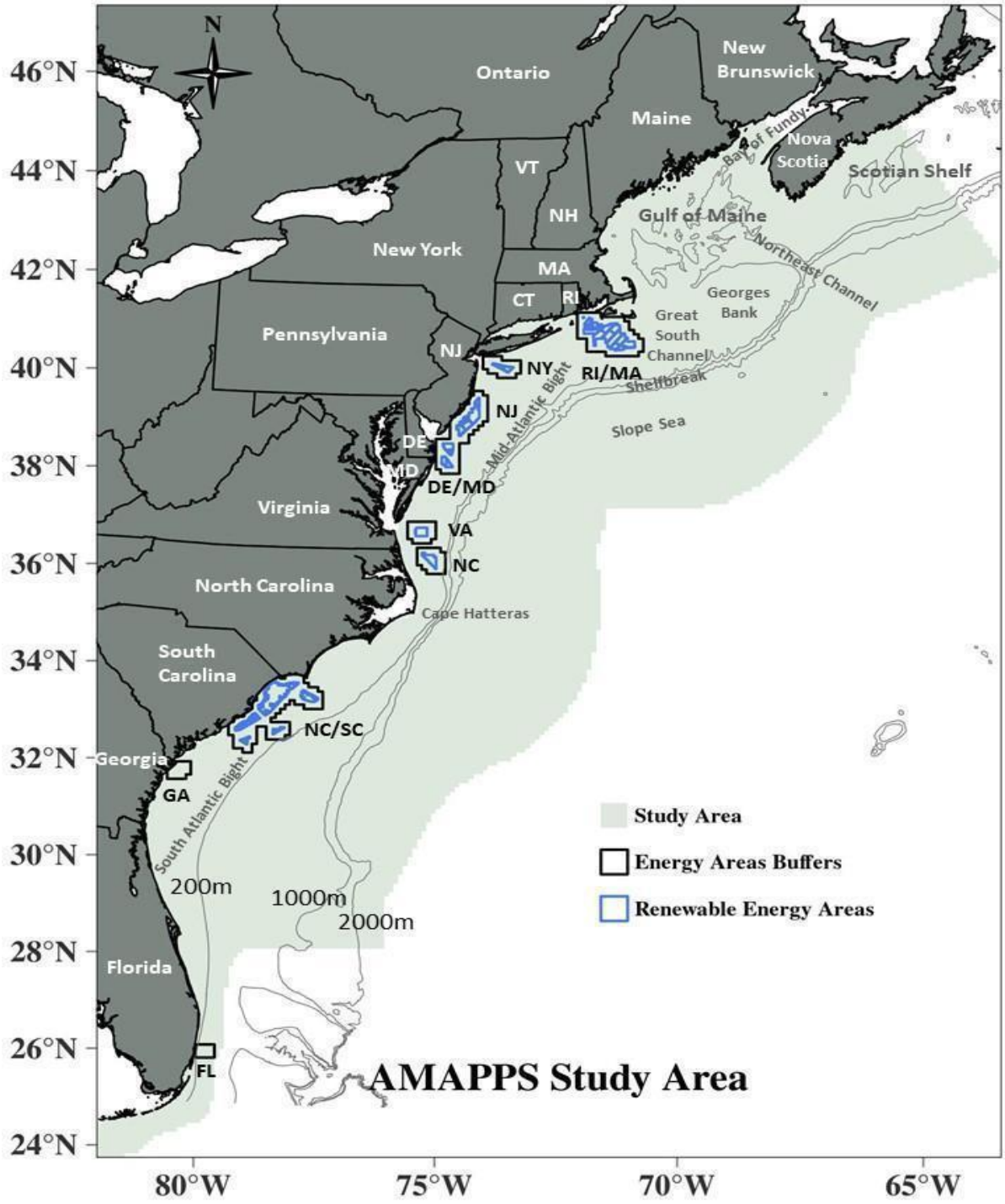

Figure 2-1. AMAPPS study area and wind-energy study areas

References Cited

[BOEM] Bureau of Ocean Energy Management. 2021. Outer Continental Shelf (accessed 10 April 2021).

[NOAA Fisheries] National Oceanic and Atmospheric Administration Fisheries. 2021a. Marine Mammal Protection Act (MMPA) polices, guidance, and regulations. (Accessed 10 April 2021).

[NOAA Fisheries] National Oceanic and Atmospheric Administration Fisheries. 2021b. Endangered Species Act (ESA). (accessed 10 April 2021).

[NOAA Fisheries] National Oceanic and Atmospheric Administration Fisheries. 2021c. National Environmental Policy Act (NEPA). (accessed 10 April 2021).

[USFWS] U.S. Fish and Wildlife Service. 2021. Executive Order 13186, Responsibilities of Federal Agencies to Protect Migratory Birds (accessed 10 April 2021).

2 Background and Objectives

2.1 Background

Human activities are increasing in our oceans and exerting increasing pressures on the ocean's ecosystem. Activities having impacts on marine ecosystems worldwide include maritime traffic, tourism, fisheries, aquaculture, hydrocarbon exploration, marine renewable energy development, and naval activities. (Azzellino et al. 2012). At the same time, the ocean's ecosystem is changing. Over the last two decades the ocean temperatures in the Northeast Atlantic, and in the Gulf of Maine particularly, have warmed faster than the global ocean (Cheng et al. 2022; Karmalkar et al. 2021; Pershing et al. 2015; Saba et al 2016; Todd and Ren 2023). These physical oceanic changes are related to shifts in the geographic ranges of many species of fish (Kleisner et al. 2017) and cetaceans (Chavez-Rosales et al. 2022).

The combination of dynamic natural variability and increasing human activities present complex challenges for the management of marine populations that interact with human activities (Maxwell et al. 2015; Hobday et al. 2016). Spatial management techniques target regions of high risk for anthropogenic impacts (Maxwell et al. 2015). Static management approaches are generally ineffective for highly migratory species and for species undergoing distributional shifts (Lascelles et al. 2014). In contrast, dynamic management involves adapting processes in real-time to guide the spatiotemporal managed activity to more align with the changing environment, species distributions, and managed resources. The goal of a dynamic approach is to result in smaller, dynamic boundaries that provide greater opportunities to the resource users, while at the same time providing the protection to the protected species. Dynamic management uses flexible systems, continuous feedback, and data-driven decision-making to account for variability and uncertainty. Key elements include frequent reassessments, dynamic resource allocation, and using technology to automate tasks and improve response times. Environmental data are commonly used to inform dynamic management by integrating environmental conditions into distributional models of marine species (Becker et al. 2016). For risk assessment and mitigation of impacts, it is necessary to have information on the seasonal and interannual variability in distribution, ecology, and behavior at small spatial scales to estimate the potential for mortality or other impacts on protected species due to localized human activities.

The goal of AMAPPS was to provide updated information on the seasonal and interannual variability in distribution and behavior of protected species (cetaceans, sea turtles and seabirds) in the U.S. Atlantic waters and to evaluate these data within an ecosystem context where the results are accessible to managers, scientists and the public.

2.2 Objectives

Ideally, results from studies that are gathering information on the seasonal and interannual variability in distribution and behavior of protected species could discriminate between changes in wildlife populations due to natural environmental variability and changes due to anthropogenic impacts, but that is a difficult task. Wiebe et al. (2009) concluded that to understand the effects of anthropogenic activities on wildlife populations within the complexities of their ecosystem, scientists need to use a range of study tools on a range of taxonomic trophic levels. The objectives of AMAPPS followed this strategy. The specific objectives of AMAPPS III were to:

1) Collect broad-scale data over multiple years on the seasonal distribution and abundance of marine mammals (cetaceans and pinnipeds), marine turtles, and seabirds using fixed passive acoustic monitoring and direct aerial and shipboard surveys of coastal U.S. Atlantic Ocean waters;
2) Collect distribution and abundance data at finer scales at several sites of particular interest to BOEM, NMFS, and partners using visual and acoustic survey and net sampling techniques;

3) Conduct tagging studies of protected species to develop corrections for availability bias in the abundance survey data and to investigate behavior and ecology of species in areas of interest;
4) Collect additional data on life-history and ecology, including habitat use, residence time, frequency of use, and behavior;
5) Identify currently used, viable technologies and explore alternative platforms and technologies to improve population assessment studies, if necessary;
6) Assess the population size of surveyed species at regional scales; and develop models and associated tools to translate these survey data into seasonal, spatially-explicit density estimates incorporating habitat characteristics; and
7) Collect opportunistic plankton sampling off the northeast U.S. Shelf and Slope Sea.

The primary species we targeted under AMAPPS were protected species: cetaceans, sea turtles, and seabirds (species listed in **Appendix A**). However, to fully understand these species, we also needed to investigate other parts of the ecosystem ranging from the physical attributes of the ocean's waters to biological attributes such as potential prey like plankton and fish species.

In AMAPPS III, we adopted a comprehensive approach to study the ecosystem, employing a diverse array of tools. These tools included the collection of visual, acoustic, and telemetry data for protected species, alongside both direct (e.g., trawl and active acoustics) and indirect (photographic and satellite imagery) sampling of other trophic levels. Recognizing the inherent strengths and weaknesses of each tool, we used a complementary suite of data collection and analysis methods to effectively address AMAPPS objectives. For instance, aerial and shipboard visual data offered species-specific estimates of surface abundance, spatiotemporal distribution, and limited insights into behavior and demographics. In contrast, passive acoustic data provided information on the spatiotemporal presence of vocalizing species below the surface, along with limited information on behavior or demographics. Animal-borne tag data provided detailed individual-specific information on distribution, behavior, and demographics. Despite the individual limitations of each data type, the integrated use of all these data sources offered the most robust means to comprehend the abundance, distribution, ecology, and behavior of these animals within an ecosystem context.

This document details the findings of AMAPPS III, addressing its objectives through multiple data sources and analysis methodologies. We investigated seasonal and annual distribution patterns, abundance estimates, and trends of cetaceans and sea turtles (Chapter 4), along with the ecology and behavior of cetaceans (Chapters 5 and 6), sea turtles (Chapter 7), seabirds (Chapter 8), and other trophic levels (Chapter 9). Chapter 10 provides an overview of all data collected under AMAPPS I-III, describing the data processing methods, and where the public can access these data. Chapter 10 provides an overview of the Geospatial Artificial Intelligence for Animals (GAIA) initiative to explore satellite-based whale detections to monitor marine mammals across their range, augmenting traditional surveys, especially in remote areas.

2.3 Permits

We conducted cetacean fieldwork during the AMAPPS I, II, and III reporting periods under U.S. Permits Nos. 17355, 21371, 21719, and 27066 issued to NEFSC.

We conducted sea turtle fieldwork during this reporting period under U.S. Permit No. 21233 issued to the SEFSC (2019-2025), U.S. Permit No. 22218 issued to the NEFSC Turtle Ecology program (2019-2021), U.S. Permit No. 18526 issued to Coonamessett Farm Foundation (2019), U.S. Permit No. 17225 issued to the NEFSC Gear Research Team (2021), and U.S. Permit No. 23639 issued to Coonamessett Farm Foundation (2021-2025).

2.4 Acknowledgements

The studies in this document were funded by two Interagency agreements with the United States Department of the Commerce, National Oceanic and Atmospheric Administration (NOAA), National Marine Fisheries Service (NMFS), Northeast Fisheries Science Center (NEFSC). One interagency agreement was with the United States Department of the Interior, Bureau of Ocean Energy Management (M14PG00005, M10PG00075, and M19PG00007). The other interagency agreement was with the U.S. Navy, U.S. Fleet Forces Command (NEC 11-009, NEC 15-004, and NEC-16-011-01; N4657922GTC).

2.5 References Cited

Azzellino A, Panigada S, Lanfredi C, Zanardelli M, Airoldi S, Notarbartolo di Sciara G. 2012. Predictive habitat models for managing marine areas: Spatial and temporal distribution of marine mammals within the Pelagos Sanctuary (Northwestern Mediterranean sea). Ocean Coast Manag. 67:63–74.

Becker EA, Forney KA, Fiedler PC, Barlow J, Chivers SJ, Edwards CA, Moore AM, Redfern JV. 2016. Moving Towards Dynamic Ocean Management: How Well Do Modeled Ocean Products Predict Species Distributions? Remote Sens. 8(2):149. https://doi.org/10.3390/rs8020149

Chavez-Rosales S, Josephson E, Palka D, Garrison L. 2022. Detection of Habitat Shifts of Cetacean Species: A Comparison Between 2010 and 2017 Habitat Suitability Conditions in the Northwest Atlantic Ocean. Front Mar Sci. 9. https://doi.org/10.3389/fmars.2022.877580

Cheng L, von Schuckmann K, Abraham JP, Trenberth KE, Mann ME, Zanna L, England MH, Zika JD, Fasullo JT, Yu Y, et al. 2022. Past and future ocean warming. Nat Rev Earth Environ. 3(11):776–794. https://doi.org/10.1038/s43017-022-00345-1

Hobday AJ, Alexander LV, Perkins SE, Smale DA, Straub SC, Oliver ECJ, Benthuysen JA, Burrows MT, Donat MG, Feng M, et al. 2016. A hierarchical approach to defining marine heatwaves. Prog Oceanogr. 141:227–238. https://doi.org/10.1016/j.pocean.2015.12.014

Karmalkar AV, Horton RM. 2021. Drivers of exceptional coastal warming in the northeastern United States. Nat Clim Chang. 11(10):854–860. https://doi.org/10.1038/s41558-021-01159-7

Kleisner KM, Fogarty MJ, McGee S, Hare JA, Moret S, Perretti CT, Saba VS. 2017. Marine species distribution shifts on the U.S. Northeast Continental Shelf under continued ocean warming. Prog Oceanogr. 153:24–36. https://doi.org/10.1016/j.pocean.2017.04.001

Lascelles B, Notarbartolo Di Sciara G, Agardy T, Cuttelod A, Eckert S, Glowka L, Hoyt E, Llewellyn F, Louzao M, Ridoux V, Tetley MJ. 2014. Migratory marine species: their status, threats and conservation management needs. Aquat Conserv. 24(S2):111–127. https://doi.org/10.1002/aqc.2512

Maxwell SM, Hazen EL, Lewison RL, Dunn DC, Bailey H, Bograd SJ, Briscoe DK, Fossette S, Hobday AJ, Bennett M, et al. 2015. Dynamic ocean management: Defining and conceptualizing real-time management of the ocean. Mar Policy. 58:42–50. https://doi.org/10.1016/j.marpol.2015.03.014

Pershing AJ, Alexander MA, Hernandez CM, Kerr LA, Le Bris A, Mills KE, Nye JA, Record NR, Scannell HA, Scott JD, et al. 2015. Slow adaptation in the face of rapid warming leads to collapse of the Gulf of Maine cod fishery. Science. 350(6262):809–812. https://doi.org/10.1126/science.aac9819

Saba VS, Griffies SM, Anderson WG, Winton M, Alexander MA, Delworth TL, Hare JA, Harrison MJ, Rosati A, Vecchi GA, Zhang R. 2016. Enhanced warming of the Northwest Atlantic Ocean under climate change. J Geophys Res Oceans. 121(1):118–132. https://doi.org/10.1002/2015JC011346

Todd RE, Ren AS. 2023. Warming and lateral shift of the Gulf Stream from in situ observations since 2001. Nat Clim Chang. 13(12):1348–1352. https://doi.org/10.1038/s41558-023-01835-w

Wiebe P, Harris R, Werner F, Young B. 2009. BASIN: Basin-scale analysis, synthesis, and integration. Science plan and implementation strategy. GLOBEC Report 27. Plymouth, UK. https://www.na-basin.org/reports/BASIN-NAIPweb.pdf

3 Organization of Report

To address the AMAPPS objectives during AMAPPS III we conducted about 32 projects (**Table 3-1**) that yielded 60 published or in-review papers and 34 presentations at various meetings and conferences (**Table 3-2**). This report provides a summary of the papers published during AMAPPS III that utilized AMAPPS data and provides more detailed information on on-going research and their results.

In Chapter 4, we integrated the visual, passive acoustic and tag data to update the spatiotemporal distribution, abundance, and trends of cetaceans and sea turtles during 2010 - 2023.

In Chapter 5, we used the data and results from Chapter 4 to focus on new ecological information on beaked whales (Ziphiidae) and killer whales (*Orcinus orca*), along with the ecological interactions of cetaceans and their biotic and abiotic habitat ecosystem.

In Chapter 6, we used the data from Chapter 4 to focus on new information on the dive behavior and demographics of deep diving beaked and sperm whales (*Physeter macrocephalus*).

In Chapter 7, we used data collected from tag-borne loggerhead (*Caretta caretta*) and leatherback (*Dermochelys coriacea*) turtles to present new information on the turtles' biology, distribution, and dive patterns.

In Chapter 8, we used data collected during AMAPPS shipboard surveys to present updated spatiotemporal distributions of sea birds.

In Chapter 9, we used data collected during AMAPPS shipboard surveys to present updated information on plankton and fish.

In Chapter 10, we provided a comprehensive summary of all data collected during AMAPPS I, II, and III (2010-2025). We also briefly described the data processing methods and information on public access to these data.

In Chapter 11, we provided a brief summary of the Geospatial Artificial Intelligence for Animals (GAIA) initiative to explore satellite-based whale detections to monitor marine mammals across their range, augmenting traditional surveys, especially in remote area.

Table 3-1. List of projects conducted by AMAPPS III researchers and collaborators
More information on each project is in the listed chapter and appendices within this document and in other references (including papers, talks, and online sources as itemized in Table 2-2).

Category	Project	Current Target Species	Chapters	Product References
Abundance	Distribution and abundance using visual data and design-based analysis methods	Cetaceans	4	8-10, 15, 17
Abundance	Abundance using visual and passive acoustic line transect data	Whales	4	18, 23
Abundance, behavior	Abundance of subsurface animals using only passive acoustics	Sperm and beaked whales	4, 5	34
Abundance, Distribution, Ecosystem	Distribution and abundance using visual data in a 2-stage generalized additive model framework	Cetaceans, turtles	4, Appendix B-D	3, 4, 5, 7, 11, 12, 18, 19, 24
Abundance, Distribution, Ecosystem	Distribution and abundance using visual data in Bayesian hierarchical model framework	Cetaceans	4	21-23
Abundance, Distribution, Ecosystem	Distribution and abundance using visual and other trophic level data	Cetaceans	5	14, 20, 26
Distribution, Ecosystem	Habitat-distribution relationships, including habitat shifting using visual data	Cetaceans, turtles	4, 5	1, 3, 4, 5, 7, 11, 13, 18, 19
Distribution, Ecosystem	Habitat-distribution relationships using passive acoustic data	Cetaceans	4, 5	18, 28, 29, 30, 31, 32, 33
Distribution, Ecosystem	Habitat-distribution relationships using tag data	Turtles	7	35, 36, 40, 43, 45, 46
Distribution	Distribution and relative frequency of seabirds	Seabirds	8	27
Stock structure	Description of a new beaked whale	Beaked whale	5	2
Stock assessment	Assess status of stock using abundance and mortality data	Cetaceans	4	57
Abundance-supporting	Cruise report and data from abundance surveys	Cetaceans, turtles, seabirds	4	6, 12, 16
Abundance-supporting, behavior	Develop correction factors to account for availability bias of visual survey data using tag data	Turtles	4, 7	34, 38, 44, 45
Abundance-supporting, behavior	Develop correction factors to account for availability bias of visual survey data using passive acoustic data	Whales	4, 5	23, 34
Distribution-forecasting	Subseasonal forecasting of arrival of humpback whales	Cetaceans	5	25
Distribution-support	Develop methods to monitor whales with satellite imagery	Whales	11	56
Distribution - climate change	Shifts due to climate change	Cetacans, Loggerhead turtle	5, 7	11, 41, 42, 58

Category	Project	Current Target Species	Chapters	Product References
Abundance and distribution - supporting	Extract static and dynamic habitat values from satellite-based and model-based online sources	Cetaceans, turtles, birds, seals	4	-
Behavior and Abundance-supporting	Estimate dive depth from acoustic localizations of deep-diving species	Sperm and beaked whales	6	34
Ecology and Distribution - supporting	Characterize acoustic repertoire, and vocal	Whales	4, 6	31, 32
Behavior, Distribution	Spatial and within water column distribution of turtles using tag data	Leatherback turtles	7	35, 36, 40, 43, 48
Life history	Biological and life history characteristics	Loggerhead and leatherback turtles	7	37, 47, 49
Management	Spatiotemporal overlap between turtles and human activities	Loggerhead turtles	7	39
Management	Spatiotemporal overlap between cetaceans and human activities	Cetaceans	4, Appendices B-D	21, 57
Ecosystem-supporting	Distribution of ocean physical and biological (plankton, fish and other trophic levels) characteristics	Other trophic levels	9	53
Ecosystem	Fish diversity and diel migration using eDNA	Fish	9	51
Ecosystem	Otolith and species identification of mesopelagic fishes	Fish	9	55
Ecosystem, Biology	Distribution and species identification of bluefin tuna larvae	Bluefin tuna	9	50, 52, 54
Outreach	Disseminate maps and abundance estimates to the public	Cetaceans, turtles	4, Appendices B-D	57
Outreach	Publicly available field data	Cetaceans, turtles, seabirds, other trophic levels	10	16
Outreach	Annual reports of AMAPPS projects	Cetaceans, turtles, seabirds, other trophic levels	4 – 10	58-64

Table 3-2. List of products resulting from data collected under AMAPPS III
List of published and in review papers (A), conference and meeting presentations (B), databases (C), and web presence for data (D), and web presence of newsletters, blogs, news articles (E).

A. PUBLISHED AND IN-REVIEW REFEREED/TECHNICAL PAPERS

Abundance and distribution

1) Barry KP, Mullin KD, Maze-Foley K, Wilcox Talbot LA, Rosel PE, Soldevilla MS, Dias LA, Ramírez-León MR, Litz JA. 2024. **Killer whales in the Gulf of Mexico and North Atlantic off the Southeastern United States**. Front Mar Sci. 11. https://doi.org/10.3389/fmars.2024.1460314

2) Carroll EL, McGowen MR, McCarthy ML, Marx FG, Aguilar N, Dalebout ML, Dreyer S, Gaggiotti OE, Hansen SS, van Helden A, et al. 2021. **Speciation in the deep: genomics and morphology reveal a new species of beaked whale *Mesoplodon eueu***. Proceedings of the Royal Society B: Biological Sciences. 288(1961):20211213. https://doi.org/10.1098/rspb.2021.1213

3) Chavez-Rosales S, Josephson E, Palka D, Garrison L. 2022. **Detection of Habitat Shifts of Cetacean Species: A Comparison Between 2010 and 2017 Habitat Suitability Conditions in the Northwest Atlantic Ocean**. Front Mar Sci. 9. https://doi.org/10.3389/fmars.2022.877580

4) Chavez-Rosales S, Josephson E, Palka D, Garrison L. **Sea turtle habitat, occurrence, and abundance patterns on the Northeast U.S. coast**. In Review.

5) Chavez-Rosales S, Palka DL, Garrison LP, Josephson EA. 2019. **Environmental predictors of habitat suitability and occurrence of cetaceans in the western North Atlantic Ocean**. Sci Rep. 9(1):5833. https://doi.org/10.1038/s41598-019-42288-6

6) Dias L, Garrison L. 2025. **NOAA Ship Gordon Gunter Vessel Line-transect Survey 2023 (GU2301)**. OBIS-SEAMAP https://seamap.env.duke.edu/dataset/2291.

7) DiMatteo A, Roberts JJ, Jones D, Garrison L, Hart KM, Kenney RD, McLellan WA, Lomac-MacNair K, Palka D, Rickard ME, et al. 2024. **Sea turtle density surface models along the United States Atlantic coast**. Endang Sp Res. 53:227–245. https://doi.org/10.3354/esr01298

8) Garrison L. 2020. **Abundance of marine mammals in waters of the U.S. southeastern Atlantic during summer 2016**. Southeast Fisheries Science Center, Protected Resources and Biodiversity Division, 75 Virginia Beach Dr., Miami, FL 33140. PRBD Contribution # PRBD-2020-04, 17 pp. https://doi.org/10.25923/zsrw-5673

9) Garrison LP, Aichinger Dias L. 2024. **Abundance of Tamanend's Bottlenose Dolphins (*Tursiops erebennus*) along the U.S. Atlantic Coast from Aerial Surveys Conducted During Summer 2021**.

Southeast Fisheries Science Center reference document; MMTD-2024-04. https://doi.org/10.25923/21jw-pc06

10) Garrison LP, Dias LA. 2023. **Abundance of marine mammals in waters of the Southeastern U.S. Atlantic during summer 2021**. SEFSC MMTD Contribution MMTD-2023-01. https://doi.org/10.25923/ce0d-9e10

11) Hirtle N, Roberts JJ, Redfern JV, Jazen EL, Palka D, McLellan W, Garrison L, Barco S, O'Brien O, Quintana-Rizzo E, Lomac-MacNair K, Rickard M, Zoidis AM, Cotter M, Whitt AD, Boisseau O, Halpin P, Thorne L. 2026. **Modeling decisions for quantifying range shifts in the face of climate change**. Diversity and Distributions32, no. 2: e70154. https://doi.org/10.1111/ddi.70154

12) Kannan R. 2020. **Postcard from the Atlantic Ocean**. Indian Birds 15 (5). https://indianbirds.in/pdfs/IB_15_5_Kannan_AtlanticOcean.pdf

13) Miller DL, Fifield D, Wakefield E, Sigourney DB. 2021. **Extending density surface models to include multiple and double-observer survey data**. PeerJ. 9:e12113. https://doi.org/10.7717/peerj.12113

14) Orphanides CD, Jech JM, Palka DL, Collie J. 2023. **Relating marine mammal distribution to water column prey structure derived from echosounding**. Mar Ecol Prog Ser. 711:101–119. https://doi.org/10.3354/meps14290

15) Palka D. 2020. **Cetacean abundance in the U.S. Northwestern Atlantic Ocean: Summer 2016** Northeast Fish Sci Cent Ref Doc. 20-05; 60 p https://doi.org/10.25923/1mrt-tn89

16) Palka D, Garrison L, Soldevilla M, Martinez A, Dias L, Rapucci G. 2024. **Cetacean visual observations using line-transect survey methods onboard the NOAA Ship Gordon Gunter (GU) during the Atlantic Marine Assessment Program for Protected Species (AMAPPS) in the Western North Atlantic Ocean (survey GU2301) from 2023-02-04 to 2023-04-27** (NCEI Accession 0290563) NOAA National Centers for Environmental Information. Dataset. https://www.ncei.noaa.gov/access/metadata/landing-page/bin/iso?id=gov.noaa.nodc:0290563

17) Palka DL. 2023. **Cetacean abundance in the U.S. Northwestern Atlantic Ocean, summer 2021**. Northeast Fisheries Science Center reference document 23-08. https://doi.org/10.25923/7cab-7s69

18) Roberts JJ, Yack TM, Fujioka E, Halpin PN, Baumgartner MF, Boisseau O, Chavez-Rosales S, Cole TVN, Cotter MP, Davis GE, et al. 2024. **North Atlantic right whale density surface model for the U.S. Atlantic evaluated with passive acoustic monitoring**. Mar Eco Prog Ser. 732:167–192. https://doi.org/10.3354/meps14547

19) Roberts JJ, Yack TM, Halpin PN. 2013. **Marine mammal density models for the U.S. Navy Atlantic Fleet Training and Testing (AFTT) study area for the Phase IV Navy Marine Species Density Database (NMSDD)**. Report prepared for Naval Facilities Engineering Systems Command, Atlantic by the Duke University Marine Geospatial Ecology Lab, Durham, North Carolina. https://seamap.env.duke.edu/seamap-models-files/Duke/Reports/AFTT_Marine_Mammal_Density_Models_2022_v1.3.pdf

20) Roberts SM, Jacoby A-M, Roberts JJ, Leslie J, Payne KL, Read AJ, Halpin PN, Barco S, Garrison L, McLellan W, et al. 2023. **Tight spatial coupling of a marine predator with soniferous fishes: Using joint modelling to aid in ecosystem approaches to management**. Div and Dist. 29(8):1074–1089. https://doi.org/10.1111/ddi.13746

21) Sigourney D, Chavez-Rosales, Josephson E, Palka D, Garrison L. in revision. **Bayesian hierarchical density surface model to estimate seasonal distributions of large whales off the East Coast of the United States with an application to a wind energy area**. Div and Dist.

22) Sigourney DB, Chavez-Rosales S, Conn PB, Garrison L, Josephson E, Palka D. 2020. **Developing and accessing a density surface model in a Bayesian hierarchical framework with a focus on uncertainty: insights from simulations and an application to fin whales (*Balaenoptera physalus*).** PeerJ. 8:e8226. https://doi.org/10.7717/peerj.8226

23) Sigourney DB, DeAngelis A, Cholewiak D, Palka D. 2023**. Combining passive acoustic data from a towed hydrophone array with visual line transect data to estimate abundance and availability bias of sperm whales (*Physeter macrocephalus*).** PeerJ. 11:e15850. https://doi.org/10.7717/peerj.15850

24) Sparks L, DiMatteo A. 2023. **Sea Turtle Distribution and Abundance on the East Coast of the United States. Prepared under NUWC Division Newport Network Activity No. 100001678464/0010**. NUWC-NPT Technical Report 12,428. https://apps.dtic.mil/sti/citations/trecms/AD1206953

25) Stepanuk JE, Kim H, Nye JA, Roberts JJ, Halpin PN, Palka DL, Pabst DA, McLellan WA, Barco SG, Thorne LH. 2023. **Subseasonal forecasts provide a powerful tool for dynamic marine mammal management.** Front Ecol and Env. 21(3):117–123. https://doi.org/10.1002/fee.2506

26) Virgili A, Hedon L, Authier M, Calmettes B, Claridge D, Cole T, Corkeron P, Dorémus G, Dunn C, Dunn TE, et al. 2021. **Towards a better characterization of deep-diving whales' distributions by using prey distribution model outputs**. PLOS ONE. 16(8):e0255667. https://doi.org/10.1371/journal.pone.0255667

27) Winship AJ, Leiness JB, Coyne M, Howell J, Saba VS, Christensen J. 2023. **Modeling the distributions of marine birds at sea to inform planning of energy development on the US Atlantic outer continental shelf**. Sterling (VA): U.S. Department of the Interior, Bureau of Ocean Energy Management. 413 p. Report No.: OCS Study BOEM 2023-060. https://espis.boem.gov/Final%20Reports/BOEM_2023-060.pdf

Passive acoustics
(Note: papers 18 and 23 above used passive acoustics data but are not duplicated in this section)

28) DeAngelis AI, Westell A, Baumann-Pickering S, Bell J, Cholewiak D, Corkeron PJ, Soldevilla MS, Solsona-Berga A, Trickey JS, Parijs SMV. 2025. **Habitat utilization by beaked whales in the western North Atlantic Ocean using passive acoustics**. Mar Eco Prog Ser. 754:137–153. https://doi.org/10.3354/meps14771

29) Haver S, Corkeron P, DeAngelis A, Baumann-Pickering S, Cholewiak D, Davis G, Frasier K, Posdaljian N, Kadifa M, Solsona-Berga A, et al. 2025. **Exploring the biodiversity of cetacean communities along the western North Atlantic Ocean shelf-break**. Roy Soc Open Sci. 12(7):241658. https://doi.org/10.1098/rsos.241658

30) Pegg N, Roca IT, Cholewiak D, Davis GE, Van Parijs SM. 2021. **Evaluating the Efficacy of Acoustic Metrics for Understanding Baleen Whale Presence in the Western North Atlantic Ocean**. Front Mar Sci. 8. https://doi.org/10.3389/fmars.2021.749802

31) Rankin S, Sakai T, Archer FI, Barlow J, Cholewiak D, DeAngelis AI, McCullough JLK, Oleson EM, Simonis AE, Soldevilla MS, Trickey JS. 2024. **Open-source machine learning BANTER acoustic classification of beaked whale echolocation pulses**. Ecol Informatics. 80:102511. https://doi.org/10.1016/j.ecoinf.2024.102511

32) Vyacheslav L, Bailey H, Tribble CM, Fandel AD, DeAngelis AI, Pagliani B, Secor DH. Submitted. **Improving acoustic classification of two closely related species, the Atlantic bottlenose dolphin and common dolphin**. Submitted on 4 September 2025 to PLOS ONE.

33) Weiss SG, Cholewiak D, Frasier KE, Trickey JS, Baumann-Pickering S, Hildebrand JA, Van Parijs SM. 2021. **Monitoring the acoustic ecology of the shelf break of Georges Bank, Northwestern Atlantic Ocean: New approaches to visualizing complex acoustic data**. Mar Policy. 130:104570. https://doi.org/10.1016/j.marpol.2021.104570

34) Westell A, Sakai T, Valtierra R, Van Parijs SM, Cholewiak D, DeAngelis A. 2022. **Sperm whale acoustic abundance and dive behaviour in the western North Atlantic**. Sci Rep. 12(1):16821. https://doi.org/10.1038/s41598-022-20868-3

Sea Turtle Ecology

35) Crowe L, Hatch JM, Patel S, Smolowitz RJ, Haas HL. 2020. **Riders on the storm: Loggerhead sea turtles detect and respond to a major hurricane in the Northwest Atlantic Ocean**. Mov Ecol. 8(32). https://movementecologyjournal.biomedcentral.com/articles/10.1186/s40462-020-00218-6

36) Rider MJ, Avens L, Haas HL, Patel SH, Sasso, CR. **Distribution models reveal important coastal habitats for endangered leatherback sea turtles**. submitted. Diversity and Distributions.

37) Forbes Z, Patel S, Scro A, Haas HL, Smolowitz R, Sharon G. in review. **Bacterial communities of wild-captured loggerhead (*Caretta caretta*) sea turtles in the Northwest Atlantic**.

38) Hatch JM, Haas HL, Sasso CR, Patel SH, Smolowitz RJ. 2022. **Estimating the complex patterns of survey availability for loggerhead turtles**. J Wildl Manage. 86(4):e22208. https://doi.org/10.1002/jwmg.22208

39) Hatch JM, Murray KT, Patel S, Smolowitz R, Haas HL. 2023. **Evaluating simple measures of spatial-temporal overlap as a proxy for encounter risk between a protected species and commercial fishery**. Front Conserv Sci. 4. https://doi.org/10.3389/fcosc.2023.1118418

40) Logan J, Dourdeville K, Choate K, Nielsen J, Patel SH, Prescott R, Haas HL. Submitted. **Niche overlap and trophic position estimates of multiple sea turtle species cold-stunned in the northwest Atlantic.**

41) Patel SH, Winton MV, Hatch JM, Haas HL, Saba VS, Fay G, Smolowitz RJ. 2021. **Projected shifts in loggerhead sea turtle thermal habitat in the Northwest Atlantic Ocean due to climate change**. Sci Rep. 11(1):8850. https://doi.org/10.1038/s41598-021-88290-9

42) Patel, Winton, Hatch J, Haas H, Saba V, Fay G, Smolowitz R. 2021. **Data compendium for projected shifts in loggerhead sea turtle thermal habitat in the Northwest Atlantic Ocean due to climate change**. https://doi.org/10.5281/zenodo.4790359

43) Rider M, Avens L, Haas H, Patel S, Sasso C. 2026. **Distribution models reveal important coastal habitats for endangered leatherback sea turtles**. Diversity and Distributions 32, no. 1: e70131. https://doi.org/10.1111/ddi.70131

44) Rider M, Haas H, Sasso C. 2022. **Surface availability metrics of leatherback turtles (*Dermochelys coriacea*) tagged off North Carolina and Massachusetts, United States**. NOAA technical memorandum NMFS-NE ; 286. https://doi.org/10.25923/82c1-4a85

45) Rider MJ, Avens L, Haas HL, Harms CA, Patel SH, Snodgrass D, Sasso CR. 2024. **Regional variation in leatherback dive behavior in the northwest Atlantic**. Endang Species Res. 55:169–185. https://doi.org/10.3354/esr01365

46) Rider MJ, Avens L, Haas HL, Hatch JM, Patel SH, Sasso CR. 2024. **Where the leatherbacks roam: movement behavior analyses reveal novel foraging locations along the Northwest Atlantic shelf**. Front Mar Sci. 11. https://doi.org/10.3389/fmars.2024.1325139

47) Robinson NJ, García-Párraga D, Stacy BA, Costidis AM, Blanco GS, Clyde-Brockway CE, Haas HL, Harms CA, Patel SH, Stacy NI, Fahlman A. 2021. **A baseline model for estimating the risk of gas embolism in sea turtles during routine dives**. Front Physiol. 12. https://doi.org/10.3389/fphys.2021.678555

48) Rogers R, Choate KH, Crowe LM, Hatch JM, James MC, Matzen E, Patel SH, Sasso CR, Siemann LA, Haas HL. 2024. **Investigating leatherback surface behavior using a novel tag design and machine learning**. J Exp Mar Bio and Ecol. 576:152012. https://doi.org/10.1016/j.jembe.2024.152012

49) Yang T, Haas HL, Patel S, Smolowitz R, James MC, Williard AS. 2019. **Blood biochemistry and haematology of migrating loggerhead turtles (*Caretta caretta*) in the Northwest Atlantic: reference intervals and intra-population comparisons**. Conserv Physiol. 7(1):coy079. https://doi.org/10.1093/conphys/coy079

Ecosystem

50) Díaz-Arce N, Gagnaire P-A, Richardson DE, Walter III JF, Arnaud-Haond S, Fromentin J-M, Brophy D, Lutcavage M, Addis P, Alemany F, et al. 2024. **Unidirectional trans-Atlantic gene flow and a mixed spawning area shape the genetic connectivity of Atlantic bluefin tuna**. Mol Ecol. 33(1):e17188. https://doi.org/10.1111/mec.17188

51) Govindarajan AF, Llopiz JK, Caiger PE, Jech JM, Lavery AC, McMonagle H, Wiebe PH, Zhang W (Gordon). 2023. **Assessing mesopelagic fish diversity and diel vertical migration with environmental DNA**. Front Mar Sci. 10. https://doi.org/10.3389/fmars.2023.1219993

52) Hernández CM, Richardson DE, Rypina II, Chen K, Marancik KE, Shulzitski K, Llopiz JK. 2022. **Support for the Slope Sea as a major spawning ground for Atlantic bluefin tuna: evidence from larval abundance, growth rates, and particle-tracking simulations**. Can J Fish Aquat Sci. 79(5):814–824. https://doi.org/10.1139/cjfas-2020-0444

53) Holzwarth-Davis T. 2023. **Oceans and Climate Branch CTD Data Report: CTD_REPORT_2021002HB**. Northeast Fisheries Science Center. https://doi.org/10.25923/jx96-4v91

54) Richardson DE, Manancik KE, Adamus M, Broughton EA, Cowen RK, Gerard T, Hernandez CM, Hoey JJ, Llopiz JK, Lutcavage ME, Malca E, Palka DL, Vasquez-Yeomans L, Walsh HJ, Willis CM, Zapfe GA. In press. **A re-evaluation of Atlantic bluefin tuna (*Thunnus thynnus*) spawning distribution in the western Atlantic Ocean**. Prog. Oceanogr. Volume 242. https://doi.org/10.1016/j.pocean.2026.103687

55) Quigley LA, Caiger PE, Govindarajan AF, McMonagle H, Jech JM, Lavery AC, Sosik HM, Llopiz JK. 2023. **Otolith characterization and integrative species identification of adult mesopelagic fishes from the western North Atlantic Ocean**. Front Mar Sci. 10. https://doi.org/10.3389/fmars.2023.1217779

Satellite imagery

56) Khan CB, Goetz KT, Cubaynes HC, Robinson C, Murnane E, Aldrich T, Sackett M, Clarke PJ, LaRue MA, White T, et al. 2023. **A biologist's guide to the galaxy: Leveraging artificial intelligence and very high-resolution satellite imagery to monitor marine mammals from space**. J. Mar. Sci. Eng., 11, 595. https://doi.org/10.3390/jmse11030595

Other

57) Hayes SA, Josephson E, Maze-Foley K, Rosel P. Eds. **U.S. Atlantic and Gulf of Mexico Marine Mammal Stock Assessments** - 2019, 2020, 2021, 2022, 2023 NOAA Tech Memo NMFS. https://www.fisheries.noaa.gov/national/marine-mammal-protection/marine-mammal-stock-assessment-reports-region#2022-reports

58) Lettrich MD, Asaro MJ, Borggaard DL, Dick DM, Griffis RB, Litz JA, et al. 2023. **Vulnerability to climate change of United States marine mammal stocks in the western North Atlantic, Gulf of Mexico, and Caribbean**. PLoS ONE 18(9): e0290643. https://doi.org/10.1371/journal.pone.0290643

59) Northeast Fisheries Science Center (U.S.), Southeast Fisheries Science Center (U.S.). 2025. **2024 Annual Report of a Comprehensive Assessment of Marine Mammal, Marine Turtle, and Seabird Abundance and Spatial Distribution in U.S. waters of the Western North Atlantic Ocean : AMAPPS III**.

60) Northeast Fisheries Science Center (U.S.), Southeast Fisheries Science Center (U.S.). 2024. **2023 Annual Report of a Comprehensive Assessment of Marine Mammal, Marine Turtle, and Seabird Abundance and Spatial Distribution in U.S. waters of the Western North Atlantic Ocean : AMAPPS III**. https://doi.org/10.25923/11cy-0j88

61) Northeast Fisheries Science Center (U.S.), Southeast Fisheries Science Center (U.S.). 2023. **2022 Annual Report of a Comprehensive Assessment of Marine Mammal, Marine Turtle, and Seabird Abundance and Spatial Distribution in U.S. waters of the Western North Atlantic Ocean : AMAPPS III**. https://doi.org/10.25923/ke0y-a251

62) Northeast Fisheries Science Center (U.S.), Southeast Fisheries Science Center (U.S.). 2022. **2021 Annual Report of a Comprehensive Assessment of Marine Mammal, Marine Turtle, and Seabird Abundance and Spatial Distribution in U.S. waters of the Western North Atlantic Ocean : AMAPPS III**. https://doi.org/10.25923/jazw-5467

63) Northeast Fisheries Science Center (U.S.), Southeast Fisheries Science Center (U.S.). 2021. **2020 Annual Report of a Comprehensive Assessment of Marine Mammal, Marine Turtle, and Seabird Abundance and Spatial Distribution in U.S. waters of the Western North Atlantic Ocean : AMAPPS III**. https://doi.org/10.25923/rey7-5w09

64) Northeast Fisheries Science Center (U.S.), Southeast Fisheries Science Center (U.S.). 2020. **2019 Annual Report of a Comprehensive Assessment of Marine Mammal, Marine Turtle, and Seabird Abundance and Spatial Distribution in U.S. waters of the Western North Atlantic Ocean : AMAPPS III**. https://doi.org/10.25923/v2pq-ht50

65) Palka D, Aichinger Dias L, Broughton E, Chavez-Rosales S, Cholewiak D, Davis G, DeAngelis A, Garrison L, Haas H, Hatch J, Hyde K, Jech M, Josephson E, Mueller-Brennan L, Orphanides C, Pegg N, Sasso C, Sigourney D, Soldevilla M, Walsh H. 2021. **Atlantic Marine Assessment Program for Protected Species: FY15 – FY19**. Washington DC: U.S. Department of the Interior, Bureau of Ocean Energy Management. OCS Study BOEM 2021-051. 330 p. https://repository.library.noaa.gov/view/noaa/47287, Appendix I, Appendix II, Appendix III

B. CONFERENCE AND MEETING PRESENTATIONS

Abundance and distribution

66) Baker CS, Baird R, Cholewiak D, Constantine R, Filatova O, Jacobsen L, Notarbarolo de Sciaria G, Oleson E, Panigada S, Schorr GS, Klink H, Steel D. **Species identification of cetaceans by environmental (e)DNA metabarcoding – a new tool for surveys of the high seas**. Oral presentation at the World Marine Mammal Conference, 9-12 December 2019, Barcelona, Spain.

67) Chavez S, Palka D, Garrison D, Sigourney DB, Josephson E. **Habitat suitability as a tool to detect spatial and temporal distribution changes of marine mammals**. Poster presentation at the World Marine Mammal Conference, 9-12 December 2019, Barcelona, Spain.

68) Chavez-Rosales S. **AMAPPS**. Presented to the Marine Science Division of the United Nations Environmental Program, Nairobi Kenya 04/17/2021.

69) Cholewiak D, Allen D, Baker CS, Cerchio S, Conger L, DeAngelis A, Hickmott L, Metheny N, Pitman R, Stanistreet J, Steel D, Tremblay C, J. Trickey. **True's beaked whale: a cryptic species revealed**. Oral presentation at the World Marine Mammal Conference, 9-12 December 2019, Barcelona, Spain.

70) NEFSC & SEFSC prepared a PowerPoint presentation in December 2020 for BOEM on the Accomplishments of AMAPPS II and Plans for AMAPPS III. This was also shared with the Navy.

71) Palka D, Campbell L, Zoidis, AM, Robinson Willmott, J, Komac-MacNair, K. **A comparison of visual and image aerial surveys for marine mammals and sea turtles in the New York Offshore Planning Area**. Presented at the New York State of the Science Workshop on Offshore Wind Energy, Wildlife and Fisheries July 16-19, 2024, Long Island, New York.

72) Palka D, Garrison L, and Aichinger Dias L presented on 11 March 2022 a PowerPoint presentation on the **NEFSC and SEFSC Imagery Abundance Surveys** to BOEM and USFWS to increase collaboration between the three agencies with the goal of developing reliable and operational aerial abundance surveys using high-definition cameras.

73) Palka presented preliminary **2021 abundance estimates of harbor porpoises** using the summer 2021 AMAPPS aerial survey data to the Harbor Porpoise Take Reduction Team during a virtual meeting on 24 March 2022.

74) Palka annually presented an **update of the AMAPPS activities** to the Atlantic Scientific Review Group in 2019 - 2025.

75) Aircraft Operational Control (AOC) stakeholders virtual meeting (May 28, 2020): **NEFSC and SEFSC aircraft needs for AMAPPS**. Presented by D. Palka.

76) Palka presentation to NOAA Protected Resources Science Board (Jun 12, 2020): **AMAPPS: past and future.**

77) Sigourney DB, Chavez S, Palka D, Garrison L, Josephson E. **Application of a Bayesian hierarchical density surface model to estimate seasonal abundance of large whales in wind energy areas off the east coast of the United States.** Presented at the New York State of the Science Workshop on Offshore Wind Energy, Wildlife and Fisheries July 16-19, 2024, Long Island, New York.

78) Sigourney and Annamaria DeAngelis received a review of their draft paper on the **integration of visual and passive acoustic data** by the Navy sponsored DENMOD Density Surface Model Uncertainty Estimation working group at a virtual meeting on 12 Feb 2021.

79) Sigourney was invited to present a seminar to the SEFSC and SERO on the **development of the method to combine visual and passive acoustic data to estimate abundance of sperm whales**. Sep 2020.

80) Stepanuk J. Chong-Montenegro C, Ney J, Kim H, Roberts J, Halpin P, Palka D, Pabst A, McLellan W, Barco SG, Thorne L. **Using prey availability and environmental covariates to forecast humpback and fin whale distributions in the Northeast United States**. Oral presentation at the World Marine Mammal Conference, 9-12 December 2019, Barcelona, Spain.

81) Walsh H, Sigourney D, Palka D. **Updating Atlantic seabird distribution and bycatch**. Talk presented to the Atlantic Marine Birds Cooperative virtual meeting on 07 December 2021.

Passive acoustics

82) DeAngelis AI, Westell A, Corkeron P, Solsona Berga A, Trickey J, Rafter M, Baumann-Pickering S, Cholewiak D, Soldevilla M, Bell J, Van Parijs S. 2023. **Niche partitioning of beaked whales (family Ziphiidae) during the summer in the western North Atlantic.** Presented at the Ecological Society of America Conference, Portland, OR. (also subsequently presented as a guest lecture for BioacousTalks virtual session hosted by Cornell University)

83) DeAngelis AI. 2022. **Combining spatial and temporal acoustic datasets to examine the summer presence of beaked whales off the east coast of the U.S**. Virtual poster at the 24th Biennial Conference on the Biology of Marine Mammals: August 1 - 5 2022.

84) DeAngelis AI. 2022. **Combining spatial and temporal acoustic datasets to examine the summer presence of beaked whales off the east coast of the U.S**. Virtual poster at the Detection, Classification, Localization, and Density Estimation workshop on 9 March 2022

85) DeAngelis AI. 2023. **Passive acoustic monitoring as a versatile tool in understanding marine mammal distributions, abundance, and behavior**. Presented AMAPPS data as part of a seminar at UMASS Dartmouth on 20 Oct 2023.

86) Fritz A, DeAngelis AI. 2023. **All these clicks and whistles: building an acoustic classifier for western North Atlantic dolphins**. Presented at the Hollings Symposium in Silver Spring, MD

87) Haver SM, Corkeron P, Baumann-Pickering S, Cholewiak D, Davis G, DeAngelis A, Frasier K, Holdman A, Martin M, Pegg N, Posdaljian N, Rafter M, Schoenbeck C, Solsona Berga A, Westell A, Van Parijs SM. 2022, Dec. **Application of long-term passive acoustic monitoring to evaluate spatial and temporal patterns of multi-species acoustic assemblages of marine mammals in the western North Atlantic Ocean**. Presented at the 183rd Meeting of the Acoustical Society of America, Nashville, TN. Invited talk.

88) Haver SM, Corkeron P, Baumann-Pickering S, Cholewiak D, Davis G, DeAngelis A, Frasier K, Posdaljian N, Rafter M, Solsona Berga A, Westell A, Van Parijs SM. 2023, Aug. **Eavesdropping on multi-species marine mammal communities along the western North Atlantic Ocean shelf-break**. Presented at the Ecological Society of America, Portland, OR. Invited talk.

89) Medina M, DeAngelis AI. 2025. **Understanding beaked whale summer distributions off the northeast U.S. through passive acoustics**. Presented at the 188th Meeting of the Acoustical Society of America conference, May 2025 and at the Hollings Symposium in Silver Springs, MD.

90) Rankin S, Sakai T, Archer E, Barlow J, Cholewiak D, DeAngelis A, Keating J, Oleson E, Simonis A, Soldevilla M. 2019. **Beaker BANTER: a machine learning approach to acoustic classification of beaked whales**. Poster presentation at the World Marine Mammal Conference, 9-12 December 2019, Barcelona, Spain.

91) Redford A, Westell A. 2023. **A deep dive into sperm whale echolocation buzzes**. Presented at the Hollings Symposium in Silver Spring, MD.

92) VanParijs S, Davis G, Palka D. **Update on AMAPPS**. Oral presentation at the New York Bight Whale Monitoring Workshop, 6 June 2019, Setauket-East Setuaket, NY.

93) Weiss S, Cholewiak D, Baumann-Pickering S, Frasier K, Hildebrand J, Van Parijs SM. 2019. **Defining shelf break soundscapes of southern Georges Bank, western North Atlantic Ocean**. Poster presentation at the World Marine Mammal Conference, 9-12 December 2019, Barcelona, Spain.

94) Westell A, Sakai T, Valtierra R, Van Parijs S, Cholewiak D, DeAngelis A. 2022. **Acoustic detections of sperm whales in the western North Atlantic: insights into their foraging ecology and abundance**. Presented a virtual poster at the 24th Biennial Conference on the Biology of Marine Mammals: August 1 - 5 2022.

95) Westell A, Sakai T, Valtierra R, Van Parijs S, Cholewiak D, DeAngelis A. 2022. **Acoustic detections of sperm whales in the western North Atlantic: insights into their foraging ecology and abundance**. Presented at the Detection, Classification, Localization, and Density Estimation workshop on 9 March 2022.

96) Westell A, Sakai T, Holdman A. 2024. **Introduction to the Dive Depth Detection method.** Presented at the Detection, Classification, Localization, and Density Estimation workshop on 3 June 2024.

Ecosystem

97) Hyde K. **Applications of ocean color and SST data in fisheries science and management**. Poster presented at International Operational Satellite Oceanography Symposium, 18-20 June 2019, College Park MD.

98) Jech M, Lavery A, Wiebe P, Stanton T. **Comparison of net catches and acoustic abundance estimates of the deep-scattering layers**. Oral presentation at the ICES WGFAST meeting, 29 April - 2 May 2019, Galway, IR.

99) Jech, J. M. 2022. **Acoustic observations of nekton and zooplankton along the northeast continental shelf break**. Invited presentation at the Acoustical Society of America meeting in Nashville, TN. 5-9 December 2022.

C. DATABASES

100) *Oracle database* (housed at NEFSC) holds the marine mammal, turtle, seal, seabird, plankton, oceanography, environmental, and passive acoustic data collected during the NEFSC and SEFSC AMAPPS fieldwork.

101) *Atlantic Offshore Seabird Dataset Catalog* originally developed by U.S. Fish and Wildlife Service and currently housed at USGS hold seabird data collected by AMAPPS surveys among other surveys.

102) *OBIS-SEAMAP database* holds the marine mammal, turtle, and seal visual sightings detected during the shipboard and aerial abundance surveys.

103) A bar code library of the northwestern Atlantic salp species (*Thaliacea*) is being developed by the University of Connecticut utilizing salp specimens taken during AMAPPS shipboard surveys (Batta-Lona et al. 2016; Jue et al. 2018).

104) Palka D, Garrison L, Soldevilla M, Martinez A, Aichinger Dias L, Rappucci G. 2024. **Cetacean visual observations using line-transect survey methods onboard the NOAA Ship Gordon Gunter (GU) during the Atlantic Marine Assessment Program for Protected Species (AMAPPS) in the Western North Atlantic Ocean (survey GU2301) from 2023-02-04 to 2023-04-27**. Dataset archived at National Centers for Environmental Information (NCEI). NCEI Accession and DOI: https://doi.org/10.25921/hhxz-vm91.

105) Passive Acoustics Database Homepage: holds the Makara Database and Passive Acoustic Cetacean Map (PACM), which includes any passive acoustic detection data collected during AMAPPS fieldwork (including from towed hydrophone array data and bottom mounted hydrophone data).

D. WEB PRESENCE – DATA

106) General information on AMAPPS.

107) AMAPPS marine mammal model viewer displays average seasonal species-specific density maps resulting from the AMAPPS habitat models output. Site is interactive to allow user to highlight a boxed area of interest and then display and download the area's estimated density and abundance along with the individual density estimates for each cell in the area of interest.

108) SEFSC Population Assessments webpage describing marine mammal research surveys, including AMAPPS:

109) The distribution of tagged loggerhead turtles (from Winton et al 2018) was published within the Northeast and Mid-Atlantic Ocean Data Portals (https://www.fisheries.noaa.gov/inport/item/27337).

110) Data compendium for Patel et al. 2021 "**Projected shifts in loggerhead sea turtle thermal habitat in the Northwest Atlantic Ocean due to climate change**". https://doi.org/10.5281/zenodo.4790359

111) Marine Mammal Research Surveys in NOAA's Southeast Region displays maps of aerial and ship-based mammal sightings and links to data. https://www.fisheries.noaa.gov/southeast/population-assessments/marine-mammal-research-surveys-noaas-southeast-region%23what-we-have-learned

E. WEB STORIES

112) 2025. Feature story: **Celebrating 15 Years of Surveying Protected Species in the Northwest Atlantic**. https://www.fisheries.noaa.gov/feature-story/celebrating-15-years-surveying-protected-species-northwest-atlantic

113) 2023. **Examples of leatherback tagging off Florida** https://www.fisheries.noaa.gov/video/tagging-leatherback-turtles

114) 2023. **Leatherback tracks from North Carolina** https://my.wildlifecomputers.com/data/map/?id=6467e9162c72b06dfd1c4a15

115) 2022. **Collaborative research cruise with the Woods Hole Oceanographic Institution and the University of Rhodes Island that is studying the mesopelagic community and its role in global carbon flux from 4-18 August 2022**. https://www.whoi.edu/press-room/news-release/whoi-leads-multi-ship-study-of-northwest-atlantic/

116) 2021. **SEFSC Feature story about AMAPPS ship and aerial surveys conducted in the summer 2021** https://www.fisheries.noaa.gov/feature-story/experts-collaborate-mission-document-protected-species

117) 2021. NEFSC cruise blogs. Jun – Aug 2021. **NOAA ship Henry. B. Bigelow's AMAPPS abundance survey**. https://www.fisheries.noaa.gov/science-blog/another-week-more-surprises-sea

118) 2021. NOAA Fisheries Science Highlights.1 Sep 2021. **AMAPPS: Updated marine mammal model viewer**. https://content.govdelivery.com/accounts/USNOAAFISHERIES/bulletins/2ef2a82

119) 2021. NOAA/SEFSC Feature story. 16 Jun 2021. **Tag, you're it! Tracking sea turtle movements with satellite tags.** https://www.fisheries.noaa.gov/southeast/endangered-species-conservation/tag-youre-it-tracking-sea-turtle-movements-satellite-tags

120) 2021. NOAA/SEFSC Feature story. 16 Jul 2021. **Experts collaborate on mission to document protected species**. https://www.fisheries.noaa.gov/feature-story/experts-collaborate-mission-document-protected-species

121) 2020. Media Coverage of Crowe et al. 2020 : **Riders on the storm: Loggerhead sea turtles detect and respond to a major hurricane in the Northwest Atlantic Ocean** https://movementecologyjournal.biomedcentral.com/articles/10.1186/s40462-020-00218-6/metrics

122) 2020. NOAA Fisheries Feature News: Technology helps unlock the world of beaked whales

123) 2020. NOAA Fisheries Feature Story: **Surveys collect data year-round on marine life along the U.S. east coast. Published 23 Jan 2020**.

124) 2019. NOAA Fisheries Feature Story on AMAPPS: East Coast Marine Life Survey Renewed for Five More Years

125) 2019. NEFSC Highlights the AMAPPS model mapper and a rare bird seen by an AMAPPS observer on an EcoMon survey

126) 2019. WCAI (NPR) reports on seabirds sighted during an offshore cetacean ecology survey

127) 2019. NOAA Fisheries Feature Story on the successful tagging of 9 leatherback turtles in Cape Cod Bay in August 2019

128) 2019. NOAA Fisheries Feature Story on the record number of leatherback turtles tagged in North Carolina

4 Distribution, Abundance, and Trends Research

Primary authors: Debra Palka, Samuel Chavez-Rosales, Doug Sigourney, Annamaria DeAngelis, Annabel Westell, Elizabeth Josephson, Laura Aichinger Dias, Lance Garrison

4.1 Introduction

Effective management of human activities that impact marine life requires a comprehensive understanding of animal distribution, abundance, and habitat use. To accurately assess population trends and understand these patterns, it is important to identify the processes that drive spatiotemporal variations in animal abundance and distribution. The Atlantic Marine Assessment Program for Protected Species (AMAPPS) provides the data to facilitate this understanding. The program's objectives (Section 2.2) aim to foster a comprehensive understanding through the collection and analysis of seasonal distribution and abundance data for marine mammals, sea turtles, and seabirds. We achieved this by utilizing visual, acoustic, and telemetry data, alongside gathering information on other habitat components such as potential prey and physical oceanographic characteristics. This chapter focuses on the distribution, abundance and trend patterns of cetaceans and marine turtles to address the following AMAPPS objectives:

1) Collect broad-scale data over multiple years on the seasonal distribution and abundance of marine mammals (cetaceans and pinnipeds), marine turtles, and seabirds using fixed passive acoustic monitoring and direct aerial and shipboard surveys of coastal U.S. Atlantic Ocean waters;

2) Collect similar data at finer scales at several sites of particular interest to BOEM, NOAA, and partners using visual and acoustic survey techniques;

5) Identify currently used, viable technologies and explore alternative platforms and technologies to improve population assessment studies, if necessary;

6) Assess the population size of surveyed species at regional scales; and develop models and associated tools to translate these survey data into seasonal, spatially explicit density estimates incorporating habitat characteristics.

This chapter addresses the AMAPPS objectives by presenting updated seasonal, spatially explicit density maps and abundance estimates of cetaceans and sea turtles by extending the time series to 2010 - 2023. We also describe refined processing and analysis methods to integrate visual and passive acoustic data, aiming to improve abundance estimates for deep-diving species. Chapters 5 and 6 further utilize these AMAPPS visual and passive acoustic line transect data to investigate the ecology and behavior of cetaceans and sea turtles.

The "species-habitat models seek to quantify and unravel the complex amalgamation of physiological requirements, behavioral preferences, predatory/competitive constraints, and stochastic processes that drive where a species occurs in time and space" (Klaasen et al. 2025). These models can inform conservation planning and management actions. Examples of usages of species-habitat models in management includes:

- Sharing information across space and time and account for spatiotemporal variability to provide better estimates of abundance in areas and times that lack data and can correct for unequal sampling intensity. We applied this idea in Sections 4-6 – 4-11.
- Defining essential habitats to improve our understanding of their distributions which can be used to inform the optimal placement of anthropogenic activities such as offshore energy. These

models can identify “core” habitat areas that can provide information on a species’ relative dependency on an area thus providing more understanding on the potential impact of placing a given activity in an area. We applied this idea in Sections 4-14 and 5-4.
- Informing dynamic management that estimates the probability of encountering a species of interest in a given area in a given oceanic condition. We applied this idea in Section 4.8.
- Understanding and evaluating potential risks a changing climate may have on a species distribution or abundance. A species-habitat model can be forward projected using climate projections to predict future patterns and changes in species distributions. This can provide insight into how species distributions may change under different future conditions and so help identify areas where species may move out of or into. A collaborator applied this idea in Section 5.6.

We designed the AMAPPS abundance surveys' data collection and analysis methods to estimate absolute abundance that are precise and accurate. We collected line-transect data from ships and planes through a two-independent team data collection method. This approach allowed for the documentation of species locations and the estimation of absolute abundance that encompassed animals found throughout the entire water column.

Our analytical methods accounted for three types of bias commonly found in visual line transect data from ships and planes (McLaren 1961): availability bias, perception bias, and bias from ambiguous species identification.

- Availability bias is due to observers missing animal detections because animals were submerged and thus not available for detection at the time the shipboard or aerial sighting survey platform traveled near the animals.
- Perception bias is due to observers missing animals that were available because, for example, the animals were too far from the platform or the sighting conditions, such as sun glare or sea state, were poor.
- Ambiguous species identification bias is due to the inability of the observers to positively identify the species of a group of animals to a specific species, but instead only able to identify that the animals were one of several species (such as a fin or sei whale, or a beaked whale) or were one of many species (such as unidentified whale or unidentified dolphin).

To account for these biases, we estimated the absolute species-specific abundance in several ways.

- We multiplied the species-specific at-surface abundance estimates of visually detected animals at or near the surface (Section 4.6 - 4.8) with species-specific availability correction factors for the animals below the surface (Section 4.3).

- For sperm whales, we estimated the abundance of foraging sperm whales using passive acoustic detections (Section 4.9). We also developed a novel integrated analytical method that used visual sperm whale data for the abundance of animals at the surface and passive acoustic sperm whale data for the animals below the surface. This integrated method accounted for the sperm whales that were both seen visually and heard acoustically (Section 4.11).

- For beaked whales, we estimated the absolute abundance estimate of animals throughout the water column using a novel approach that adds the at-surface perception-bias corrected abundance estimate using visual data analyzed analyzed with design-based methods (Section 4.6) to the subsurface abundance estimate using passive acoustic data analyzed with design-based analysis methods (Section 4.10). This is appropriate since the likelihood of visually spotting a

beaked whale that was also identified by a passive acoustic array is deemed negligible during shipboard line-transect survey conducted at 10-knots.

Estimating beaked whale abundance is challenging for several reasons. First, species identification in the field is difficult because beaked whales spend very little time at the surface and share similar physical and behavioral traits. Accurate identification requires clear, unobstructed views to distinguish the subtle features that set each species apart. To fully utilize the visual sightings assigned as an ambiguous unidentified beaked whale, we developed a novel method that uses passive acoustic detections to help differentiate ambiguous visual sightings (see Section 4.4.1).

The general work flow we used to estimate abundance is as follows:

1. Data collection
    a. Conduct line transect surveys on ships and planes to collect visual and passive acoustic detections and collect data on the abiotic and biotic habitat characteristics (Section 4.2.1 and Chapter 10).
    b. Collate concurrent environmental habitat data from satellite and ocean data assimilation derived sources (Section 4.2.2 and Chapter 10).
2. Prepare data (Section 4.2 and Chapter 10)
    a. Conduct quality control checks on all data types.
    b. Process the passive acoustic data.
    c. Define the spatiotemporal strata: 10x10 km^2 and 8-day intervals starting with 4 Jan 2010.
    d. Merge environmental habitat data with the line transect data by spatiotemporal strata.
3. Conduct supportive analyses
    a. Estimate species- and platform-specific availability bias correction factors using dive and surfacing patterns derived from data collected from individual animals deployed with time-depth tags (Section 4.3).
    b. Separate ambiguous species identifications of visual sightings into separate species (Section 4.4).
    c. Build acoustic classifiers to detect passive acoustic clicks (Section 4.5).
4. Estimate species-specific abundance
    a. Using only visual data
        i. Estimate design-based bias-corrected species-specific abundance from the summer 2021 shipboard and aerial visual surveys that we reported in the Atlantic Marine Mammal Stock Assessment Report (Section 4.6).
        ii. Estimate bias-corrected species-specific abundance using generalized additive models based on the 2010-2023 shipboard and aerial visual data (Section 4.7).
        iii. Estimate bias-corrected large whale species-specific abundance using Bayesian hierarchical models based on the 2010-2023 shipboard and aerial visual data (Section 4.8).
    b. Using only passive acoustic data
        i. Estimate subsurface abundance estimate of acoustically active foraging sperm whales using passive acoustically detected events from the shipboard summer 2016 and 2021 towed hydrophone array data (Section 4.9).
        ii. Estimate subsurface abundance of vocalizing beaked whales using passive acoustically detected events for the shipboard summer 2013, 2016, and 2021 towed hydrophone array data (Section 4.10).
    c. Integrating visual and passive acoustic data
        i. Estimate bias-corrected abundance of beaked whales throughout the water column by combining model-based surface abundance estimates using visual

data and design-based subsurface abundance estimates using passive acoustic data (Section 4.10).

ii. Estimate bias-corrected abundance of sperm whales throughout the water column by integrating visual and towed array passive acoustic data that we collected simultaneously in a newly developed analysis method that combines a capture mark-recapture approach with a distance sampling analysis to estimate abundance and surface availability while accounting for transition probabilities among surfacing and diving states (Sections 4.11-4.12).

d. Estimates developed by collaborators during the AMAPPS III time period (Section 4.13)

5. Investigate spatiotemporal trends of cetaceans and sea turtles using visual and passive acoustic data (Section 4.14).

4.2 Data Collection and Processing

4.2.1 Data Collection

During AMAPPS III, our data collection objectives related to estimate abundances were to conduct the following:

- An aerial survey focusing on marine mammal and sea turtle visual sightings that covered the U.S. Atlantic continental shelf waters (out to the 2000 m or 200 m depth contour depending on the location) once each fiscal year (FY19 - FY23), where each year's survey was conducted in different seasons using the two independent-team data collection procedures.
- A shipboard survey in the summer in offshore waters focusing on marine mammals, sea turtle, and seabird visual sightings using the two independent-team data collection procedures at the same time cetacean acoustic detections were recorded using a towed passive acoustic hydrophone. We conducted the shipboard survey concurrently as the summer aerial surveys that covered coastal waters.
- A shipboard survey in a non-summer season in offshore waters using the two independent-team data collection procedures and passive acoustic monitoring data collection procedures.
- An aerial pilot study using a camera system in addition to visual observers to test the feasibility of using cameras in the future to replace or augment visual observers.

We met these objectives (**Table 4-1**). More information on the data collection and processing procedures plus a general description of the cruises can be found in the annual reports on the AMAPPS website, Chapter 10, Palka (2023) and Garrison and Aichinger Dias (2023). Scientific names of all species detected are in **Appendix A**.

Please note that in Jan - Feb 2025, using funds from AMAPPS IV, we collected additional line transect abundance data during simultaneous aerial (visual and imagery data) and shipboard (visual, passive acoustic and plankton data) surveys, which we will report on in the 2025 AMAPPS IV annual report.

Table 4-1. Abundance shipboard and aerial surveys conducted during AMAPPS III
Additional information on these surveys is in Chapter 10.

Fiscal Year	Season	Platform	On-effort Trackline (km)	Mammal Sighting Records*	Turtle Sighting Records*
19	spring 2019	NOAA aircraft Twin Otter	10,392	1,280	2
20	spring 2019	NOAA aircraft Twin Otter	6,108	127	495
21	summer 2021	NOAA aircraft Twin Otter	20,468	1,113	393
21	summer 2021	NOAA ship *Henry B. Bigelow*	5,870	1,246	39

Fiscal Year	Season	Platform	On-effort Trackline (km)	Mammal Sighting Records*	Turtle Sighting Records*
21	summer 2021	NOAA ship *Gordon Gunter*	5,926	643	4
23	spring 2023	NOAA aircraft Twin Otter	14,402	1,036	565
23	spring 2023	NOAA ship *Gordon Gunter*	5,061	445	7

* Mammal and turtle sighting counts include duplicates and resightings.

For an informal description of life on a shipboard abundance survey see Kannan (2020) and the webstores and blogs for teachers-at-sea and abundance survey observers (Table 3-2).

4.2.2 Process Habitat Data

We improved and updated the contemporaneous habitat environmental data that we used as potential covariates in the density-habitat species models (**Table 4-2**). We described the details of how we processed the static, satellite-derived, and ocean model habitat data in Section 10.2.

Table 4-2. Habitat covariates used in the 2010 – 2023 density-habitat models

Covariate Abbreviation	Description	Resolution
SST	SST multi-scale ultra-high resolution	1 km mapped to 2 km
SSTF	Strength of SST fronts	1 km mapped to 2 km
CHLA	Chlorophyll-a concentration	1 km mapped to 2 km
CHLF	Strength of chlorophyll fronts	1 km mapped to 2 km
PIC	Particulate inorganic carbon	1 km mapped to 2 km
POC	Particulate organic carbon	1 km mapped to 2 km
PP	Primary productivity	1 km mapped to 2 km
SLA	Sea Surface Height Anomaly	1/4°
MLD	Mixed layer depth	1/12°
MLP	Mixed layer thickness	1/12°
SALINITY	Surface salinity	1/12°
BTEMP	Bottom temperature	1/12°
DGSNW	Distance to the Gulf Stream north wall	meters
DGSSW	Distance to the Gulf Stream south wall	meters
Depth	Depth	3 arc-sec
Dist2shore	Distance to coastline	0.04°
Slope	Seafloor slope	3 arc-sec
Dist200	Distance to the 200 m isobath/contour	meters
Dist125	Distance to the 125 m isobath/contour	meters
Dist1000	Distance to the 1000 m isobath/contour	meters
Lat	Latitude	

4.2.3 Process Passive Acoustic Data

We deployed passive acoustic towed hydrophone arrays during shipboard abundance surveys in 2013, 2016, and 2021 (referred to as HB1303, HB1603, and HB2102, respectively) to collect vocalizations of cetaceans. We analyzed these data using the PAMGuard software (various versions throughout the years). For sperm whales, the data were decimated to a 96 kHz sample rate, and a customized sperm whale click detector searched for impulsive clicks between 2 and 20 kHz (Westell et al. 2022). For beaked whales, this involved running a click detector searching for frequency-modulated clicks between 16 and 90 kHz (DeAngelis et al. 2017). Specific detection parameters can be found in the AMAPPS II Final Report (Palka et al. 2021). For members of the Kogiidae family, a click detector searched for narrow-band high frequency clicks within the 100 - 150 kHz range. We separated incoming sperm whale, beaked whale, and Kogiidae click trains into “tracks” of individuals by aggregating signals received along a similar change in bearing. We identified beaked whale species by the spectral properties and inter-click-intervals of

clicks (e.g., Baumann-Pickering et al. 2013). At present, we cannot reliably distinguish between *Kogia sima* and *K. breviceps* clicks, thus both species are grouped into a joint "Kogia" class. Reviewing towed array data for Kogia events is time consuming because of their ephemeral presence; thus, we created a semi-automated method to reduce analyst review time. We ran all sperm, beaked whale, and Kogia tracks (hereafter referred to as "events") through PAMGuard's Target Motion Analysis module to estimate the latitude and longitude position of the echolocating submerged animal. For sperm, beaked whale, and Kogia events in which there were not enough clicks to estimate the position, or if we detected the animals during a ship's turn, we instead used the latitude and longitude of the ship's position at the start of the event.

Using the multipath arrival of a deep diver's foraging click, we can estimate the depth of each click produced by a sperm or beaked whale (DeAngelis et al. 2017; Westell et al. 2022). See more details on this method in Section 6.2. We have not tried this method on Kogia events due to the brevity of the event's tracks. We then used the depth of the click to estimate the horizontal perpendicular distance of the foraging animal that we used in standard line transect analysis methods (Sections 4.9 - 4.11).

We adapted the PAMGuard processing of Delphinidae acoustic data due to the limited understanding of how acoustic classifications link to specific behaviors in this family, unlike with sperm, beaked, and Kogia whales. To assign species identification to a delphinid acoustic event, we cross-referenced the towed array data with corresponding visual sighting data. This process, detailed in Section 4.5.2, is a step toward developing a multi-species delphinid classifier.

During each abundance survey, the acoustic technician recorded the state of the EK60 in real-time as "passive" or "active". For the HB1303 and HB1603 cruises, we altered the state on a daily scale. For HB2102, we alternated the EK60 state on a spatial scale, where the shelf break even numbered tracklines were in active mode, and the odd numbered tracklines were in passive mode. For the longer offshore tracklines, we altered the EK60 state temporally to better distribute active acoustic effort (see the HB2102 cruise report for details; NEFSC and SEFSC 2022). We assigned each sperm and beaked whale event and ship trackline an EK60 state of "active" or "passive" based on the real-time effort log maintained by the acoustic technician. With the duty-cycling of the EK60 across the three survey years, we covered the entire survey area by both EK60 states (**Figure 4-1**).

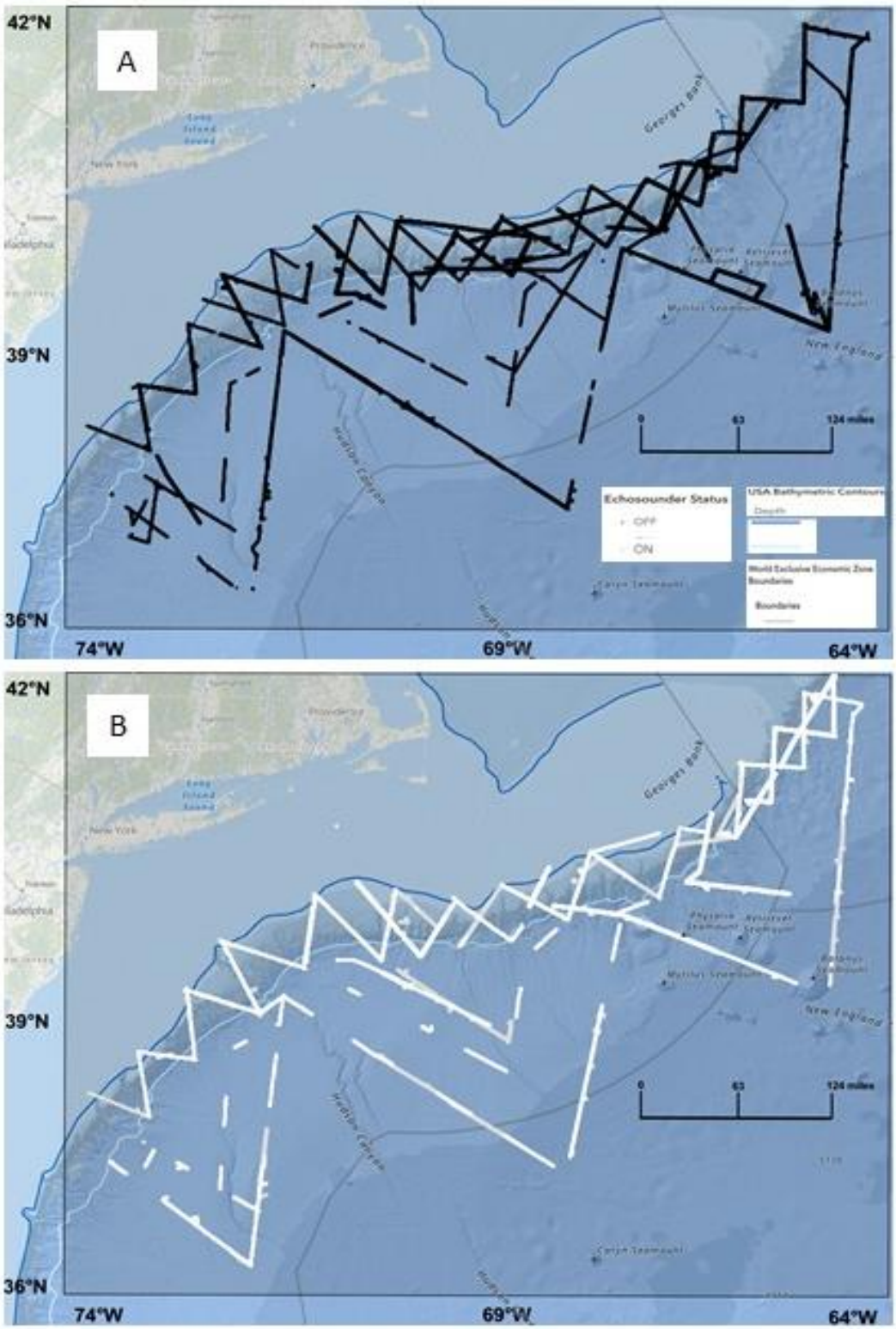

Figure 4-1. HB1303, HB1603, and HB2102 tracklines by EK60 state
When EK60 echosounders were in passive mode “off” (A) and when in actively transmitting “on” (B).

4.3 Availability Bias Correction Factors

To estimate the total abundance (N) of cetaceans and turtles, including those both at and below the ocean's surface, we adjusted the estimated at-surface abundance (N_s), which we obtained from visual line transect data, with an availability bias correction factor (a): $N = N_s/a$. We defined the correction factor as the average probability of an animal being at the surface and available for detection. For cetacean species, we estimated the species-specific availability bias correction factors (**Table 4-3**) using a two-state continuous Markov process as described in Laake et al. (1997) and further explained in Palka et al. (2021).

Table 4-3. Availability bias correction factors from Palka et al. (2017)
The – indicates not applicable. Scientific names are in Appendix A.

Species	Aerial Correction Factor	CV of Aerial Correction Factor	Shipboard Correction Factor	CV of Shipboard Correction Factor
Atlantic white-sided dolphin	0.944	0.116	1	-
Common bottlenose dolphin	0.785	0.364	1	-
Cuvier's beaked whale	0.157	0.451	0.748	0.257
Fin whale	0.368	0.331	1	-
Harbor porpoise	0.628	0.299	1	-
Humpback whale	0.649	0.185	1	-
Long/short finned pilot whale	0.629	0.270	1	-
Minke whale	0.307	0.397	1	-
Risso's dolphin	0.858	0.161	1	-
Sei whale	0.410	0.536	1	-
Common dolphin	0.930	0.138	1	-
Sperm whale	0.145	0.005	0.613	0.247
Striped dolphin	1.000	-	1	-
Pygmy/dwarf sperm whale	-	-	0.539	0.307

We equipped loggerhead (*Caretta caretta*) and leatherback (*Dermochelys coriacea*) sea turtles within the AMAPPS study area with satellite-linked transmitters (Chapter 7). These transmitters reported location and the proportion of time a turtle spent within specific depth bins that we used to estimate availability bias correction factors. AMAPPS researchers and collaborators equipped 245 loggerhead turtles during 2009-2018 with data loggers that recorded location, average dive duration and average surface duration. Hatch et al. (2022) used these data to construct spatiotemporal regression models of the average dive and surface time, resulting in monthly spatially-specific (20 km x 20 km grid cells) average dive and surface times (Section 7.4). We then used these modeled spatially-explicit monthly average dive and surface times within the two-state continuous Markov process (Laake et al. 1997) to produce monthly 20x20 km grid cell-specific estimates of the availability bias correction factor. However, because some of the AMAPPS line transect data fell outside the Hatch et al. (2022) study area, we developed a generalized additive model to estimate the correction factor for sightings outside the Hatch et al. (2022) study area (Chavez-Rosales et al. in review). This model integrated AMAPPS loggerhead sightings with oceanographic covariates and availability data from Hatch et al. (2022). We assume that environmental factors influenced the dive/surface patterns of the species, thus, allowing us to estimate availability for sightings outside the Hatch et al. (2022) study area.

For leatherback turtles that we tagged off Massachusetts and North Carolina, we used the inverse of the proportion of time the leatherbacks spent within the top two meters (Rider et al. 2022; Section 7.4) to estimate monthly averaged availability bias corrections factors (**Table 4-4**).

Table 4-4. Average monthly availability bias correction factor for leatherback sea turtles

Month	Correction factor	CV
Jan	0.78	1.35
Feb	0.62	0.80
Mar	0.57	0.88
Apr	0.69	1.17
May	0.53	0.80
Jun	0.70	0.75
Jul	0.79	0.86
Aug	0.86	1.00
Sep	0.93	1.64
Oct	0.91	2.09
Nov	0.91	2.03
Dec	0.83	1.54

For green (*Chelonia mydas*) and Kemp's ridley (*Lepidochelys kempii*) turtles, we utilized estimates derived from turtles tagged in the Gulf of America, as calculated by Roberts et al. (2022; **Table 4-5**).

Table 4-5. Estimates of availability bias correction factors for green and Kemp's ridley turtles
Source: Roberts et al. (2022)

Species	Spring	Summer	Fall	Winter
Green	0.17 (CV=1.23)	0.35 (CV=0.6)	0.20 (CV=0.91)	0.14 (CV=1.2)
Kemp's ridley	0.16 (CV=1.25)	0.14 (CV=1.28)	0.20 (CV=1.43)	0.15 (CV=1.53)

4.4 Separate Ambiguous Species Identification of Visual Sightings

In the field, during the AMAPPS shipboard and aerial abundance surveys, we were not able to identify some sightings (defined as single individuals or groups) to the species level. So, we labeled them with the lowest possible species identification. During the analyses of the visual data, to minimize bias in the absolute abundance estimates for a target species, the analysis incorporated data from two sighting categories: those identified specifically to the target species and those identified to an ambiguous species group that included the target species.

Commonly confused species that were grouped in ambiguous identifications included:

- Fin (*Balaenoptera physalus*) and sei (*Balaenoptera borealis*) whales
- Atlantic spotted dolphin (*Stenella frontalis*) and common bottlenose dolphin (*Tursiops truncatus*)
- Atlantic white-sided dolphin (*Lagenorhynchus acutus*) and short-beaked common dolphin (*Delphinus delphis*)
- Short-finned (*Globicephala macrorhynchus*) and long-finned (*G. melas*) pilot whales
- Tamanend's bottlenose (*Tursiops erebennus*) and common bottlenose dolphins
- Beaked whales
- Hard-shelled sea turtles

Sightings ambiguously identified as "unidentified whale" or "unidentified dolphin" were excluded from the analysis.

For the design-based analyses (Section 4.6), we used a common method to incorporate data from ambiguous sightings. This involved estimating the abundance of a target species as the sum of two components: the abundance derived from unambiguously identified target species, and a proportion of the abundance from ambiguous sightings that could potentially be the target species. For example, the

abundance of Atlantic spotted dolphins was the sum of the abundance derived from the positively identified sightings of Atlantic spotted dolphins plus a proportion of abundance derived from the sighting labeled as ambiguous Atlantic spotted/common bottlenose dolphins (Palka 2023).

For the model-based analyses (Sections 4.7 and 4.8), we developed an improved method to assign ambiguous sightings to an unambiguous species id that was then used to develop the density-habitat models (**Table 4-6**). First, we developed models that identify key environmental variables linked to the locations and times of unambiguous species sightings. This allowed us to apply the environmental "signature" of the modeled unambiguous species to ambiguous sightings to predict the individual species identification of the ambiguous sightings. We then combined the data from the newly assigned sightings with the data from the unambiguous sightings, and estimated abundance using standard methods.

For the model-based analyses (Sections 4.7 and 4.8), we implemented an enhanced approach for assigning ambiguous sightings to a specific species identification, which we then used to develop the density-habitat models (**Table 4-6**). Our first step was to model the relationship between key environmental variables and the locations and times of unambiguous species sightings. We explored several different statistical modeling techniques. This modeling established an environmental "signature" for each unambiguous species, which we then applied to the ambiguous sightings to predict the individual species identity. We then combined the newly classified data with the original unambiguous sightings, allowing us to estimate abundance using established standard methods.

Table 4-6. Methods used to assign species identifications to ambiguous sightings

Ambiguous species group	Statistical Method used to Assign Species Ids	Environmental Variables in Model	Reference
Fin or sei whale	Binomial logistic regression based on sighting locations	Sea surface temperature, Distance to the shore, Primary productivity	Palka et al. 2017
Large-finned or short-finned pilot whales	Binomial logistic regression based upon a genetic analysis of tissues	Sea surface temperature, Latitude	Garrison and Rosel 2017
Loggerhead, green, Kemp's ridley, or other hardshell turtles	Hierarchical clustering and principal components analysis based on sighting locations	Distance to the North and South Gulf Stream wall, Latitude, Bottom temperature, Depth, Distance to the coast, Distances to the 1000, 200 and 125 m isobaths	Chavez-Rosales et al. in review and section 4.4.2
Tamanend's bottlenose dolphins or common bottlenose dolphin	Binomial logistic regression based upon a genetic analysis of tissues	Depth, Latitude, Depth*Latitude	Garrison and Aichinger Dias 2024
Beaked whales	Discriminant analysis based on locations of passive acoustically detected beaked whales	Chlorophyll concentration, Chlorophyll front intensity, Primary productivity	This paper section 4.4.1

4.4.1 Beaked Whales

Visual line-transect shipboard surveys often struggled to identify beaked whale sightings to the species level due to their cryptic nature and brief surface times. However, a simultaneous passive acoustic monitoring towed hydrophone array yielded a larger sample of positively identified beaked whale species. This was attributed to the whales' long dive times and the distinct species-specific calls captured by the hydrophone array (Baumann-Pickering et al. 2013). To utilize these acoustic identifications, a discriminant analysis function, developed using habitat variables to classify the acoustic detections, was applied to the ambiguous visual sightings of beaked whales to classify them to the species level.

4.4.1.1 Methods

We considered multiple concurrent habitat covariates in a discriminant analysis, conducted using the lda function from the MASS package in r (version 1.5.2; Chang 2024) with the passive acoustic detections classified to a known single species that we collected during 11 separate cruises from 2013 through 2021 (**Table 4-7**). To assign covariates to the known species of the acoustic beaked whale detections, we first assigned the acoustic detections to the AMAPPS grid cells and 8-day time intervals using the date, latitude and longitude of each detection. We then utilized the full suite of AMAPPS spatiotemporal-specific habitat covariates (**Table 4-2**) to develop the discriminant analysis function. In addition, we explored covariates available from the Environmental Research Division's Data Access Program (ERDDAP) website (https://www.ncei.noaa.gov/erddap/) since DeAngelis et al. (2025) used ERDDAP variables in a random forest analysis to classify acoustic detections of beaked whales into different habitat guilds. To assign ERDDAP covariates to the acoustic detections we used the R package PAMPal (v. 0.19.1, Sakai 2023). We initially attempted to use the same covariates that DeAngelis et al. (2025) demonstrated were important; however, some covariates were unavailable for this dataset that encompassed more recent years. The final covariates we included from ERDDAPP website were sst_mean, analysed_sst_mean, mean_sst_mean and standard_deviation_mean and we gathered them from the jplMURSST41 data set (daily resolution, https://www.ghrsst.org).

Many acoustic detections were categorized as True's/Gervais' because True's and Gervais' beaked whales have similar vocalization patterns that can be hard to distinguish if few clicks are detected (DeAngelis et al. 2018). Reliable differentiation of these two species requires cruise data to be analyzed post-cruise, when inter-click-interval information can be estimated. To date, post-processing of the towed array datasets for beaked whales has occurred for data collected from 2013-2017, and 2021. Data collected from the 2018 and 2019 beaked whale surveys have not been post-processed, thus classification was left at the True's/Gervais' level. To separate the acoustic detections into either a True's or Gevais' beaked whale, we applied the discriminant analysis function to the True's/Gervais' category. To accomplish this step, we first separated the True's/Gervais' detections into a test dataset and the positively identified True's and Gervais' passive acoustic detections into a training dataset. We applied a discriminant analysis to this training dataset and used the resulting function to assign all True's/Gervais' detections into either the True's or the Gervais' category. This step substantially increased the sample size of both True's and Gervais' in our dataset of species-specific acoustic detections.

We next applied the discriminant analysis function to our expanded dataset of species identified acoustic detections and used the resulting function to assign visual sightings to species' categories. As a comparison of the discriminant analysis function to the visual observers we first used the discriminant analysis function to classify positively identified visual sightings. Finally, we applied the discriminant analysis function to the unknown visual sightings and assigned a species identification. We then combined these assigned ambiguous visual sightings with the known visual sightings to perform the density surface modelling described in Section 4.6.

4.4.1.2 Results

Goose-beaked beaked whales were the most common species in the acoustic data and Sowerby's were the least common (**Table 4-8**). A total of 472 acoustic detections were initially categorized as True's/Gervais'. Of these, 455 were subsequently assigned to True's and 17 to Gervais', reflecting a high classification rate for this group, demonstrating high confidence in the discriminant analysis function to classify these detections into specific species groups (**Table 4-9**). The ordination plot demonstrated clear discrimination between the two species along the first linear discriminant axis (**Figure 4-2**). However, when the model was applied to the full expanded dataset, the overall classification accuracy decreased (**Table 4-10**). The discriminant analysis function had the highest classification success with Blainville's

(**Table 4-10**) and lowest with Sowerby's. The ordination plot revealed substantial overlap among Sowerby's, True's, and Goose-beaked whales (**Figure 4-3**). The linear discriminant coefficients indicated that chlorophyll concentration, chlorophyll front intensity, and primary productivity were among the most influential environmental covariates driving species separation.

A total of 391 ambiguous visual sightings were classified to species using the discriminant analysis model. The majority were assigned to Goose-beaked whales, while the fewest were assigned to Sowerby's beaked whales (**Table 4-11**). Posterior probabilities of classification success were highest for Blainville's and lowest for True's beaked whales (**Table 4-11**).

Table 4-7. Cruises with acoustic beaked whale detections used in the discriminant analysis

Cruise	Date	Number of Acoustic Detections
GU1304	6/16/13 – 9/15/13	17
GU1402	3/12/14 – 4/27/14	3
GU1605	7/1/16 – 8/24/16	263
GU1803	7/21/18 – 8/1/18	693*
HB1303	7/2/13 – 8/18/13	192
HB1403	7/25/14 – 7/30/14	28
HB1503	6/10/15 – 7/1/15	54
HB1603	6/28/16 – 8/24/16	217
HB2102	6/17/21 – 8/20/21	62
HRS1701	9/8/17 – 9/17/17	240
HRS1910	8/18/19 – 8/27/19	39*

* Denotes datasets in which only real-time analysis exists; thus, they may overrepresent the number of events (individuals) and also have high autocorrelation as the same groups of beaked whales were tracked over multiple days

Table 4-8. Summary of numbers of passive acoustic detections
For the original data (True's/Gervais' not separated) and the expanded dataset (True's/Gervais' separated into species using the discriminant analysis classification)

Species	Original Number of Detections	Expanded Number of Detections
Blainville's	48	48
Goose-beaked	994	994
Gervais'	81	98
Sowerby's	18	18
True's	194	649
True's/Gervais'	472	0

Table 4-9. Classification table applied to the Gervais' and True's beaked whale acoustic detections
Classification success rate=99.3%.

Observed	Predicted Gervais'	Predicted True's
Gervais'	80	1
True's	1	193

Table 4-10. Classification table applied to the expanded dataset
Classification success rate=57.3%.

Observed	Predicted Gervais'	Predicted True's	Predicted Cuvier's	Predicted Blainville's	Predicted Sowerby's
Gervais'	71	1	29	12	0

Observed	Predicted Gervais'	Predicted True's	Predicted Cuvier's	Predicted Blainville's	Predicted Sowerby's
True's	3	297	264	0	2
Goose-beaked	16	347	671	0	12
Blainville's	8	0	9	36	0
Sowerby's	0	4	21	0	4

Table 4-11. Numbers of ambiguous visual sightings assigned to a species
Using the discriminant analysis function.

Species	Number Assigned (%)	Mean Posterior Probability (range)
Gervais'	111 (28.4)	0.94 (0.49 – 1.00)
True's	50 (12.8)	0.57 (0.47 – 0.82)
Goose-beaked	169 (43.2)	0.64 (0.39 – 0.97)
Blainville's	28 (7.2)	0.96 (0.60 – 1.00)
Sowerby's	33 (8.4)	0.78 (0.40 – 1.00)

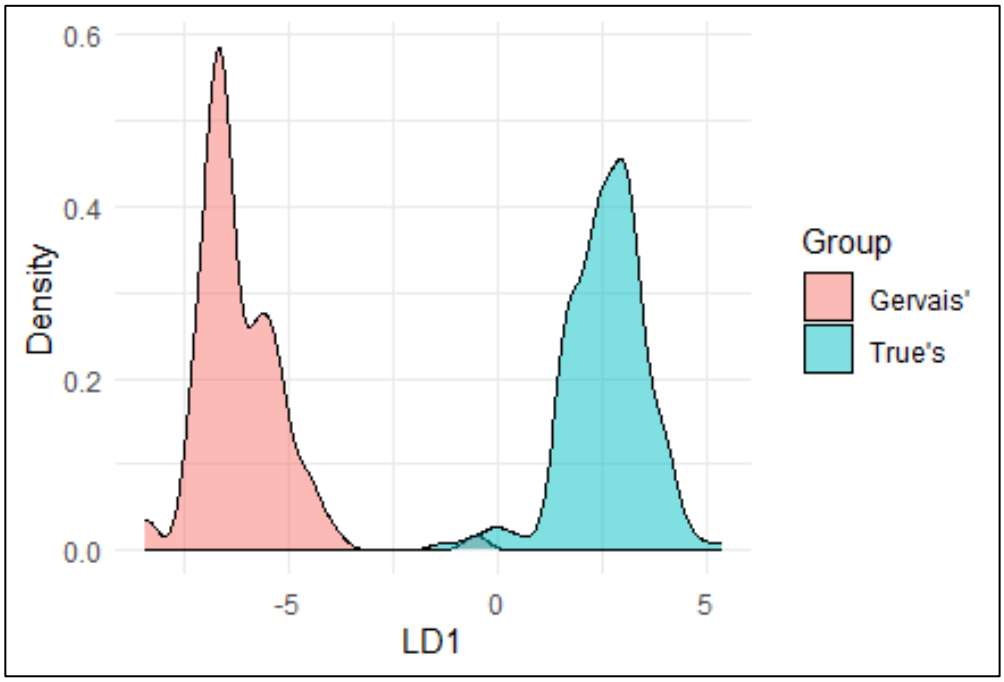

Figure 4-2. Ordination plot of True's and Gervais' beaked whale acoustic detections
Derived from only the positively identified species.

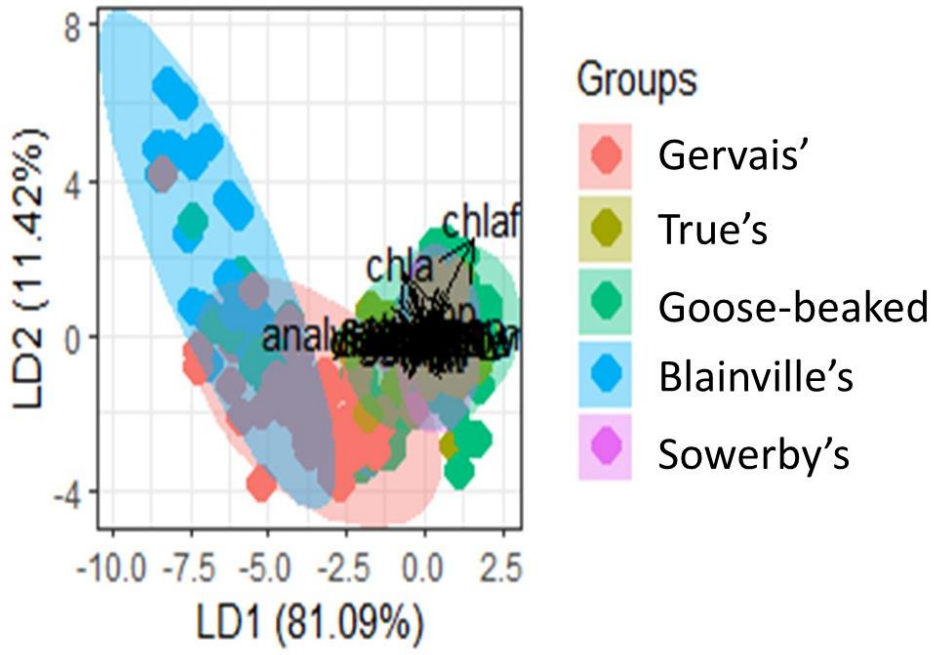

Figure 4-3.Ordination plot of acoustic beaked whale's detections
Relative to concurrent habitat covariates

4.4.1.3 Discussion

Previously DeAngelis et al. (2025) reported some habitat segregation among beaked whale species in the western North Atlantic. Building on this, we augmented our AMAPPS dataset with ERDDAP variables, as suggested by DeAngelis et al. (2025). Our initial results indicate a modest improvement in classification accuracy with the inclusion of ERDDAP-derived covariates. Consistent with DeAngelis et al. (2025), chlorophyll concentration and chlorophyll front intensity were significant predictors of habitat segregation among beaked whale species.

Discriminant analysis effectively differentiated between species, though considerable overlap was observed, particularly with goose-beaked whales. This overlap is likely due to the broad distribution of goose-beaked whales in offshore waters that they share with other beaked whale species (MacLeod et al., 2005). Within these overlapping regions, the model allocates species assignments proportionally based on their relative frequencies.

When conducting discriminant analyses, prorating species based on the sample sizes of positively identified sightings is a standard method. While discriminant analysis is a valid approach for species classification, its effectiveness diminishes when species share similar habitat preferences. Future research could explore additional variables, such as day/night cycles or behavioral cues, to potentially improve the categorization of beaked whale species.

Overall, the passive acoustic data were useful in characterizing habitat differences among vocalizing beaked whale species. These habitat differences were then useful in classifying the ambiguous visual sightings of beaked whales to a single species. However, there are still important caveats in the acoustic data that need further consideration as they may bias the results from the discriminant analysis. Most notably are two factors that affect the chances of recording a vocalizing beaked whale: the differential

effects of the presence or absence of the ship's echosounder and the differential distances for which we can detect a click due to species-specific frequency of the clicks. That is, the echosounder appears to affect beaked whale behavior; thus, we have a smaller chance of detecting beaked whales when the echosounder is on (Cholewiak et al. 2017 and Section 6.7). In addition, we know lower frequency clicks travel further than higher frequency clicks, and there are some habitat properties that will further exaggerate this; thus, we have a smaller chance to detect species using higher frequency clicks. Future analyses could compare results using data collected when the echosounder is on versus when the echosounder is off. Integrating the detection probability into a discriminant analyses would be challenging but an important advancement to derive unbiased characterization of habitat utilization and increase the efficacy of discriminant functions to accurately classify unknown visual sightings of beaked whales into their correct species categories.

4.4.2 Hardshell Turtles

Due to their cryptic nature, small size, and brief surface times, identifying hardshell turtles to the species level during visual line transect aerial surveys often proved challenging. Consequently, we had to categorize many aerial sightings as "unidentified hardshell turtles". To address this issue for abundance estimates, we employed a hierarchical clustering and principal components analysis (Chavez-Rosales et al. in review), utilizing confirmed species sightings and their associated environmental covariates.

In this analysis, we used 6,327 positively confirmed loggerhead aerial sightings to identify three clusters: 3,408 sightings in the first, 2,822 in the second, and 97 in the third. The first two clusters distinguished by nine environmental covariates, included distance to the North and South Gulf Stream walls, latitude, bottom temperature, bottom depth, and distance to the coast and the 100, 200, and 125 m isobaths. About 40% of the turtle sightings were classified as an unidentified hardshell turtle. Of these unidentified hardshell turtle sightings, about 80% of their associated environmental values aligning with the first two clusters and thus were predicted to be loggerheads. These were then combined with positively identified loggerheads for abundance estimation (Section 4.7).

We subsequently differentiated the remaining unidentified hardshell turtle sightings, not allocated to loggerheads, into green and Kemp's ridley turtles using a hierarchical clustering and principal component model developed from positively identified green and Kemp's ridley turtles. This model assigned 778 unidentified hardshell sightings to green turtles and 346 to Kemp's ridleys. However, there were still 84 unidentified hardshell sightings that we could not assign using this two-step procedure; thus, they we excluded them from abundance estimates.

4.5 Acoustic Classifiers to Assign Species to Acoustic Clicks

Section 4.4.1 describes how passive acoustic array detections were utilized to help resolve ambiguous species identifications for animals observed visually. We intend to apply this methodology to other uncertain visual sightings; however, this requires establishing high-confidence species identifications for the acoustic data first. This section details our work in identifying acoustic detections for delphinids and Kogiidae.

4.5.1 Kogiidae

Kogiidae family members are known for their very high-frequency, narrow-bandwidth clicks (Merkens et al. 2018; Cohen et al. 2022). These clicks differ significantly from the clicks made by sperm whales and members of the Delphiniidae family, as well as the frequency-modulated pulses produced by members of the Ziphiidae family (Morisaka and Connor 2007). Due to their high frequency, Kogiidae clicks experience rapid attenuation, resulting in a shorter detection range compared to other species.

Consequently, during shipboard abundance surveys, which we typically conduct at speeds of about 10 knots, the detection window for Kogiidae clicks is extremely short, lasting less than one minute (Palka et al. 2021).

In previous AMAPPS analyses, the acoustic presence of Kogiidae required a manual review process. This manual review consumed a month of analyst time per abundance survey (Palka et al. 2021). To address this, we developed an acoustic classifier during AMAPPS III to automatically detect Kogiidae clicks, thereby reducing the time needed for analyst review.

The towed array we used during HB2102 contained HTI-96-Min hydrophones that collected the passive acoustic data. When building a classifier, it is preferable to remain within the same hydrophone make and model, as different models and manufacturers have different sensitivities and recording characteristics. In AMAPPS II, the shipboard abundance survey HB1603 and ITS.DEEP survey GU1803 used the same hydrophone make and model as HB2102. We have manually reviewed these two surveys for the presence of Kogiidae (Palka et al. 2021). Thus, they provide a foundation for developing and testing a classifier, as well as establishing a more efficient analyst workflow compared to manual browsing.

4.5.1.1 Methods

From the HB2102 and GU1803 surveys, we selected a representative Kogiidae click as the template for a matched click template classifier. This came from the GU1803 Leg 1 dataset. Then we used the rest of Leg 1 to train the classifier, and GU1803 Leg 2 and all of HB1603 to test the click classifier. Additionally, we tested the robustness of the classifier by applying the classifier on data collected from a drifting acoustic recorder that we already manually reviewed for Kogiidae clicks. This drifting acoustic recorder contained similar hydrophone specifications as those used in the towed arrays.

Within the program PAMGuard is a Matched Template Classifier that uses a representative click as input for a match, along with a reject template (**Figure 4-4**). We used the Kogiidae click from GU1803 Leg 1 as the match, and a standard delphinid impulsive click that comes with the Matched Template Classifier module within PAMGuard as the reject template. We set the Fast Fourier Transform length to 512 samples, and we tested various thresholds to obtain optimal performance. Optimal in this case meant that at least 1 click from every manually annotated Kogiidae event was classified.

Once we found a suitable threshold, we processed the entire dataset using the Matched Template Classifier and then imported into R using the package PAMPal (Sakai 2025). From there, custom R scripts aggregated Matched Template Classifier classified clicks into PAMGuard "events". These had to meet the criteria of a Matched Template Classifier score > 0.5, and contain at least 2 Matched Template Classifier labeled clicks that were within 20 s apart. We set events to be no longer than 60 s (as it is highly unlikely that it would be the same group given prior results from the manual analyses). The R script then exported each potential Kogiidae event into the PAMGuard database that an analyst reviewed within PAMGuard. We calculated precision and recall scores for each of the five datasets to understand the overall method's performance. We defined precision as the number of true Kogiidae events divided by the sum of the number of true Kogiidae events and the number of false labeled Kogiidae events. We defined recall as the number of true Kogiidae events divided by the sum of the number of true Kogiidae events and the number of Kogiidae events that the method missed.

4.5.1.2 Results and Discussion

Within PAMGuard, we determined a Matched Template Classifier threshold of 0.4 provided the optimal performance. After generating the PAMGuard events to review, we found that most of them were false positives, with few false negatives (**Table 4-12**). This led to high recall scores > 87% and low precision scores (≤25%). The highest number of false positive events to review was 147 events for HB1603 Leg 2.

This equated to about 10 min of analyst review time. As this is much less than the one month of manual review, we deemed the Matched Template Classifier method was suitable to use the HB2102 dataset. HB2102 Leg 1 had a total of 24 false positives, and no events that contained characteristics of Kogiidae clicks. HB2102 Leg 2 had a total of 11 false positive events, and also no Kogiidae events. This resulted in no Kogiidae being acoustically detected for HB2102.

As a validation step, we processed the recordings within the AMAPPS study area from a drifting recorder with the Matched Template Classifier method. The recorder contained 33.6 hrs of audio data that we manually reviewed and found one Kogiidae event. The Matched Template Classifier successfully identified the Kogiidae event, with few false positives, again leading to a high recall score and low precision (**Table 4-12**).

Most of the false positives from the towed array datasets were the same currently unknown source click type (**Figure 4-5**). When using this click type as the reject template, overall method performance decreased. Future work could explore alternative approaches for incorporating this additional click type as a reject class to reduce the number of false positives requiring analyst review.

Table 4-12. Performance of the Matched Template Classifier method across datasets
We consider the manually annotated events as the "truth". We calculated precision and recall scores from the number of true positive, false positive, and false negative events created from the Matched Template Classifier method.

Dataset	Number of Manual Events	True Positive Events	False Positive Events	False Negative Events	Precision	Recall (%)
GU1803 Leg 1	4	4	36	0	10	100
GU1803 Leg 2	7	7	21	1	25	87.5
HB1603 Leg 1	1	1	110	0	>1	100
HB1603 Leg 2	6	6	147	0	3.9	100
Drifting recorder	1	1	4	0	20	100

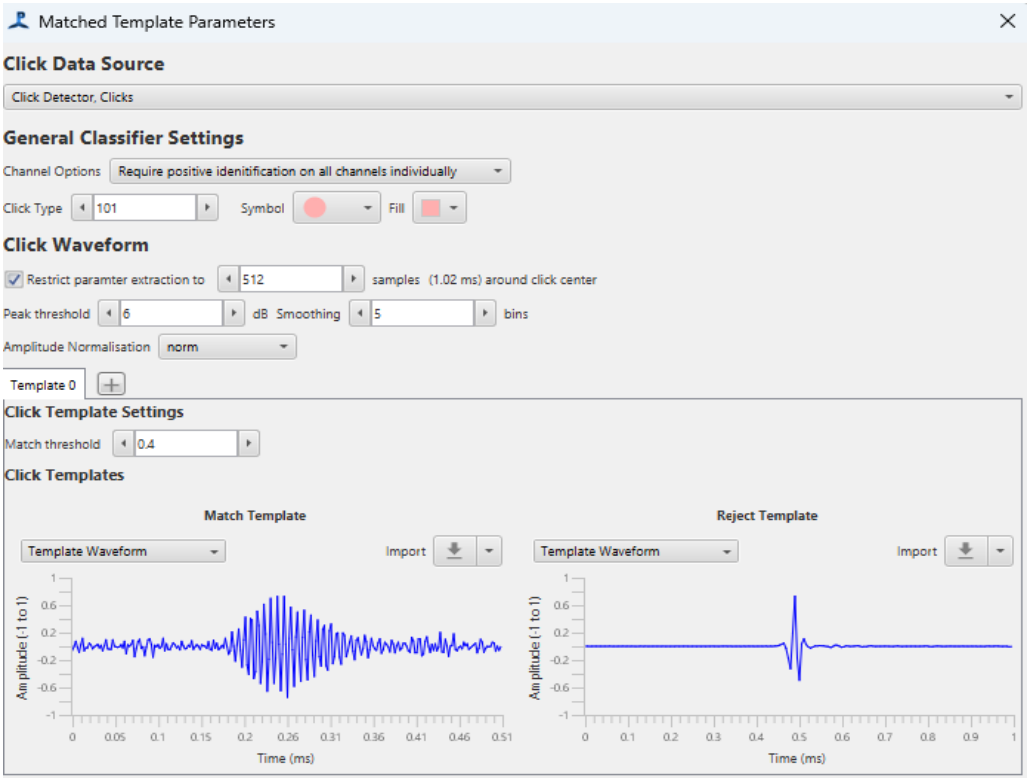

Figure 4-4. Matched Template Classifier settings within PAMGuard
The match template Kogiidae click's waveform is on the left, and the reject template on the right, which is a generic delphinid impulsive click. Also shown are the settings used in the Matched Template Classifier.

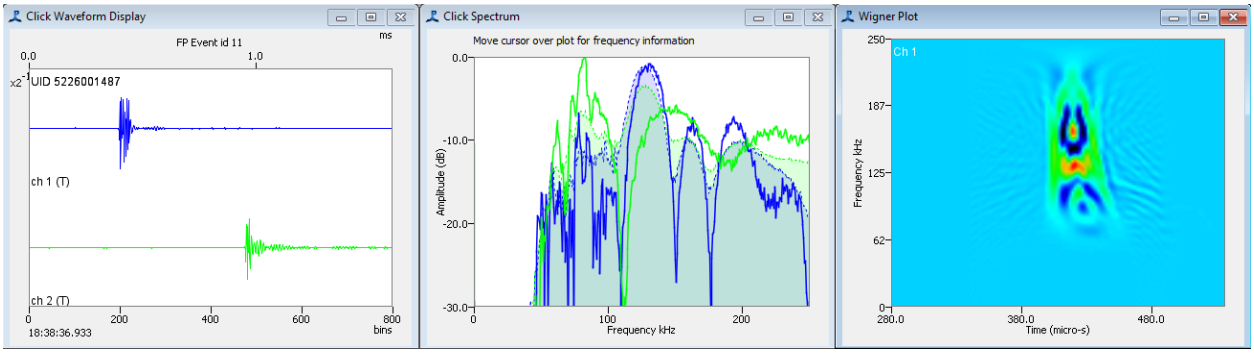

Figure 4-5. Waveform, power spectrum, and Wigner-ville plot of a common Kogiidae false positive

4.5.2 Delphinids

Delphinid passive acoustic classification to a species level is notoriously difficult because of the diverse repertoire between and within species, especially in areas that host a diverse group of overlapping species (e.g. Cohen et al. 2022, Palka et al. 2021). McCullough et al. (2021) and Zahn et al. (2021) made advancements in single species, and binary classification systems in areas less diverse than our study area. The waters off the East Coast of the United States contains a diverse number of delphinid species, with at

least three species of blackfish[1] and at least seven smaller delphinids, that co-occur frequently. Given this context, we aimed to evaluate whether a multi-species passive acoustic classifier could be effectively applied to the AMAPPS dataset. The multi-species classifier BANTER seems promising as it has a holistic approach to classification, being able to take as inputs the full delphinid repertoire of whistles, clicks and burst pulses (Rankin et al. 2017). Additionally, this classification system can also function as a binary classifier, depending on the number of species within a study area (e.g., McCullough et al. 2021. Zahn et al. 2021).

4.5.2.1 Methods

We utilized data collected from the HB1603 and HB2102 NEFSC shipboard abundance surveys. We used two different hydrophone arrays in these surveys, but they were both of the HTI-96-Min model. We used PAMGuard to run several whistle and moan detectors, a cepstrum detector for the burst pulses, and a click detector with a suite of click classifications (Keating and Barlow 2013). We used the HB1603 survey's 192 kHz data stream and the HB2102 survey 500 kHz data stream. This led to slightly different signal processing parameters, where the whistle and moan detector had a smaller fast Fast Fourier Transform size (thus more frequency bins) for the 2016 dataset than the 2021 dataset (93.75 s for 2016 and 122.07 s for 2021). The click detector also had different sample rates, which meant that the last click classifier's frequency search range extended to 125 kHz as opposed to 96 kHz, which should not affect delphinid classification as most of their click energy spans 20 - 80 kHz (Cohen et al. 2022).

As a first step, an acoustic analyst reviewed the passive acoustic monitoring data in PAMGuard to identify time periods (encounters) containing a single species. We used the criteria set developed by McCullough et al. (2021), which included reviewing concurrent visual sightings data to find time periods where visual observers detected only one delphinid species that was 18.5 min between different species sightings. Then, within PAMGuard, the analyst would localize the incoming acoustic signals to confirm that the encounter was indeed of a single species by using a combination of the Target Motion Analysis module for clicks with an overlay of whistle bearings.

We then brought all single species encounters into R using the PAMPal package, which formatted the data for use within the BANTER package (Sakai 2025; Rankin et al. 2017). Within BANTER, the analyst configured which species to select by setting a threshold for the number of encounters to include. The analyst also configured how many trees to use to assess how stable the model was. BANTER then exported a confusion matrix to evaluate the model performance, the distribution of what each species was classified as by using the percent of votes the trees assigned each encounter, and a proximity plot showing the acoustic similarity/dissimilarity of the input species.

4.5.2.2 Results and Discussion

Table 4-13 lists the delphinid species that were in either of the HB2102 and HB1603 datasets. We added sperm whales as another species class due to their prevalence in both datasets. We conducted multiple model-runs where we adjusted the number of trees and the encounter threshold to improve model performance. Atlantic spotted dolphins achieved the highest correct classification percentage, 83%, where the number of trees was 25,000, the encounter threshold was five, and we excluded sperm whales, false killer whales, spinner dolphins, and Clymene dolphins. The confidence intervals for the correct classification percentage for this species and the other species were large, indicating that the model is still unstable. At this time, we attribute the poor model performance to small sample sizes, as other multi-class

[1] Blackfish is an informal term used for several larger darker delphinids that lack a prominent, elongated beak: long-finned and short-finned pilot whales, killer whales, pymgy killer whales, false killer whales, melon-headed whales, and Risso's dolphins.

species classifiers also performed poorly on this dataset (e.g., DelphinID). Machine learning models such as random forests are notorious for being data hungry thus these results are not surprising. Future work could look into using BANTER in a binary approach (e.g., Zahn et al. 2021) while we collect more data to boost the sample size.

Table 4-13. Numbers of confirmed single species encounters in the HB1603 and HB2102 datasets
Species scientific names are in Appendix A.

Species	HB1603 Sample Size	HB2102 Sample Size	Total Sample Size
Sperm whale	5	0	5
Pilot whale sp.	5	4	9
False killer whale	1	2	3
Common dolphin	6	3	9
Risso's dolphin	4	3	7
Offshore bottlenose dolphin	2	15	17
Stripe dolphin	8	11	19
Atlantic spotted dolphin	1	5	6
Spinner dolphin	0	1	1
Clymene dolphin	0	1	1

4.6 Design-Based Abundance Estimates of 2021 Surveys

During the AMAPPS III period, we utilized design-based methods to analyze data from the summer 2021 U.S. Atlantic coastwise shipboard and aircraft line transect abundance surveys (Garrison and Aichinger Dias 2023; 2024; Palka 2023). We subsequently published the resulting abundance estimates in the Atlantic Marine Mammal Stock Assessment Report (Hayes et al. 2024) to update the species-specific Potential Biological Removal levels.

4.6.1 Methods

During the 2021 surveys, we collected line-transect data covering 11,238 km by ship and 15,510 km by plane (**Table 4-14**; **Figure 4-6**). To account for perception bias, Garrison and Aichinger Dias (2023; 2024) and Palka (2023) calculated abundance estimates by using a standard two-independent team mark-recapture distance sampling approach, assuming point independence (Laake and Borchers, 2004) and implemented in the R package MRDS (Laake et al. 2022). To address species-specific detectability, we modeled sighting detection functions for pooled species groups, which were specific to the survey and platform. We also incorporated factors such as weather and viewing conditions to enhance the detection function models. For deep-diving species observed during shipboard surveys (e.g., sperm whales, beaked whales, and *Kogia* spp.) and all species detected during aerial surveys, we also corrected estimates for availability bias (see Section 4-3 for details). To resolve some types of ambiguous sightings, we developed statistical separation models (see Section 4.4 for details). For other ambiguously identified sightings, we partitioned the estimated abundance among unambiguous species based on the proportions of unambiguous sightings (see Section 4.4 for details).

Table 4-14. Summary of 2021 summer abundance surveys

Region	Platform	Area (km^2)	On-effort Track length (km)	Number of Cetacean sightings	Number of Turtle Sightings
Northeast	NOAA ship *Henry B. Bigelow*	249,245	5,867	1,246	39
Northeast	NOAA Twin Otter aircraft	215,247	6,191	480	1,127
Southeast	NOAA ship *Gordon Gunter*	416,501	5,371	541	21
Southeast	NOAA Twin Otter aircraft	178,096	9,319	210	1,086
GRAND TOTAL		1,059,089	26,748	2,477	2,273

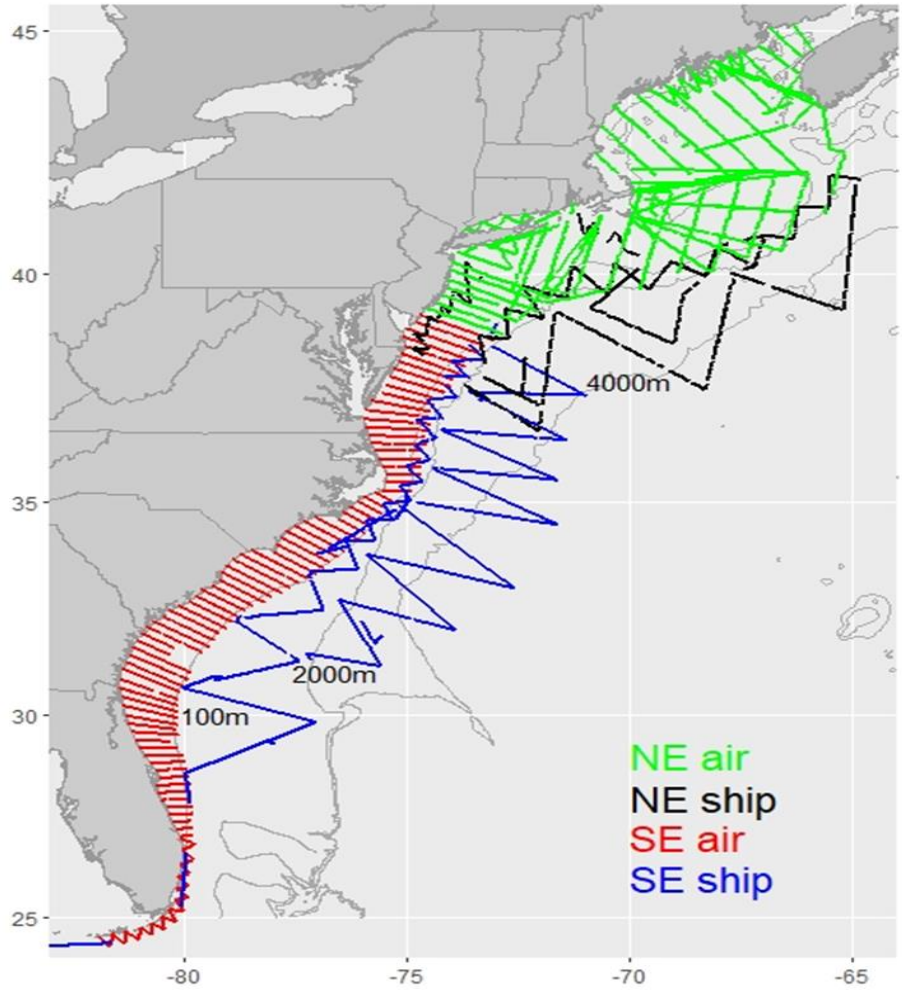

Figure 4-6. On-effort track lines during summer 2021 abundance survey using ships and planes

4.6.2 Results and Discussion

Using the shipboard and aerial survey data we estimated that there were 503,333 individuals of 32 species or species groups inhabiting the U.S. Atlantic waters (**Table 4-15**).

We used these updated abundance estimates to update the assessment of the populations relative to human-caused mortalities and injuries (Hayes et al. 2024). Of significance is these updated assessments indicate that for only two populations its estimated human-caused mortalities and injuries was larger than

its calculated Potential Biological Removal levels, which is a function of the abundance estimates. The two exceptions were the short-finned pilot whale (*Globicephala macrorhynchus*) and the Tamanend' bottlenose dolphin stock in the Northern North Carolina estuarine system (*Tursiops erebennus*).

In addition, the updated abundance estimates showed a significant decline in the Tamanend' bottlenose dolphin coastwide population occurred between the 2010-2011 period and the 2016 survey, which corresponded with a major Unusual Mortality Event caused by a morbillivirus outbreak from 2013-2015 (Garrison and Aichinger Dias 2024). The 2021 coastwide estimate suggested a partial recovery from the 2016 low of 19,471 and is consistent with estimates from years prior to the mortality event. At the individual stock level, high uncertainty in the estimates makes assessing trends difficult. The only stock with a statistically significant interannual trend was the Southern Migratory stock, which had higher abundances in the 2002-2004 period and significantly lower numbers in the following years. Most other coastal bottlenose dolphin stocks showed a decline between 2011 and 2016, followed by an increase in 2021, although these changes were not statistically significant.

Table 4-15. Design-based abundance estimates from 2021 surveys by region for each species
Scientific names are in Appendix A. – indicates an abundance of zero that does not have an estimated coefficient of variation (CV).

Species	Northeast Abundance	CV Northeast Abundance	Southeast Abundance	CV Southeast Abundance	Total Abundance	CV of Total
Atlantic spotted dolphin	8,112	0.22	23,394	0.37	31,506	0.28
Beaked whale, Blainville's	-	-	2,936	0.26	2,936	0.26
Beaked whale, Cuvier's	1,742	0.39	2,927	0.31	4,670	0.24
Beaked whale, Gervais'	-	-	8,595	0.24	8,595	0.24
Beaked whale, Sowerby's	492	0.50	-	-	492	0.50
Beaked whale, True's	4,480	0.34	-	-	4,480	0.34
Blue whale	26	1.02	-	-	26	1.02
Bottlenose dolphin, Offshore	37,721	0.34	26,866	0.34	64,587	0.24
Bottlenose, Central Florida	-	-	2,541	0.46	2,541	0.46
Bottlenose, Northern Florida	-	-	3,619	0.35	3,619	0.35
Bottlenose, South Carolina/Georgia	-	-	9,121	0.28	9,121	0.28
Bottlenose, Northern Migratory	-	-	10,244	0.50	10,244	0.50
Bottlenose, Southern Migratory	-	-	2,626	0.74	2,626	0.74
Bottlenose, Southern North Carolina	-	-	4,373	0.67	4,373	0.67
Clymene dolphin	2,268	0.50	19,510	0.80	21,778	0.72
Common dolphin	5,035	0.61	8,065	0.86	93,100	0.56
False killer whale	753	1.13	545	0.68	1,298	0.72
Fin whale	2,240	0.39	12	1.02	2,252	0.39
Harbor porpoise	85,765	0.53	-	-	85,765	0.53
Humpback whale	863	0.36	7	1.04	870	0.36
Killer whale	-	-	73	0.99	73	0.99
Kogia spp.	4,012	0.54	5,462	0.47	9,474	0.36
Minke whale	5,630	0.58	-	-	5,630	0.58
Pantropical Spotted Dolphin	-	-	2,757	0.50	2,757	0.50
Pilot whale, Long-finned	5,711	0.62	-	-	5,711	0.62
Pilot whale, Short-finned	3,722	0.67	15,004	0.38	18,726	0.33
Risso's dolphin	39,612	0.50	4,455	0.45	44,067	0.45
Sei whale	34	0.99	-	-	34	0.99
Sperm whale	3,789	0.38	2,106	0.44	5,895	0.29
Spinner dolphin	3,181	0.65	-	-	3,181	0.65
Striped dolphin	38,522	0.34	9,752	0.49	48,274	0.29
White-sided dolphin	4,632	0.55	-	-	4,632	0.55
TOTAL	338,342		164,990		503,333	

4.7 Generalized Additive Model-Based Abundance Estimates

We developed seasonal, spatially explicit density estimates by employing density surface models that incorporated habitat characteristics. Our modeling utilized two approaches: generalized additive modeling (GAM), presented here in Section 4.7, and Bayesian hierarchical analysis techniques, presented in Section 4.8. These spatiotemporal density-habitat models enabled the creation of seasonal maps and abundance estimates.

Density surface models use known locations of individuals of a species and information on environmental conditions at those locations and times to predict species distribution patterns. We used contemporaneous environmental candidate covariates that measured characteristics of the sea surface (e.g. sea surface temperature (SST) and chlorophyll-a as obtained from satellite sources), sea bottom (e.g. bottom temperature, bottom depth and slope), and water column characteristics (e.g. salinity from ocean models like HYCOM (HYbrid Coordinate Ocean Model). See Section 4.2.2 and Table 4.2 for the full list of the covariates we used.

In this current development of density surface models, our primary objective was to construct predictive frameworks potentially capable of forecasting future trends by carefully balancing bias and variance to prevent overfitting. To achieve this, we intentionally excluded certain spatiotemporal covariates, such as interactions between latitude and longitude or random effects of temporal factors like year and season. While this predictive framework is theoretically designed to generate reliable long-term predictive maps, such as seasonal averages across the 2010 - 2023 study period, it may be less effective at predicting at finer scales, such as specific monthly distributions within a single year. Consequently, our subsequent analyses will investigate more explanatory models that incorporate complex covariates, including, for example, interactions between year-8 day layers and sea surface temperature or random effects of year.

4.7.1 Methods

We created spatiotemporal density estimates and maps from the density surface models. To do this, we used visual data from shipboard and aerial line-transect surveys. We also factored in survey conditions, animal group details, static and dynamic environmental data (both spatially and temporally specific), and species-specific availability bias correction factors.

Prior to developing the density surface models, we executed steps 1-3 of the general workflow detailed at the beginning of Chapter 4, which included data collection, preparation (Section 4.2), and supportive analyses (Sections 4.3 - 4.6). Below we outline the workflow for deriving abundance estimates from density surface models, with further details provided in Palka et al. (2021) and Chavez-Rosales et al. (2019).

1) We calculated the density of marine species (or species groups) at the ocean surface for each surveyed 10x10 grid cell and 8-day time period (hereafter referred to spatiotemporal strata). We divided these spatiotemporal strata into four distinct analyses based on ship-based surveys in the northeast, aerial surveys in the northeast, ship-based surveys in the southeast, and aerial surveys in the southeast. The Northeast Fisheries Science Center (NEFSC) performed the northeast surveys, while the Southeast Fisheries Science Center (SEFSC) conducted the southeast surveys. To account for observational biases, we employed distance sampling analysis methods (Thomas et al. 2010). To address perception bias, we utilized mark-recapture distance sampling analyses of the two-team data from each platform. This involved estimating a detection function and p(0)—the probability of detecting a group directly on the transect line—by incorporating key survey parameters such as sighting conditions, group size, and animal behavior.

2) For each spatiotemporal stratum surveyed, we calculated bias-corrected density estimates. This involved applying species- and platform-specific availability bias correction factors (detailed in Section 4.3) to the ocean surface density estimates, which had already accounted for perception bias.

3) We then developed an animal density-habitat GAM model utilizing the density estimates from each spatiotemporal strata with survey effort. To select the most suitable model, we employed several goodness-of-fit tests (**Table 4-16**) to evaluate the relationship between the strata's bias-corrected density and its associated static and dynamic habitat covariates. **Figures 4-7 to 4-10** display examples of spatial maps for static covariates.

4) Next, we predicted animal density and its associated uncertainty for all spatiotemporal strata by using the modeled animal density-habitat relationship and the strata-specific values of the habitat covariates in the model. We defined the seasons as:

- Spring (1 March to 31 May)
- Summer (1 June to 31 August)
- Fall (1 September to 30 November)
- Winter (1 December to 28 (29) February), unless specified.

5) Lastly, we displayed results by plotting maps of spatially explicit densities and associated measures of uncertainty, trend lines of abundance and associated uncertainties, and we tabulated the seasonal abundance averaged over 2010 - 2023 and its associated uncertainty.

Table 4-16. Diagnostic tests and criteria used to evaluate density-habitat model performance

Test	Description	Criteria	Calculated From	Formula
DE	Percentage of deviance explained from the model	Higher value	GAM model	
R^2	Coefficient of determination from the model	Higher value	GAM model	
RHO	Spearman's rank correlation	Higher value	None-zero data. 1) Initial testing and; 2) k-fold cross-validation.	
ASPE	Mean square prediction error	Lower value	All data. 1) Initial testing and; 2) k-fold cross-validation	$\sum \frac{(observed - predicted)^2}{n}$
MAPE	Mean absolute percentage error	Lower value	None-zero data. 1) Initial testing and; 2) k-fold cross-validation	$\frac{1}{n}\sum_{i=1}^{n}\left\lvert\frac{observed - predicted}{observed}\right\rvert * 100$
MAE	Mean absolute error	Lower value	All data. 1) Initial testing and; 2) k-fold cross-validation.	$\frac{1}{n}\sum_{i=1}^{n}\lvert observed - predicted\rvert$

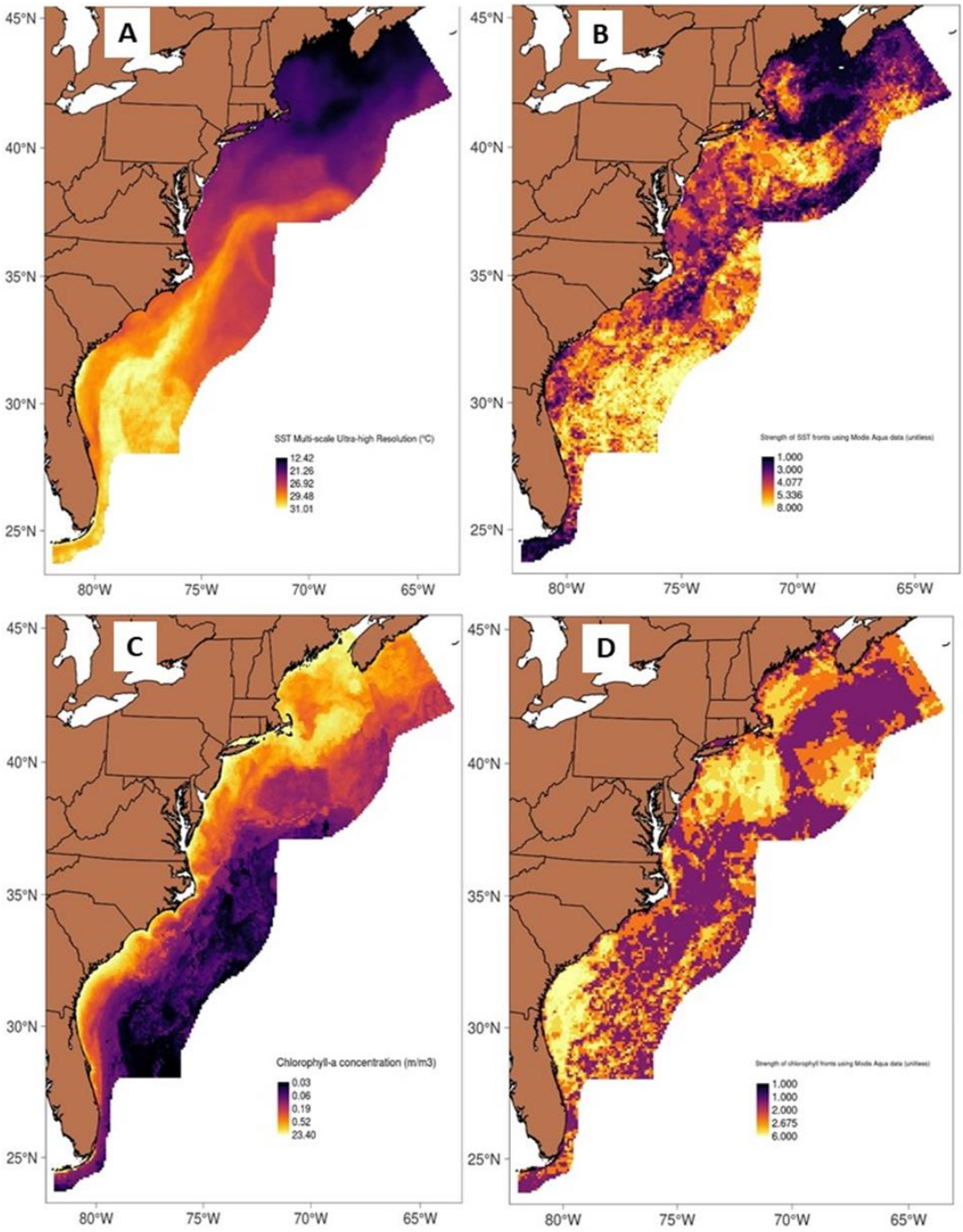

Figure 4-7. Habitat covariate maps – A) SST, B) SST fronts, C) Chlorophyll, D) chlorophyll fronts
Example of covariates from layer 25 in 2016 (4 to 11 July 2016). Abbreviations explained in Table 4-2.

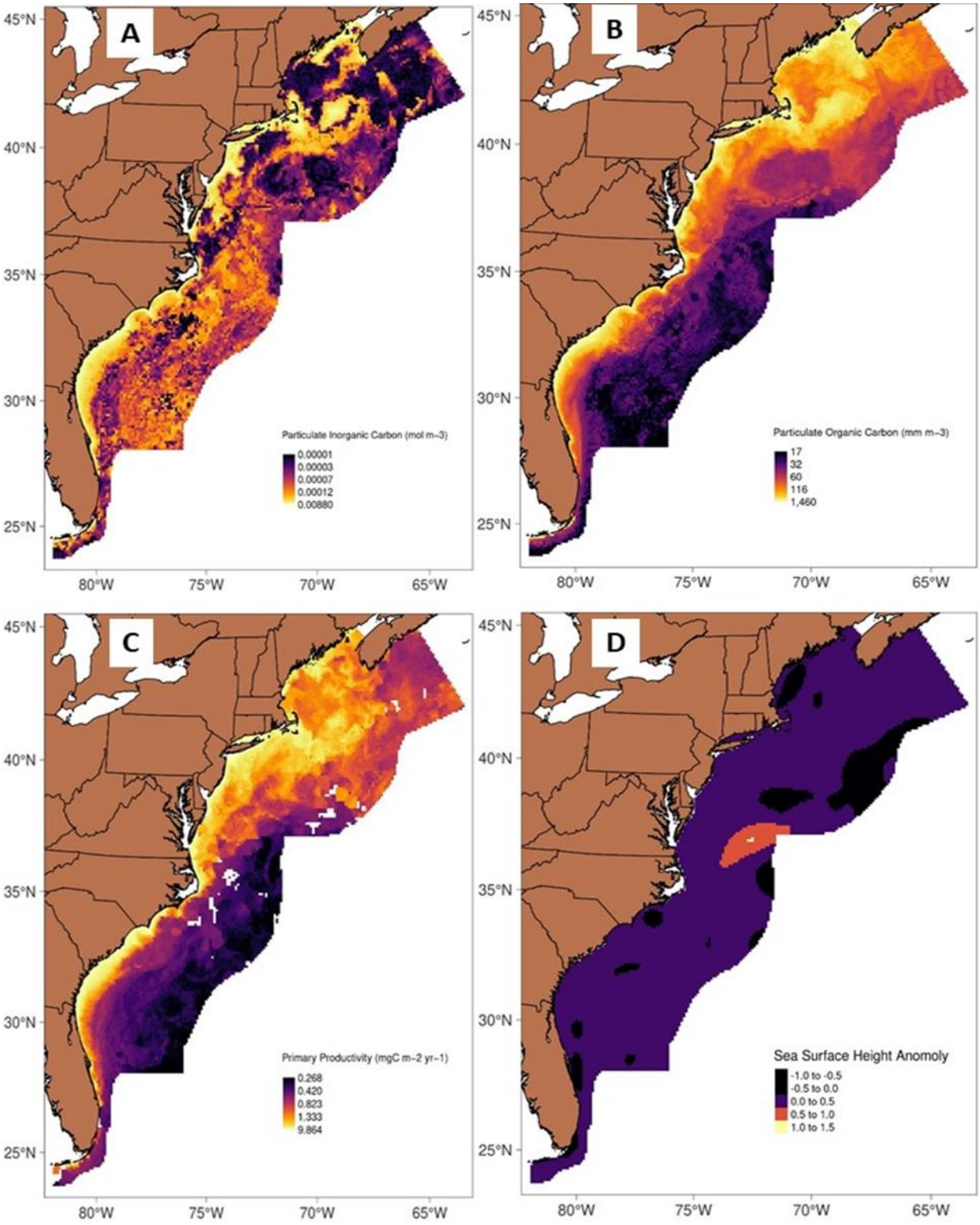

Figure 4-8. Habitat covariate maps – A) PIC, B) POC, C) PP, and D) SLA
Example of covariates from layer 25 in 2016 (4 to 11 July 2016). Abbreviations explained in Table 4-2.

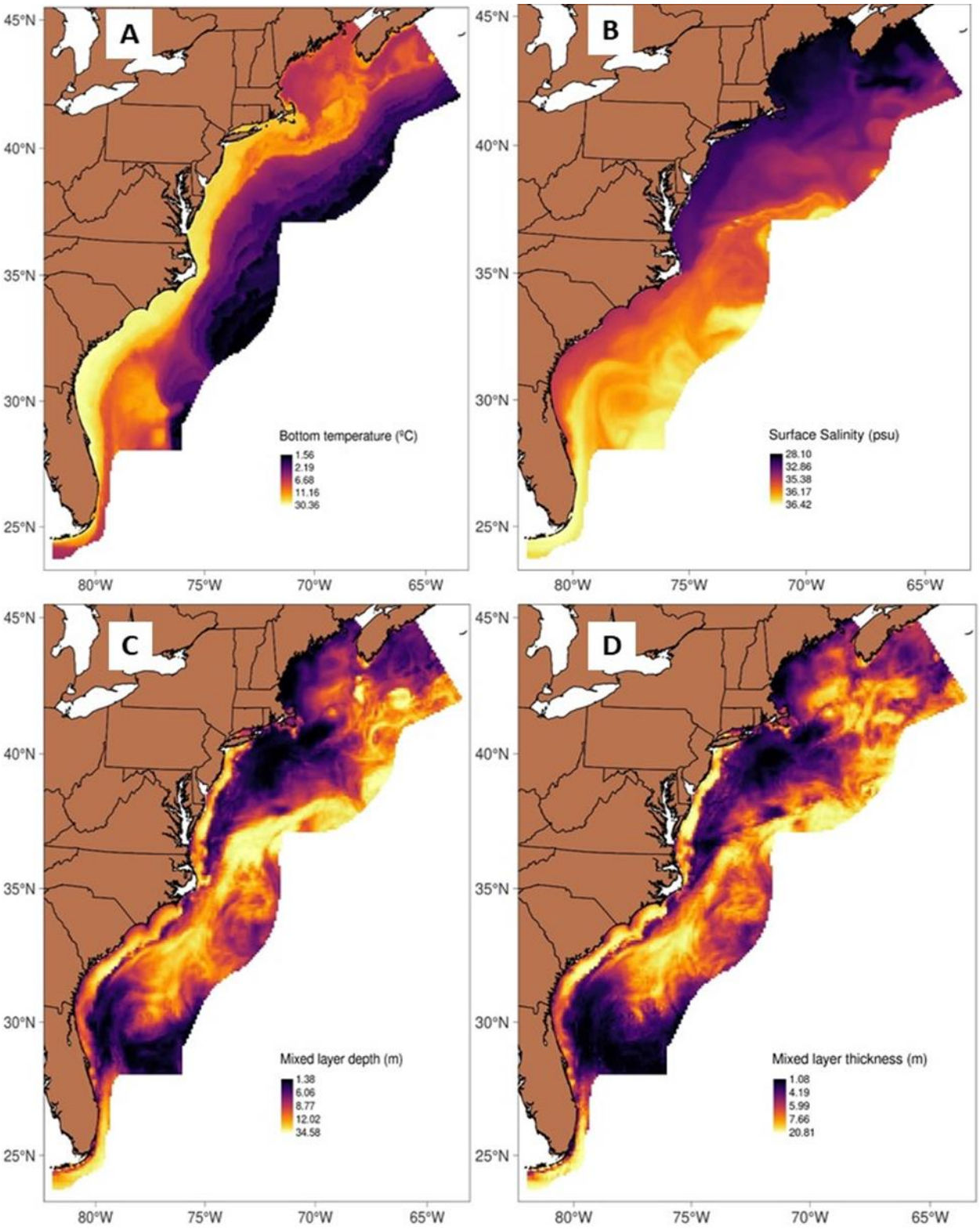

Figure 4-9. Habitat covariate maps – A) BTEMP, B) SALINITY, C) MLD, and D) MLP
Example of covariates from layer 25 in 2016 (4 to 11 July 2016). Abbreviations explained in Table 4-2.

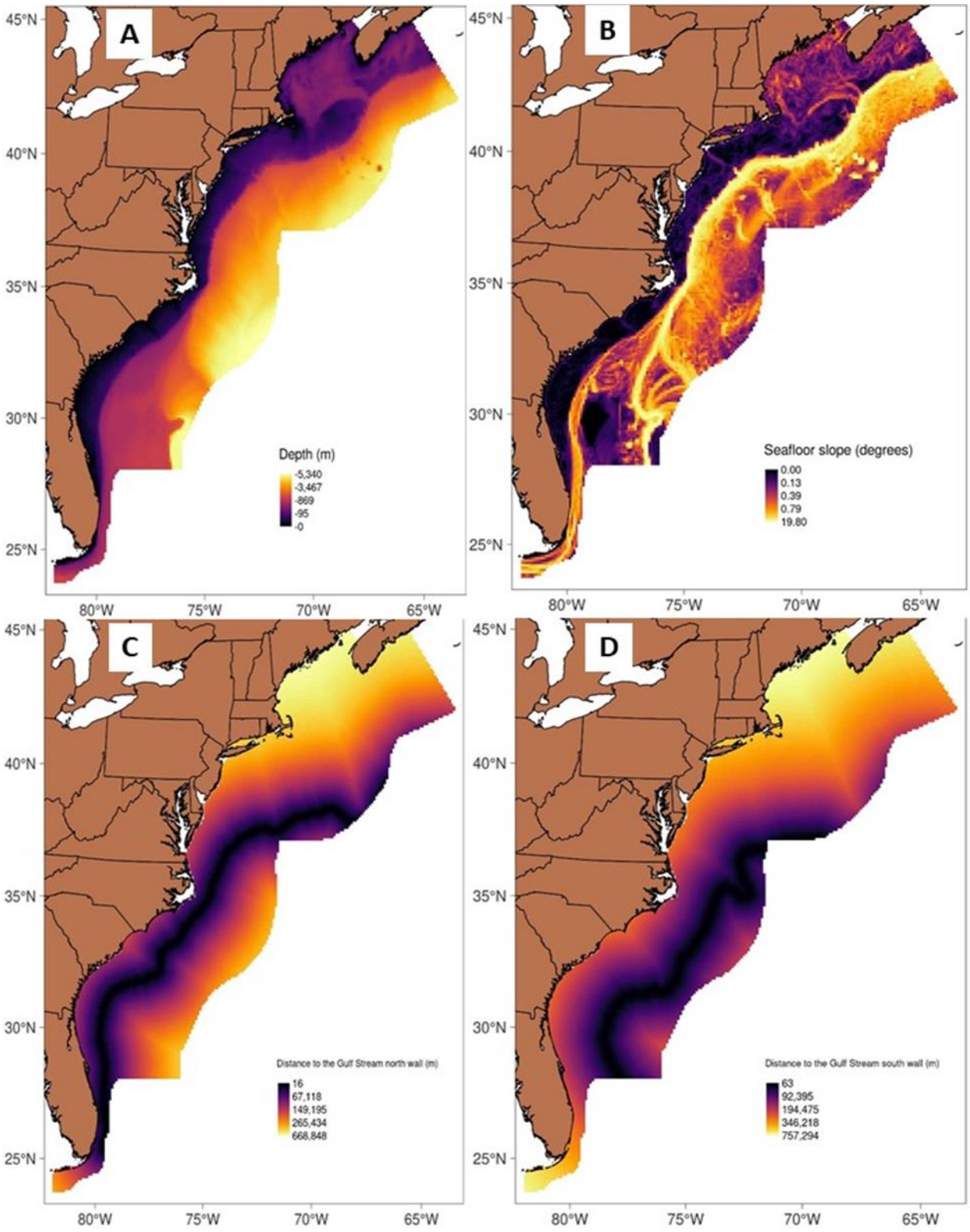

Figure 4-10. Habitat covariate maps – A) Depth, B) Slope, C) DGSNW, and D) DGSSW
Example of covariates from layer 25 in 2016 (4 to 11 July 2016). Abbreviations explained in Table 4-2.

4.7.2 Results and Discussion

We developed density surface models for marine megafauna using line-transect visual sightings data collected under AMAPPS. Specifically, we created 22 single-species models and one model for a species guild (pygmy/dwarf sperm whales) using cetacean data collected from 2010 to 2023 (Appendices B: Whales and C: Small Cetaceans). We used sea turtle data from 2010 to 2021 to develop four single-species models (Appendix D). For all species models, we incorporated data from all four seasons when available.

We did not develop density surface models for species that we sighted infrequently (e.g., Clymene's dolphins, killer whales) or for sightings broadly categorized (e.g., unidentified dolphin, unidentified whales). The distribution maps showing the locations of these rare species are presented in Appendix E. Finally, Chapter 8 discusses the seabird sightings that were collected during the AMAPPS abundance surveys.

4.7.2.1 Survey Effort

The 2010 – 2023 data we used in the density spatial models came from about 417,000 km of on-effort track lines from AMAPPS shipboard and aerial surveys (**Table 4-17** and **Figure 10-1**) that resulted in nearly 12,400 groups of cetaceans of over 145,600 individuals and over 7,710 groups of sea turtles of nearly 8,840 individuals (**Tables 4-18 and 4-19**).

Table 4-17. On-effort track line effort (km) from 2010 – 2023 by season and platform
Survey effort used in the species density models.

Platform	Spring	Summer	Fall	Winter	TOTAL
NE Shipboard	8,883	49,064	0	0	57,947
NE Aerial	38,839	52,003	87,311	24,747	202,900
SE Shipboard	2,604	18,331	2,673	302	23,910
SE Aerial	48,634	43,285	21,153	19,151	132,223
TOTAL	98,960	162,683	111,137	44,200	416,980

Table 4-18. Number of groups of species by season used in the species density models
Scientific names of species in Appendix A.

Species	Spring (Mar-May)	Summer (Jun-Aug)	Fall (Sep – Nov)	Winter (Dec - Feb)	TOTAL
Humpback whale	283	123	89	9	504
Fin whale	104	536	94	9	743
Sei whale	43	28	5	2	78
Minke whale	77	142	59	3	281
Sperm whale	76	581	20	0	677
Goose-beaked whale	29	345	9	0	383
Sowerby's beaked whale	8	62	4	2	76
Gervais' beaked whale	1	130	4	0	135
True's beaked whale	0	66	0	0	66
Pygmy or dwarf sperm whales	14	384	2	0	400

Species	Spring (Mar-May)	Summer (Jun-Aug)	Fall (Sep – Nov)	Winter (Dec - Feb)	TOTAL
Short-finned pilot whale	21	404	81	5	511
Long-finned pilot whale	54	44	23	0	121
Risso's dolphin	110	733	96	32	971
Atlantic white-sided dolphin	151	103	168	18	440
Common dolphin	508	871	570	126	2,075
Atlantic spotted dolphin	79	274	62	25	440
Striped dolphin	20	303	7	8	338
Common bottlenose dolphin	799	1,146	362	289	2,596
Harbor porpoise	519	421	541	66	1,547
TOTAL CETACEANS	2,896	6,696	2,196	594	12,382
Loggerhead turtle	1,761	2,635	1,206	652	6,254
Leatherback turtle	130	346	205	54	735
Green turtle	47	384	53	69	553
Kemp's ridley turtle	52	68	27	23	170
TOTAL TURTLES	1,990	3,433	1,491	798	7,712

Table 4-19. Number of individuals of species by season in species density models
Scientific names of species in Appendix A.

Species	Spring (Mar-May)	Summer (Jun-Aug)	Fall (Sep - Nov)	Winter (Dec - Feb)	TOTAL
Humpback whale	406	187	126	9	728
Fin whale	143	780	124	9	1,056
Sei whale	68	38	11	5	122
Minke whale	85	147	76	3	311
Sperm whale	150	1033	50	0	1,233
Goose-beaked whale	58	930	18	0	1,006
Sowerby's beaked whale	15	195	5	2	217
Gervais' beaked whale	4	323	6	0	333
True's beaked whale	0	169	0	0	169
Pygmy or dwarf sperm whales	24	477	2	0	503
Short-finned pilot whale	332	4,980	1,197	38	6,547
Long-finned pilot whale	350	452	112	0	914
Risso's dolphin	686	5,426	793	146	7,051
Atlantic white-sided dolphin	1,099	1,213	2,856	183	5,351
Common dolphin	12,892	34,706	10,502	4,414	62,514
Atlantic spotted dolphin	1,335	7,713	1,369	548	10,965
Striped dolphin	854	13,879	325	61	15,119
Common bottlenose dolphin	7,110	14,034	4,589	2,042	27,775
Harbor porpoise	716	963	1,942	100	3,721
TOTAL CETACEANS	26,327	87,645	24,103	7,560	145,635
Loggerhead turtle	2,073	3,023	1,366	786	7,248
Leatherback turtle	141	367	213	55	776
Green turtle	48	410	55	126	639
Kemp's ridley turtle	62	70	28	26	186
TOTAL TURTLES	2,324	3,870	1,662	993	8,849

4.7.2.2 Stage One

The area-platform mark-recapture distance-sampling (MRDS) models for pooled groups of cetacean and turtle species that we used to estimate perception bias-corrected densities for spatiotemporal strata with survey effort, demonstrated a good fit to the data, as confirmed by the Cramér–von Mises goodness-of-fit tests (Appendix C; **Tables 4-20 and 4-21**). Beaufort sea state and/or glare magnitude were the most frequent significant covariates in the distance sampling component of the detection functions (**Figures 4-11 to 4-14**). In the mark-recapture component models, the observer team was a significant covariate in many instances, suggesting that team or observer position influenced the shape of the detection function (**Figures 4-11 to 4-14**). Additionally, Beaufort sea state and group size were frequently significant covariates for the mark-recapture components.

Table 4-20. Results of the mark-recapture distance sampling analyses for aerial survey data
Scientific names of species in Appendix A.

Analysis Set	Truncation Distance (m) in Step 1/ Step2	Primary Team p(0)	CV[p(0)]	Cramér–von Mises p-value
NE aerial-1 (fin, sei, fin/sei whales)	500/1000	0.54	0.12	0.97
NE aerial-2 (minke, beaked whales)	380/600	0.75	0.07	0.70
NE aerial-3 (humpback, blue, right, sperm, northern bottlenose whales)	900/900	0.66	0.07	0.96
NE aerial-4 (bottlenose dolphin)	380/550	0.31	0.18	0.94
NE aerial-5 (harbor porpoise)	360/350	0.38	0.06	0.56
NE aerial-6 (Risso's dolphin)	460/600	0.49	0.12	0.91
NE aerial-7 (Pilot whales)	460/460	0.66	0.12	0.95
NE aerial-8 (white-sided and white-beaked dolphins)	400/460	0.62	0.06	0.74
NE aerial-9 (common and striped dolphins)	480/550	0.58	0.04	0.79
NE aerial-10 (loggerhead turtle)	350/450	0.60	0.05	0.95
NE aerial-11 (leatherback turtle)	350/340	0.61	0.14	0.59
SE aerial-1 (Atlantic spotted dolphin)	360/360	0.79	0.06	0.98
SE aerial-2 (Bottlenose and Clymene's dolphins)	460/460	0.86	0.02	0.78
SE aerial-3 (Common and striped dolphins)	380/380	0.85	0.04	0.89
SE aerial-4 (fin, minke, humpback, right, sperm, beaked whales)	550/550	0.86	0.07	0.89
SE aerial-5 (pilot whales, Risso's dolphin, false killer whale, rough toothed dolphin)	400/400	0.76	0.09	0.83
SE aerial-6 (loggerhead turtle)	430/300	0.60	0.01	0.61
SE aerial-7 (leatherback turtle)	350/340	0.60	0.06	0.96
SE aerial-8 (green turtle)	330/340	0.49	0.05	0.87
SE aerial-9 (Kemp's ridley turtle)	350/350	0.42	0.09	0.95

Table 4-21. Results of the mark-recapture distance sampling analyses for shipboard survey data
Scientific names of species in Appendix A.

Analysis Set	Truncation (m)	Primary Team *p(0)*	CV[*p(0)*]	CvM p-value
NE ship-1 (Atlantic spotted, Pantropical spotted dolphins)	2300	0.91	0.04	0.99
NE ship-2 (Striped dolphin)	5100	0.70	0.08	0.93
NE ship-3 (Bottlenose dolphin)	4100	0.64	0.07	0.79
NE ship-4 (Risso's dolphin, rough toothed dolphin, killer whale, false killer whale, pygmy killer whale)	4500	0.51	0.10	0.55

Analysis Set	Truncation (m)	Primary Team *p(0)*	CV[*p(0)*]	CvM p-value
NE ship-5 (Common, white-sided, Clymene's dolphins, harbor porpoise)	5000	0.39	0.14	0.55
NE ship-6 (Beaked whales, dwarf sperm and pygmy sperm whales)	3900	0.43	0.12	0.81
NE ship-7 (Pilot whales)	4000	0.67	0.09	0.92
NE ship-8 (Humpback whale)	10,000	0.39	0.17	0.92
NE ship-9 (Sperm whale)	6000	0.56	0.08	0.93
NE ship-10 (Fin, sei, minke, blue, right whales)	4500	0.54	0.08	0.95
SE ship-1 (Atlantic spotted, Pantropic spotted, striped, common, Clymene's, white-sided, spinner dolphins)	4000	0.59	0.10	0.52
SE ship-2 (bottlenose dolphin and harbor porpoise)	5000	0.56	0.12	0.73
SE ship-3 (Pilot whales, Risso's dolphin, rough toothed dolphin, false killer whale, killer whale)	5000	0.60	0.14	0.66
SE ship-4 (Beaked whales)	5000	0.35	0.26	0.91
SE ship-5 (Fin, humpback, right, sperm, Bryde, minke, killer whale, blue whale, sei whales)	9000	0.58	0.12	0.61
SE ship-6 (Dwarf and pygmy sperm whales)	3000	0.42	0.23	0.96

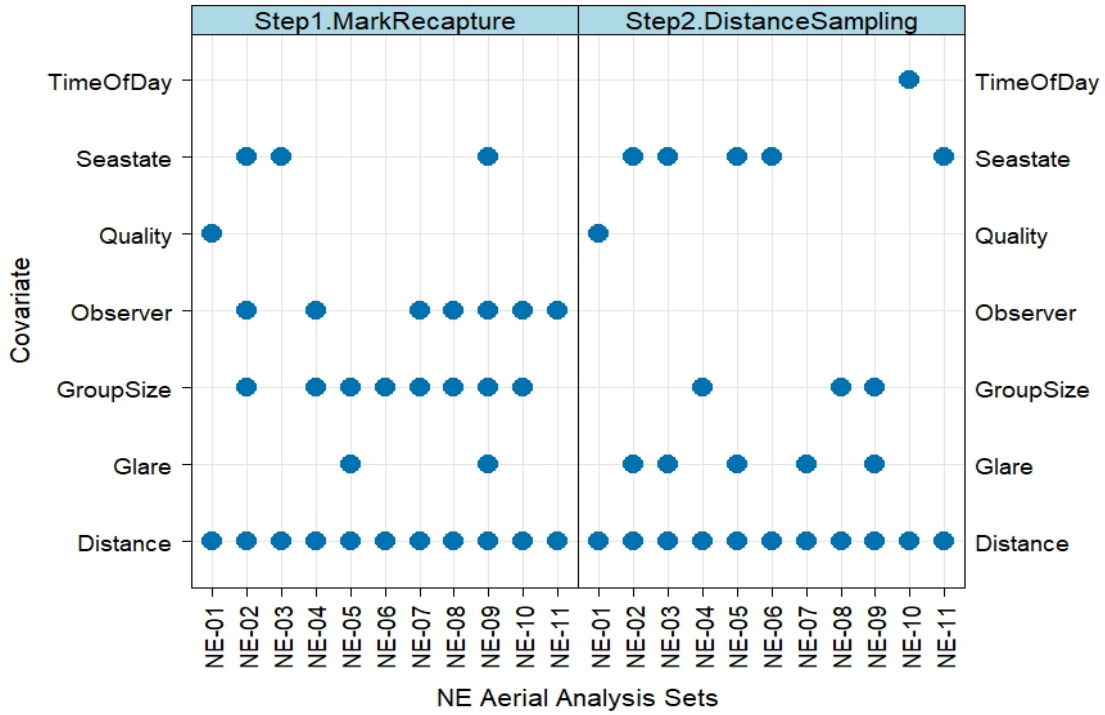

Figure 4-11. Significant covariates for Northeast (NE) aerial models

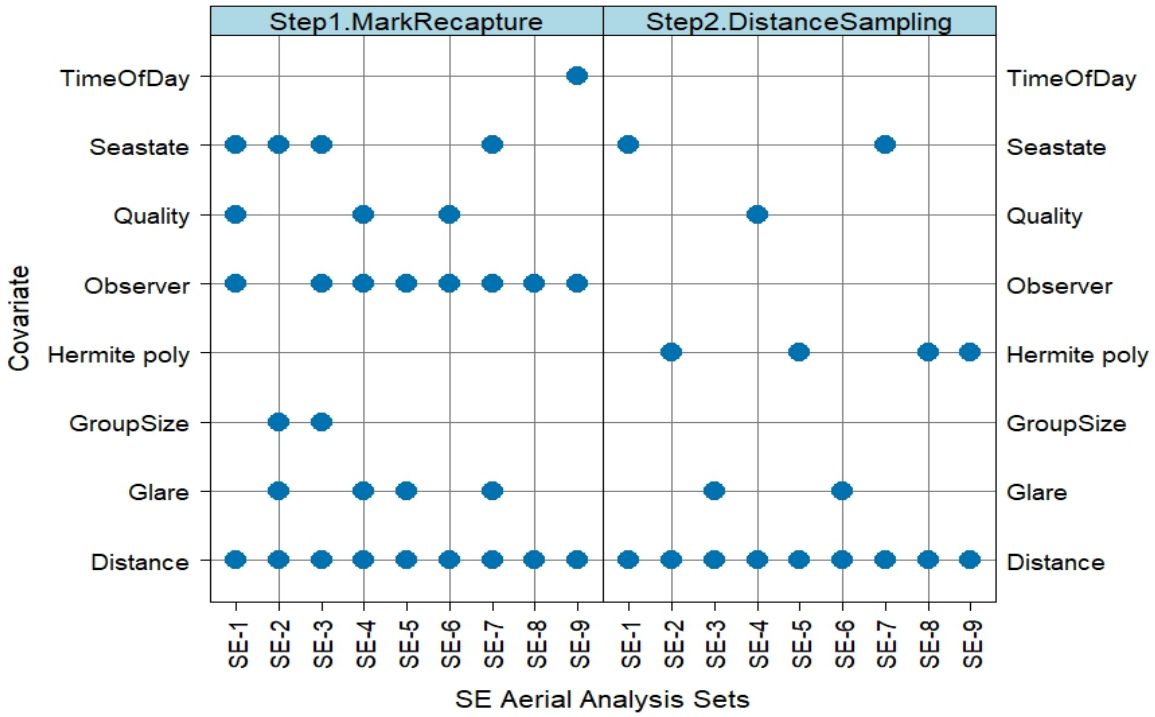

Figure 4-12. Significant covariates for Southeast (SE) aerial models

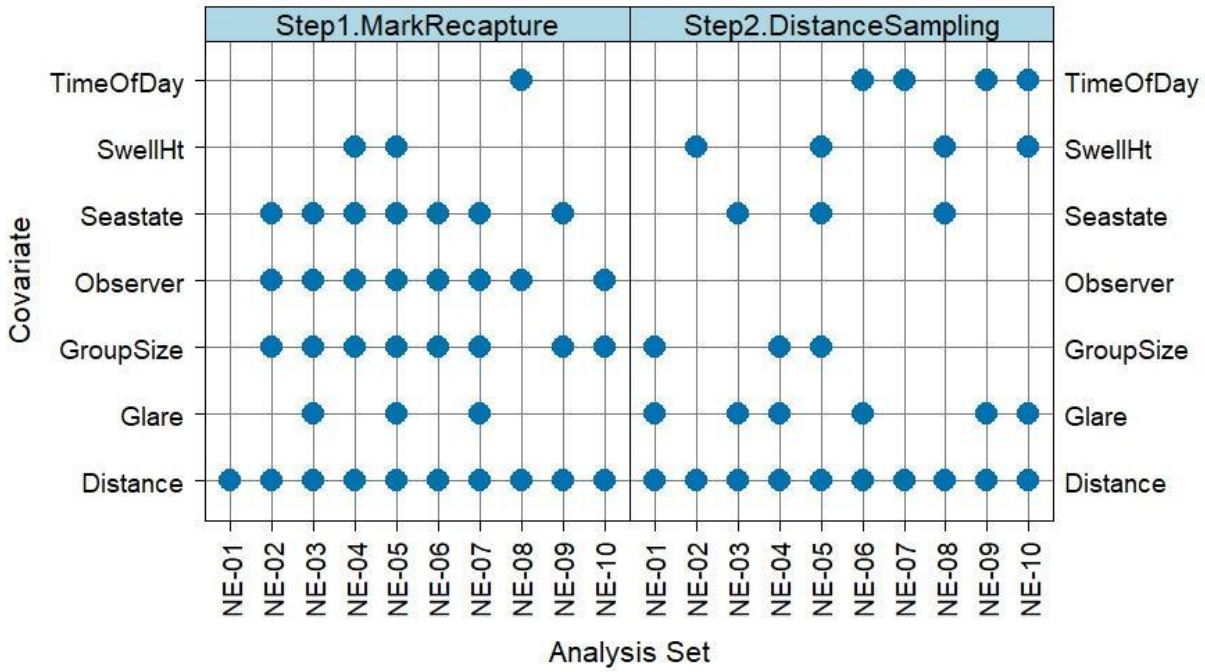

Figure 4-13. Significant covariates for Northeast (NE) shipboard cetacean models

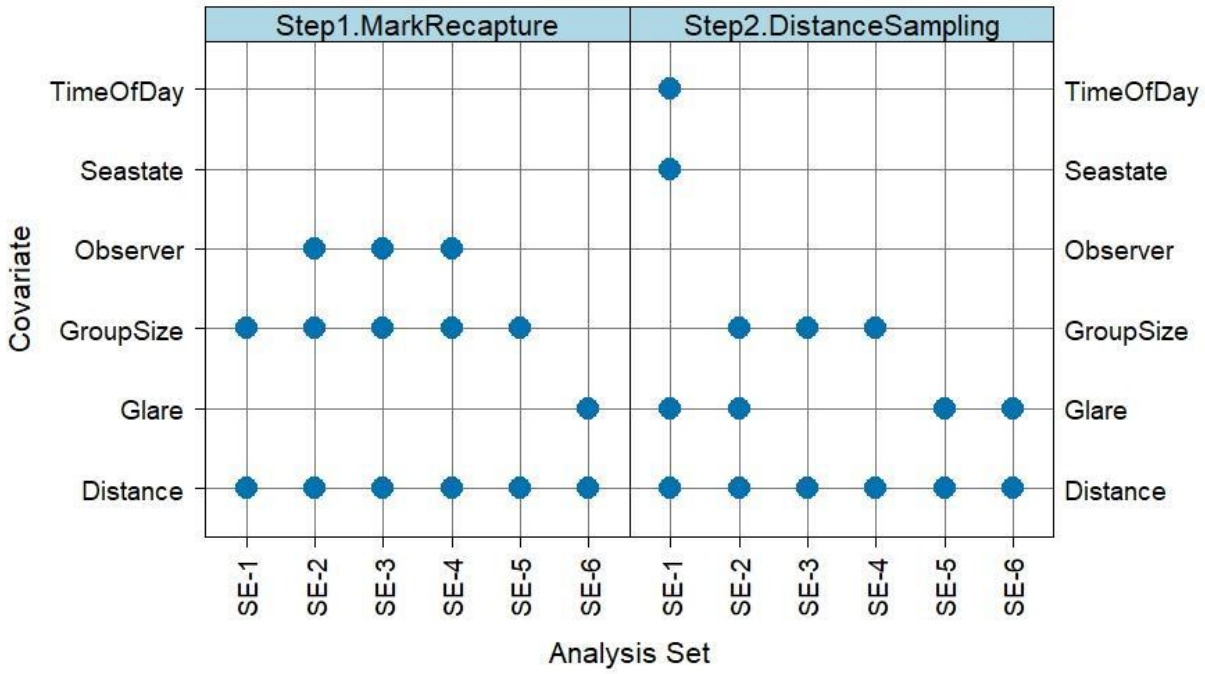

Figure 4-14. Significant covariates for Southeast (SE) shipboard cetacean models

4.7.2.3 Stage Two

The GAM models effectively predicted the relationship between density estimates (corrected for perception and availability bias) and habitat covariates, as confirmed by four diagnostic tests (**Table 4-22**). These GAM models, summarized in **Figures 4-15 - 4-17**, explained an average of 47% of the deviance, with a range from 35% for common bottlenose dolphins to 63% for Kemp's ridley turtles. The most frequently identified significant habitat covariates were latitude, bottom temperature, distance to the 1000 m isobath, mixed layer thickness and sea surface temperature (**Figure 4-18**). Conversely, chlorophyll, particulate organic, and inorganic carbon were the least frequently selected covariates. Depth was the primary explanatory covariate for whales (**Figure 4-15**), SST for dolphins (**Figure 4-16**), and latitude for turtles (**Figure 4-17**).

Table 4-22. Results of diagnostic tests to evaluate fit of density-habitat GAM models
Diagnostic tests are the Spearman's rank correlation (RHO), mean absolute percentage error (MAPE) and mean absolute error (MAE). See **Table 4-16** for more details on the tests. Scientific names of species in Appendix A.

Species	Non-Zero RHO[1]	Non-Zero MAPE	Random RHO	Random MAE
Atlantic spotted dolphin	0.447	91.39	0.123	0.014
Atlantic white-sided dolphin	0.077	89.49	0.113	0.014
Beaked whale – Gervais'	0.113	90.61	0.095	0.001
Beaked whale – Goose-beaked	0.291	90.62	0.129	0.002
Beaked whale – Sowerby's	0.399	96.90	0.058	0.0004
Beaked whale - True's	0.351	91.94	0.065	0.0004
Common dolphin	0.233	110.32	0.176	0.244
Common bottlenose dolphin	0.302	83.69	0.172	0.311
Fin whale	0.552	86.93	0.319	0.118
Harbor porpoise	0.315	83.36	0.186	0.239

Species	Non-Zero RHO[1]	Non-Zero MAPE	Random RHO	Random MAE
Humpback whale	0.451	92.70	0.088	0.006
Pygmy or dwarf sperm whale	0.219	87.33	0.115	0.001
Minke whale	0.311	76.59	0.109	0.008
Pilot whale – long finned	0.367	92.60	0.149	0.017
Pilot whale – short finned	0.296	85.50	0.130	0.024
Risso's dolphin	0.335	78.91	0.173	0.110
Sei whale	0.110	98.73	0.057	0.0002
Sperm whale	0.271	85.89	0.160	0.002
Striped dolphin	0.268	76.72	0.189	0.031
Loggerhead turtle	0.406	69.15	0.464	0.953
Leatherback turtle	0.209	91.52	0.137	0.129
Green turtle	0.301	83.05	0.213	0.217
Kemp's ridley turtle	0.676	104.02	0.493	1.000

[1] Color coding is:

RHO:	Poor= x<0.05	Fair to good =0.05<=x<0.3	Excellent= x>0.3
MAPE:	Poor= x>150%	Fair to good= 150%>=x>50%	Excellent= x<=50%
MAE:	Poor= x>1	Fair to good = 1>=x>0.25	Excellent= x<=0.25

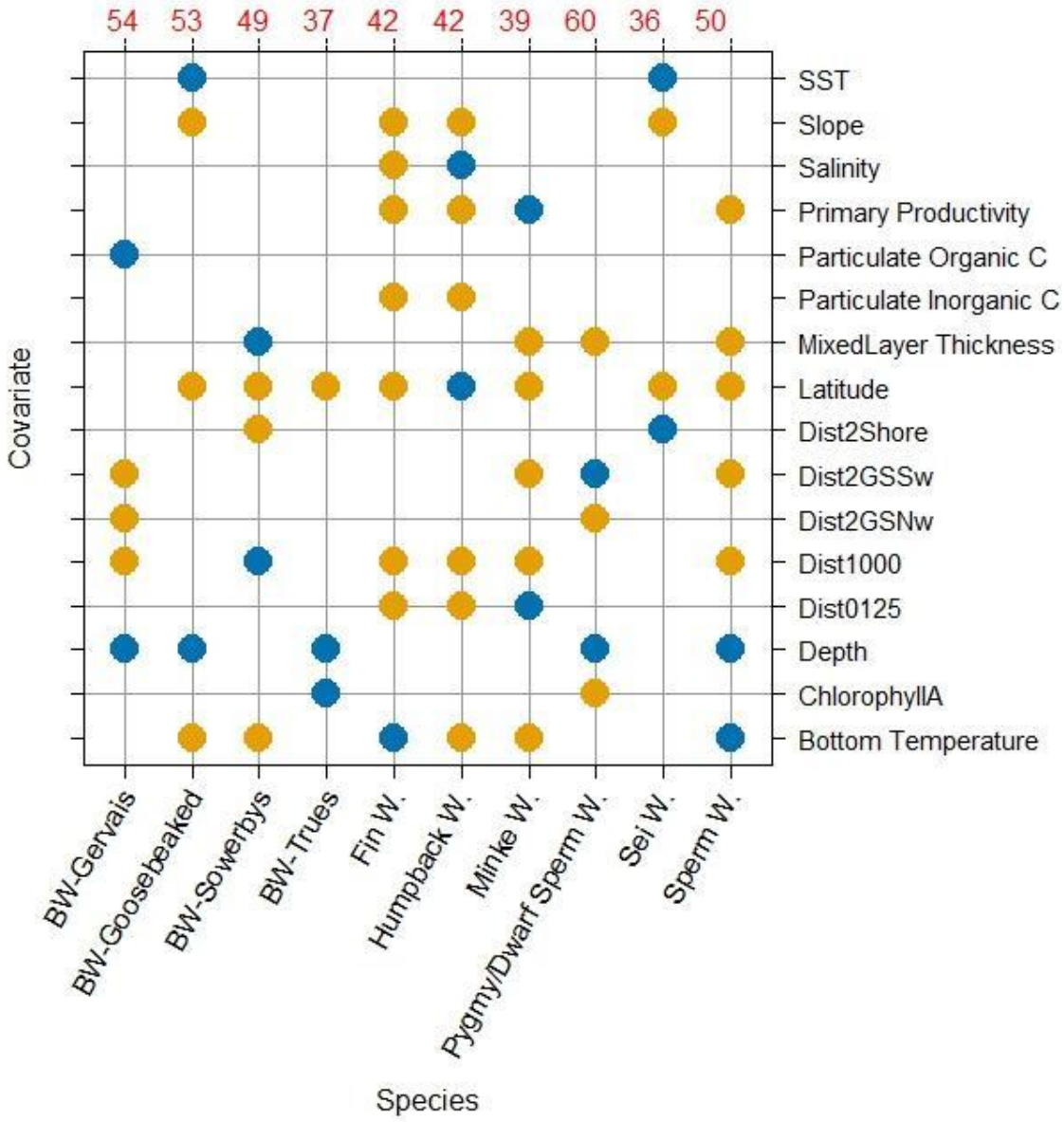

Figure 4-15. Significant habitat covariates for the density-habitat models for whales
Blue circles are the covariates that contributed the most to the species-specific model. If that covariate was a static covariate, then the dynamic covariate that contributed the most was also colored blue. Orange circles are the other covariates in the best fitting model. Percent deviance explained are the red numbers on the top axis. Habitat covariates are described in Table 4-2. Scientific names of species in Appendix A.

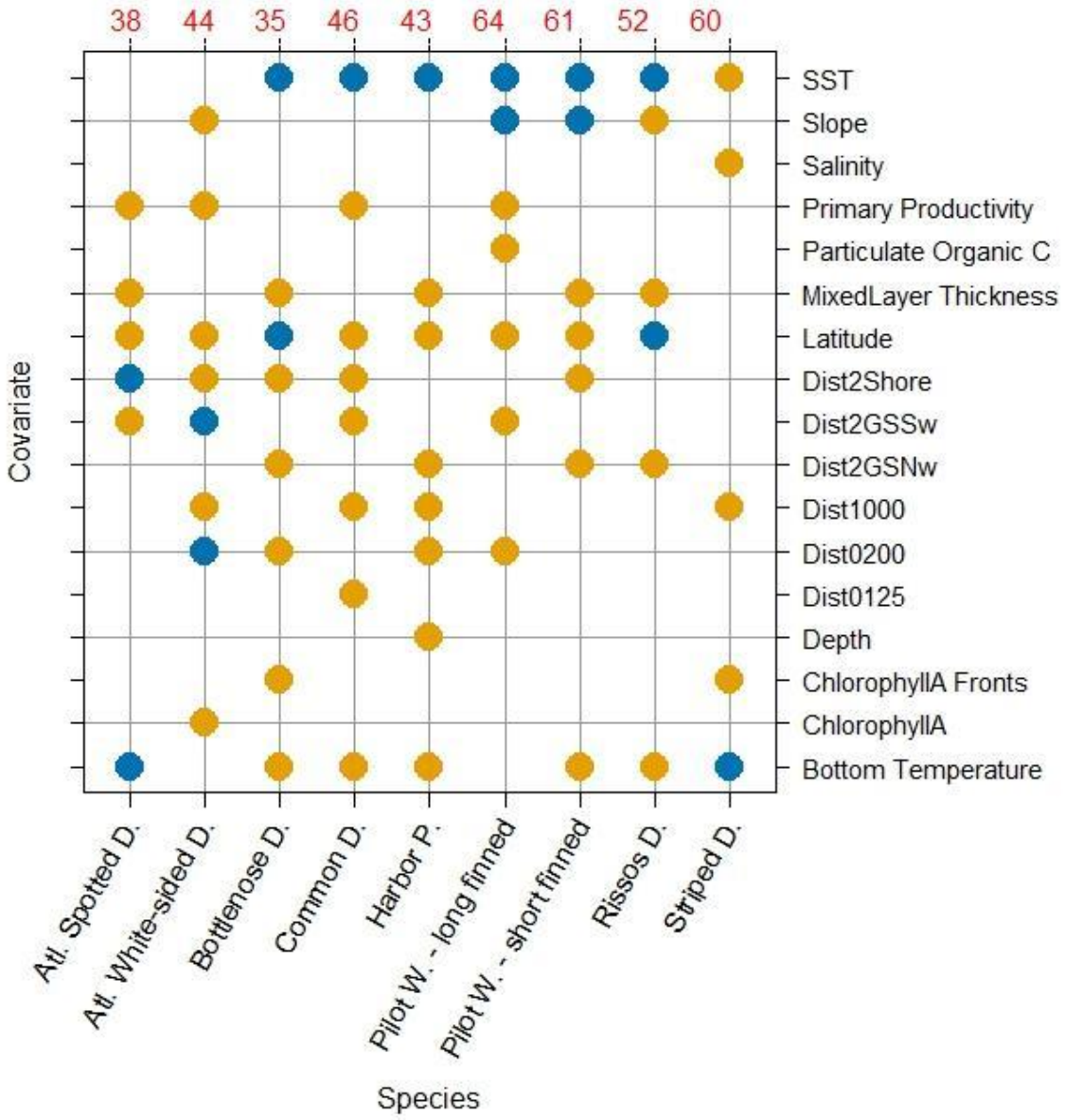

Figure 4-16. Significant habitat covariates for the density-habitat models for dolphins
Blue circles are the covariates that contributed the most to the species-specific model. If that covariate was a static covariate then the dynamic covariate that contributed the most was also colored blue. Orange circles are the other covariates in the best fitting model. Percent deviance explained are the red numbers on the top axis. Habitat covariates are described in Table 4-2. Scientific names of species in Appendix A.

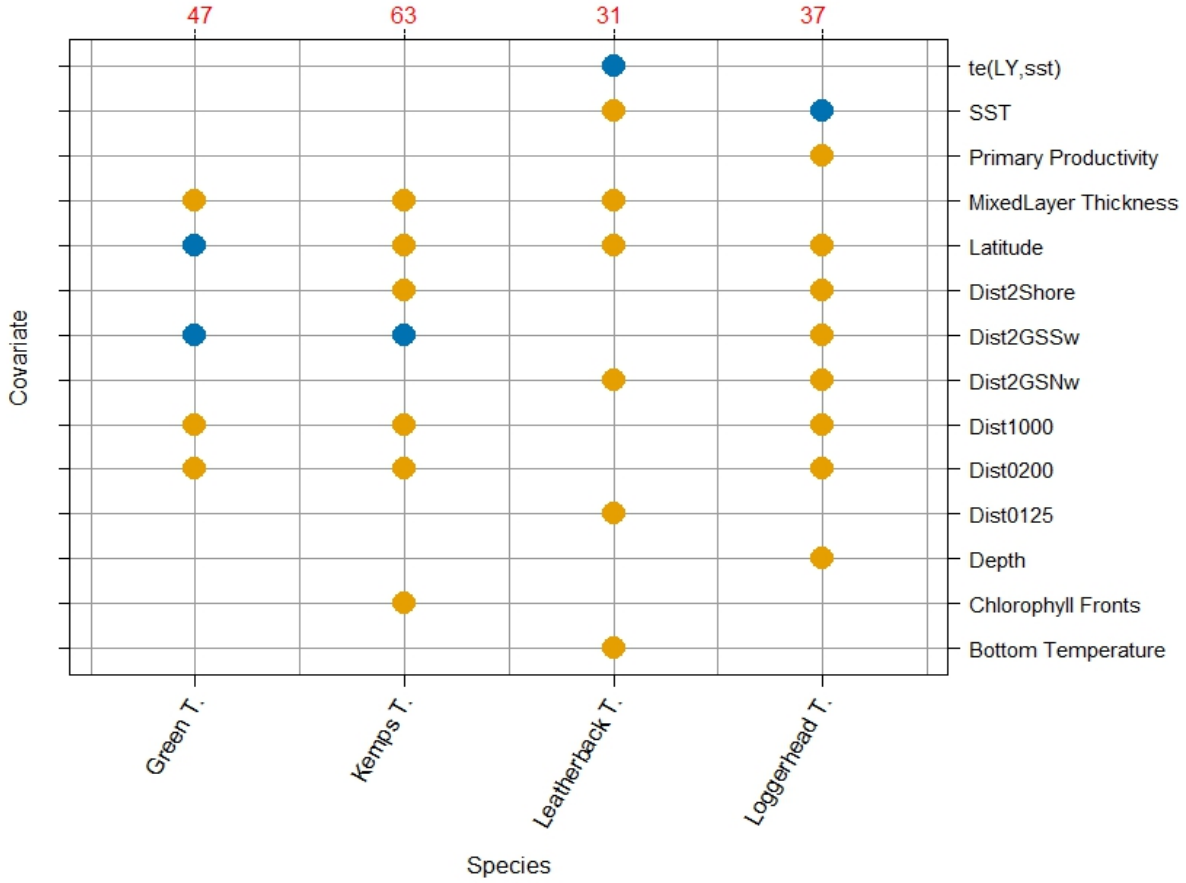

Figure 4-17. Significant habitat covariates for the density-habitat models for sea turtles
Blue circles are the covariates that contributed the most to the species-specific model. If that covariate was a static covariate then the dynamic covariate that contributed the most was also colored blue. Orange circles are the other covariates in the best fitting model. Percent deviance explained are the red numbers on the top axis. Habitat covariates are described in Table 4-2. Scientific names of species in Appendix A.

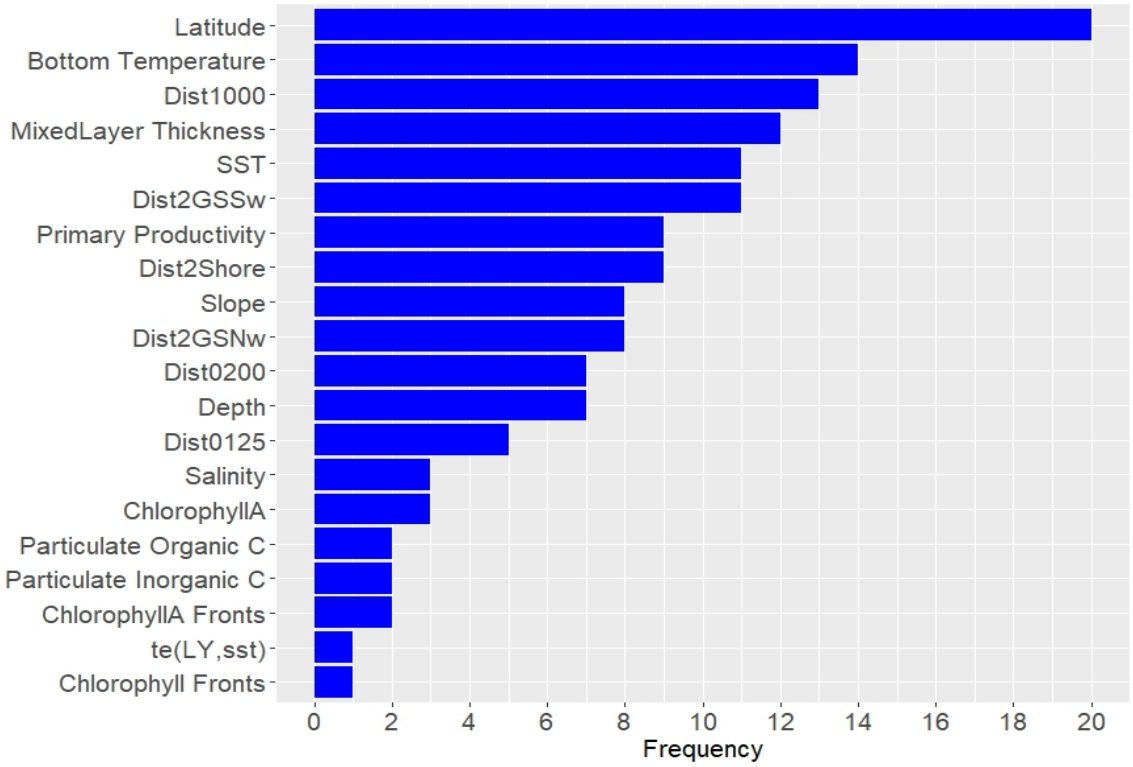

Figure 4-18. Frequency of habitat covariates in density-habitat models

4.7.2.4 Seasonal Average Abundance Estimates

The GAM models predicted the seasonal average abundance, including the associated coefficient of variation (CV) and the lower and upper 95% confidence intervals (CI 2.5% and CI 97.5%) (**Table 4-23**).

Table 4-23. Average 2010 to 2023 seasonal abundances for each species or species guild
Scientific names of species in Appendix A.

Species and Season	Abundance	CV	CI 2.5%	CI 97.5%
Atlantic spotted dolphin				
Spring (Mar-May)	11,166	0.38	5,436	22,936
Summer (Jun-Aug)	20,922	0.35	10,746	40,735
Fall (Sep-Nov)	8,915	0.36	4,497	17,671
Winter (Dec-Feb)	2,544	0.45	1,096	5,903
Atlantic white-sided dolphin				
Spring	3,788	0.36	1,911	7,509
Summer	2,689	0.36	1,357	5,330
Fall	3,500	0.35	1,798	6,814
Winter	4,493	0.34	2,350	8,592
Beaked whales - Gervais’				
Spring	1,474	0.27	876	2,479
Summer	2,815	0.23	1,804	4,393
Fall	1,965	0.25	1,213	3,184
Winter	1,001	0.33	533	1,880
Beaked whales - Goose-beaked				
Spring	2,803	0.35	1,440	5,457

Species and Season	Abundance	CV	CI 2.5%	CI 97.5%
Summer	5,177	0.25	3,195	8,388
Fall	4,937	0.26	2,991	8,150
Winter	2,742	0.35	1,408	5,339
Beaked whales - Sowerby's				
Spring	233	0.43	104	522
Summer	502	0.36	253	995
Fall	268	0.41	124	580
Winter	93	0.62	30	284
Beaked whales - True's				
Spring	165	0.59	57	482
Summer	851	0.45	367	1,975
Fall	467	0.50	185	1,179
Winter	284	0.53	107	753
Common bottlenose dolphin				
Spring	68,186	0.29	39,067	119,010
Summer	55,155	0.26	33,410	91,053
Fall	54,424	0.26	32,967	89,846
Winter	49,587	0.30	27,892	88,156
Common dolphin				
Spring	82,694	0.32	44,843	152,494
Summer	123,574	0.28	72,122	211,731
Fall	142,093	0.28	82,931	243,462
Winter	87,419	0.30	49,172	155,414
Fin whale				
Spring	5,833	0.31	3,221	10,562
Summer	9,414	0.30	5,295	16,736
Fall	8,550	0.29	4,899	14,923
Winter	4,863	0.31	2,686	8,805
Harbor porpoise				
Spring	82,130	0.31	45,358	148,713
Summer	80,391	0.23	51,516	125,450
Fall	64,140	0.24	40,336	101,992
Winter	52,033	0.34	27,211	99,498
Humpback whale				
Spring	1,570	0.32	851	2,895
Summer	2,987	0.32	1,620	5,508
Fall	2,104	0.31	1,162	3,810
Winter	1,312	0.32	711	2,419
Long-finned pilot whale				
Spring	4,268	0.71	1,220	14,930
Summer	5,634	0.66	1,734	18,309
Fall	5,061	0.62	1,655	15,478
Winter	5,538	0.67	1,679	18,268
Minke whale				
Spring	2,793	0.38	1,360	5,737
Summer	5,259	0.37	2,606	10,612
Fall	2,694	0.36	1,359	5,340
Winter	1,422	0.39	680	2,973
Pygmy or dwarf sperm whale				
Spring	1,313	0.35	674	2,556
Summer	5,436	0.24	3,419	8,644

Species and Season	Abundance	CV	CI 2.5%	CI 97.5%
Fall	2,054	0.32	1,114	3,788
Winter	340	0.64	108	1,072
Risso's dolphin				
Spring	46,038	0.34	24,076	88,034
Summer	99,351	0.23	63,666	155,037
Fall	66,372	0.27	39,463	111,630
Winter	52,095	0.41	24,058	112,805
Sei whale				
Spring	304	0.55	111	833
Summer	125	0.56	45	384
Fall	147	0.55	54	403
Winter	284	0.55	104	778
Short-finned pilot whale				
Spring	3,740	0.47	1,558	8,978
Summer	13,831	0.37	6,854	27,910
Fall	8,744	0.40	4,109	18,606
Winter	2,527	0.53	953	6,701
Sperm whale				
Spring	4,435	0.25	2,737	7,186
Summer	5,713	0.22	3,731	8,748
Fall	3,957	0.23	2,536	6,175
Winter	2,760	0.30	1,552	4,907
Striped dolphin				
Spring	24,556	0.71	7,020	85,902
Summer	48,317	0.38	23,522	99,247
Fall	51,468	0.43	22,957	115,385
Winter	20,830	0.79	5,320	81,558
Loggerhead turtle				
Spring	231,900	0.13	179,931	298,879
Summer	219,086	0.14	166,733	287,877
Fall	244,310	0.12	193,268	308,832
Winter	233,777	0.11	188,560	289,837
Leatherback turtle				
Spring	21,819	0.45	9,404	50,625
Summer	39,959	0.40	18,779	85,025
Fall	60,117	0.42	27,284	132,462
Winter	19,877	0.57	7,028	56,214
Green turtle				
Spring	52,540	0.32	2,8491	96,888
Summer	73,524	0.28	42,911	125,976
Fall	44,087	0.33	23,477	82,791
Winter	39,288	0.26	23,799	64,859
Kemp’s ridley turtle				
Spring	12,606	0.40	5,924	26,823
Summer	23,714	0.31	13,097	42,939
Fall	18,532	0.35	9,518	36,081
Winter	12,216	0.38	5,947	25,093

4.8 Bayesian Hierarchical Model-Based Abundance Estimates

During AMAPPS II (2015-2019), we developed a Bayesian hierarchical framework to estimate the abundance and spatial density of cetacean species, as detailed in Palka et al. (2021). This framework utilized two-independent team distance sampling from both aircraft and ships, incorporated a platform- and species-specific availability bias correction factor and accounted for variance across all estimation aspects.

In the AMAPPS III time period, we published this framework and applied it to estimate fin whale abundance and spatial density (Sigourney et al. 2020). This work inspired Miller et al. (2021a) to enhance the R package DMS (version 2.3.1 Miller et al. 2021b). The expanded package now supports data from multiple distance sampling platforms within a single spatial model, propagating variance throughout the framework. Miller et al. (2021a) also compared their results to those presented in Sigourney et al. (2020).

More recently during the AMAPPS III period, we significantly enhanced our Bayesian framework. Key improvements included:

- Hierarchical Distance-Sampling: Integrated a component to model detection probabilities.
- Rigorous Model Selection: Implemented a thorough process for model selection.
- Extrapolation Diagnosis: Developed code to identify extrapolations within the study area.
- Parallel Implementation: Introduced code for parallel processing to reduce computation time.
- Streamlined Code: Optimized code for increased efficiency and improved interpretability.

Additionally, we re-coded the model framework using the new R package NIMBLE (de Valpine et al. 2017). This transition substantially reduced computation time compared to the JAGS software (Plummer 2003) previously used by Sigourney et al. (2020).

We applied the Bayesian framework for density-habitat models to a wind energy area off Long Island, NY (**Figure 4-19**). We leveraged the unique features of a Bayesian model to quantify the posterior probability that the abundance within the wind energy area exceeds a user-defined threshold. As an example, we selected the species-specific Potential Biological Removal (PBR) level as the threshold. Our findings revealed predicted seasonal changes in abundance within the wind energy area and the seasonal probability of humpback whale abundance surpassed the user-specific threshold, PBR (**Figure 4-20**). We presented this work at the State of the Science Workshop in Stony Brook, NY in July 2024.

Expanding this framework, we wrote a manuscript that is currently in review (Sigourney et al. *in revision*, below) that focuses on the Massachusetts-Rhode Island wind energy area. For the threshold value in this manuscript, we chose the species-specific level B take levels within various areas of impact relative to the central centroid location of the wind energy area. We took the level B take levels from an incidental harassment authorization document for one of the wind-energy projects in this wind energy area. We also provided seasonal density estimates for the entire AMAPPS area with Bayesian uncertainty levels as described in Sigourney et al (2020). Then in Sigourney et al. (*in revision*) we applied this refined model framework to eight years of line transect survey data to develop Bayesian hierarchical density surface models for fin whales, humpback whales, minke whales, sei whales, and sperm whales.

Use of a Bayesian hierarchical density surface model to estimate seasonal distributions of large whales off the East Coast of the United States with an application to a wind energy area by Sigourney et al. (in revision)

> ***ABSTRACT: "Aim:*** *Offshore wind energy development off the East Coast of the United States is in the nascent but growing stage with consequences for wildlife. Marine*

mammals are particularly sensitive to pile driving activity, and therefore, it is critical to provide guidance about where and when impacts are most likely to be minimized. The aim of this study was to develop Bayesian hierarchical density surface models (BHDSMs) for five species of large whales and use model outputs specifically to characterize seasonal abundance within a wind energy area (WEA) off the East Coast of the United States.

Location: *Western Atlantic, USA*

Methods: *We use eight years of line transect survey data to develop BHDSMs for fin whales (*Balaenoptera physalus*), humpback whales (*Megaptera novaeangliae*), minke whales (*Balaenoptera acutorostrata*), sei whales (*Balaenoptera borealis*) and sperm whales (*Physeter macrocephalus*). We produced seasonal maps of densities at a basin-wide scale with associated measures of uncertainty. We then apply our models to a WEA off the Massachusetts-Rhode Island coast and estimate seasonal shifts in abundance and calculate the probability of abundance exceeding user-defined thresholds for each species.*

Results: *Seasonal distributions were largely consistent with previous studies of large whales for this region. Application to the WEA demonstrated an interaction between seasonal peaks in abundance and species. Posterior probabilities of abundance exceeding the user-defined threshold tracked seasonal changes in abundance, with differences among species in the magnitude of the probabilities.*

Main conclusions: *This application of a BHDSM demonstrates the multipurpose use of habitat models to examine both large scale patterns in density with robust measures of uncertainty and localized variation in abundance in a probabilistic framework that can be used to assess risk. Model outputs can be readily applied to additional areas off the East Coast of the U.S. that are of interest."*

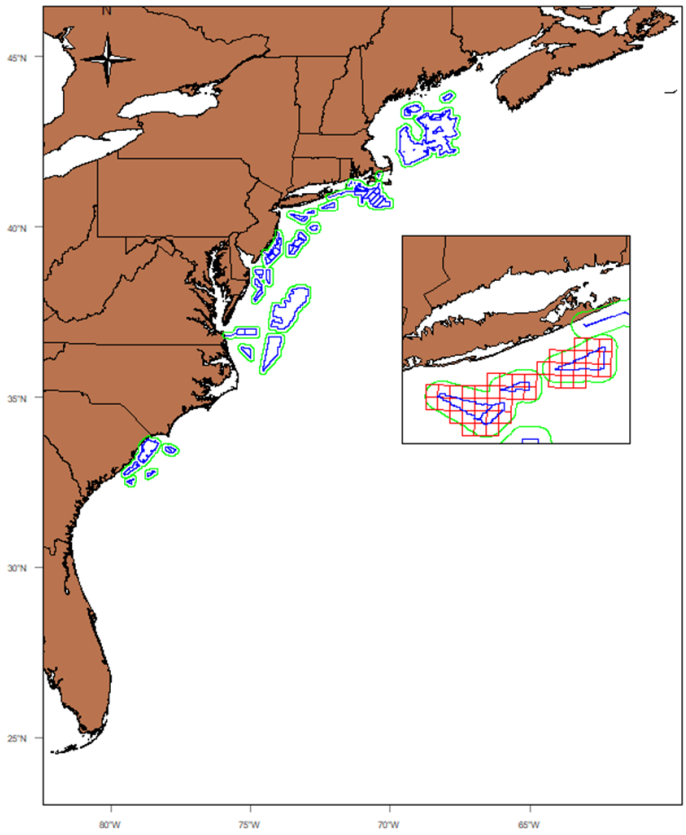

Figure 4-19. Map of wind energy areas and targeted New York area

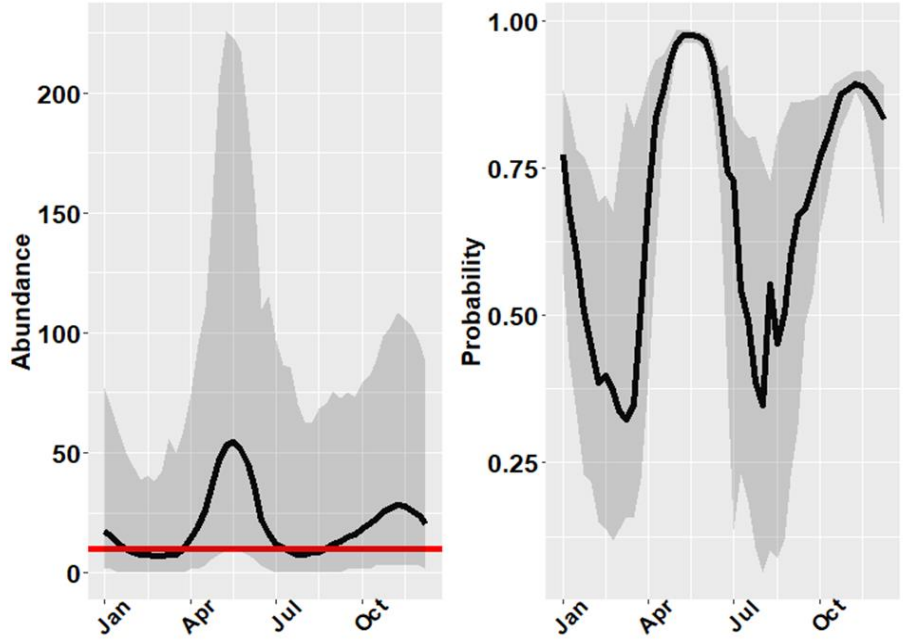

Figure 4-20. Seasonal abundance of humpback whales in New York wind energy area
Used a Bayesian hierarchical density surface model, where the gray shading is the 95% credibility interval. Left panel: Median seasonal abundance (black line) and Potential Biological Removal (PBR) threshold value (red line),

over 2010 - 2021. Right panel: Seasonal change in median posterior probability of abundance exceeding the PBR level threshold value.

4.9 Acoustic Abundance Estimate of Subsurface Sperms Whales

After we processed the passive acoustic data (Section 4.2.3), we estimated the abundance of foraging sperm whales below the ocean's surface using passive acoustic detections. Estimating the abundance of passive acoustic detected events using standard line transect analysis methods depends on converting the slant distance between the array hydrophone and location of the subsurface animal to a horizontal perpendicular distance between the track line and location of the animal transferred to the ocean surface. We estimated the depth of each click following the methods in DeAngelis et al. (2017). We then used the depth of the click to estimate the horizontal perpendicular distance (similar to that esimated in visual surveys), which we then used in standard line transect analysis methods.

Westell et al. (2022) used acoustic towed array data collected during the summer 2016 Northeast shipboard survey (HB1603, Palka et al. 2016) to estimate the acoustic abundance of foraging sperm whales in the study region and to explore the sperm whale's dive behavior. We estimated whether echosounder usage had an effect on the daily detection rate of sperm whales. We described preliminary methodology developments and results in AMAPPS 2021, 2022 and 2023 Annual Reports (**Table 3-2**).

In summary, Westell et al. (2022) used the passive acoustic data collected between 27 June 2016 and 25 August 2016 on more than 5500 km of on-effort acoustic line transects between North Carolina and Maine. We processed over 350 hours of acoustic data using the PAMGuard sperm whale click detector (Gillespie et al. 2008). We manually annotated the sperm whale click trains produced by individual animals into "events" and then we used 699 events in the Target Motion Analysis module's 2D Simplex Optimisation algorithm. This localization estimated the 2D distance between the detected animal and the trackline, known as the slant range, which ranged from 31 m to more than 30 km. Of the 699 events, we included 690 events across 38 survey days in the echosounder analysis. Using the R package MASS (Venables & Ripley, 2002) a negative binomial generalized linear model (GLM) with a log link function was fitted to the total daily acoustic detections of sperm whales. Covariates included echosounder state (active versus passive), month (June, July, August), and habitat type (slope versus abyssal). To account for varying daily effort the track line distance covered per day we included daily effort as an offset. We selected the best fitting model using backwards stepwise selection using Akaike's information criterion (AIC) and the single-term deletion method using Chi-squared goodness-of-fit tests.

At the 95% significance level, echosounder state did not have a significant impact on the number of daily acoustic detections or the number of detections available for acoustic localization. Month was the only significant covariate using both backwards stepwise model selection or the single term deletion method ($P < 0.05$). Thus, we used all sperm whale events, regardless of echosounder state, for abundance estimation.

When possible we applied the methods established by DeAngelis et al. (2017) to use the multipath arrival of surface reflected echoes to estimate the depth of each click. To improve the horizontal distance estimates used for acoustic distance sampling we calculated the average depth and a depth corrected horizontal perpendicular distance (3D localization) for 274 events. For events that could not be localized in 3D, we applied the first quartile (25th percentile) of the average depths (411 m) as the assumed depth to calculate the depth corrected horizontal perpendicular distance.

We included 431 events in the acoustic distance sampling. We explored the effects of using the slant distance versus the depth corrected horizonal perpendicular distance in distance sampling abundance estimates of subsurface foraging sperm whales in the shipboard survey study areas. To do so, we truncated the events at a slant range of 6500 m. Then we used the R Package Distance (Thomas et al.

2010) to conduct two distance analyses using (1) slant distances and (2) depth corrected perpendicular distances. We selected the best detection function from each analysis based on the Akaike's Information Criterion score, the Kolmogorov-Smirnov test, the Cramer-von Mises test, and the quantile-quantile plots.

The best fitting detection function for the slant ranges was a hazard rate key function with no adjustment terms (**Figure 4-21**). This produced an abundance estimate of submerged foraging sperm whales within the shipboard study area of 1,969 (CV = 14.1%, SE = 278), with an average probability of detection of 0.784 (CV = 3.6%) and an effective strip half width (ESHW) of 5,099 m (SE = 182 m). The best fitting function for depth corrected perpendicular distances was a half normal key function with simple polynomial adjustment terms of order two. This produced an abundance estimate of submerged foraging sperm whales within the shipboard study area of 2,199 (CV = 14.6%, SE = 322), with an average probability of detection of 0.702 (CV = 5.2%), and an ESHW of 4,566 m (SE = 236 m). The corresponding density estimates of submerged foraging sperm whales within the shipboard study area were 7.5 whales per 1000 km^2 using slant ranges and 8.3 per 1000 km^2 using depth-corrected perpendicular distances.

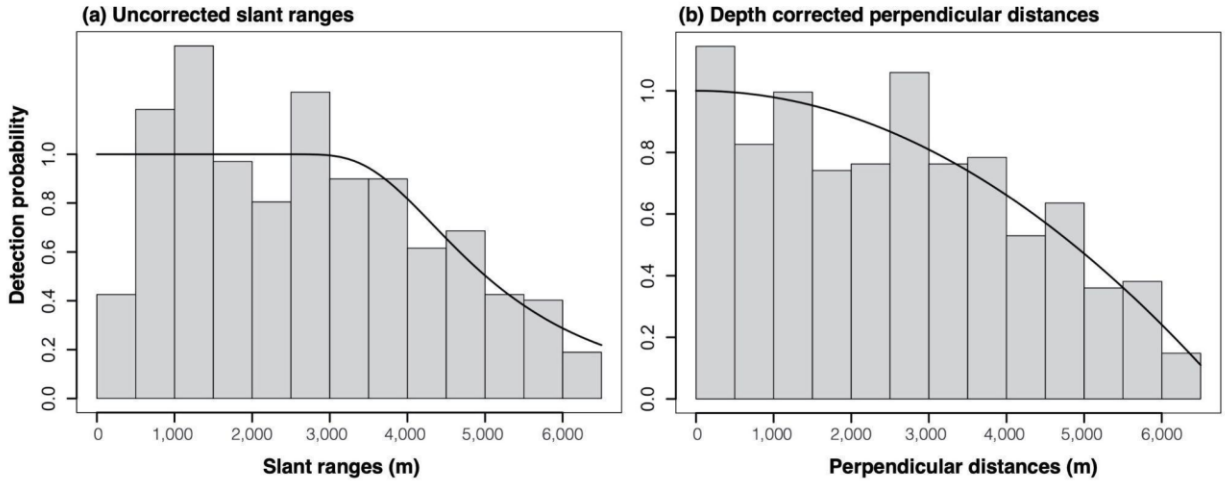

Figure 4-21. Fitted line transect models for acoustic detections of sperm whales
The solid line represents the best fitting model. The histogram bars represent the (a) perpendicular slant distances and (b) depth-corrected perpendicular horizontal distances.

The distribution of slant ranges was atypical for line transect sampling as the number of detections within 1000 m of the trackline were less than at 1000 - 1500 m, and all models fitted to the slant ranges failed the Kolmogorov-Smirnov goodness of fit test at the 95% level. Distance sampling using depth-corrected perpendicular distances resulted in a 10.5% change in the acoustic abundance estimate and a detection function that was a better fit for the data.

As these acoustic surveys recorded only foraging sperm whales and did not account for unavailable animals (for example sperm whales at the surface or subsurface sperm whales not foraging) and did not account for perception bias (for example, vocalizing foraging sperm whales unable to estimate depth accurately). Thus, these acoustic abundance estimates cannot be directly compared to those of the concurrent visual survey. For further discussion of the results see Westell et al. (2022).

In 2024 we applied the same methods to towed array data collected during the summer 2021 Northeast shipboard survey and we presented preliminary results in the AMAPPS 2024 Annual Report (Palka et al. 2021). However, more work is needed to finalize the analysis of the 2021 sperm whale acoustic events.

4.10 Acoustic Abundance Estimates of Beaked Whales

In the past we estimated abundance of the beaked whale species using visual line transect data in design-based analysis methods (Section 4.6) and model-based analysis methods (Section 4.7). These methods used an availability bias correction factor to account for animals below the surface when estimating the total-water-column abundance. We derived this correction factor from data collected from time-depth tags deployed on individual animals, where the estimated correction factor for all the beaked whale species was 1.309 (CV = 0.246).

With the advances in processing and analyzing passive acoustic data, we used the passive acoustic data to gain insights into the abundance of the animals below the surface that were not available to visual observers. In essence, now it is possible that the beaked whale towed hydrophone passive acoustic data that we collected simultaneously with the visual data could replace the availability bias correction factor we previously used in estimates derived from shipboard surveys.

The probability of visually sighting an acoustically detected beaked whale during a shipboard line-transect cruise surveying at 10 knots in passing mode is considered negligible. This is because of the beaked whale's extended dive times, brief surface intervals, and the fact that they only vocalize at depths below what can be seen by a visual observer (e.g. Tyack et al. 2006, Shearer et al. 2019). This low probability allows us, in theory, to simply add a visual at-surface abundance estimate and a passive acoustic below-surface abundance to estimate the total-water-column abundance within the area surveyed by the shipboard abundance cruise.

In reference to estimating abundance of subsurface acoustic detections, perception bias is due to two types of animal behaviors. One, vocalizing subsurface animals that we missed and/or were not able to process even though they were potentially able to be detected and processed. And two, non-vocalizing subsurface animals. Furthermore, in reference to estimating abundance of subsurface acoustic detections, availability bias of an acoustic abundance estimate refers to the animals not able to be detected acoustically when at the surface.

In this section, we used standard line transect methods to estimate abundance of below-surface beaked whales by using passive acoustic detections. Then we added corresponding at-surface abundance estimates to estimate the species-specific total-water-column abundance of animals in the shipboard survey study area. While availability bias correction factors for missed animals at or below the surface and for duplicates are likely small, they are not zero. This is primarily because most beaked whales are either visible at the surface or can be acoustically detected when submerged. Further research is required to determine the number of subsurface animals that remain undetected acoustically due to being submerged and not vocalizing.

4.10.1 Methods

In this section, we estimated the total-water-column abundance estimate of beaked whales by adding a) the at-surface abundance estimate accounting for perception bias derived from the visual data but not accounting for the availability bias correction factor and b) the below-surface abundance derived from the passive acoustic data as a replacement for the availability bias correction factor.

To estimate the below-surface abundance we used the passively acoustically detected events in a standard line transect analysis framework. However, first, we converted the slant distance between the array and the subsurface animal's location to a horizontal perpendicular distance at the surface (DeAngelis et al. 2017, Boisseau et al. 2023). We defined the horizontal perpendicular distance at the surface as the distance between the trackline and the animal's location when reflected to the surface. Similar to what we did with sperm whale passive acoustic events (Section 4.9) we employed the innovations developed in

DeAngelis et al. (2017) to use the multipath arrival of surface reflected echoes to estimate the depth of a beaked whale click. We then used the depth of the beaked whale clicks and simple geometry to estimate the horizontal perpendicular distance that we used in standard line transect distance-sampling analysis methods.

We could not estimate depth for 35% of the 713 beaked whale acoustic events (n = 253). In a similar situation for uncorrected sperm whale acoustic events, we assumed the first quartile (25th percentile) of the average sperm whale depth for the depth of the uncorrected events that we then used to calculate a depth-corrected horizontal perpendicular distance. Here we explored a different approach for beaked whales. We assumed the probability of detecting the non-corrected events was similar to the probability of detecting the corrected events. We then derived the detection function from only the events that were depth corrected, and applied it to the encounter rate of both the corrected and uncorrected events to estimate the abundance of below-surface animals.

We used beaked whale passive acoustic data collected during three years that were on four shipboard line transect cruises on two ships that used three types of passive acoustic hydrophone arrays (**Table 4-24**). We only used beaked whale acoustic data collected when the ship's active acoustic echosounder was in passive mode, since beaked whales are rarely acoustically detected when the echosounder is in active mode (Cholewiak et al. 2017 and Section 6.7). In addition, we only used the data collected between 6 am and 7 pm local time to correspond to the times when the visual observers were collecting data. As shown in Section 4.2.3 the beaked whale data collected while in passive mode were spatially and temporally distributed within the study area (**Figure 4-1**); thus, we assume the data collected during passive mode were representative of the entire study area and appropriate to be used to derive a design-based line transect abundance estimate. We also assumed that each beaked whale acoustic event represented a single animal; that is, the group size of the detection was always one. In the handful of rare cases where a single event showed evidence of two animals vocalizing along the same bearing such that the two could not be confidently separated into their own events, we created two rows of data to represent each animal that had the same data associated with each individual. Beaked whales forage in tight synchrony (Alcazar-Trevino et al. 2021, Cioffi et al. 2021) which could be the cause of this coupling of received bearings. At this time, we have not yet estimated the depths of beaked whales detected in 2021 (HB2102); thus, we did not use them in the estimation of the detection function.

Table 4-24. Survey information for the analysis of acoustic beaked whale events

Year	Cruise	Ship[1]	Array Type	Survey Area (km^2)	Acoustic Trackline Length[2]
2013	HB1303	Bigelow	A	249,245	2,446
2016	HB1603	Bigelow	B	252,446	3,640
2016	GU1605	Gunter	C	400,418	5,725
2021	HB2102	Bigelow	B	249,245	3,030

[1] Bigelow is the NOAA ship *Henry B. Bigelow* and Gunter is the NOAA ship *Gordon Gunter*.
[2] Trackline length of GU1605 is preliminary since some off-effort time periods have not yet been removed.

Using depth-corrected horizontal perpendicular distances (**Table 4-25**) truncated at 6 km from the ship, we estimated species-specific detection functions using standard multiple covariate distance sampling techniques in the R package mrds (version 3.0.1; Laake et al. 2025). To identify the best fitting detection function, we assessed array type, species, and time of day as potential covariates, and the half-normal and hazard rate models as potential key models. We also investigated whether species exhibited different detection function shapes. Because of the small sample sizes, we explored pooling species data to estimate the detection function. We then selected the optimal detection function based on Akaike's Information Criterion score, Cramer-von Mises test, quantile-quantile plots, and a visual assessment of the sighting histograms and predicted detection functions.

Because we wanted to use the passive acoustic detections that we were unable to derive corrected horizontal perpendicular distances, we used the species- and array type-specific detection function's effective half strip width (w_{sc}) to estimate the below-surface abundance of each species (s) for each cruise (c) (N_{sc}) by :

$$N_{sc} = \frac{n_{sc} \cdot A_c}{2 w_{sc} L_c}$$

where n_{sc} is the total number of recorded events of species on cruise c that included the corrected and uncorrected detections; A_c is the area covered by cruise c; L_c is the track line covered by cruise c.

This formula also allowed us to estimate the abundance of beaked whales from HB2102, for which we have not yet estimated the depths of the events. Since HB2102 used the same array type as HB1603, we used the species-specific detection functions derived for HB1603 to represent that for HB2102. This assumed that the detection process was similar for HB1603 and HB2102.

One could consider that when we used the total number of corrected and uncorrected events in the encounter rate, then we partially accounted for the acoustic perception bias.

We estimated the variance of N_{sc} using the standard delta method:

$$CV(N_{sc}) = \sqrt{CV^2\left({}^{n_{sc}}/_{L_c}\right) + CV^2(w_{sc}) + CV^2(A_c)}$$

4.10.2. Results and Discussion

4.10.2.1 Subsurface Abundance Estimates

Ideally, we would define species-specific detection functions using only data from that particular species (**Table 4-25**). However, due to limited sample sizes for most species (excluding goose-beaked whales) the other species were pooled. For goose-beaked whales, the detection function was based solely on their detections, revealing array type as a significant covariate (**Figures 4-22, 4-23; Table 4-26**). For other beaked whale species, we pooled their data and found both array type and species were important covariates for the detection function (**Figures 4-22, 4-23; Table 4-26**). In both detection function models, the addition of a time-of-day covariate did not improve the models.

Table 4-25. Numbers of beaked whale events by cruise and species used in abundance estimation
Numbers outside parentheses represent the total number of depth-corrected and depth-uncorrected events, which we used for the encounter rate and final abundance estimate. Number inside parentheses is the number of depth-corrected events used to define the detection function, that was truncated at 6 km. Scientific names of species in Appendix A.

Cruise	Blainville	Goose-beaked	Gervais'	Gervais' or True's	Sowerby's	True's
GU1605	44 (37)	102 (74)	73 (57)	12 (7)	2 (1)	12 (7)
HB1303	0 (0)	108 (77)	4 (3)	17 (7)	1 (0)	48 (41)
HB1603	0 (0)	76 (64)	4 (4)	6 (5)	4 (4)	60 (46)
HB2102	0 (0)	42 (0)	0 (0)	8 (0)	6 (0)	42 (0)

Table 4-26. Detection function for the species groups of passive acoustic beaked whale events
Numbers of events are those within the truncation distance, 6 km. Scientific names of species in Appendix A.

Species	Number of events	Truncation Distance (km)	Key Model	Covariate function	Cramer-von Mises p-value
Goose-beaked	213	6	Half Normal	Perpendicular distance + ArrayType	0.18
True's, Gervais', Sowerby's, Blaninville's, Gervais'/True's	219	6	Half Normal	Perpendicular distance + ArrayType + Species	0.45

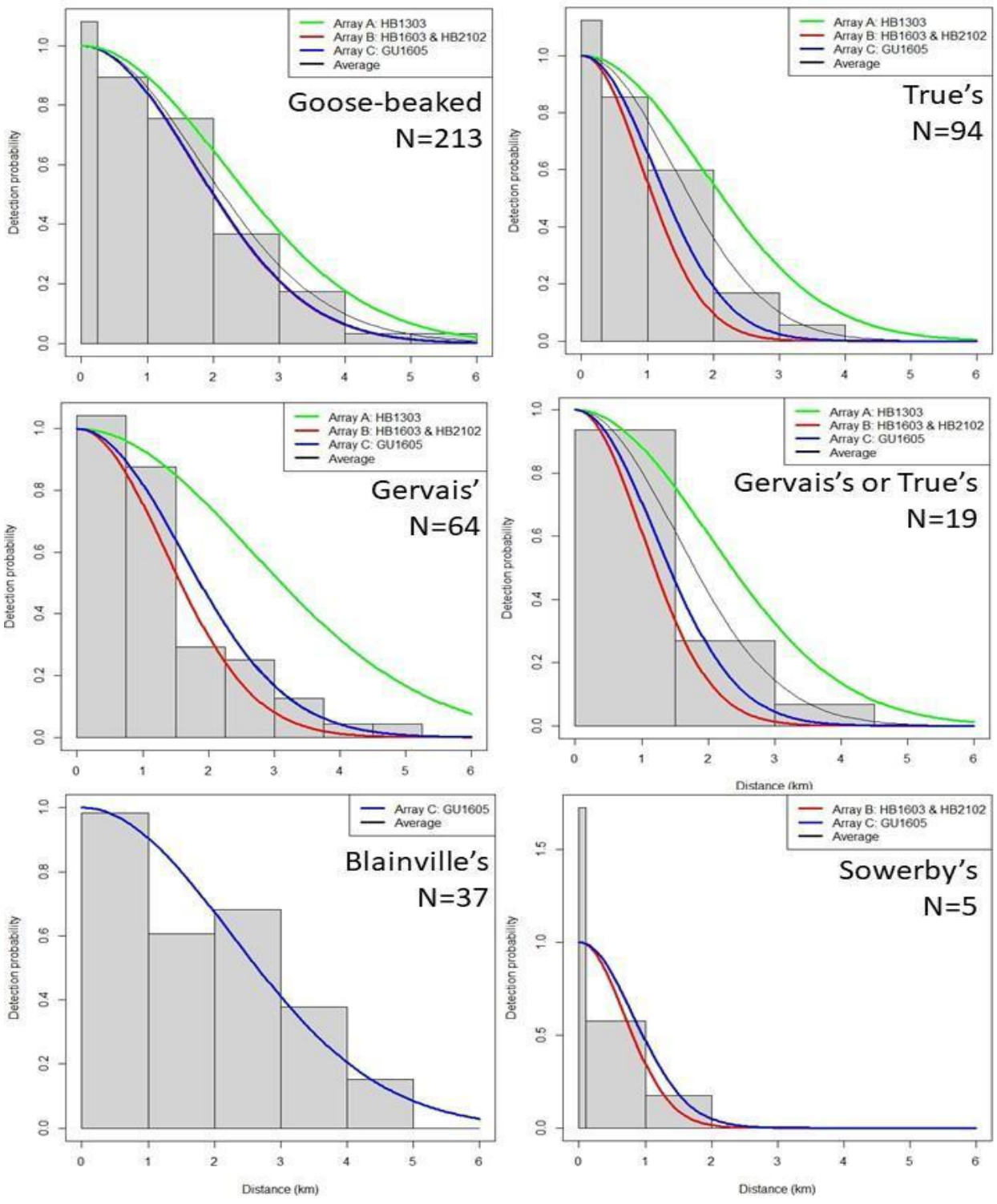

Figure 4-22. Detection functions for each beaked whale species
Histograms represent distribution of detections of only the specific species. Colored curves are the predicted detection function for the arrays that detected the specific species. The number of species-specific detections used to develop the detection (N) is embedded in each plot. Scientific names of species in Appendix A.

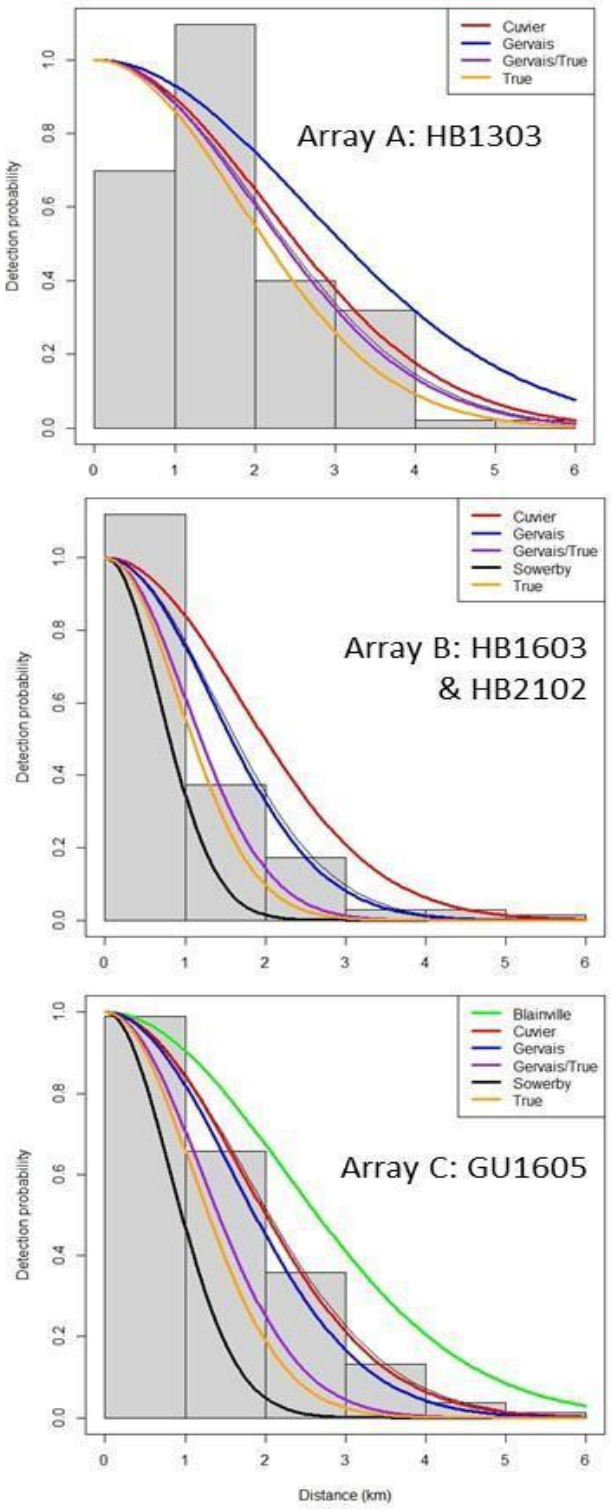

Figure 4-23. Detection functions of beaked whale species for each array type
Histograms represent the distribution of detections recorded by each array. Colored curves are the predicted detection function for the species as detected by the array type. Scientific names of species in Appendix A.

The estimated species- and array-specific effective strip half-widths ranged from 0.86 to 3.23 km, with an overall average of 1.896 km (**Table 4-27**). Goose-beaked whales had the largest estimated average effective strip half-width at 2.3 km, while Sowerby's beaked whales had the smallest at 1.19 km (based on only seven detections). This pattern is consistent with the acoustic characteristics of these species, as the low-frequency clicks of goose-beaked whales travel farther, and the high-frequency clicks of Sowerby's beaked whales travel the least distance (Zimmer et al. 2005; Clarke et al. 2019).

The species-specific below-surface abundance estimates from the GU1605 and HB1303 surveys are in Table 4-28. Because there are no comparable at-surface abundance estimates for these surveys, we did not estimate the total-water-column abundance estimates for these two surveys. However, for HB1603 and HB2102 we estimated the total-water-column abundance estimates that we reported in the next section.

In a future analysis of these data, we will assign the ambiguous Gervais'/True's beaked whale detections to a specific species, using methods described in Section 4.4. In addition, we will estimate the depth-corrected horizontal perpendicular distance of the acoustic beaked whale detections made during HB2102. Both of these actions will augment sample sizes, which should increase the precision of the below-surface abundance estimates.

Table 4-27. Effective strip half widths (ESHW), in km, for the below-surface species by survey
Scientific names of species in Appendix A.

Species	Survey	ESHW (km)	CV(ESHW)
Goose-beaked	GU1605	2.14	0.08
Goose-beaked	HB1303	2.68	0.09
Goose-beaked	HB1603	2.13	0.07
Goose-beaked	HB2102	2.13	0.07
Gervais's	GU1605	1.99	0.08
Gervais's	HB1303	3.23	0.19
Gervais's	HB1603	1.68	0.19
Sowerby's	GU1605	1.02	0.49
Sowerby's	HB1303	1.70	0.49
Sowerby's	HB1603	0.86	0.47
Sowerby's	HB2102	0.86	0.47
True's	GU1605	1.38	0.20
True's	HB1303	2.29	0.13
True's	HB1603	1.16	0.09
True's	HB2102	1.16	0.09
Blainville's	GU1605	2.80	0.14
Gervais'/True's	GU1605	1.51	0.19
Gervais'/True's	HB1303	2.50	0.23
Gervais'/True's	HB1603	1.27	0.23
Gervais'/True's	HB2102	1.27	0.23

Table 4-28. Estimates of beaked whale below-surface abundance for GU1605 and HB1303
Scientific names of species in Appendix A.

Cruise	Species	Below-Surface Abundance	CV(Below-Surface Abundance)
GU1605	Goose-beaked	1,670	0.37
GU1605	Gervais's	1,284	0.22
GU1605	Sowerby's	68	1.11
GU1605	True's	305	0.74
GU1605	Blainville's	550	0.38
GU1605	Gervais'/True's	279	0.44
HB1303	Goose-beaked	2,054	0.26
HB1303	Gervais's	63	0.84
HB1303	Sowerby's	30	1.11
HB1303	True's	1,069	0.37
HB1303	Gervais'/True's	346	0.52

4.10.2.2 Abundance Estimates for the Total Water Column

Improved knowledge in identifying beaked whale species from both visual sightings and acoustic detections allowed us to calculate species-specific total-water-column abundance estimates using the visual and acoustic data. These estimates combine below-surface abundance, calculated in this section, with at-surface abundance estimates, which account for visual observer perception bias but not availability bias (**Table 4-29**; Palka 2020; 2023; methods described in this document Section 4.6).

The species-specific total-water-column abundance estimates calculated using visual and acoustic data for HB1603 and HB2102 (**Table 4-29**) were similar to the total-water-column abundance estimates calculated using the design-based analyses of the visual sightings data to estimate the at-surface estimate accounting for perception bias and the time-depth tag data to estimate for the availability bias correction factor to account for the below-surface animals that could not be seen by the visual observers (**Figures 4-24 and 4-25**).

Table 4-29. Estimates of beaked whale total water column abundance for HB1603 and HB2102
We corrected the at-surface abundance estimates for perception bias but not availability bias. As a reference, the availability bias correction factor derived from tag data on beaked whales was 1.309 (CV=0.246). Scientific names of species in Appendix A. NA = not available.

Species	Cruise	Below-surface Abun	CV(Below-surface Abun)	At-surface Abun	CV(At-surface Abun)	Total Abun	CV(Total Abun)
Goose-beaked	HB1603	1,240	0.29	4,021	0.28	5,261	0.22
Gervais's	HB1603	83	0.79	4,452	0.17	4,535	0.17
Sowerby's	HB1603	161	0.74	537	0.15	698	0.21
True's	HB1603	1,793	0.37	1,957	0.13	3,750	0.19
Gervais'/True's	HB1603	164	0.48	NA	NA	NA	NA
Blainville's	HB1603	0	0	42	0.4	42	0.4
Goose-beaked	HB2102	813	0.33	1,331	0.3	2144	0.22
Sowerby's	HB2102	286	0.98	376	0.39	662	0.48
True's	HB2102	1,488	0.37	3,422	0.23	4,910	0.2
Gervais'/True's	HB2102	259	0.48	NA	NA	NA	NA

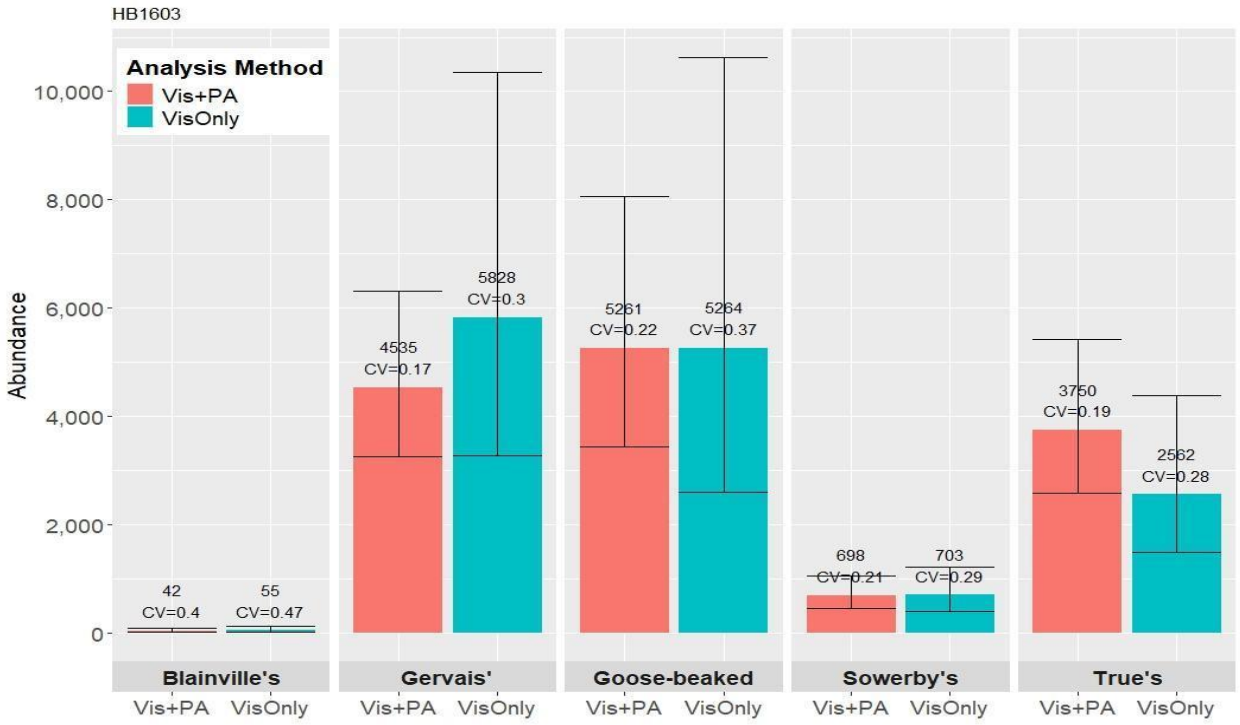

Figure 4-24. Comparison of total-water-column beaked whale abundance estimates for HB1603
Colored bars with numbers on top represent the species-specific abundance estimates. Black colored error bars represent the 95% confidence interval. Scientific names of species in Appendix A.

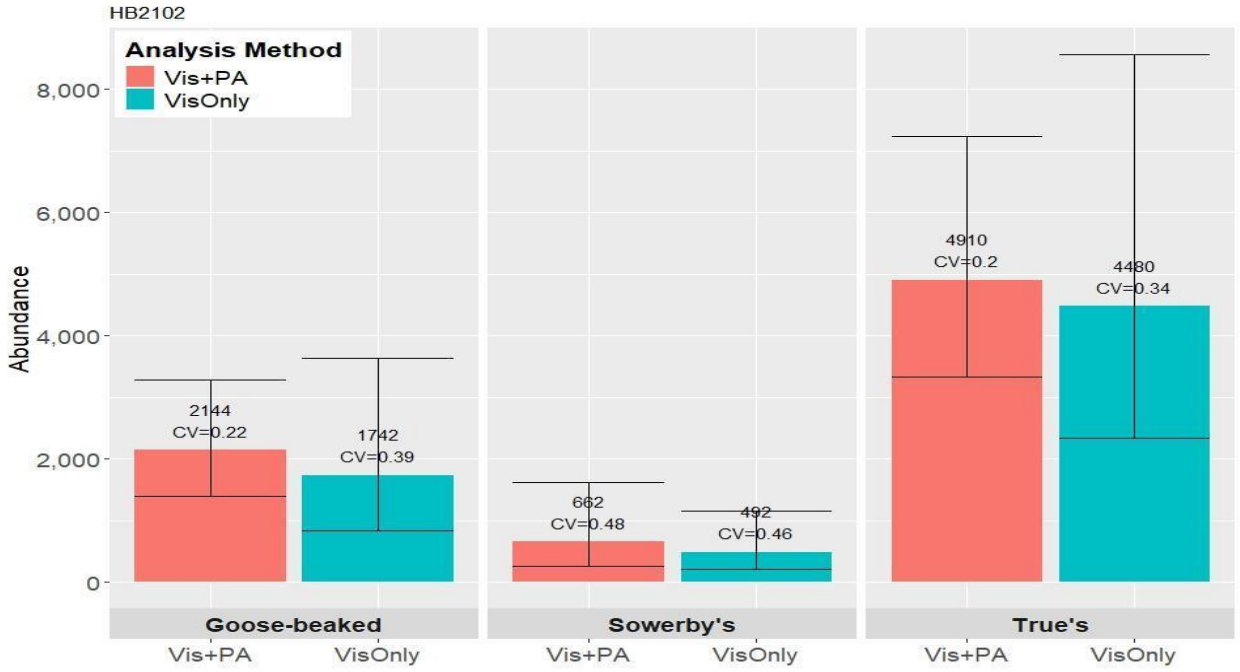

Figure 4-25. Comparison of total-water-column beaked whale abundance estimates for HB2102
Colored bars with numbers on top represent the species-specific abundance estimates. Black colored error bars represent the 95% confidence interval. Scientific names of species in Appendix A.

Future research will investigate applying spatial density modeling to passive acoustic detections. This could allow for a comprehensive abundance estimate of beaked whales across the entire water column. This estimate would combine spatial modeling from visual data (representing non-foraging, at-surface behavior) and passive acoustic data (representing subsurface foraging).

4.11 Integrating Visual and Passive Acoustic Data to Estimate Sperm Whale Abundance

Line transect sampling has long been the cornerstone of abundance estimation for cetaceans, providing a statistically rigorous framework to account for detectability and generate unbiased population estimates. Reliable abundance estimates derived from line transects form the basis for conservation status assessments, management of human impacts, and evaluation of long-term population trends. However, the value of abundance estimates is closely tied to their precision. In recent decades, the advent of passive acoustic monitoring has offered new tools to complement visual line transects. This technology has proven valuable, especially for species that are rarely seen but reliably heard, by providing opportunities to integrate visual and acoustic survey data to improve abundance estimates (e.g. Boisseau et al. 2023, 2024).

4.11.1 Methods

Under AMAPPS II, Sigourney et al. (2023) developed a method to integrate visual line transect and passive acoustic data collected simultaneously during shipboard surveys, addressing the challenge of avoiding double counting individual animals detected by both visual observers and passive acoustic monitors. This is particularly applicable to sperm whales. Some individual sperm whales can be detected at the surface by visual observers at far distances ahead of the ship and then later detected by passive acoustics after the whale dives and starts clicking during a foraging bout or vice versa. Sigourney et al. (2023) tested their approach using simulations that depicted this situation. They then applied the methods to a subset of 2013 AMAPPS visual and passive acoustic survey data.

During AMAPPS III, we apply the Sigourney et al. (2023) method to data collected during 2016 and 2021 on the NOAA ship *Henry B. Bigelow* to estimate sperm whale abundance in the Northeast shelf region of the U.S. Atlantic. On the NOAA ship *Henry B. Bigelow*, we simultaneously collected visual and passive acoustic data between June 27 and August 27 in 2016 and between June 16 and August 23 in 2021. These surveys covered about 6,600 km and 5,350 km of line transect effort in 2016 and 2021, respectively. We described the methods used to collect the visual and passive acoustic data in Sections 4.2. Sigourney et al. (2023) used the slant range distances estimated by PAMGuard's Target Motion Analysis 2D Simplex Optimization algorithm. With these more recent data we applied the methods described by DeAngelis et al. (2017) to estimate 3D localizations, the depth of the click event, and a depth corrected horizontal perpendicular distance. Thus, now we assigned to each event a latitude and longitude position, timestamp, bearing angle to each click in the event, and an ID number. Using this information and the GPS location of the ship, we calculated a radial distance for each annotated click.

To estimate abundance using the combined passive acoustic and visual line transect data we employed the *Hybrid Method* described in Sigourney et al. (2023). The *Hybrid Method* combined estimates of abundance of animals at the surface ($N_{Surface}$) and estimates of foraging animals below the surface (N_{Forage}) and adjusted for the number of duplicates both at and below the surface to achieve an unbiased estimate of total abundance of animals throughout the water column (N_{Total}). To calculate duplicates, we used a subset of the passive acoustic data to develop capture histories that we then used to estimate average transition rates between foraging (below surface) and non-foraging states (at the surface). Additionally,

we used the estimates of N_{Total} and $N_{Surface}$ to derive an estimate of the surface availability correction factor, like what we used in Sections 4.6 through 4.8.

For the capture histories we used a subset of 124 fully annotated click trains from the 2016 dataset and applied it to both the 2016 and 2021 analyses. To estimate N_{Forage} we applied a simple distance sampling analysis to the depth corrected horizontal perpendicular distances calculated from the passive acoustic data using a hazard rate function. To estimate $N_{Surface}$ we applied a mark-recapture distance sampling approach.

Similar to Sigourney et al (2023), we compared both the abundance estimates to a traditional analysis using only the visual line transect data. With the traditional analysis we adjusted for availability bias using an estimate of surface availability for sperm whales calculated from tag data (see Palka et al. 2021). We also compared our derived estimate of availability bias to the estimate calculated from tag data (Palka et al., 2021).

4.11.2 Results and Discussion

We compared 2016 and 2021 estimates of abundance in the covered region around the track lines from the *Hybrid Method* to estimates using traditional methods (**Figure 4-26**). The 2016 estimates were nearly identical. While for 2021, the estimate from the *Hybrid Method* was approximately 25% higher than the estimate from the traditional visual line transect method. Both methods estimated higher overall abundance in 2016 than in 2021. Credible intervals for abundance estimates were substantially narrower for the *Hybrid Method* in both 2016 and 2021, highlighting the ability of the *Hybrid Method* to increase precision. We derived the estimates of abundance of the entire shipboard surveyed area in Section 4.11.

Estimates of surface availability from the *Hybrid Method* were also comparable to the estimates derived from tag data (**Figure 4-27**). As with the abundance estimates, the 2016 surface availability value closely matched the estimate derived from tag data, while the 2021 estimate was lower. The CV for the Hybrid Method availability bias correction factor estimates were 9.8% in 2016 and 10.1% in 2021, both substantially less than the 25% CV obtained from the tag data by Palka et al. (2021).

This analysis showed that the *Hybrid Method* can estimate abundance as accurately as traditional visual-only approaches but with greater precision. Unlike the traditional method, which needs extra tag data to adjust for surface availability bias, the *Hybrid Method* directly corrects for surface availability bias using the visual and acoustic data when they are simultaneously collected.

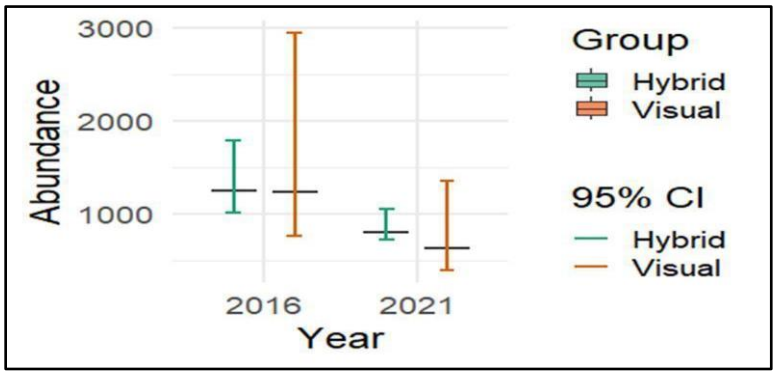

Figure 4-26. Sperm whale abundance derived from the *Hybrid Method* and visual-only method
Abundance is for the covered region only around the track lines, not the entire surveyed area. Colored vertical bars are the derived 95% credible intervals (CI).

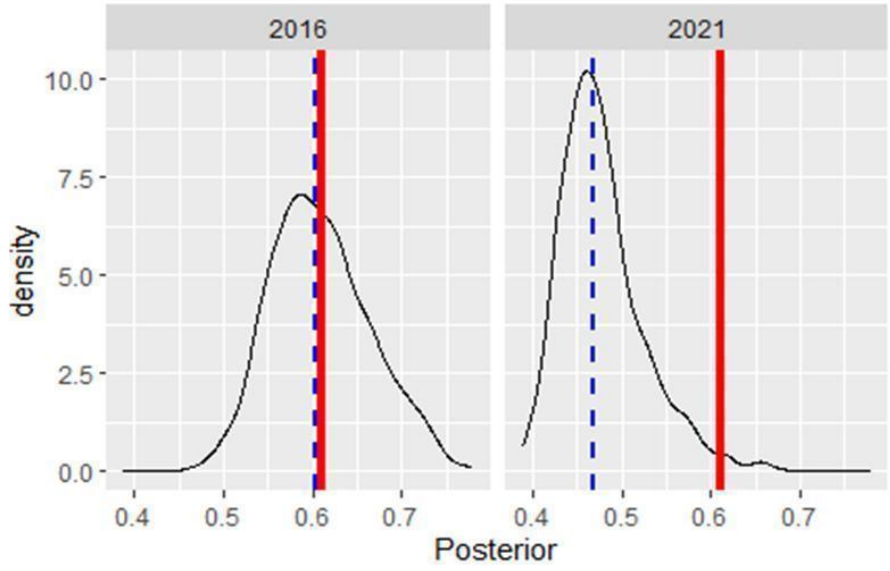

Figure 4-27. Posterior distributions of sperm whale surface availability correction factor
Probability densities of the posterior distributions are displayed. Solid black line indicates *the Hybrid Method* posterior distribution. Dashed blue lines indicate median values of the posterior distributions. Red solid lines indicate the availability bias correction factor estimate derived from tag data used by Palka et al. (2021).

4.12 Comparison of Sperm Whale Abundance Estimation Methods

During AMAPPS shipboard line-transect abundance surveys, we collected both visual and passive acoustic data to study cetaceans. We collected direct visual observations of animals at or near the surface, alongside passive acoustic echolocation clicks (grouped into "events") indicating submerged animals. Historically, we only used the visual data for abundance estimates.

This section focuses on comparing various estimates of sperm whale total-water-column abundance derived from the shipboard survey study area that use various sources of data. We specifically compared comparable estimates from the NEFSC surveys conducted during the summers of 2016 (termed HB1603) and 2021 (termed HB2102) because they occurred in the same time periods and locations and collected both visual and passive acoustic data. We conducted these surveys aboard the NOAA ship *Henry B. Bigelow* (represented by the black lines in **Figure 4-6**in Section 4.6) that covered the shelf break and deeper waters stretching from south of Massachusetts to north of Delaware.

4.12.1 Methods

We estimated the total-water-column abundance of sperm whales for the study areas covered by HB1603 and HB2102 using the following four analysis methods (**Table 4-30**).

1. *Design-based MRDS method*. We developed an annual summer abundance estimate from a design-based covariate mark-recapture distance sampling (MRDS) analysis separately using visual data from only the shipboard surveys in the summers of 2016 and 2021 (Section 4.6). This analysis incorporated a correction for perception bias for missed animals at the surface using the two-independent team visual data. The analysis also incorporated an availability bias correction factor for missed animals subsurface derived from time-depth tag data collected independently of the abundance survey.

2. *GAM SDM method*. We developed an average summer abundance estimate for only the area covered by the shipboard surveys HB1603 and HB2102 from a mark-recapture spatial density-habitat model (SDM) developed by generalized additive models (Section 4.7). This method utilized results from a covariate mark-recapture distance sampling analysis of two-independent team visual data from shipboard and aerial surveys conducted from 2010-2023 across all seasons in a generalized additive model of the relationship between animal density and environmental habitat variables. This analysis incorporated a correction for perception bias for missed animals at the surface using two-independent teams collecting the visual data. The analysis also incorporated the same availability bias correction factor for missed animals below the surface used in the *design-based MRDS method*.
3. *Bayesian SDM method.* We developed an average summer abundance estimate for only the area covered by the shipboard surveys HB1603 and HB2102 derived from a mark-recapture spatial density-habitat model developed by hierarchical Bayesian models (Section 4.8). This method utilized results from a covariate mark-recapture distance sampling analysis of two-independent team visual data from shipboard and aerial surveys conducted from 2010-2023 across all seasons in a hierarchical Bayesian model of the relationship between animal density and environmental habitat variables. This analysis incorporated a correction for perception bias for missed animals at the surface using two-independent teams collecting the visual data. The analysis also incorporated the same availability bias correction factor for missed animals below the surface used in the *design-based MRDS method*.
4. *Integrated visual-PAM hybrid method.* We developed an annual summer abundance estimate for only the area covered by the shipboard surveys HB1603 and HB2102 from the integrated *Hybrid Method* (Section 4.9) that accounts for duplicate detections. This method used the simultaneously collected visual and passive acoustic data from the HB1603 and HB2102 shipboard surveys. We estimated the at-surface abundance with the two-team visual data in a MRDS analysis that incorporated a correction for perception bias for missed animals at the surface. We estimated the subsurface abundance using the passive acoustic data in a conventional distance sampling (CDS) analysis. The analysis accounted for duplicate detections using the *Hybrid Method* that used a subset of the passive acoustic data to develop capture histories that we then used to estimate average transition rates between foraging (subsurface) and non-foraging states (at the surface).

As a reference, we also estimated just the subsurface abundance using:

5. *Design-based CDS method.* We developed an annual summer subsurface foraging sperm whale abundance estimate for each shipboard study area covered during HB1603 and HB2102 using a design-based conventional distance sampling analysis. This analysis used the passive acoustic data from shipboard surveys conducted in the summers of 2016 and 2021. These estimates were not corrected for perception bias of the acoustic data (for example, did not account for foraging animals below the surface we missed even though they were potentially able to be detected and processed, and did not account for non-foraging animals below the surface). We also did not correct these estimates for availability bias for, in this case, animals at the surface that were never below the surface during the time the ship was passing by.

Table 4-30. Analytical methods to estimate sperm whale abundance in NEFSC shipboard area

Method Name	Surface Data Source	Subsurface Data Source	Surface Analysis method	Subsurface Analysis Method	Surface Perception Bias Accounted For	Subsurface Perception Bias Accounted For	Method to Account for Availability Bias	Reference
1. Design MRDS	Visual sightings	Time-depth tags	Design-based 2-team mark-recapture distance-sampling	2-state continuous Markov process	Y	Y	Correction factor	Section 4.6
2. GAM SDM	Visual sightings	Time-depth tags	Two-team MRDS and generalized additive model spatial density-habitat model	2-state continuous Markov process	Y	Y	Correction factor	Section 4.7
3. Bayes SDM	Visual sightings	Time-depth tags	Two-team MRDS and Bayesian spatial density-habitat model	2-state continuous Markov process	Y	Y	Correction factor	Section 4.8
4. Integrated Visual-PAM	Visual sightings	Passive acoustic detections	Design-based 2-team mark-recapture distance-sampling	Conventional distance sampling	Y	N	Average transition rate in Hybrid Method	Section 4.11
5. Design CDS	None	Passive acoustic detections	Design-based 1-team conventional distance sampling	None	N	N	None	Section 4.9

4.12.2 Results and Discussion

Abundance estimates and associated uncertainty intervals differed across methods and between survey years (**Figure 4-28**). However, confidence intervals for the estimates within a survey overlap, with one exception. The only outlier was the estimate for the HB1603 survey derived from the *Integrated Vis-PAM* method.

Several factors may account for variation in point estimates among methods, which we discussed below.

- The *Integrated Vis-PAM* method yielded higher point estimates (particularly in HB1603) and narrower confidence intervals compared to other approaches. This was the only method that utilized passive acoustic data to account for subsurface animals. **Figure 4-28** indicated that the correction factors for subsurface animals, as determined by both the *Integrated Vis-PAM* and *Design Visual* methods, were similar in 2016 (Section 4.11). Therefore, the discrepancy in the HB1603 Integrated Vis-PAM results likely stems from differing calculations of the at-surface abundance estimate.

- The *Bayesian SDM*, *GAM SDM*, and *Design MRDS* methods all utilized the same surface availability bias correction factor. We derived this factor from data collected in separate field

projects using time-depth tags on individual Atlantic animals, which provided full dive cycle data. In contrast, the *Integrated Vis-PAM* method directly estimated abundance using passive acoustic data collected simultaneously with the visual data. For the *Integrated Vis-PAM* method, we used passive acoustic data from only a subsample of acoustically detected animals that were only foraging near the ship to determine the transition rate between at-surface and subsurface animals.

- The *GAM SDM* and *Bayesian SDM* habitat-model based analyses produced the lowest abundance estimates with minimal uncertainty. We applied these methods to visual line-transect data collected across all seasons over many years, 2010 to 2023, then predicted the abundance for just the area and timing of the shipboard surveys. As with most models, extreme small scale localized high abundance regions are typically smoothed out, which may explain the slightly lower estimates.

- Among the model-based methods, the *Bayesian SDM* yielded higher abundance estimates compared to the *GAM SDM*. This outcome is expected because of the strongly skewed posterior distribution of abundance derived from the *Bayesian SDM*, which can lead to elevated overall abundance estimates (Conn et al. 2015). Furthermore, the *Bayesian SDM* employed a distinct formulation of the spatial density model equation, inherently contributing to differences in the resulting estimates.

- The *design MRDS* estimate, derived from a single summer survey, utilized a systematically designed approach. However, this survey had some small gaps in coverage. These uncovered regions could introduce either positive or negative biases. While model-based estimation methods, such as the *GAM SDM* and *Bayesian SDM* could theoretically address these biases more effectively if the modeled relationship between animal density and environmental condition is valid.

Future sensitivity analyses of these methods could clarify which model components most significantly impact abundance estimates. This would also help to elucidate differences when compared to alternative methodologies.

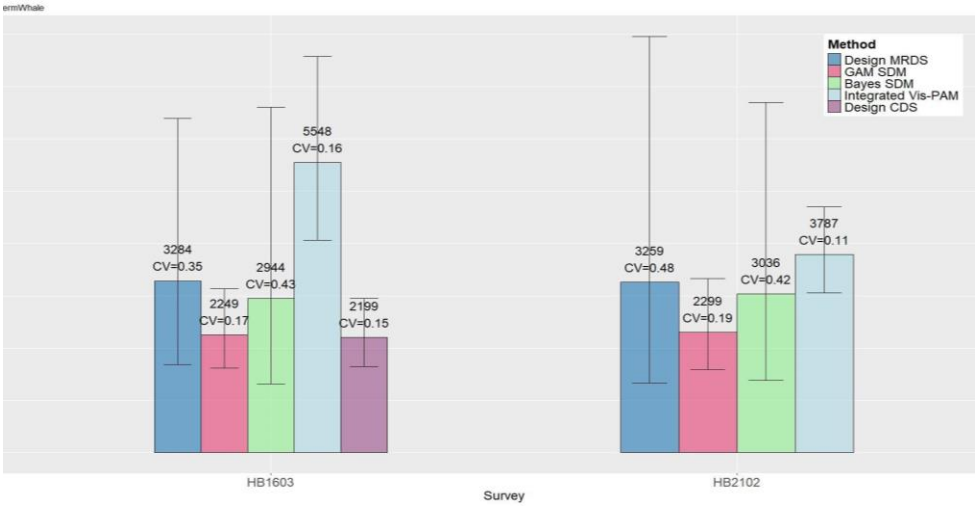

Figure 4-28. Comparison of 2016 and 2021 shipboard abundance estimate of sperm whales
Error bars represent the 95% confidence intervals. Abundance estimates are the number of animals only within the shipboard survey area.

4.13 Abundance Estimates Developed by Collaborators

Abstracts from published papers that used AMAPPS data are below.

North Atlantic right whale density surface model for the U.S. Atlantic validated with passive acoustic monitoring by Roberts et al. 2024 https://doi.org/10.3354/meps14547

ABSTRACT: *"The Critically Endangered North Atlantic right whale* Eubalaena glacialis *entered a population decline around 2011. To save this species without closing the ocean to human activities requires detailed information about its intra-annual density patterns that can be used to assess and mitigate human-caused risks. Using 2.9 million km of visual line-transect survey effort from the U.S. Atlantic and Canadian Maritimes conducted in 2003–2020 by 11 institutions, we modeled the absolute density (ind. km–2) of the species using spatial, temporal, and environmental covariates at a monthly time step. We accounted for detectability differences between survey platforms, teams, and conditions, and corrected all data for perception and availability biases, accounting for platform differences, whale dive behavior, group composition, and group size. We produced maps of predicted density and evaluated our results using independently collected passive acoustic monitoring (PAM) data. Densities correlated positively ($r = 0.46$, $\rho = 0.58$, $\tau = 0.46$) with acoustic detection rates obtained at 492 stationary PAM recorders deployed across the study area (mean recorder duration = 138 d). This is the first study to quantify the concurrence of visual and acoustic observations of the species in U.S. waters. We summarized predictions into mean monthly density and uncertainty maps for the 2003–2009 and 2010–2020 eras, based on the significant changes in the species' spatial distribution that began around 2010. The results quantify the striking distribution shifts and provide effort- and bias-corrected density surfaces to inform risk assessments, estimations of take, and marine spatial planning."*

Sea turtle density surface models along the United States Atlantic coast by DiMatteo et al. 2024. https://doi.org/10.3354/esr01298

ABSTRACT: *"Spatially explicit estimates of marine species distribution and abundance are required to quantify potential impacts from human activities such as military training and testing, fisheries interactions, and offshore energy development. There are 4 protected species of sea turtle loggerhead, green, Kemp's ridley, and leatherback) commonly found along the east coast of the USA, our study area, and which require impact assessments. Data from 7 different survey organizations were used to create density surface models for the 4 sea turtle species utilizing 1.2 million km of line transect surveys. A substantial portion (29.7%) of available sightings were not identified to the species level. Not including these sightings would underestimate density, so a conditional random forest model was used to assign unidentified sightings to species. Higher densities of loggerhead, green, and Kemp's ridley sea turtles were predicted south of the Outer Banks in cool months, transitioning northwards in late spring to occupy seasonal neritic habitats. The highest leatherback densities were predicted off the coasts of Georgia and Florida. Leatherbacks were also predicted throughout offshore areas. The predicted distribution patterns generally matched satellite tracking and strandings data, indicating the models reproduced established seasonal movements. Surveys rarely detect sea turtles smaller than 40 cm, so these age classes are not represented. The models are the first for the study area to apply availability bias estimates developed in or near the study area and attempt to classify unidentified sightings to the species level, providing an updated, critical tool for conservation management along the eastern seaboard."*

Sea turtle distribution and abundance of the east coast of the United States by Sparks and DiMatteo 2023. https://apps.dtic.mil/sti/citations/trecms/AD1206953

ABSTRACT: *"Spatially explicit estimates of species distribution and abundance are required to quantify potential impacts from human activities, such as military training and testing. On the U.S. East Coast, four protected species of sea turtles can commonly be found and require impact assessments. An area of 1.2 million kilometers of line transect surveys from seven different survey organizations were collated to create spatial density models for these species. Almost a third of the available sightings were unidentified turtles. A random forest model was used to assign these unidentified sightings to the species level. Hardshell turtles were predicted to be farther south in cool months, moving northwards in late spring and early summer to occupy seasonal nearshore habitats. Leatherback turtles were predicted to be in high abundance off Florida year-round and at low-to-moderate densities off the continental shelf and in the Gulf of Maine year-round. The models presented here are the first to apply availability bias estimates that have been developed in or near the study area and to classify unidentified sightings to the species level in the region, providing an updated, critical tool to managers responsible for the conservation of these species."*

Marine mammal density models for the U.S. Navy Atlantic Fleet Training and Testing (AFTT) study area for the Phase IV Navy Marine Species Density Database (NMSDD). Document version 1.3 by Roberts et al. 2023. https://seamap.env.duke.edu/seamap-models-files/Duke/Reports/AFTT_Marine_Mammal_Density_Models_2022_v1.3.pdf

4.14 Trends

From 2010 to 2023, AMAPPS I-III gathered line transect abundance data across all seasons. This extensive time series enabled us to investigate the spatial and temporal trends of cetaceans and sea turtles throughout the AMAPPS time period. This section focuses on examining the shifts in observed spatial distribution and abundance trends.

In the first section (4.14.1) we report on the spatiotemporal distribution shifts documented from 2010 to 2017 that used visual abundance data and we published in Chavez-Rosales et al. (2022). In Section 4.14.2 we update the distribution shifts by extending the time series: 2010 - 2023. Next in Section 4.14.3 using passive acoustic and visual data, we focus on distribution changes of beaked whales, while also examining in further detail species-specific responses to the shipboard echosounders used in our surveys.

4.14.1 Cetacean Distribution Shifts from 2010 to 2017

Chavez-Rosales et al. (2022) compared the spatiotemporal distribution patterns of cetaceans from 2010 versus 2017 using the AMAPPS line transect visual sightings survey data. They examined 16 cetacean species habitat suitability in the western North Atlantic Ocean using generalized additive models. They based the models on observed species distributions as a function of 21 environmental covariates and then compared species-specific core habitats between 2010 and 2017. They identified seasonal differences in patterns of habitat change across guilds and an average northward shift of 178 km across the AMAPPS study area (**Figure 4-29**; **Table 4-31**).

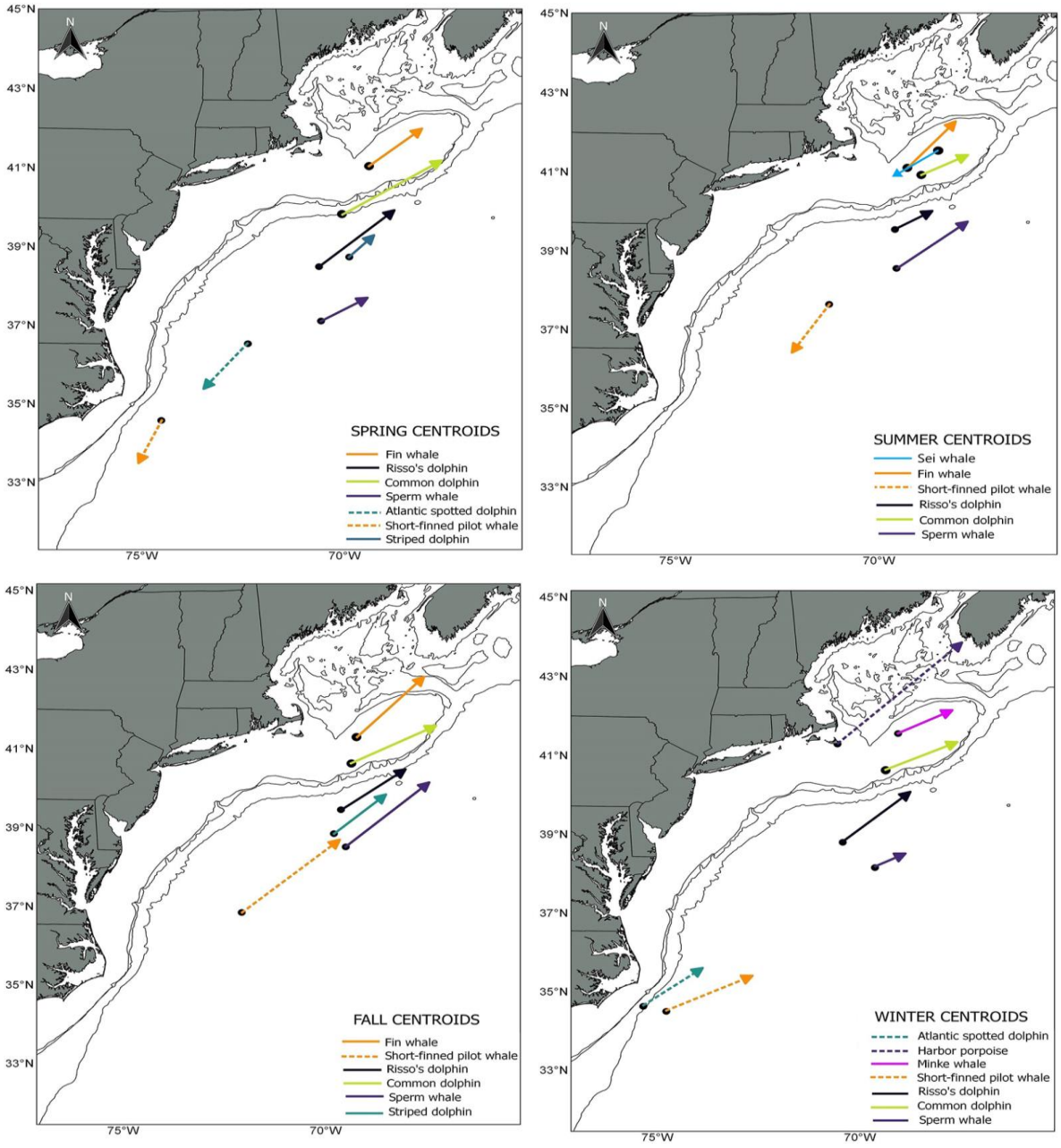

Figure 4-29. Direction and magnitude of core habitat shifts of cetaceans between 2010 and 2017
From Figure 2 of Chavez-Rosales et al. (2022). We only plotted species with more than a 70 km shift difference. The black dot represents the 2010 location of the seasonal weighted centroid for a species, while the tip of the arrow is the corresponding 2017 location.

Table 4-31. Difference in km and direction of the core habitat weighted centroid shift: 2010 to 2017
From Table 3 in Chavez-Rosales et al. (2022). Scientific names of species in Appendix A. NA indicates not available.

Species	Spring Diff	Spring Direction	Summer Diff	Summer Direction	Fall Diff	Fall Direction	Winter Diff	Winter Direction
Atlantic spotted dolphin	151	SW	25	SE	15	SE	165	NE
Beaked whale, Cuvier's	NA	NA	69	NE	NA	NA	NA	NA
Beaked whale, Sowerby's	NA	NA	5	SE	NA	NA	NA	NA
Common bottlenose dolphin	294	NE	505	NE	753	NE	211	NE
Fin whale	154	NE	162	NE	223	NE	33	NE
Harbor porpoise	17	SW	3	NE	10	SW	397	NE
Humpback whale	17	S	17	S	14	NW	3.9	SW
Minke whale	40	NE	14	NW	10	W	133	NE
Short-finned pilot whale	120	SW	149	SW	296	NE	218	NE
Long-finned pilot whale	39	NE	38	NE	69	E	2	NE
Risso's dolphin	232	NE	89	NE	182	NE	202	NE
Sei whale	70	SW	97	SW	134	SW	179	SW
Common dolphin	267	NE	111	NE	216	NE	205	NE
Sperm whale	114	NE	202	NE	255	NE	71	NE
Striped dolphin	71	NE	41	NE	155	NE	30	NE
White-sided dolphin	29	NE	13	W	23	NW	26	NE
Mean	115		96		168		134	

4.14.2 Updated Spatiotemporal Distribution Shifts using Visual Data

We are in the process of writing a document that updates the spatiotemporal patterns of cetaceans and sea turtles that we will submit to a peer-reviewed journal. This section provides a sample of what we are considering for this document for the species humpback whales (**Figure 4-30**), harbor porpoises (**Figure 4-31**), and loggerhead turtles (**Figure 4-32**). In this update, we investigated the spatiotemporal patterns using the generalized additive habitat-density models (Section 4.7). These models, developed from visual sightings data collected during shipboard and aerial surveys from 2010 to 2023 across all seasons, predict animal density (number of animals/km^2) and abundance (density * area). We generated seasonal predictions for 10km x 10km grid cells every 8 days, starting January 4, 2010, within the AMAPPS study area, where the average seasonal maps are in **Appendices B-D**.

To analyze trends within a season for cetaceans, we calculated and plotted the average seasonal abundance for each grid cell separately for the years 2010 and 2023. To highlight spatial differences between these years, we subtracted the 2010 seasonal abundance estimate from the 2023 estimate for each grid cell and plotted the difference (**Figures 4-30 - 4-31**, panels A-D). Red cells indicate regions where 2021 abundance exceeded 2016, while blue cells indicate a reduction. Because we completed the sea turtle analyses before the 2022 and 2023 data were available, we used the average seasonal abundance patterns for 2010 versus 2021 (**Figure 4-32**, panels A-D).

We illustrated overall within-year patterns by plotting the total abundance of the AMAPPS study area per 8-day time series for each year (**Figures 4-30 - 4-31**, panel E). We illustrated overall between-year patterns by plotting the time series of seasonal average abundances (colored lines in **Figures 4-30 - 4-32**, panel F) plotted over the time series of 8-day abundances (light gray line in **Figures 4-30 - 4-32**, panel F).

To assess simple annual growth rates, we used a quasi-Poisson generalized linear model, with the seasonal average abundance as the response variable and year (continuous) and season (factor) as predictors. We then estimated the approximate annual growth rate as { [exp(coefficient of the year variable) * 4 seasons] - 1} and annotated panel F with the estimated average growth rate.

We found that the generalized additive models for humpback whales predicted an overall annual increase of 1.1% within the AMAPPS study area between 2010 and 2023 (**Figure 4-30**). Within the study area, more humpback whales were present in the summer and were increasingly congregating around the coastal waters between southern Maine and Long Island, NY, especially in the summer.

We found that the generalized additive models for harbor porpoises predicted an overall annual increase of 2.8% within the AMAPPS study area between 2010 and 2023 (**Figure 4-31**). Within the study area, more harbor porpoises were present in the spring and fall and were increasingly shifting northeastern with the largest increases in Canadian waters south of Nova Scotia.

We found that the generalized additive models for loggerhead turtles predicted an overall annual decrease of 1.9% within the AMAPPS study area between 2010 and 2023 (**Figure 4-32**). Within the study area, more loggerheads were in the continental shelf waters from southern New Jersey to northern North Carolina, particularly in the summer to winter time period.

We also want to explore the temporal and larger scale spatial trends as described by the summer abundance time series of design-based abundance estimates developed from 1991 to 2021. Furthermore, we want to explore the locations of the core habitats of each species.

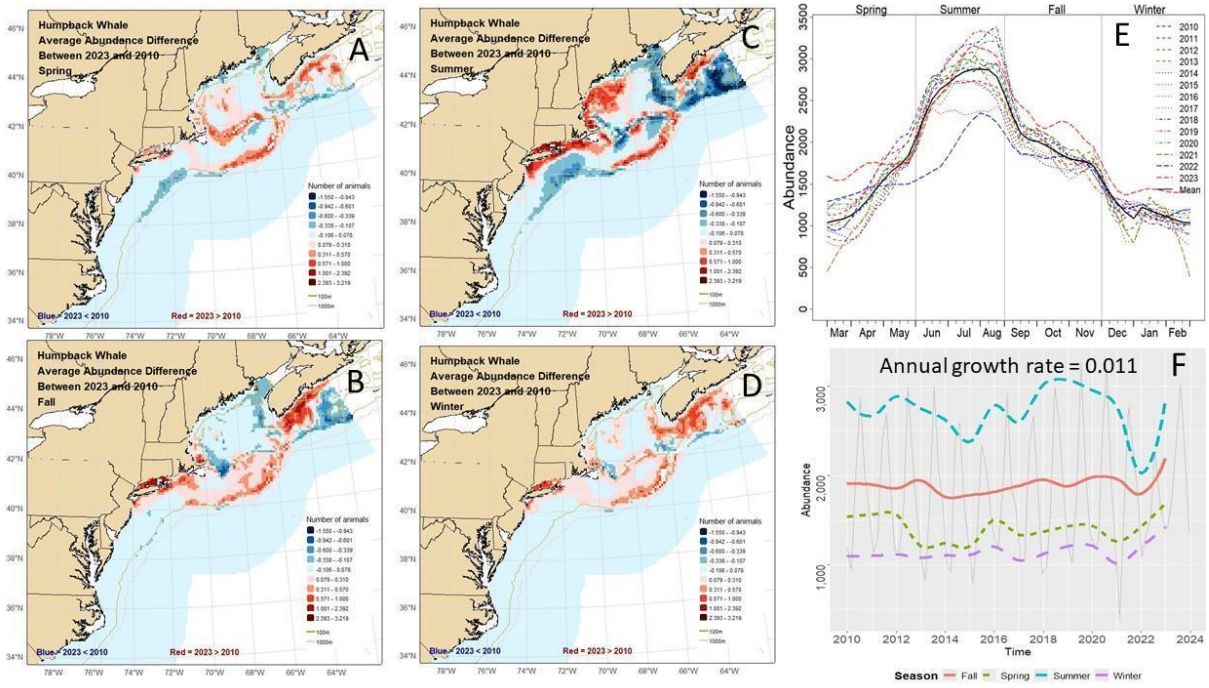

Figure 4-30. Spatiotemporal trends of humpback whales based on generalized additive models
Panels A-D illustrate the difference in abundance between 2021 and 2010, with red cells indicating areas where 2021 abundance exceeded that of 2010. Panel E displays the within-year time series of abundance for each year, distinguished by different colors and line types. Panel F presents the between-year seasonal time series of abundances and the estimated annual growth rate, which we calculated using a quasi-Poisson generalized additive model of the seasonal abundance estimates.

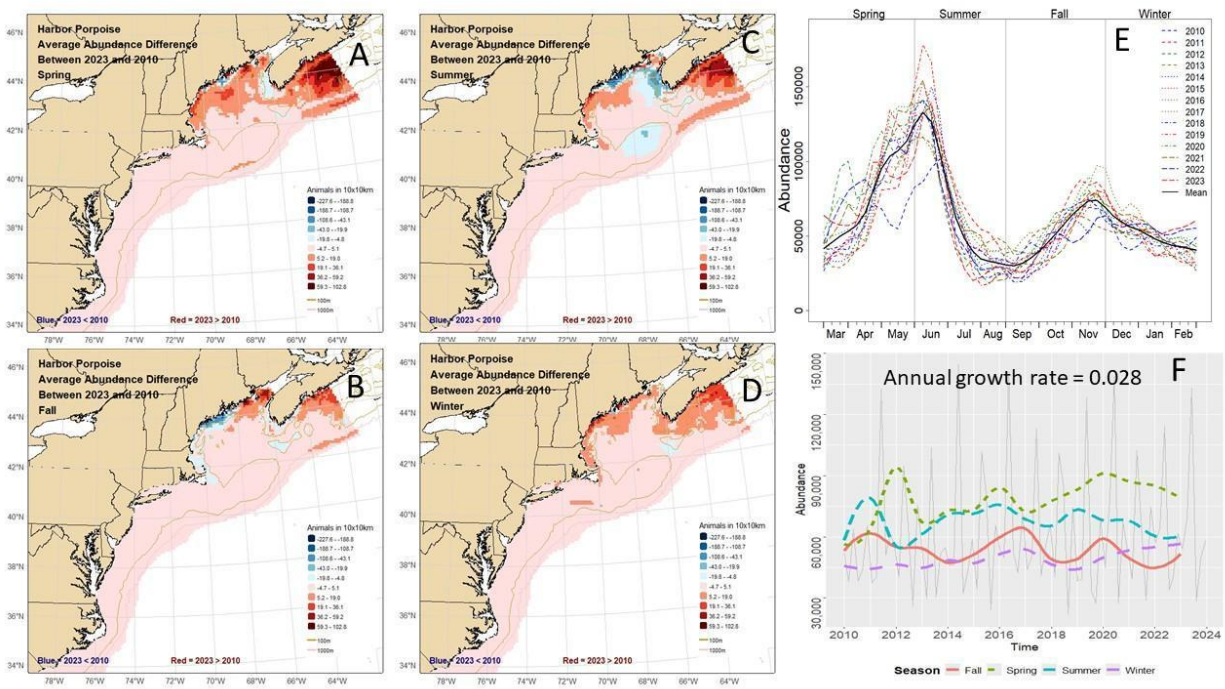

Figure 4-31. Spatiotemporal trends of harbor porpoises based on generalized additive models
Panels A-D illustrate the difference in abundance between 2021 and 2010, with red cells indicating areas where 2021 abundance exceeded that of 2010. Panel E displays the within-year time series of abundance for each year, distinguished by different colors and line types. Panel F presents the between-year seasonal time series of abundances and the estimated annual growth rate, which we calculated using a quasi-Poisson generalized additive model of the seasonal abundance estimates.

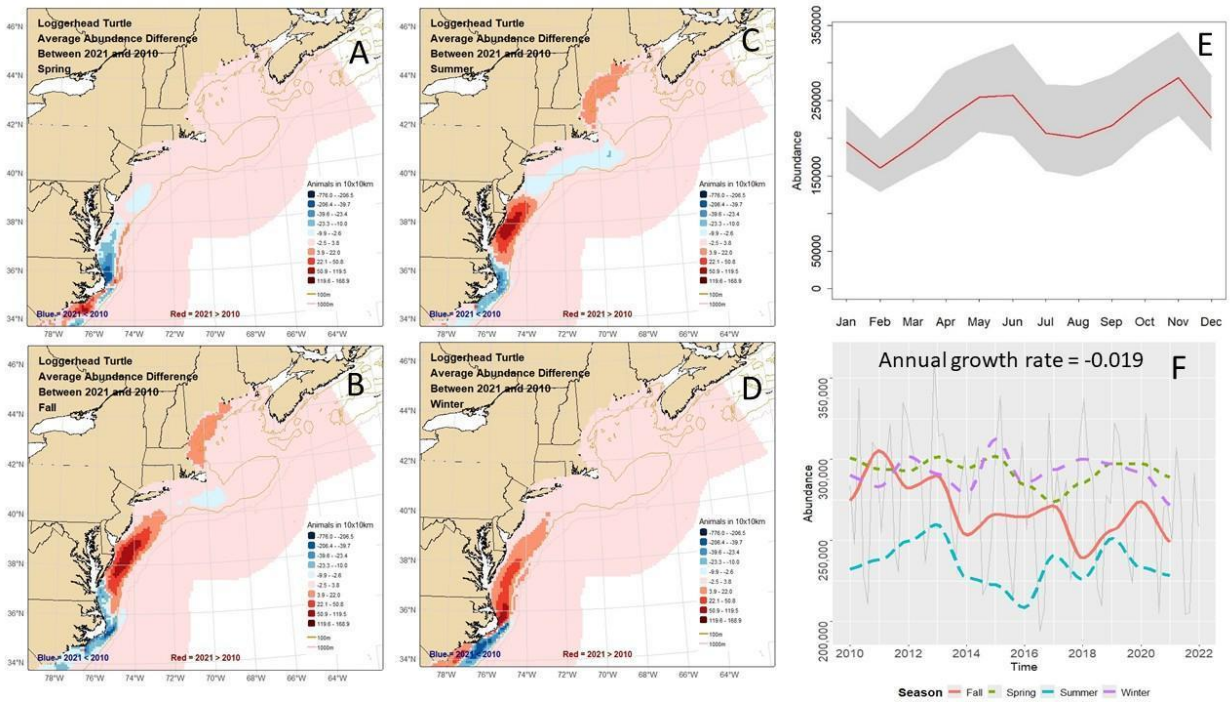

Figure 4-32. Spatiotemporal trends of loggerhead turtles based on generalized additive models
Panels A-D illustrate the difference in abundance between 2021 and 2010, with red cells indicating areas where 2021 abundance exceeded that of 2010. Panel E displays the within-year time series of abundance for each year, distinguished by different colors and line types. Panel F presents the between-year seasonal time series of abundances and the estimated annual growth rate, which we calculated using a quasi-Poisson generalized additive model of the seasonal abundance estimates.

4.14.3 Updated Spatiotemporal Distribution Shifts of Beaked Whales

As mentioned above in Section 4.14.1 the previous study by Chavez-Rosales et al. (2022) compared the abundance patterns using visual data from 2010 to 2017, revealing shifts in the core habitat centroids for goose-beaked and Sowerby's beaked whales during the summer. Specifically, the core habitat centroid for goose-beaked whales showed a 69 km shift to the northeast, while Sowerby's beaked whales shifted 5 km to the southeast (**Table 4-31**).

During AMAPPS III, we improved our understanding of beaked whale spatiotemporal patterns by integrating new visual and passive acoustic data. This allowed us to update previous investigations into potential changes in their distribution across time and space. Our analysis relied on two main approaches. The first approach used passive acoustic detections, where we tabulated and plotted the passive acoustic detections from towed hydrophone arrays used during NEFSC shipboard surveys conducted in the summers of 2013, 2016, and 2021. Note, these acoustic data were also integral to estimating the abundance of vocalizing beaked whales (Sections 4.2.3 and 4.10). The second approach used the spatial generalized additive models that we developed from visual shipboard and aerial survey data collected across all seasons from 2010 to 2023 (see Section 4.7 for model details).

The goose-beaked whale' passive acoustic distribution map for the three summer surveys (**Figure 4-33 top left**) and predicted summer visual abundance spatial distribution maps for 2016 and 2021 (**Figures 4-34A and 4-34C**) revealed the overall large scale distribution patterns were similar. The predicted summer abundance was similar each summer during 2010 to 2023 (**Figure 4-34D**). However, on a finer scale, the predicted visual distribution shifted slightly towards the northeastward along the shelf break, particularly in waters less than 1000 m depth, although the magnitude of the difference between 2016 and 2021 was

small (**Figures 4-34B and 4-34D**). This was also the case when comparing 2010 to 2017 (**Table 4-31**; Chavez-Rosales et al. 2022).

The overall abundance of Sowerby's beaked whales within the AMAPPS study area appears to be increasing at about 3.6% annually (**Figure 4-35D**). The Sowerby's beaked whales' distribution of acoustic detections (**Figure 4-33 top right**) and visual detections (**Figures 4-35 A-C**) appear to have shifted northward between 2016 and 2021.

The overall abundance of True's beaked whales within the AMAPPS study area appears to have decreased (3.6%) between 2010 and 2023 (**Figure 4-36D**). There was not an obvious shift of the distribution of the True's between the 2016 and 2021 surveys, but rather areas of consistent detections were observed across the New England seamount chain and the nearby canyons along the southern edge of Georges Bank (**Figures 4-33 bottom left and 4-36**).

No conclusions could be drawn about Gervais' beaked whale due to the paucity of detections (**Figure 4-33 bottom right**). However, the very offshore presence of Gervais' beaked whales in the north aligns with what was reported in DeAngelis et al. (2025), which is presence in the Gulf Stream.

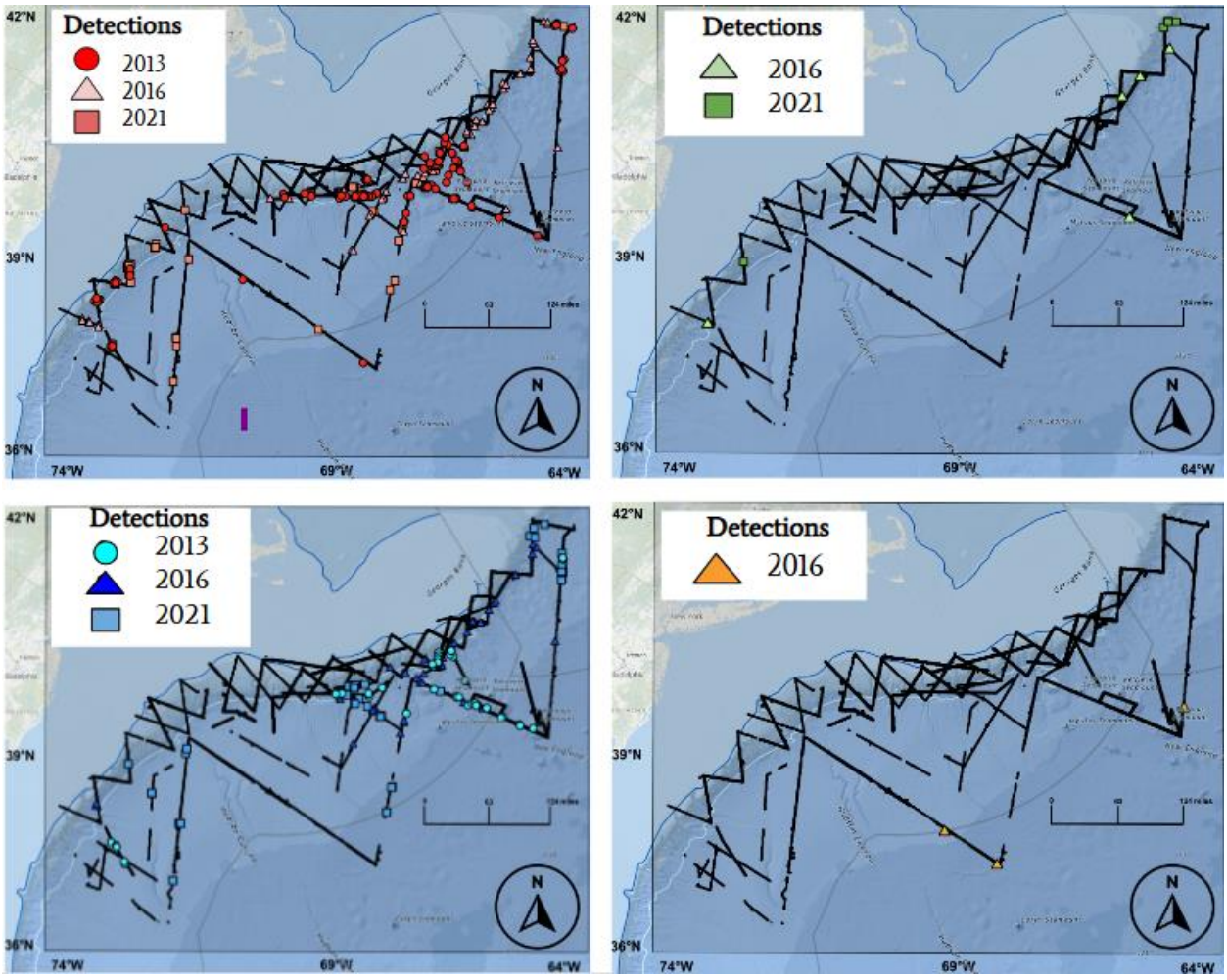

Figure 4-33. Maps of beaked whale acoustic detections by species and survey
Acoustic detected collected from passive acoustic towed hydrophones from HB1303 (circles), HB1603 (triangles), and HB2102 (squares). Top left: goose-beaked, top right: Sowerby's, bottom left: True's, bottom right: Gervais' beaked whale detections.

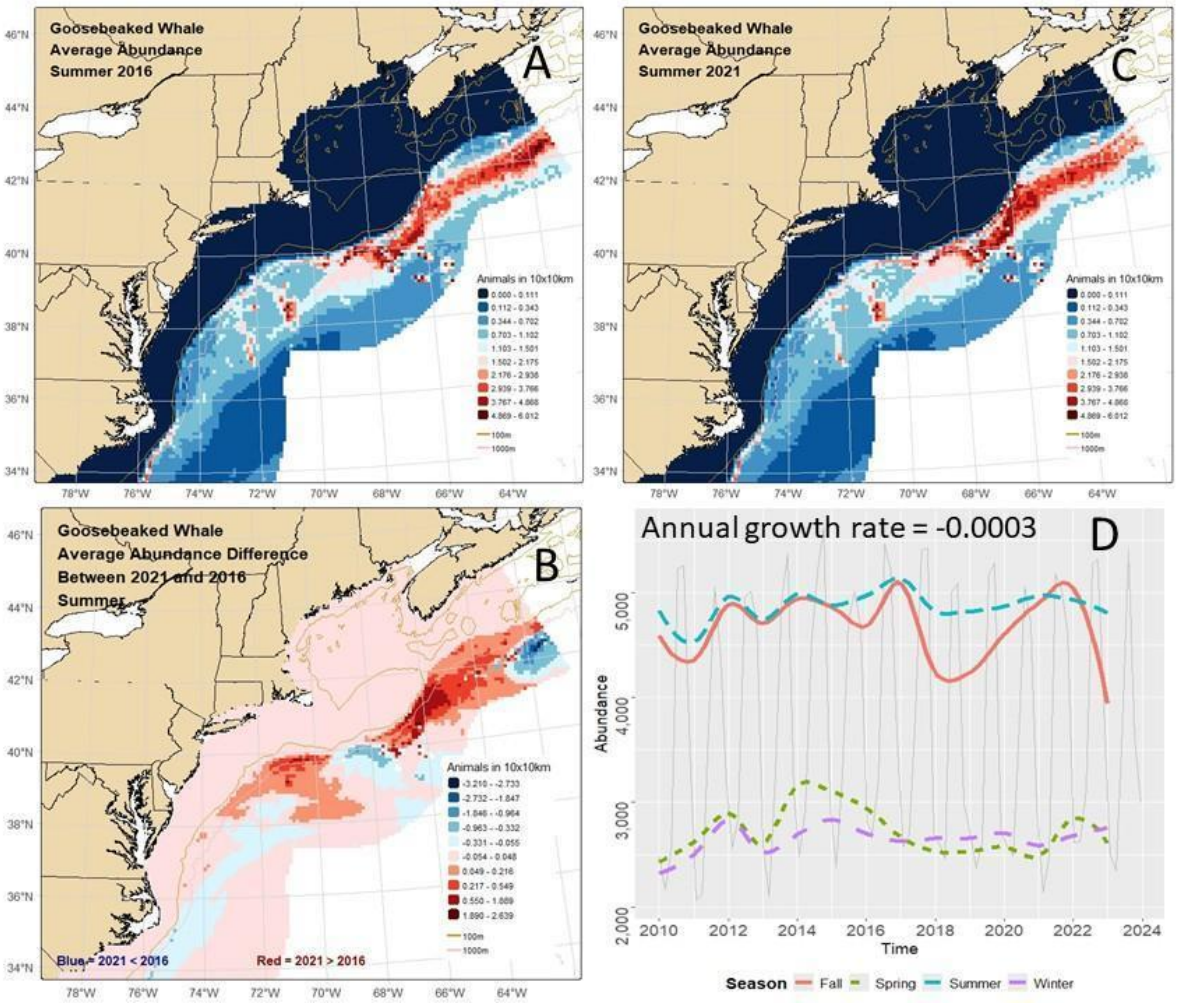

Figure 4-34. Spatiotemporal trends of goose-beaked whales based on generalized additive models
Panels A and C illustrate the spatial distribution of the summer abundance of 2016 and 2021, respectively, that corresponds to HB1603 and HB2102. Panel B illustrates the difference in abundance between 2021 and 2016, with red cells indicating areas where 2021 abundance exceeded that of 2016. Panel D presents the seasonal time series of abundances and the estimated annual growth rate, which we calculated using a quasi-Poisson generalized additive model of the seasonal abundance estimates.

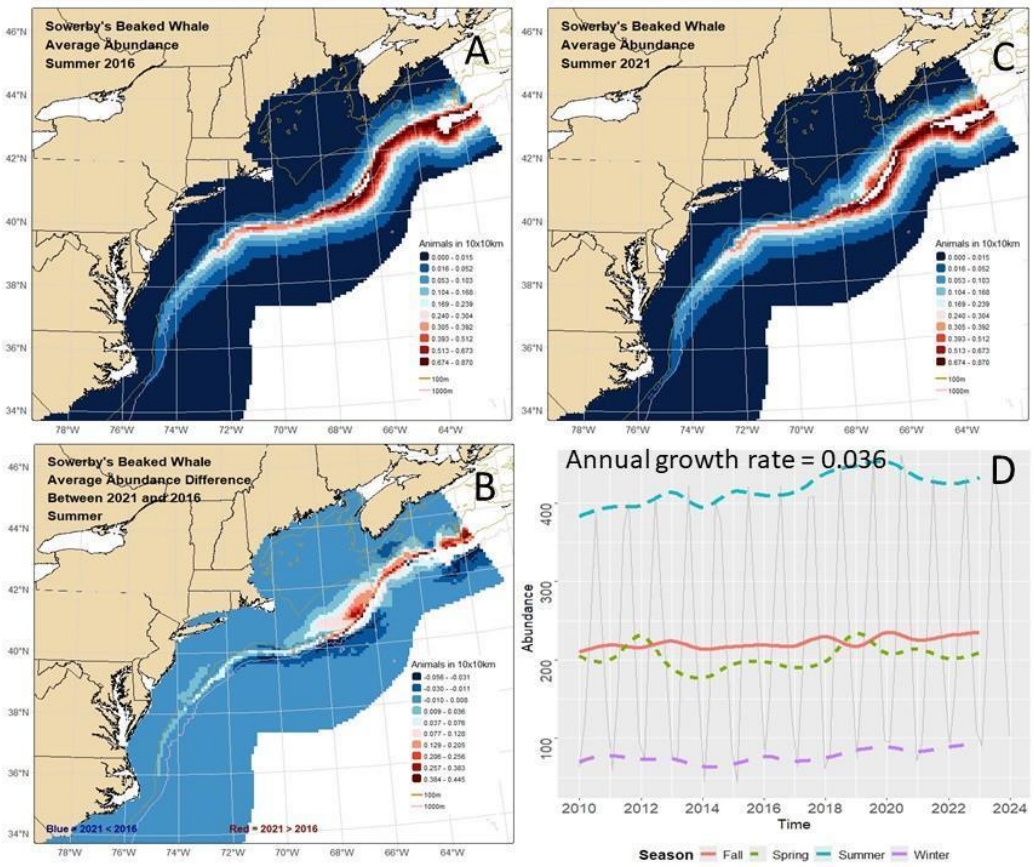

Figure 4-35. Spatiotemporal trends of Sowerby's beaked whales based on generalized additive models

Panels A and C illustrate the spatial distribution of the summer abundance of 2016 and 2021, respectively, that corresponds to HB1603 and HB2102. Panel B illustrates the difference in abundance between 2021 and 2016, with red cells indicating areas where 2021 abundance exceeded that of 2016. Panel D presents the seasonal time series of abundances and the estimated annual growth rate, which we calculated using a quasi-Poisson generalized additive model of the seasonal abundance estimates.

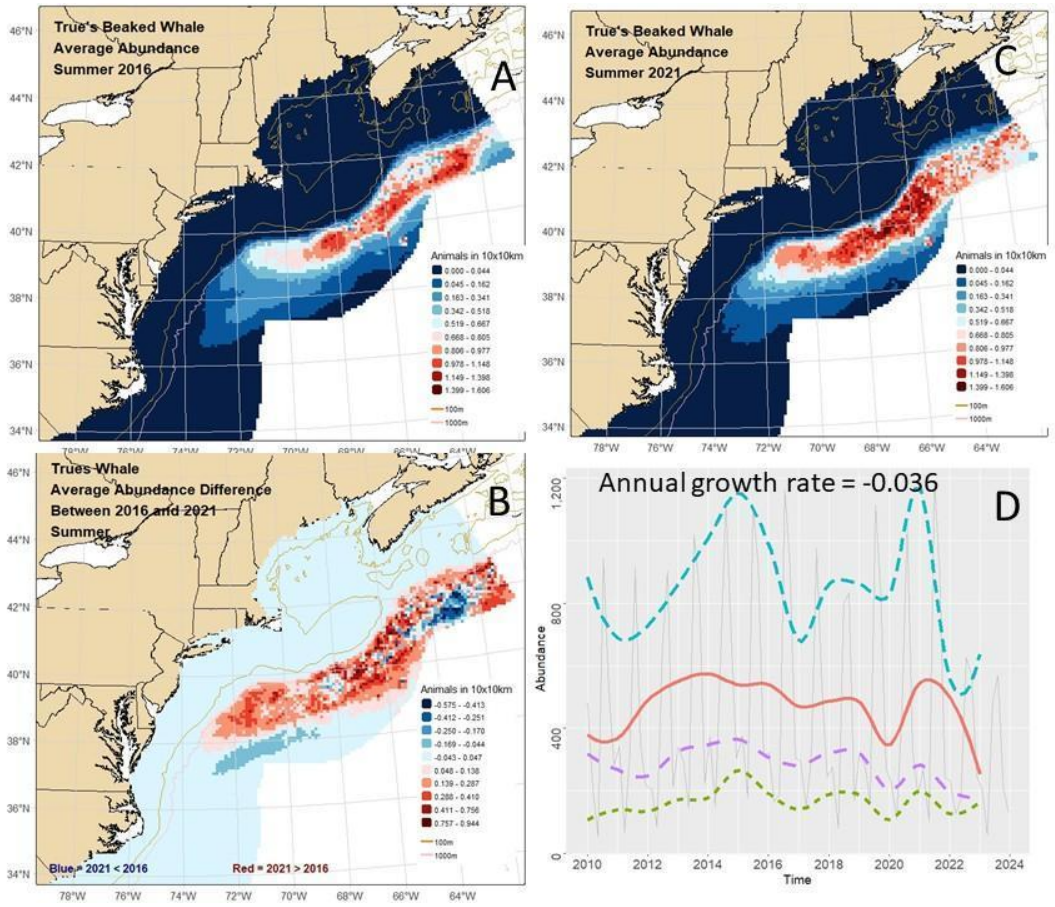

Figure 4-36. Spatiotemporal trends of True's beaked whales based on generalized additive models
Panels A and C illustrate the spatial distribution of the summer abundance of 2016 and 2021, respectively, that corresponds to HB1603 and HB2102. Panel B illustrates the difference in abundance between 2021 and 2016, with red cells indicating areas where 2021 abundance exceeded that of 2016. Panel D presents the seasonal time series of abundances and the estimated annual growth rate, which we calculated using a quasi-Poisson generalized additive model of the seasonal abundance estimates.

4.15 References Cited

Alcázar-Treviño J, Johnson M, Arranz P, Warren VE, Pérez-González CJ, Marques T, Madsen PT, Aguilar de Soto N. 2021. Deep-diving beaked whales dive together but forage apart. Proc R Soc B. 288(1942):20201905. https://doi.org/10.1098/rspb.2020.1905

Baumann-Pickering S, McDonald MA, Simonis AE, Solsona Berga A, Merkens KPB, Oleson EM, Roch MA, Wiggins SM, Rankin S, Yack TM, Hildebrand JA. 2013. Species-specific beaked whale echolocation signals. J Acoust Soc Am. 134(3):2293–2301. https://doi.org/10.1121/1.4817832

Baumann-Pickering S, Trickey J, Wiggins S, Oleson E. 2016. Odontocete occurrence in relation to changes in oceanography at a remote equatorial Pacific seamount. Mar Mamm Sci. 32(2):805–825.

Boisseau O, Nowacek D, Pabst DA, Roberts J, Blawas A, Clabaugh A, McLanaghan R, Moscrop A, Levenson JJ. 2024. Passive acoustic surveys demonstrate high densities of sperm whales off the mid-

Atlantic coast of the USA in winter and spring. Mar Env Res. 201:106674. https://doi.org/10.1016/j.marenvres.2024.106674

Boisseau O, Nowacek D, Roberts J, Pabst DA, Clabaugh A, Moscrop A, McLanaghan R, Yack T, Levenson JJ. 2023. Acoustic density estimates of beaked whales off the mid-Atlantic coast of the USA in winter and spring. Deep Sea Res Part I: Ocean Res Papers. 199:104108. https://doi.org/10.1016/j.dsr.2023.104108

Broadus L, Carroll G, Gonzalez-Sols J, Henry L-A, Leitner A, Stæhr SU, Göke C, Holbach A, Neves V, Paiva V, et al. 2025. A perspective on quantifying the attractiveness of seamounts for marine megafauna. Authorea. https://doi.org/10.22541/au.174599647.77520271/v1

Chang J. Collapsed Gibbs Sampling Methods for Topic Models. R package version 1.5.2. 10.22541/au.174599647.77520271/v1

Chavez-Rosales S, Josephson E, Palka D, Garrison L. 2022. Detection of habitat shifts of cetacean species: A comparison between 2010 and 2017 habitat suitability conditions in the Northwest Atlantic Ocean. Front Mar Sci. 9. https://doi.org/10.3389/fmars.2022.877580

Chavez-Rosales S, Palka DL, Garrison LP, Josephson EA. 2019. Environmental predictors of habitat suitability and occurrence of cetaceans in the western North Atlantic Ocean. Sci Rep. 9(1):5833. https://doi.org/10.1038/s41598-019-42288-6

Chavez-Rosales S, Palka DL, Garrison LP, Josephson EA. in review. Sea turtle habitat, occurrence, and abundance patterns on the Northeast U.S. coast.

Cholewiak D, DeAngelis AI, Palka D, Corkeron PJ, Van Parijs SM. 2017. Beaked whales demonstrate a marked acoustic response to the use of shipboard echosounders. R Soc Open Sci. 4(12):170940. https://doi.org/10.1098/rsos.170940

Cioffi WR, Quick NJ, Foley HJ, Waples DM, Swaim ZT, Shearer JM, Webster DL, Friedlaender AS, Southall BL, Baird RW, et al. 2021. Adult male Cuvier's beaked whales (*Ziphius cavirostris*) engage in prolonged bouts of synchronous diving. Mar Mam Sci. 37(3):1085–1100. https://doi.org/10.1111/mms.12799

Clarke E, Feyrer LJ, Moors-Murphy H, Stanistreet J. 2019. Click characteristics of northern bottlenose whales (Hyperoodon ampullatus) and Sowerby's beaked whales (Mesoplodon bidens) off eastern Canada. J Acoust Soc Am. 146(1):307. https://doi.org/10.1121/1.5111336

Cohen RE, Frasier KE, Baumann-Pickering S, Wiggins SM, Rafter MA, Baggett LM, Hildebrand JA. 2022. Identification of western North Atlantic odontocete echolocation click types using machine learning and spatiotemporal correlates. PLOS ONE. 17(3):e0264988. https://doi.org/10.1371/journal.pone.0264988

Conn P, Johnson D, Hoef J, Hooten B, London J, Boveng P. 2015. Using spatiotemporal statistical models to estimate animal abundance and infer ecological dynamics from survey counts. Ecol Monog. 85(2):235–252.

DeAngelis AI, Stanistreet JE, Baumann-Pickering S, Cholewiak DM. 2018. A description of echolocation clicks recorded in the presence of True's beaked whale (Mesoplodon mirus). J Acoust Soc Am. 144(5):2691. https://doi.org/10.1121/1.5067379

DeAngelis AI, Valtierra R, Van Parijs SM, Cholewiak D. 2017. Using multipath reflections to obtain dive depths of beaked whales from a towed hydrophone array. J Acoust Soc Am. 142(2):1078. https://doi.org/10.1121/1.4998709

DeAngelis AI, Westell A, Baumann-Pickering S, Bell J, Cholewiak D, Corkeron PJ, Soldevilla MS, Solsona-Berga A, Trickey JS, Parijs SMV. 2025. Habitat utilization by beaked whales in the western North Atlantic Ocean using passive acoustics. Mar Eco Prog Ser. 754:137–153. https://doi.org/10.3354/meps14771

DeRuiter SL, Southall BL, Calambokidis J, Zimmer WMX, Sadykova D, Falcone EA, Friedlaender AS, Joseph JE, Moretti D, Schorr GS, et al. 2013. First direct measurements of behavioural responses by Cuvier's beaked whales to mid-frequency active sonar. Biol Let. 9(4):20130223. https://doi.org/10.1098/rsbl.2013.0223

Garrison L, Barry K, Hoggard W. 2017. The abundance of coastal morphotype bottlenose dolphins on the U.S. east coast: 2002-2016. Southeast Fisheries Science Center Reference Document PRBD-2017-01. https://repository.library.noaa.gov/view/noaa/50343

Garrison L, Rosel P. 2017. Partitioning short-finned and long-finned pilot whale bycatch estimates using habitat and genetic information. Southeast Fisheries Science Center, Protected Resources and Biodiversity Division, 75 Virginia Beach Dr., Miami, FL 33140. PRBD Contribution # PRBD-2016-17.

Garrison LP, Aichinger Dias L. 2024. Abundance of Tamanend's Bottlenose Dolphins (Tursiops erebennus) along the U.S. Atlantic Coast from Aerial Surveys Conducted During Summer 2021. Southeast Fisheries Science Center reference document ; MMTD-2024-04. https://doi.org/10.25923/21jw-pc06

Garrison LP, Dias LA. 2023. Abundance of marine mammals in Waters of the Southeastern U.S. Atlantic During Summer 2021.SEFSC MMTD Contribution MMTD-2023-01. https://doi.org/10.25923/ce0d-9e10

Gillespie D, Gordon J, McHugh R, McLaren D, Mellinger D, Redmond P. 2008. PAMGUARD: Semiautomated, open source software for real-time acoustic detection and localization of cetaceans. Proc Inst Acoust. 30(5). https://pubs.aip.org/asa/jasa/article/125/4_Supplement/2547/698127/PAMGUARD-Semiautomated-open-source-software-for

Hatch JM, Haas HL, Sasso CR, Patel SH, Smolowitz RJ. 2022. Estimating the complex patterns of survey availability for loggerhead turtles. J Wildl Manage. 86(4):e22208. https://doi.org/10.1002/jwmg.22208

Hayes SA, Josephson E, Maze-Foley K, Rosel PE, McCordic J, Brossard A, Chavez-Rosales S, Cole TVN, Garrison LP, Hatch J, et al. 2024. U.S. Atlantic and Gulf of Mexico Marine Mammal Stock Assessments 2023. NOAA Technical Memorandum NMFS-NE-321. https://www.fisheries.noaa.gov/s3/2025-01/Atlantic-MMSAR-122025.pdf

Hazen EL, Nowacek DP, Laurent LS, Halpin PN, Moretti DJ. 2011. The relationship among oceanography, prey fields, and beaked whale foraging habitat in the Tongue of the Ocean. PLOS ONE. 6(4):e19269. https://doi.org/10.1371/journal.pone.0019269

Kannan R. 2020. Postcard from the Atlantic Ocean. Indian Birds [Internet]. 15(5). https://indianbirds.in/pdfs/IB_15_5_Kannan_AtlanticOcean.pdf

Keating JL, Barlow J. 2013. Summary of P amguard beaked whale click detectors and classifiers used during the 2012 Southern California behavioral response study. NOAA-TM-NMFS-SWFSC-517. https://repository.library.noaa.gov/view/noaa/4535

Laake J, Borchers D, Thomas L, Miller D. 2022. mrds: Mark-Recapture Distance Sampling. R package version 2.2.7.

Laake J, Miller D, Petersma F. 2025. mrds: Mark-Recapture Distance Sampling. R package version 3.0.1. https://CRAN.R-project.org/package=mrds

Laake JL, Borchers DL. 2004. Methods for incomplete detection at distance zero. In: Buckland ST, Andersen DR, Burnham KP, Laake JL, Thomas L, editors. Advanced distance sampling. New York: Oxford University Press; p. 108–189.

Laake JL, Calambokidis J, Osmek SD, Rugh DJ. 1997. Probability of detecting harbor porpoise from aerial surveys: Estimating g(0). J Wildl Manage. 61(1):63–75. https://doi.org/10.2307/3802415

MacLeod CD, Perrin WF, Pitman R, Barlow J, Ballance L, D'Amico A, Gerrodette T, Joyce G, Mullin KD, Palka DL, Waring GT. 2005. Known and inferred distributions of beaked whale species (Cetacea: Ziphiidae). J Cetacean Res Manage. 7(3):271–286. https://doi.org/10.47536/jcrm.v7i3.737

McCarthy E, Moretti D, Thomas L, DiMarzio N, Morrissey R, Jarvis S, Ward J, Izzi A, Dilley A. 2010. Changes in spatial and temporal distribution and vocal behavior of Blainville's beaked whales (*Mesoplodon densirostris*) during multiship exercises with mid-frequency sonar. Mar Mam Sci. http://nova.wh.whoi.edu/prospecieslit/McCarthy et al. - 2010 - Changes in spatial and temporal distribution and v.pdf

McCullough JLK, Simonis AE, Sakai T, Oleson EM. 2021. Acoustic classification of false killer whales in the Hawaiian islands based on comprehensive vocal repertoire. JASA Express Lett. 1(7):071201. https://doi.org/10.1121/10.0005512

McLaren I. 1961. Methods of determining the numbers and availability of ringed seals in the Eastern Canadian Arctic. Arctic. 14(3):162–175.

Merkens K, Mann D, Janik VM, Claridge D, Hill M, Oleson E. 2018. Clicks of dwarf sperm whales (*Kogia sima*). Mar Mam Sci. 34(4):963–978. https://doi.org/10.1111/mms.12488

Miller D, Rextad E, Burt L, Bravington M, Hedley S. 2021. dsm: Density Surface Modelling of Distance Sampling Data. R package version 2.3.1. https://cran.r-project.org/web/packages/dsm/index.html

Miller DL, Fifield D, Wakefield E, Sigourney DB. 2021. Extending density surface models to include multiple and double-observer survey data. PeerJ. 9:e12113. https://doi.org/10.7717/peerj.12113

Morato T, Miller PI, Dunn DC, Nicol SJ, Bowcott J, Halpin PN. 2016. A perspective on the importance of oceanic fronts in promoting aggregation of visitors to seamounts. Fish and Fisheries. 17(4):1227–1233. https://doi.org/10.1111/faf.12126

Morisaka T, Connor RC. 2007. Predation by killer whales (*Orcinus orca*) and the evolution of whistle loss and narrow-band high frequency clicks in odontocetes. J Evol Biol. 20(4):1439–1458. https://doi.org/10.1111/j.1420-9101.2007.01336.x

Northeast Fisheries Science Center (U.S.), Southeast Fisheries Science Center (U.S.). 2021 Annual Report of a Comprehensive Assessment of Marine Mammal, Marine Turtle, and Seabird Abundance and Spatial Distribution in U.S. waters of the Western North Atlantic Ocean : AMAPPS III: 2022. https://doi.org/10.25923/jazw-5467

Palka D. 2020. Cetacean Abundance in the U.S. Northwestern Atlantic Ocean: Summer 2016. Northeast Fish Sci Cent Ref Doc. 20-05. https://doi.org/10.25923/1mrt-tn89

Palka D, Aichinger Dias L, Broughton E, Chavez-Rosales S, Cholewiak D, Davis G, DeAngelis A, Garrison L, Haas H, Hatch J, et al. 2021. Atlantic Marine Assessment Program for Protected Species: FY15-FY19.OCS Study BOEM 2021-051 https://repository.library.noaa.gov/view/noaa/47287

Palka D, Chavez-Rosales S, Josephson E, Cholewiak D, Haas H, Garrison L, Jones M, Sigourney D, Waring G, Jech M, et al. 2017. Atlantic Marine Assessment Program for Protected Species: FY10-FY14. Washington: U.S. Dept. of the Interior, Bureau of Ocean Energy Management, Atlantic OCS Region.

Palka D, Cholewiak D, Broughton EJ, Jech M. 2016. Appendix A: Northern leg of shipboard abundance survey during 27 June - 25 August 2016: Northeast Fisheries Science Center in: 2016 Annual Report of a Comprehensive Assessment of Marine Mammal, Marine Turtle, and Seabird Abundance and Spatial Distribution in U.S. Waters of the Western North Atlantic Ocean – AMAPPS II. https://doi.org/10.25923/gbap-g480

Palka DL. 2023. Cetacean Abundance in the U.S. Northwestern Atlantic Ocean, Summer 2021. Northeast Fisheries Science Center reference document 23-08. https://doi.org/10.25923/7cab-7s69

Plummer M. 2003. JAGS: A program for analysis of Bayesian graphical models using Gibbs sampling. Proceedings of the Third International Workshop on Distributed Statistical Computing. Vienna, Austria: R Project for Statistical Computing

Rider M, Haas H, Sasso C. 2022. Surface Availability Metrics of Leatherback Turtles (Dermochelys coriacea) Tagged off North Carolina and Massachusetts, United States. NOAA technical memorandum NMFS-NE 286. https://doi.org/10.25923/82c1-4a85

Roberts KE, Garrison LP, Ortega-Ortiz J, Hu C, Zhang Y, Sasso CR, Lamont M, Hart KM. 2022. The influence of satellite-derived environmental and oceanographic parameters on marine turtle time at surface in the Gulf of Mexico. Rem Sens. 14(18):4534. https://doi.org/10.3390/rs14184534

Sakai T. 2023. PAMpal: Load and Process Passive Acoustic Data:0.19.1 https://CRAN.R-project.org/package=PAMpal

Sakai T. 2025. PAMpal: Load and Process Passive Acoustic Data:1.4.4. doi:10.32614/CRAN.package.PAMpal

Sigourney DB, Chavez-Rosales S, Conn P, Garrison L, Josephson E, Palka D. 2018. Development of a species distribution model for fin whales (Balaenoptera physalus) within a Bayesian hierarchical framework: Implications for uncertainty. PeerJ. https://doi.org/10.7287/peerj.preprints.27424v1

Sigourney DB, DeAngelis A, Cholewiak D, Palka D. 2023. Combining passive acoustic data from a towed hydrophone array with visual line transect data to estimate abundance and availability bias of sperm whales (Physeter macrocephalus). PeerJ. 11:e15850. https://doi.org/10.7717/peerj.15850

Sigourney D, Chavez-Rosales S, Josephson E, Palka D, Garrison L. in review. Use of a Bayesian hierarchical density surface model to estimate seasonal distributions of large whales off the East Coast of the United States with an application to a wind energy area. Div and Dist.

Thomas L, Buckland ST, Rexstad EA, Laake JL, Strindberg S, Hedley SL, Bishop JR, Marques TA, Burnham KP. 2010. Distance software: design and analysis of distance sampling surveys for estimating population size. J Appl Ecol. 47(1):5–14.

Tyack PL, Johnson M, Aguilar Soto N, Sturlese A, Madsen PT. 2006. Extreme diving of beaked whales. J Exp Biol. 209(21):4238–4253.

de Valpine P, Turek D, Paciorek CJ, Anderson-Bergman C, Lang DT, Bodik R. 2017. Programming With Models: Writing Statistical Algorithms for General Model Structures With NIMBLE. J Comp and Graph Stat. 26(2):403–413. https://doi.org/10.1080/10618600.2016.1172487

Varghese HK, Lowell K, Miksis-Olds J, DiMarzio N, Moretti D, Mayer L. 2021. Spatial analysis of beaked whale foraging during Two 12 kHz multibeam echosoundersurveys. Front Mar Sci. 8. https://doi.org/10.3389/fmars.2021.654184

Venables WN, Ripley BD. 2002. Modern Applied Statistics with S. New York, NY: Springer.. https://doi.org/10.1007/978-0-387-21706-2

Westell A, Sakai T, Valtierra R, Van Parijs SM, Cholewiak D, DeAngelis A. 2022. Sperm whale acoustic abundance and dive behaviour in the western North Atlantic. Sci Rep. 12(1):16821. https://doi.org/10.1038/s41598-022-20868-3

Zimmer WMX, Johnson MP, Madsen PT, Tyack PL. 2005. Echolocation clicks of free-ranging Cuvier's beaked whales (*Ziphius cavirostris*). J Acoust Soc Am. 117(6):3919–3927. https://doi.org/10.1121/1.1910225

5 Cetacean Ecology Research

Primary authors: Annamaria DeAngelis, Annabel Westell, Danielle Cholewiak, Debra Palka, Samuel Chavez-Rosales, Elizabeth Josephson

This chapter presents new ecological information on cetaceans, drawing from recent data collections and analyses conducted during 2019-2025 within the Atlantic Marine Assessment Program for Protected Species III (AMAPPS III). This focuses on addressing the following AMAPPS objectives (all objectives in Section 2.2):

8) Collect additional data on life-history and ecology, including habitat use, residence time, frequency of use, and behavior;
9) Identify currently used, viable technologies and explore alternative platforms and technologies to improve population assessment studies, if necessary;

The definition of ecology is the study of the interactions between living organisms and their abiotic and biotic surroundings. Ecological information is commonly used to inform management. For instance, ecological information has been used in marine spatial planning or fishery management plans to facilitate the equitable sharing of ocean resources among various users while simultaneously ensuring the protection of marine species. Ecological information has also been used to understand species response to climate variability, which is useful in developing robust marine spatial planning and fishery management plans.

In this chapter we highlight a new beaked whale species (Section 5.1), ecology of beaked whales and killer whales (Sections 5.2 and 5.3), species-habitat interactions (Section 5.4), species-prey interactions (Section 5.5), and using models to forecast short-term future distribution patterns (Section 5.6).

5.1 A New Beaked Whale Species

Using data collected on AMAPPS surveys among other field research activities conducted world-wide, Carroll et al. (2021) described a new species of beaked whale.

Speciation in the deep - genomics and morphology reveal a new species of beaked whale *Mesoplodon eueu* by Carroll et al. (2021)
https://royalsocietypublishing.org/doi/10.1098/rspb.2021.1213

ABSTRACT: *"The deep sea has been described as the last major ecological frontier, as much of its biodiversity is yet to be discovered and described. Beaked whales (ziphiids) are among the most visible inhabitants of the deep sea, due to their large size and worldwide distribution, and their taxonomic diversity and much about their natural history remain poorly understood. We combine genomic and morphometric analyses to reveal a new Southern Hemisphere ziphiid species, Ramari's beaked whale,* Mesoplodon eueu*, whose name is linked to the Indigenous peoples of the lands from which the species holotype and paratypes were recovered. Mitogenome and ddRAD-derived phylogenies demonstrate reciprocally monophyletic divergence between* M. eueu *and True's beaked whale (*M. mirus*) from the North Atlantic, with which it was previously subsumed. Morphometric analyses of skulls also distinguish the two species. A time-calibrated mitogenome phylogeny and analysis of two nuclear genomes indicate divergence began circa 2 million years ago (Ma), with geneflow ceasing 0.35–0.55 Ma. This is an example of how deep-sea biodiversity can be unravelled through increasing international collaboration and genome sequencing of archival specimens. Our consultation and involvement with Indigenous peoples offers a model for broadening the cultural scope of the scientific naming process."*

5.2 ITS.DEEP Dedicated Cruises

Cetaceans in the beaked whale family (Ziphiidae) forage at meso- and bathypelagic depths and only infrequently come to the surface for short time periods (minutes) where they display cryptic behaviors. These characteristics make finding and studying these species difficult. To learn more about these species' ecology, we used data collected on dedicated shipboard cruises and from passive acoustic hydrophones.

From 2-17 July 2025 using AMAPPS III funds, we conducted a multidisciplinary survey in the slope and offshore waters of Georges Bank, with the following primary objectives: 1) collect visual and passive acoustic data on cetacean distribution to assess multispecies occurrence in deep-water habitats; 2) collect seabird distribution data; 3) collect oceanographic and mesopelagic prey data in areas and depths relevant for deep-diving odontocetes, including targeted samples in areas where animals have been documented foraging; 4) deploy uncrewed aircraft systems (UASs) to collect photogrammetry and other data, as feasible; and 5) assess the performance of infrared camera systems for detecting large and small cetaceans, as compared to trained visual observers.

The primary survey region included the shelf break and offshore waters of Georges Bank, within U.S. waters, from approximately 39° – 41° N and 64° – 70.5° W. The visual and acoustic teams surveyed nearly 1600 km of trackline (**Figure 5-1**). We visually detected 33 beaked whale groups, comprising about 82 animals, and we acoustically logged at least 112 beaked whale events (most corresponding to different groups than the visual sightings). In addition, we visually detected at least 15 other cetacean taxa, ranging from killer whales (*Orcinus orca*) to a variety of other delphinids, baleen whales, and *Kogia*.

We prepared two Astro UASs for separate mission profiles: photogrammetry and biologging tag deployments. We equipped the photogrammetry platform with a Sony A7R IV camera paired with a Sigma 24mm f3.5 mapping lens. This UAS also featured two custom carbon fiber catch handles for hand-launch and retrieval, and a Lightware LW20/C laser altimeter mounted adjacent to the camera lens, which continuously recorded distance off the water. Field conditions and challenges associated with tracking beaked whales precluded operational UAS flights until 14 July 2025, when weather conditions improved

sufficiently, achieving a Beaufort sea state ≤ 2 with winds of 6 - 8 knots. The UAS successfully located and captured high-resolution (9504 x 6336 px) imagery of the group from approximately 2 km away from the vessel and at 45 meters altitude, obtaining 102 nadir images over three minutes. Still imagery captured six individual whales, including two adult males distinguished by extensive white scarring across most of the body (**Figure 5-2**).

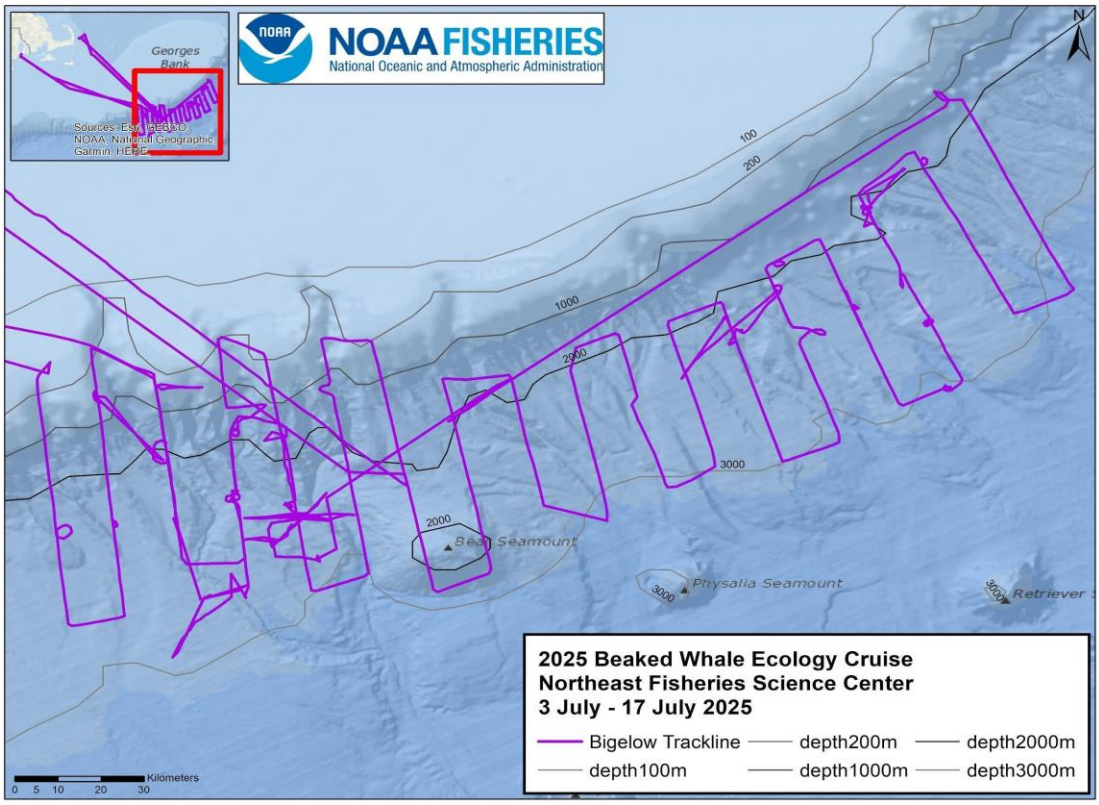

Figure 5-1. Tracks covered during the July 2025 beaked whale ecology cruise

Figure 5-2. High-resolution uncrewed aerial system imagery over six *Ziphius cavirostris*
This shows the relative distribution of animals and body size.

We used a midwater trawl to sample mesopelagic organisms at depths where beaked whales are thought to feed. The midwater trawl is a modified balloon design with a mouth opening of 10 m x 10 m and mesh sizes starting at 6.35 cm (2.5 inch stretch mesh) and grading down to a knotless cod-end liner with 0.635 cm (0.25 inch) mesh. We attached a cod-end aquarium to the end of the cod end to minimize damage to the specimens. We deployed tows between 2300 and 0630 (local time) each night. We selected locations where we visually sighted beaked whales or detected them on a passive acoustic array during daylight hours to deploy the tows. We deployed the midwater trawls to depth for 40 min. We then sorted the net catches to the lowest taxonomic level possible that varied from Class (e.g., gelatinous organisms) to Genus and species (most of the fish). We completed ten midwater tows during the cruise, ranging from the deepest at about 1400 m to the shallowest at 350 m. The trawls captured 112 different types of animals with taxonomic resolution ranging from order (e.g., gelatinous animals) to species (fish).

We will provide more information on this survey in the AMAPPS 2025 annual report.

5.3 Killer Whale Ecology

Visual sightings of killer whales collected on AMAPPS surveys off Florida to North Carolina contributed to a paper exploring the distribution and ecology of killer whales in Atlantic waters.

Killer whales in the Gulf of Mexico and North Atlantic off the Southeastern United States by Barry et al. (2024). https://doi.org/10.3389/fmars.2024.1460314

ABSTRACT: *"Killer whales occur in the Gulf of Mexico (GoMex) and the North Atlantic, including off the southeastern United States (SEUS). Data from cetacean surveys during 1990 – 2021 and other sources were combined to assess killer whale biology, including spatial and temporal distribution, social structure, genetics, morphology, acoustics, and predatory behavior. GoMex records occurred predominantly in oceanic waters (>200 m) during spring and summer. SEUS records occurred primarily in winter and spring off the North Carolina region along the shelf-edge and deeper waters, and off the east coast of Florida. Photo-identification analysis of GoMex killer whales resulted in 49 individuals sighted up to seven times with sighting histories up to 26 years, and social analysis provided evidence of long-term relationships up to 16 years. The GoMex genetic samples revealed two mtDNA haplotypes, one of which does not match any outside the GoMex. Most GoMex whales had wide non-faint saddle patches and many had cookiecutter shark scars while no scars were noted on SEUS whales. Three groups recorded in the GoMex made few calls, but a group harassing sperm whales produced many. Cetaceans and tuna are known prey in the GoMex and SEUS, respectively. Directed studies of killer whales in the GoMex areas would be difficult to implement as this species is very rare. It is therefore important to pursue ongoing efforts to collect behavioral, acoustic and any biological samples that will contribute to improve our understanding of the biology and ecology of killer whales in tropical and subtropical regions."*

5.4 Species-Habitat Associations

Throughout AMAPPS I-III we conducted multi-year, all-season aerial and shipboard surveys, collecting visual and passive acoustic data on animals. During AMAPPS III we utilized several methods to identify species-habitat associations. For example, DeAngelis et al. (2025) defined habitat segregation among the beaked whale species by using classification tree analysis techniques on towed array passive acoustic recordings of beaked whales collected from AMAPPS surveys and concurrent values of depth, sea surface temperature, salinity, and chlorophyll (**Figure 5-3**).

Habitat utilization of beaked whales in the western North Atlantic Ocean using passive acoustics. by DeAngelis et al. 2025.https://doi.org/10.3354/meps14771

ABSTRACT: *"Beaked whales (family Ziphiidae) are cryptic, deep diving cetaceans found offshore. Passive acoustic monitoring of this family allows identification to species and is instrumental in expanding knowledge of their behavior, distribution, and habitat use. From 28 June – 25 August 2016, two broadscale shipboard surveys towed a hydrophone array in the western North Atlantic. Concurrently, 11 bottom-mounted recorders collected continuous passive acoustic data during July and August 2016 along the 1,000 m contour. Five beaked whale species (goose-beaked [*Ziphius cavirostris*], Gervais' [*Mesoplodon europaeus*], True's [*M. mirus*], Sowerby's [*M. bidens*], and Blainville's [*M. densirostris*] beaked whales) were present in both datasets. Beaked whales were commonly detected at the bottom-mounted sites (71% total days present), with sites off the United States' Mid-Atlantic Bight containing the greatest species diversity. Overall, daily co-occurrence was uncommon (35% of study period). Using the towed array, Blainville's and Gervais' beaked whales were found in the Gulf Stream, True's beaked whales were more common in abyssal waters, and Sowerby's were more common on the continental slope. Goose-beaked whales were present throughout. Using multipath reflections, click depths were examined for 192*

beaked whale events. Among three species tested (goose-beaked, Gervais', and True's beaked whales), only goose-beaked whales were found to significantly forage in proximity to the seafloor. This is the first study of its kind to provide a comprehensive overview of how these whales utilize their habitat across latitudes, longitudes, and at depth."

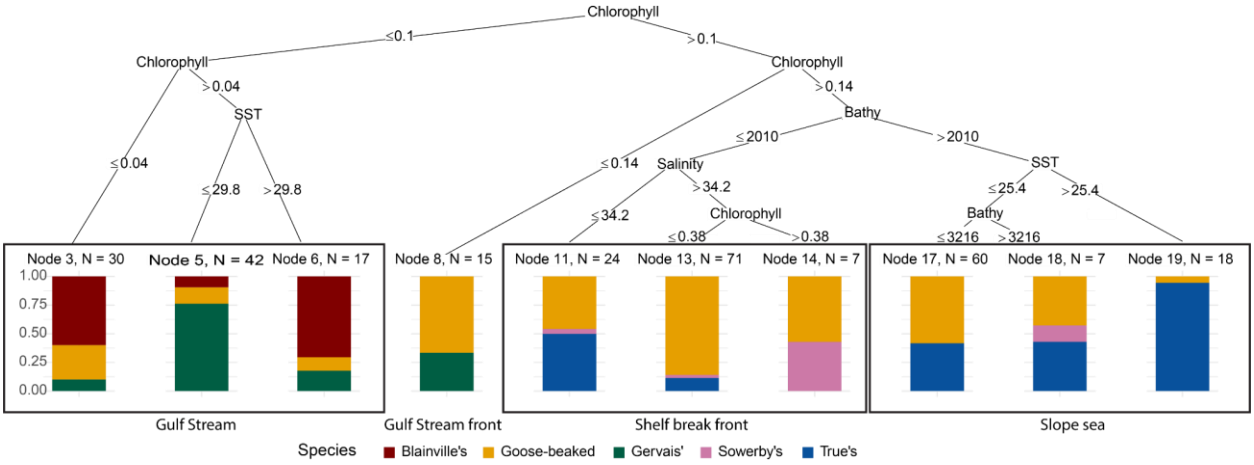

Figure 5-3. Classification tree of proportion of beaked whale species detection events
From Figure 4 in DeAngelis et al. (2025).

We also used generalized additive modelling techniques to choose from 16 - 22 habitat covariates to uncover the spatiotemporal distributions of cetacean species and the habitat factors associated with the animal's distribution and abundance. We converted line transect survey data collected by shipboard and aerial surveys into seasonal, spatially-explicit density estimates, taking into account habitat characteristics (see Section 4.7 in this paper for details). In Chavez-Rosales et al. (2019) we used survey data collected during 2010 - 2013 in all seasons except winter and 16 habitat covariates (7 static and 9 dynamic covariates), where we found the most common covariates were sea surface temperature, sea surface temperature, latitude, bottom temperature, primary productivity and bottom slope, in order of prevalence (**Table 5-1** black text).

Environmental predictors of habitat suitability and occurrence of cetaceans in the western North Atlantic by Chavez-Rosales et al. (2019). https://doi.org/10.1038/s41598-019-42288-6

ABSTRACT: *"The objective of this study was to identify the main environmental covariates related to the abundance of 17 cetacean species/groups in the western North Atlantic Ocean based on generalized additive models, to establish a current habitat suitability baseline, and to estimate abundance that incorporates habitat characteristics. Habitat models were developed from dedicated sighting survey data collected by NOAA-Northeast and Southeast Fisheries Science Centers during July 2010 to August 2013. A group of 7 static physiographic characteristics and 9 dynamic environmental covariates were included in the models. For the small cetacean models, the explained deviance ranged from 16% to 69%. For the large whale models, the explained deviance ranged from 32% to 52.5%. Latitude, sea surface temperature, bottom temperature, primary productivity and distance to the coast were the most common covariates included and their individual contribution to the deviance explained ranged from 5.9% to 18.5%. The habitat-density models were used to produce seasonal average abundance estimates and habitat suitability maps that provided a good correspondence with observed sighting locations and historical sightings for each species in the study area. Thus, these models, maps and abundance estimates established a current habitat characterization of cetacean species in these waters*

and have the potential to be used to support management decisions and conservation measures in a marine spatial planning context."

To update the species-habitat relationships described in Chavez-Rosales (2019), we analyzed the 2010 - 2017 AMAPPS line transect data from all four seasons using generalized additive model techniques and we added 5 additional dynamic covariates: distance to the northern and southern walls of the Gulf Stream, SST fronts, chlorophyll fronts, mixed layer thickness, and the winter North Atlantic Oscillation index (Palka et al. 2021). We found the most common covariates were latitude, bottom temperature, distance to the 1000 m depth contour, and sea surface temperature, in order of prevalence (**Table 5-1** blue text).

More recently we updated the generalized additive density-habitat models by analyzing the 2010 - 2023 AMAPPS line transect data from all four seasons, but excluded the SST and chlorophyll fronts and mixed layer depth covariates because they were not available at the time of the analyses (Section 4.6 in this document). We found the most common covariates were latitude, bottom temperature, distance to the 1000 m depth contour, sea surface temperature, and mixed layer thickness (**Table 5-1** red text).

In summary, increased data over more years and expanded survey efforts during non-summer months led to general better fits in the generalized additive density-habitat models (higher percent deviance explained). These models became more effective at explaining variability both within and between years. The most commonly chosen significant habitat factors in these models were latitude and water temperature, with bottom temperature proving more influential than surface temperature.

Table 5.1. Percent deviance explained (DE) by term for species density-habitat models

Models built on data collected in different time series (ending year): during 2010 - 2013 (black text), 2010 - 2017 (blue), and 2010 - 2023 (red). Habitat covariate terms defined in Table 4-2.

Species	Ending Year	SST	BTEMP	PP	CHLA	PIC	POC	SALINTY	MLD/MLP	SLA	Lat	Depth
Atlantic spotted dolphin (summer)	2013			3.59		2.52		3.43			6.66	
Atlantic spotted dolphin	2017		4.38						4.44		15.96	
Atlantic spotted dolphin	**2023**		**8.22**	**5.28**					**3.74**		**6.88**	
Beaked whale group (summer)	2013	0.8									13.64	23.11
Beaked whale group (summer)	2017		13.27								4.76	
Beaked whale, Cuvier's (summer)	2013	1.13	11.08								10.92	4.08
Beaked whale, Cuvier's (summer)	2017		6.25		2.96						18.4	1.66
Beaked whale, Cuvier's	**2023**	**6.84**	**0.01**								**7.11**	**35.17**
Beaked whale, Gervais'	**2023**						**8.80**					**33.57**
Beaked whale, Sowerby's (summer)	2013	6.49						1.09	3.54	22.96		
Beaked whale, Sowerby's (summer)	2017		7.83					1.94			16.31	
Beaked whale, Sowerby's	**2023**		**4.48**						**6.92**		**9.14**	
Beaked whale, True's	**2023**				**7.35**						**12.60**	**17.00**
Common bottlenose dolphin	2013	0.4		3.11					1.02			
Common bottlenose dolphin	2017		2.67	5.40	1.93			1.18				
Common bottlenose dolphin	**2023**	**5.80**	**2.79**		**0.42**				**1.03**		**10.88**	
Common dolphin	2013	14.53									9.39	
Common dolphin	2017	11.8	19.25								1.72	
Common dolphin	**2023**	**14.02**	**8.24**	**0.38**							**7.19**	
Dwarf/Pygmy sperm whale group (summer)	2013				1.41			0.57				28.27
Dwarf/Pygmy sperm whale group (summer)	2017		20.95				1.62		1.85			
Dwarf/Pygmy sperm whale group	**2023**				**1.19**				**1.16**			**49.42**
Fin whale	2013		7.86		0.98						15.79	
Fin whale	2017			5.16					1.78		4.51	
Fin whale	**2023**		**18.92**	**11.37**		**9.83**		**7.40**			**7.40**	
Harbor porpoise (fall)	2013	2.62									10.8	
Harbor porpoise (spring)	2013			2.6							40.87	

Species	Ending Year	SST	BTEMP	PP	CHLA	PIC	POC	SALINTY	MLD/MLP	SLA	Lat	Depth
Harbor porpoise (summer)	2013					1.48			4.7		60.17	2.95
Harbor porpoise (Nov - May)	2017		1.08					15.47	5.61			
Harbor porpoise (Jun - Oct)	2017								4.85		29.29	
Harbor porpoise	**2023**	**16.17**	**5.68**						**8.30**		**7.98**	**0.74**
Humpback whale	2013	9.14		6.48	0.65						9.97	
Humpback whale	2017	2.95		8.07		0.79			1.96		9.24	
Humpback whale	**2023**		**2.94**			**0.08**	**0.95**	**5.02**			**15.91**	
Minke whale	2013	5.88		9.59			4.51				10.7	
Minke whale	2017	4.9		1.35			0.67		4.59		9.95	
Minke whale	**2023**		**0.24**	**7.34**					**0.26**		**9.07**	
Risso's dolphin	2013	6.12	5.67									
Risso's dolphin	2017		7.95		6.06				4.27		0.74	4.96
Risso's dolphin	**2023**	**6.18**	**5.99**						**3.87**		**19.06**	
Sei whale	2013	20.18							3.69			
Sei whale	2017					3.24						
Sei whale	**2023**	**6.42**									**11.32**	
Pilot whale, Long/Short-finned	2013		5.76	11.97		6.53					10.21	
Pilot whale, Long-finned	2017					1.42					44.31	
Pilot whale, Long-finned	**2023**	**9.18**		**1.34**			**4.22**				**16.20**	
Pilot whale, Short-finned	2017		15.15		6.12			5.26	5.33			1.65
Pilot whale, Short-finned	**2023**	**10.92**	**9.11**						**0.79**		**3.93**	
Sperm whale	2013	7.24	10.07	5.35	1.35							
Sperm whale	2017	10.79	2.16								6.06	10.58
Sperm whale	**2023**		**5.28**	**5.26**					**1.42**		**6.16**	**21.88**
Striped dolphin (summer)	2013	6.79	41.52	1.39								
Striped dolphin	2017		2.37								23.99	31.23
Striped dolphin	**2023**	**9.98**	**44.97**		**0.92**			**4.40**				
White-sided dolphin	2013	4.38			2.63				2.9			
White-sided dolphin	2017	6.73				6.56						
White-sided dolphin	**2023**			**2.84**	**3.25**						**13.36**	

Species	Ending Year	Slope	Dist2shore	Dist125	Dist200	Dist1000	Interact	DGSSW	DGSNW	SSTF	CHLAF	Total % Deviance
Atlantic spotted dolphin (summer)	2013											16.2
Atlantic spotted dolphin	2017		4.48	8.12							0.39	37.8
Atlantic spotted dolphin	**2023**		**10.84**					**2.75**				**37.7**
Beaked whale group (summer)	2013	0.56										38.1
Beaked whale group (summer)	2017					2.58					3.63	24.2
Beaked whale, Cuvier's (summer)	2013	6.79										34.0
Beaked whale, Cuvier's (summer)	2017			2.70								32.0
Beaked whale, Cuvier's	**2023**	**4.67**										**53.8**
Beaked whale, Gervais'	**2023**					**6.35**		**2.73**	**1.66**			**53.1**
Beaked whale, Sowerby's (summer)	2013				7.02							41.1
Beaked whale, Sowerby's (summer)	2017					11.41				3.72		41.2
Beaked whale, Sowerby's	**2023**		**0.35**			**27.76**						**48.7**
Beaked whale, True's	**2023**											**37.0**
Common bottlenose dolphin	2013	0.19	1.48		2.88		13.22					22.3
Common bottlenose dolphin	2017	2.41					8.66		5.66			27.9
Common bottlenose dolphin	**2023**		**6.79**		**5.29**				**1.50**			**34.5**
Common dolphin	2013		10.53			7.64						42.1
Common dolphin	2017	3.88	3.88				5.83		4.42			50.3
Common dolphin	**2023**		**1.87**	**1.86**		**4.07**		**8.25**				**45.9**
Dwarf/Pygmy sperm whale group (summer)	2013	0.8				2.65						33.7
Dwarf/Pygmy sperm whale group (summer)	2017							3.21				27.6
Dwarf/Pygmy sperm whale group	**2023**							**6.27**	**1.86**			**59.9**
Fin whale	2013			10.06								34.7
Fin whale	2017				16.4		14.38					42.2
Fin whale	**2023**	**9.09**		**1.10**		**0.51**						**65.6**
Harbor porpoise (fall)	2013		42.97		10.21							66.6
Harbor porpoise (spring)	2013		4.39		2.03							49.9
Harbor porpoise (summer)	2013											69.3
Harbor porpoise (Nov - May)	2017						8.68					30.8
Harbor porpoise (Jun - Oct)	2017		3.29		4.42		13.86					55.7

Species	Ending Year	Slope	Dist2shore	Dist125	Dist200	Dist1000	Interact	DGSSW	DGSNW	SSTF	CHLAF	Total % Deviance
Harbor porpoise	**2023**				**1.02**	**1.61**			**1.94**			**43.4**
Humpback whale	2013			5.66								31.9
Humpback whale	2017			8.88		1.7	8.13					41.7
Humpback whale	**2023**	**1.21**		**13.14**		**2.99**						**42.2**
Minke whale	2013		5.65	3.57								39.9
Minke whale	2017				4.27	2.73					1.06	29.5
Minke whale	**2023**			**11.39**		**9.21**		**1.02**				**38.5**
Risso's dolphin	2013	6.39	20.25	11.16								49.6
Risso's dolphin	2017		9.95		8.1			5.58		4.64		52.3
Risso's dolphin	**2023**	**11.83**							**5.07**			**52.0**
Sei whale	2013		24.76	3.87								52.5
Sei whale	2017						26.37			9.51		39.1
Sei whale	**2023**	**1.57**	**16.87**									**36.2**
Pilot whale, Long/Short-finned	2013	21.73										56.2
Pilot whale, Long-finned	2017					11.32			5.95		0.49	63.5
Pilot whale, Long-finned	**2023**	**27.60**			**2.38**			**2.72**				**63.6**
Pilot whale, Short-finned	2017					14.6		17.68				65.8
Pilot whale, Short-finned	**2023**	**19.1**	**7.52**						**9.15**			**60.5**
Sperm whale	2013	9.49										33.5
Sperm whale	2017					22.17			0.52			52.3
Sperm whale	**2023**					**7.29**		**3.01**				**50.3**
Striped dolphin (summer)	2013					3.12						52.8
Striped dolphin	2017								2.43	5.63	5.96	71.6
Striped dolphin	**2023**					**0.15**						**60.4**
White-sided dolphin	2013	1.02		7.57								18.5
White-sided dolphin	2017				4.81		28.18					46.2
White-sided dolphin	**2023**	**2.28**	**2.12**		**14.26**	**1.61**		**3.98**				**43.7**

5.5 Interactions with Prey Species

The density-habitat models (Sections 4.6, 4.7, and 5.4) primarily utilize readily available physical habitat characteristics to describe the physical and biological ecosystems of the animals. Some of these characteristics serve as proxies for the biological ecosystem. It is well-established that prey distribution influences the distribution of predators like the cetaceans, sea turtles, and seabirds targeted by AMAPPS. However, obtaining spatiotemporal distributions of prey species is challenging. AMAPPS collaborators, Roberts et al. (2022) and Orphanides et al. (2023), detailed below, published innovative approaches to use AMAPPS data to identify prey indices associated with the targeted cetacean species.

Tight spatial coupling of a marine predator with soniferous fishes: Using joint modelling to aid in ecosystem approaches to management by Roberts, SL et al. 2022 .https://doi.org/10.1111/ddi.13746

> ABSTRACT: *"Aim: Understanding the distribution of marine organisms is essential for effective management of highly mobile marine predators that face a variety of anthropogenic threats. Recent work has largely focused on modelling the distribution and abundance of marine mammals in relation to a suite of environmental variables. However, biotic interactions can largely drive distributions of these predators. We aim to identify how biotic and abiotic variables influence the distribution and abundance of a particular marine predator, the bottlenose dolphin (*Tursiops truncatus*), using multiple modelling approaches and conducting an extensive literature review.*
>
> *Location: Western North Atlantic continental shelf.*
>
> *Methods: We combined widespread marine mammal and fish and invertebrate surveys in an ensemble modelling approach to assess the relative importance and capacity of the environment and other marine species to predict the distribution of both coastal and offshore bottlenose dolphin ecotypes. We corroborate the modelled results with a systematic literature review on the prey of dolphins throughout the region to help explain patterns driven by prey availability, as well as reveal new ones that may not necessarily be a predator–prey relationship.*
>
> *Results: We find that coastal bottlenose dolphin distributions are associated with one family of fishes, the Sciaenidae, or drum family, and predictions slightly improve when using only fish versus only environmental variables. The literature review suggests that this tight coupling is likely a predator–prey relationship. Comparatively, offshore dolphin distributions are more strongly related to environmental variables, and predictions are better for environmental-only models. As revealed by the literature review, this may be due to a mismatch between the animals caught in the fish and invertebrate surveys and the predominant prey of offshore dolphins, notably squid."*

Relating marine mammal distribution to water column prey structure derived from echosounding by Orphanides et al. 2023 https://doi.org/10.3354/meps14290

> ABSTRACT: *"Managing human impacts on marine mammal populations depends on understanding their distributions in space and time. Knowledge of these distributions is becoming increasingly important due to offshore energy development and climate-induced shifts in oceanic habitat. Most models assessing pelagic marine mammal abundance and distribution primarily use ocean surface or ocean floor variables as proxies for water column habitat. Here, we used a ship-based marine mammal sighting survey to test the utility of echosounder-based predictive variables for modeling marine mammal*

distribution and abundance. We assessed the distribution of 7 marine mammal taxa and 3 feeding guilds along the shelf break off the northeast USA relative to prey structure derived from acoustic data. We classified prey into 4 categories: (1) fish with swimbladders; (2) small resonant bubbles as phytoplankton, fish larvae, and gelatinous zooplankton; (3) fluid-like scatterers such as krill and copepods; and (4) fish with no swimbladder. We quantified the spatial structure of prey by calculating backscattering strength, location, dispersion, occupied areas, evenness, and aggregation. Spatial resolution along the survey track line was set to bins 1000 m in distance and either 50 or 200 m in depth. We then built generalized additive models (GAMs) using these acoustically derived variables to explain marine mammal distribution. The resulting GAMs explained between 9 and 38% of deviance, with model fit often reflecting aspects of foraging depth and prey preference. This approach could contribute to improved management through more accurate species distribution models that employ direct measurements of prey."

5.6 Forecasting using Species Distribution Models

Dynamic management, which involves adjusting the spatial and/or temporal area of concern between animals and human activities, can improve the management of mobile species such as cetaceans, sea turtles, and seabirds targeted by AMAPPS. Ideally, this approach would predict future areas of concern, which requires anticipating the future distributions of these target animals. One method for achieving this is to utilize ecological forecasting tools and density-habitat models. For instance, an AMAPPS collaborator, Stepanuk et al. (2022), published an innovative study demonstrating the use of subseasonal global environmental forecasts and AMAPPS line transect data to predict the arrival of migrating humpback whales (*Megaptera novaeangliae*).

Subseasonal forecasts provide a powerful tool for dynamic marine mammal management by Stepanuk et al. (2022) https://esajournals.onlinelibrary.wiley.com/doi/10.1002/fee.2506

ABSTRACT: *"Adaptive approaches are needed to effectively manage dynamic marine systems, and ecological forecasts can help managers anticipate when and where conservation issues are likely to arise in the future. The recent development of subseasonal global environmental forecasts provides an opportunity to inform management by forecasting species distributions in advance over operational timeframes. We demonstrate the utility of environmental forecasts for managing marine mammals by integrating species distribution models with subseasonal forecasts to predict the arrival of migratory humpback whales (*Megaptera novaeangliae*) at foraging grounds in the Northeast US. Environmental forecasts showed high model skill at lead times of up to 2 weeks and resulting humpback whale models performed well in predicting humpback arrival. Forecasts of whale distribution can shape management efforts to minimize both impacts on whales and economic costs. Applying subseasonal forecasts to anticipate future risk presents a powerful tool for the dynamic management of marine mammals."*

5.7 References Cited

Barry KP, Mullin KD, Maze-Foley K, Wilcox Talbot LA, Rosel PE, Soldevilla MS, Dias LA, Ramírez-León MR, Litz JA. 2024. Killer whales in the Gulf of Mexico and North Atlantic off the Southeastern United States. Front Mar Sci. 11. https://doi.org/10.3389/fmars.2024.1460314

Carroll EL, McGowen MR, McCarthy ML, Marx FG, Aguilar N, Dalebout ML, Dreyer S, Gaggiotti OE, Hansen SS, van Helden A, et al. 2021. Speciation in the deep: genomics and morphology reveal a new species of beaked whale *Mesoplodon eueu*. Proceedings of the Royal Society B: Biological Sciences. 288(1961):20211213. https://doi.org/10.1098/rspb.2021.1213

Chavez-Rosales S, Palka DL, Garrison LP, Josephson EA. 2019. Environmental predictors of habitat suitability and occurrence of cetaceans in the western North Atlantic Ocean. Sci Rep. 9(1):5833. https://doi.org/10.1038/s41598-019-42288-6

DeAngelis AI, Westell A, Baumann-Pickering S, Bell J, Cholewiak D, Corkeron PJ, Soldevilla MS, Solsona-Berga A, Trickey JS, Parijs SMV. 2025. Habitat utilization by beaked whales in the western North Atlantic Ocean using passive acoustics. Mar Eco Prog Ser. 754:137–153. https://doi.org/10.3354/meps14771

Orphanides CD, Jech JM, Palka DL, Collie J. 2023. Relating marine mammal distribution to water column prey structure derived from echosounding. Mar Ecol Prog Ser. 711:101–119. https://doi.org/10.3354/meps14290

Palka D, Aichinger Dias L, Broughton E, Chavez-Rosales S, Cholewiak D, Davis G, DeAngelis A, Garrison L, Haas H, Hatch J, et al. 2021. Atlantic Marine Assessment Program for Protected Species: FY15-FY19. https://repository.library.noaa.gov

Roberts SM, Jacoby A-M, Roberts JJ, Leslie J, Payne KL, Read AJ, Halpin PN, Barco S, Garrison L, McLellan W, et al. 2023. Tight spatial coupling of a marine predator with soniferous fishes: Using joint modelling to aid in ecosystem approaches to management. Diversity and Distributions. 29(8):1074–1089. https://doi.org/10.1111/ddi.13746

Stepanuk JE, Kim H, Nye JA, Roberts JJ, Halpin PN, Palka DL, Pabst DA, McLellan WA, Barco SG, Thorne LH. 2023. Subseasonal forecasts provide a powerful tool for dynamic marine mammal management. Frontiers in Ecology and the Environment. 21(3):117–123. https://doi.org/10.1002/fee.2506

6 Cetacean Behavior Research

Primary authors: Annabel Westell, Annamaria DeAngelis, Elizabeth Josephson

6.1 Introduction

The Atlantic Marine Assessment Program for Protected Species (AMAPPS) project utilized both active and passive acoustics during shipboard surveys to gather data on marine species. We employed active acoustics emitted by an EK60 or EK80 mounted to the bottom hull of the ship to map prey fields, which were then linked to the distribution and abundance of target species (Orphanides et al. 2023; Section 5.5). Passive acoustics involved towing a specialized hydrophone array behind the survey vessel to record the presence and distribution of soniferous species, with a focus on detecting and tracking odontocetes. The resulting passive and active signals provided valuable insights into the animals' distribution, ecology, and behavior. This chapter focuses on the behavioral information extracted from the passive and active acoustic data to address the AMAPPS objective of collecting data on life-history and ecology, including habitat use, residence time, frequency of use, and behavior.

We analyzed the acoustic data in several ways throughout this chapter:

- **Animal Depth and Abundance (Section 6.2):** We used passive acoustic recordings to estimate the depth of clicking, diving animals (DeAngelis et al. 2017). We then used this depth information to correct the slant distance between the array and the clicking animal, allowing for the estimation of the horizontal perpendicular distance. Subsequently we used this measure in a distance sampling analysis to estimate the abundance of subsurface animals (Sections 4-9 – 4-12).
- **Sperm Whale Body Length (Section 6.3):** We leveraged the automated dive depth methodology introduced in Section 6.2 to also automatically extract the inter-pulse interval of clicking sperm whales using a new processing methodology. We then used the inter-pulse interval to estimate the body length of the clicking sperm whale.
- **Sperm Whale Foraging Behavior (Sections 6.4 and 6.5):** We analyzed the characteristics of the buzzes made by sperm whales, which we recorded with a passive acoustic array, in two distinct ways to study their use of the water column for foraging. Westell et al. (2022) previously described these methods and results using sperm whale data from the summer 2016 northeast shipboard survey. For this report, we added the data from the summer 2021 northeast shipboard survey to report preliminary results of an analysis of sperm whale dive and foraging behavior based on acoustic dive profiles.
- **Diet and Foraging Integration (Section 6.6):** We combined the dive profile information from Section 6.5 with the associated EK60 active acoustic data to enhance the understanding of sperm whale diet and foraging behavior.
- **Active Acoustic Propagation Range and Beaked Whale Response (Section 6.7):** We characterized the propagation range of the EK60 active acoustic signals in the open ocean relative to what beaked whales might perceive. Passive acoustic moorings, positioned at the typical foraging depth of beaked whales, served as a proxy for a foraging beaked whale. We estimated the received level that a foraging animal would experience to better understand the acoustic cessation response of beaked whales during shipboard surveys.

6.2 Leveraging Surface Reflections of Clicks to Estimate Depth

To facilitate the estimation of the horizontal perpendicular distance of animals below the surface, DeAngelis et al. (2017) developed an acoustic localization method for estimating the depth of a beaked whale acoustically detected on a towed hydrophone array. This method used the multipath arrivals of surface reflected echoes of a click train collected using a towed hydrophone array.

In 2021, we further automated the DeAngelis et al. (2017) multipath arrival process and applied it to sperm whale data collected during the 2016 northeast shipboard abundance survey (HB1603; Westell et al. 2022; see Section 4.9). The new process involves automating and streamlining the multipath arrival method to efficiently use it to process new data consisting of thousands of clicks (**Figure 6-1**). The process involves six steps, from processing towed acoustic array data in PAMGuard to estimating the depth of the animal and calculating a depth corrected horizontal perpendicular distance for acoustic density estimation. In addition, this automated method makes it easy to analyze acoustic dive profiles for sperm whales (Sections 6.4 and 6.5) and the inter-pulse intervals of sperm whales for acoustic body length estimation (Section 6.3). We incorporated this process into specialized functions in the PAMPal package within the R computing language (Sakai, 2024). Then in 2024, we fully converted the code to R and presented it at the Detection, Classification, Localization, and Density Estimation workshop in Rotterdam, Netherlands (Westell et al. 2024a).

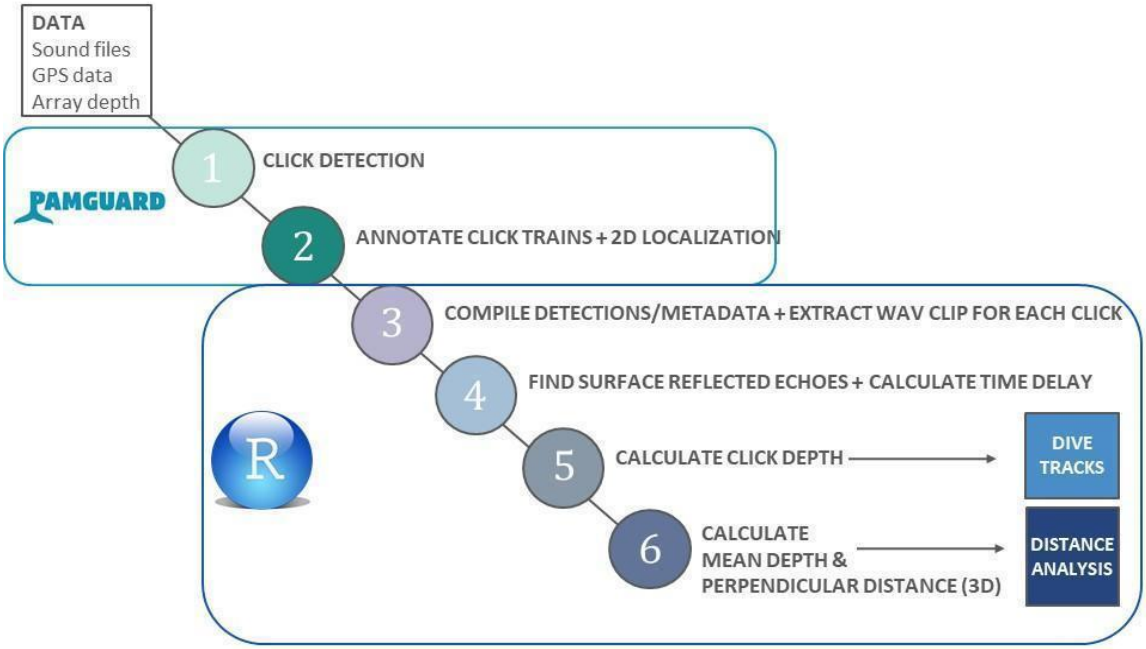

Figure 6-1. Procedure involved in the dive depth detection method using PAMGuard and R.

6.3 Demographics of Sperm Whales using the Towed Hydrophone Array

Studying demographic composition provides information about population structure and habitat use, for example if an area is frequented by adult females and immature animals it is likely an important area for social groups (Whitehead 2003). Passive acoustic clicks of sperm whales are one way to determine the demography of sperm whales.

A unique feature of sperm whales is that we can estimate the size of an individual based on the click structure of their foraging clicks. Sperm whales are sexually dimorphic and this is reflected in their body size, acoustic signals, social behavior and distribution (e.g., Best 1979, Growcott et al. 2011). The production of an echolocation click by a sperm whale results in a series of acoustic reflections within its head (Norris and Harvey, 1972, Mohl et al. 2003). As a result, each click consists of a set of pulses (identified as P0, P1, P2, etc.) with a relatively stable (± 0.05 ms, Growcott et al. 2011) inter-pulse interval. The inter-pulse interval ranges from less than 2 ms to greater than 9 ms (e.g., Beslin et al. 2018). As a sperm whale's head is approximately one third of the total body length, we can use the inter-pulse

interval to estimate the acoustic body length, which can then be used to infer sex and/or maturity stage (e.g., Gordon, 1991, Growcott et al. 2011, Rice, 1989).

6.3.1 Methods

We processed the acoustic data from the 2021 NEFSC abundance survey (HB2102) through a PAMGuard sperm whale click detector and annotated the click trains of each detected individual whale into "events" (e.g., Westell *et al.* 2022). We then processed the annotated click trains using a dive depth detection method (Section 6.2 this report; Sakai 2024) to identify surface reflected echoes, estimate depth, and estimate a depth corrected horizontal perpendicular distance (Sections 4.2.3 and 4.9). As part of the automated dive depth detection method, we developed a new method to plot the average waveform of all the clicks in an event and estimate the inter-pulse interval by automatically identifying the highest amplitude peak after the initial detection of the click. For each event, an analyst reviewed the output who then rejected, accepted, or modified the average inter-pulse interval based on the waveform (**Figure 6-2**). We excluded events that were under two minutes as a stable inter-pulse interval can be difficult to verify for short events.

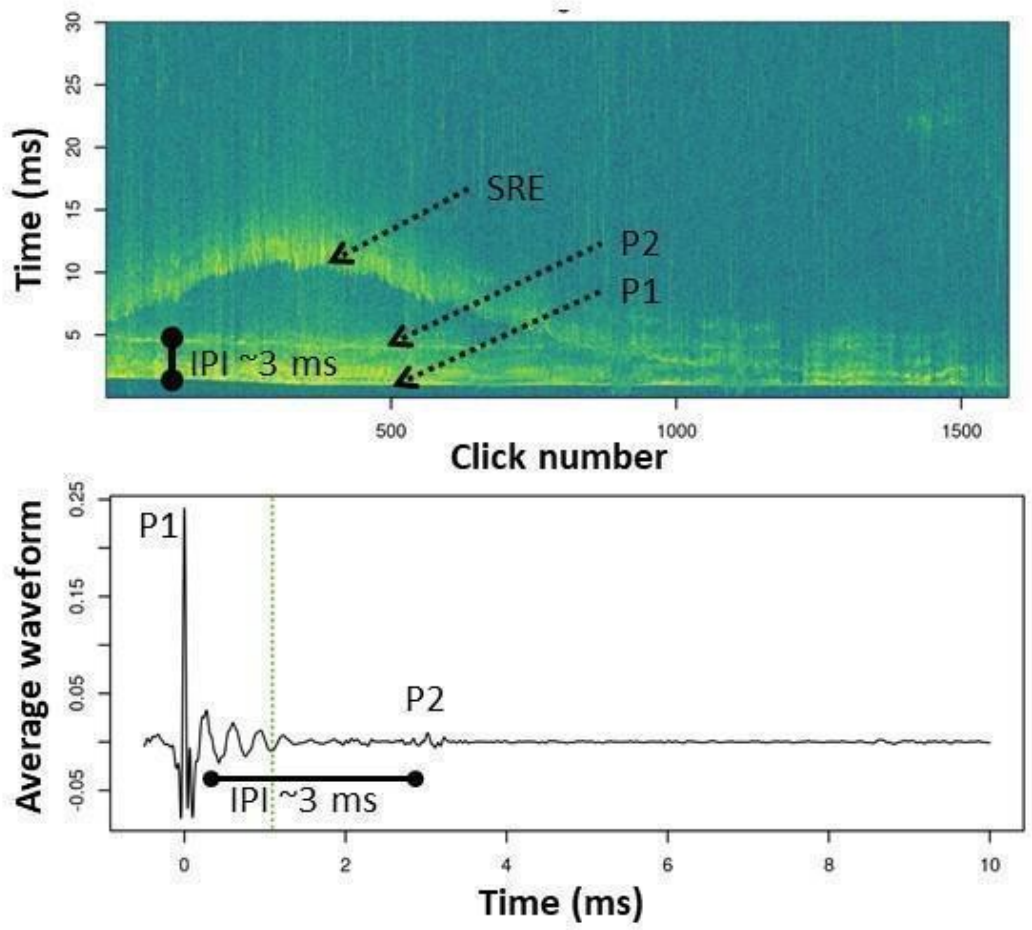

Figure 6-2. Example echogram and average waveform for one sperm whale event
The echogram displays the energy of the P1 and P2 pulses of the click, with a relatively stable inter-pulse interval (IPI) of ~3 ms. It also displays the detection of surface reflected echoes (SRE) of these pulses, used for the dive depth method. We marked by a vertical green dotted line the P2 automatically detected feature. We then manually reviewed and adjusted it to record the actual P2 at ~3 ms after P1.

We estimated acoustic body length using one of three equations. We used the Ferrari et al. (2024) method for an average IPI less than 2 ms, the Gordon (1991) method for an average IPI between 2 - 4 ms and the Growcott et al. (2011) method for an average IPI greater than 4 ms. We also categorized the body lengths into three age categories: immature animals (<9 m), adult females or juvenile males (9 - 12 m), and adult males (>12 m) (e.g., Barile et al. 2024, Caruso et al. 2015, Solsona-Berga et al. 2022).

6.3.2 Results and Discussion

We processed and reviewed a total of 441 sperm whale events. The average inter-pulse interval was accepted for 115 events (26%) and ranged from 1.5 - 7.4 ms (mean: 3 ms, SD: 0.9 ms) (**Table 6-1**). The estimated acoustic body length ranged from 3.9 - 15.1 m (mean: 9.2 m, SD: 1.5 m). It is important to note that individuals may have been detected more than once and thus these results may not represent 115 different whales. Based on the estimated acoustic body lengths, 21 detections could be categorized as immature (<9 m), 92 as adult female or juvenile (9 - 12 m), and two as adult male (>12 m) (**Figure 6-3**).

Table 6-1. Estimated acoustic body length for events with various inter-pulse intervals

Number of sperm whale events	Average inter-pulse interval range (ms)	Equation	Estimated acoustic body length (m)
4	<2	Ferrari et al. 2024	3.9 - 4.8
98	2 – 4	Gordon 1991	7.7 - 10.6
13	>4	Growcott et al. 2011	10.8 - 15.1

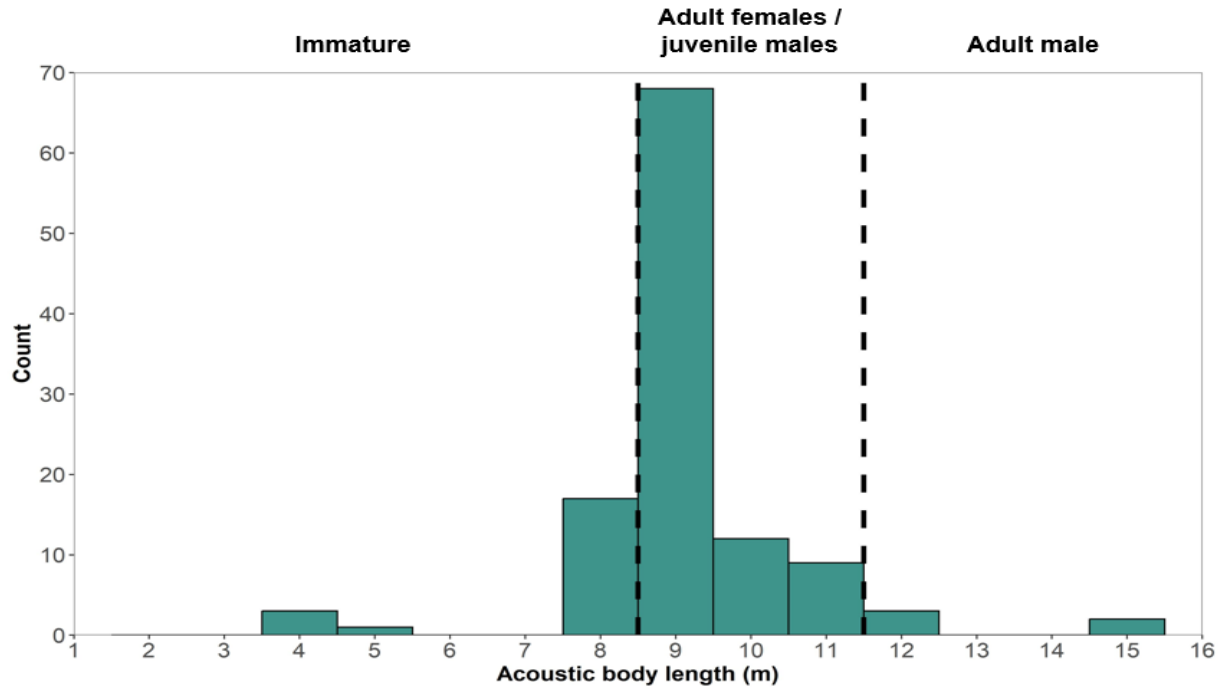

Figure 6-3. Estimated acoustic body length of sperm whales based on inter-pulse intervals
We categorized the 115 sperm whale click trains (events) into three demographic categories as indicated by the vertical dashed lines.

These results suggest that, of the sperm whale click trains detected and analyzed, 98% may have been produced by an adult female, juvenile male, or immature animal. The majority of these whales (78%) were in groups that could be social groups or groups of juvenile males (Whitehead 2003). These results are consistent with the theory that sperm whales, including social groups consisting of related females and their offspring, spend the summer and fall in the productive waters of the western North Atlantic (e.g., Best, 1979, Westell et al. 2024b).

This data represents 26% of the click trains detected and annotated in the HB2102 dataset. Future analysis could verify the accuracy of the average inter-pulse interval estimation and determine if the analyzed click trains are representative of the sperm whales detected in the study area at that time (summer of 2021).

6.4 Investigating the Foraging Phase of Sperm Whales using Recorded Buzzes

Sperm whales produce echolocation clicks to navigate and detect prey (Weilgart & Whitehead, 1988). We associate buzzes made by the sperm whales with times when the whale is foraging and attempting to capture prey (Griffin et al. 1960). Thus, based on acoustic and movement data from tagged animals, we define the foraging phase of a sperm whale as the period between the first and last foraging buzz (e.g., Watwood et al. 2006). Sperm whales use multiple and adaptive foraging strategies and have been recorded alternating between shallow and deep dives (e.g., Fais et al. 2015; Teloni et al. 2008). The deep dives are typically U-shaped dives, where that are a steep descent, horizontal bottom phase at a targeted prey layer, and then a steep ascent.

As sperm whales emit thousands of clicks while foraging, which are relatively low frequency, we receive many, but not all of those clicks by the towed hydrophone array. Sperm whale foraging buzzes are distinguished from echolocation clicks by an increase in click rate (i.e., faster clicking) and decrease in amplitude. This decrease in amplitude means foraging buzzes are more difficult to record and detect using an automated detector (Madsen et al. 2002). Thus, to study the dive profiles of sperm whales, we defined the foraging phase of their dive in two ways: 1) identify the times in which buzzes are audibly heard and/or detected and use the presence of the first and last buzz to define the foraging phase (this section) and 2) use a percentage of the maximum dive depth to identify the start and end of the dive phase (Section 6.5).

6.4.1 Methods

We selected a subset of sperm whale dives collected during the 2016 northeast shipboard survey (HB1603) where we could identify the U-shaped dive (a descent, bottom phase, and ascent) produced by one whale using methods documented in Westell et al. (2022). We used PAMGuard v. 2.01.05 (Gillespie et al. 2008) to review the 44 sperm whale dives to determine if the detected foraging buzzes could be associated with an individual whale. We then reviewed the nine dives that met the criteria in Raven Pro 1.6 (K. Lisa Yang Center for Conservation Bioacoustics at the Cornell Lab of Ornithology 2023) to record the times and durations of breaks in the click train using audible buzzes and possible buzzes. We defined a possible buzz as an increase in the usual click rate and decrease in click amplitude followed by a pause in the click train, possibly indicating an inaudible foraging buzz occurred. We then plotted the dive profiles (click depths over time) and detected buzzes to visualize patterns in dive behavior and acoustic behavior. Based on foraging behavior of tagged sperm whales (Teloni et al. 2008), we categorized buzzes produced at depths <500 m as “shallow” foraging dives and buzzed produced as depths >500 m as “deep” foraging dives.

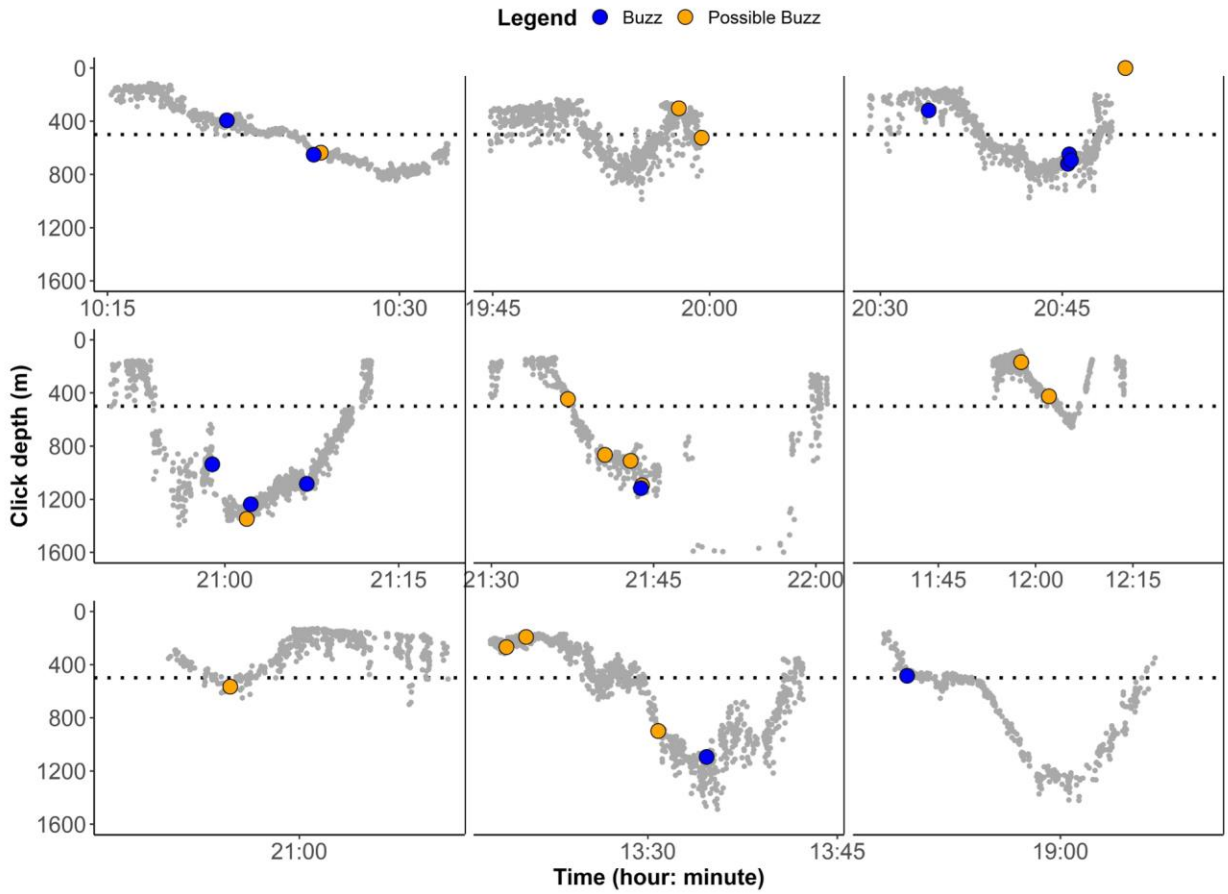

Figure 6-4. Estimated click depth (m) over time for nine individual sperm whales
We marked regular echolocation clicks in grey; depth and time of detected buzzes as a blue dot; depth and time of possible buzzes ked as an orange dot; and transition between shallow and deep foraging as a horizontal dotted line at the 500 m depth.

6.4.2 Results and Discussion

We manually detected sperm whale foraging buzzes in all nine dives and confirmed foraging activity in various layers of the water column between 200 and 1300 m (**Figure 6-4**). Across all analyzed dives, we recorded 12 audible buzzes, 15 possible buzzes, and 106 breaks in the click train. The number of audible foraging buzzes detected per dive ranged from 1 - 4 (mean: 1.3). The audible buzz duration ranged from 0.79 – 5.7 s (mean: 2.1). Audible and possible buzzes occurred at estimated depths between 150 - 1300 m. Seven dives included shallow foraging (<500 m) and two included deep foraging (>500 m) dives.

This study confirms it is possible to detect sperm whale foraging buzzes using a towed hydrophone array and gain insights into foraging behavior. However, the results are likely an underestimate of the number of foraging buzzes produced during a foraging dive and thus do not fully represent sperm whale foraging behavior and phases. This analysis recorded an average 1.3 buzzes per dive while Fais et al. (2016) reported sperm whale dives which include an average of 24 (±4) foraging buzzes. For the data reviewed, the underlying behavior causing 80% of the observed breaks in click trains was unknown. These could be due to a pause or undetected buzz during a prey capture attempt but may also be the result of undetected echolocation clicks or a pause used by the whale to recycle air (Madsen et al. 2002).

These preliminary results from a set of nine acoustic dive profiles indicate that the detected sperm whales were foraging in multiple layers of the water column, displaying both shallow and deep foraging, which is consistent with sperm whale data collected using animal borne tags (e.g., Fais et al. 2016, Teloni et al. 2008, Watwood et al. 2006). The detection of foraging buzzes may indicate areas of prey preference and/ or adaptive foraging strategies. Where possible, these results will be combined with the project combining active EK60 data with sperm whale acoustic dive profiles to confirm foraging by the sperm whale (Section 6.6).

6.5 Using Maximum Depth of Sperm Whale Dives to Infer Foraging Phase

To study the dive profiles of sperm whales, we defined the foraging phase of their dive in two ways: 1) identify the times in which buzzes are audibly heard and/or detected and use the presence of the first and last buzz to define the foraging phase (Section 6.4) and 2) use a percentage of the maximum dive depth to identify the start and end of the dive phase (this section). This second method follows three previous tagging studies that reported the starting depth of the foraging phase was within 27-55% (mean: 40%) and the end depth of the foraging phase was within 26-44% (mean: 35%) of the maximum dive depth (Guerra et al. 2017, Teloni et al. 2008, Watwood et al. 2006).

6.5.1 Methods

We detected and localized sperm whale click trains recorded during the 2016 (HB1603) and 2021 (HB2102) northeast shipboard surveys as described by Westell et al. (2022). An acoustic dive profile refers to estimated click depth over time for an individual whale. If the duration of an acoustic dive profile was longer than 5 min and a descent, bottom phase, and ascent were visually discernible (e.g., Watwood et al. 2006), it was categorized as U-shaped. Other patterns included descent, ascent, and a flat dive (Westell et al. 2022). For the U-shaped dives, we tested a new method to define the foraging phase. For each acoustic dive profile, we defined the estimated start and end of the foraging phase conservatively as 50% of the maximum dive depth, based on results from tagging studies. As an initial method for grouping results, we categorized the dives based on the minimum depth of the start/end of the foraging phase: shallow (<400 m), medium (400 - 800 m), and deep (>800 m).

6.5.2 Results and Discussion

The data from 2016 and 2021 cruises included, respectively, 265 and 120 click trains localized in 3D (**Table 6-2**). A total of 81 U-shaped acoustic dive profiles were analyzed from both datasets (**Figure 6-5**).

Table 6-2. Numbers of sperm whale acoustic dive profiles localized in 3D
We used the U-shaped dives in this section.

Dataset	Total click trains	U shaped	Descent	Ascent	Flat	Partial
2016	265	44	70	31	9	111
2021	120	37	27	15	8	33
Total	385	81	97	46	17	144

Analyzed U-shaped dives ranged in duration between 5.5 – 41.9 min (mean: 16 min ± 6.5) (**Table 6-3**). The minimum depth ranged from 52 - 698 m (mean: 243m ± 131) and the maximum depth ranged from 377 - 2919 m (mean: 1139 m ± 494). The estimated start / end of the foraging phase ranged from 189 - 1459 m (mean: 569 m ± 247). For 23 dives (28%) the foraging phase started at <400 m (shallow) and

ended at <800 m (**Figure 6-6**). For 47 dives (58%) the foraging phase started between 400 - 800 m (medium) and ended at depths <1600 m. For 11 dives (14%) the foraging phase started at a depth >800 m (deep) and ended at depths <2900 m.

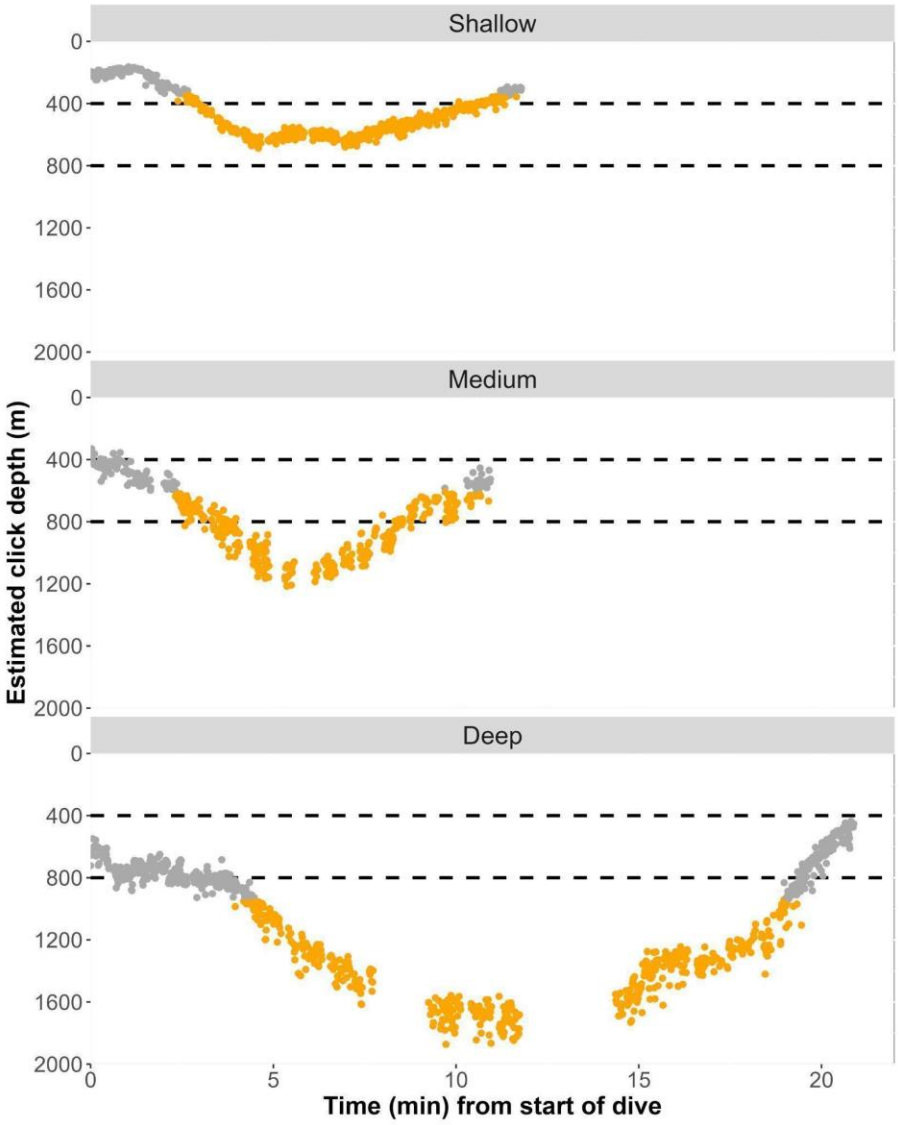

Figure 6-5. Examples of acoustic dive profiles (estimated click depth over time)
We categorized the profiles as shallow (<400 m), medium (400 - 800 m), and deep (>800 m) foraging dives. Each estimated click depth is plotted as a point. Depths within the estimated foraging phase are colored orange and depths outside of the foraging phase are colored grey. Horizontal dashed lines were added at 400 m and 800 m for reference. Note the duration of each dive is limited to when the clicks were detected and localized (i.e., the start and end of the dives are not included).

Table 6-3. Summary of sperm whale acoustic dive profiles by foraging phase category

Category	Start depth (m) of foraging phase	No. of dives (%)	Min. start depth (m) of foraging phase	Max. start depth (m) of foraging phase	Max. dive depth (m)	Duration (min)
Shallow	<400	23 (28%)	188	399	798	5.5 - 20.2
Medium	400-800	47 (58%)	405	767	1533	6.4 - 27.4
Deep	>800	11 (14%)	801	1459	2919	12.1 - 41.9

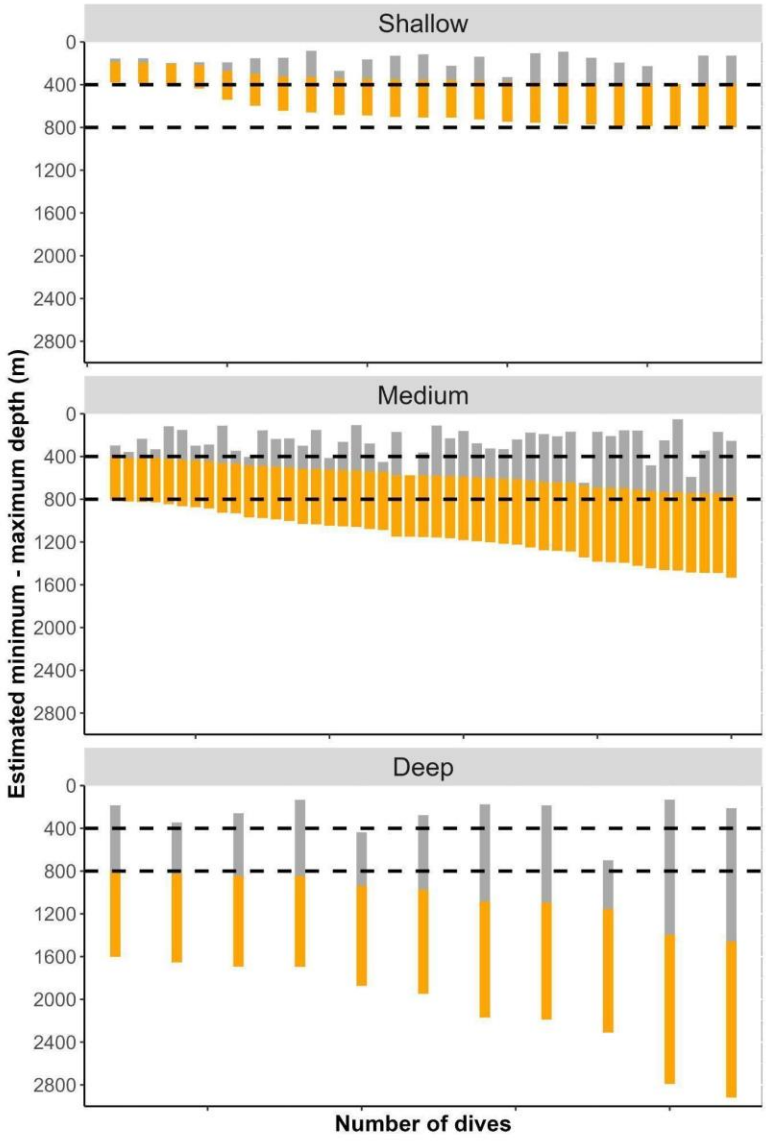

Figure 6-6. Minimum and maximum estimated depth for each categorized acoustic dive profile
The minimum depth to the start of the foraging phase is colored grey. The foraging phase is colored orange. Horizontal dashed lines were added at 400 m and 800 m for reference.

Forging depths and maximum depths are consistent with previous studies; however, shallow and deep foraging have been categorized differently in various publications depending on the study region and

results (e.g., Fais et al. 2015, Teloni et al. 2008). Using a subset of the same data, Westell et al. (2022) reported that the whales exhibited multiple foraging strategies and targeted prey in both the mesopelagic (200 - 1000 m) and bathypelagic (>1000 m) zones. Incorporating data collected in 2021 nearly doubled the sample size. Estimated foraging depths and dive durations vary, but for the majority of analyzed dives (84%) some or all of the foraging phase occurred between 400 - 800 m depth in the mesopelagic zone. For 6% of the dives the estimated foraging phase started deeper than 1000 m in the bathypelagic zone.

We were limited to estimating depths when the whale produced clicks, we detected the clicks, and we detected a surface reflected echo. To account for possible error in these estimated depths, we interpreted the results by 400 m depth intervals. We expected that we excluded most whales in the epipelagic zone (<200 m) due to the difficulty of detecting surface reflected echoes at these shallow depths. Thus, this method does not account for any dive or foraging activity in very shallow waters (<200 m).

Sperm whale foraging behavior is flexible, adjusting to factors like prey preference, availability, habitat type, and potentially sex and age (Teloni et al. 2008). To improve our understanding of sperm whale habitat usage off the eastern U.S. coast, future studies should focus on analyzing a larger number of dives and sampling a wider area. This can be achieved more efficiently and cost-effectively by utilizing passive acoustic data and the dive detection method, as opposed to the more challenging collection of animal-borne tag data.

Future analysis will involve further testing and improvement of methods for estimating the foraging phase of the acoustic dive profiles, categorizing dive behavior, determining if the whales were foraging in the water column or to the sea floor, and assessing if foraging strategies varied by dive depth or habitat type (e.g., on the continental slope versus over the abyssal plains).

6.6 Examine Relationship Between Deep Scattering Layer and Sperm Whale Behavior

The NOAA ship *Henry B. Bigelow* has active acoustic scientific Kongsberg EK60 echosounders with split-beam transducers mounted to a retractable centerboard. The full suite of frequencies is18, 38, 70, 120, and 200 kHz, although not all frequencies were available for every survey. When the EK60 is in active mode, we transmitted a 1.024-ms continuous wave narrowband acoustic pulse (aka “ping”) at nominally 6-s intervals and recorded digitized echoes. When the EK60 is in passive mode, the EK60 did not transmit a pulse and only recorded ambient reverberation. The 18-kHz transducer has a beam width of 11º and all other transducers have a beam width of 7º. Some of the EK60 echosounders transmit sound within marine mammal hearing and communication frequencies, thus, there is interest in determining whether the EK60 impacts odontocete presence and acoustic detections, and what its propagation range is in the open ocean.

Cholewiak et al. (2017) demonstrated that when the EK60 echosounders actively transmitted sound there were fewer beaked whale detections recorded on the towed hydrophone array, which may mean there was a negative impact on their foraging behavior. At the time of the publication, it was unclear whether this meant a complete cessation of foraging, a change of heading away from the vessel but continuously foraging (thus not being detected), or eavesdropping on the echoes of the EK60 to forage and not use their own signals. For sperm whales there was no visible change in their overall acoustic detections and thus foraging behavior (Westell et al. 2022). This makes sperm whales a perfect candidate species for combining passive acoustic data with the active acoustic EK60 data to examine the relationship between prey fields and cetacean foraging behavior.

The objective of this project was to combine active acoustic data with sperm whale acoustic dive profiles to better understand how the tracked whales were targeting prey layers in the continental shelf waters off

the northeast coast of the U.S. We collected these data in the summer of 2016 during the northeast shipboard abundance survey (HB1603). Then we annotated and localized the sperm whale dives as described in Westell et al. (2022) and Sections 6.4 and 6.5.

As sperm whales typically forage at depths greater than 200 m (e.g., Watwood et al., 2006), we used the 18 and 38 kHz narrowband EK60 active acoustic data to map the vertical distributions of the mesopelagic fish and plankton communities. We binned the acoustic data into 2.0-m vertical by 10-s horizontal cells. We created a simple classification system based on the relationship between the volume backscattering amplitudes (*Sv* dB re m^2 m^{-3}) between the two frequencies (*Sv*(18) and *Sv*(38)). Subsequently we coded the data as: *Sv*(18) > *Sv*(38) (code=1), *Sv*(18) = *Sv*(38) (code=1), and *Sv*(18) < *Sv*(38) (code=3), where we considered the differences between *Sv*(18) and *Sv*(38) of less than or equal to 3 dB as equal. Broadly, code 1 indicates organisms with a gas inclusion (e.g., fish with a gas filled swimbladder or siphonophores), code 2 is still uncertain and code 3 indicates organisms that do not have a gas inclusion (e.g., squid or other non-gas bearing fish).

Based on when the EK60 was active, we selected 14 U-shaped sperm whale acoustic dive profiles to combine with the active acoustic data. To account for variation and/or error in the estimated depth of the whale, we applied a LOESS smoothing with a span of 0.2 (**Figure 6-7**). We then combined the smoothed acoustic dive profile with the EK60 data by synchronizing the two data types by time and depth. As a preliminary indicator of foraging behavior and prey preference, we calculated the proportion of time a whale spent in each code and at various depth intervals.

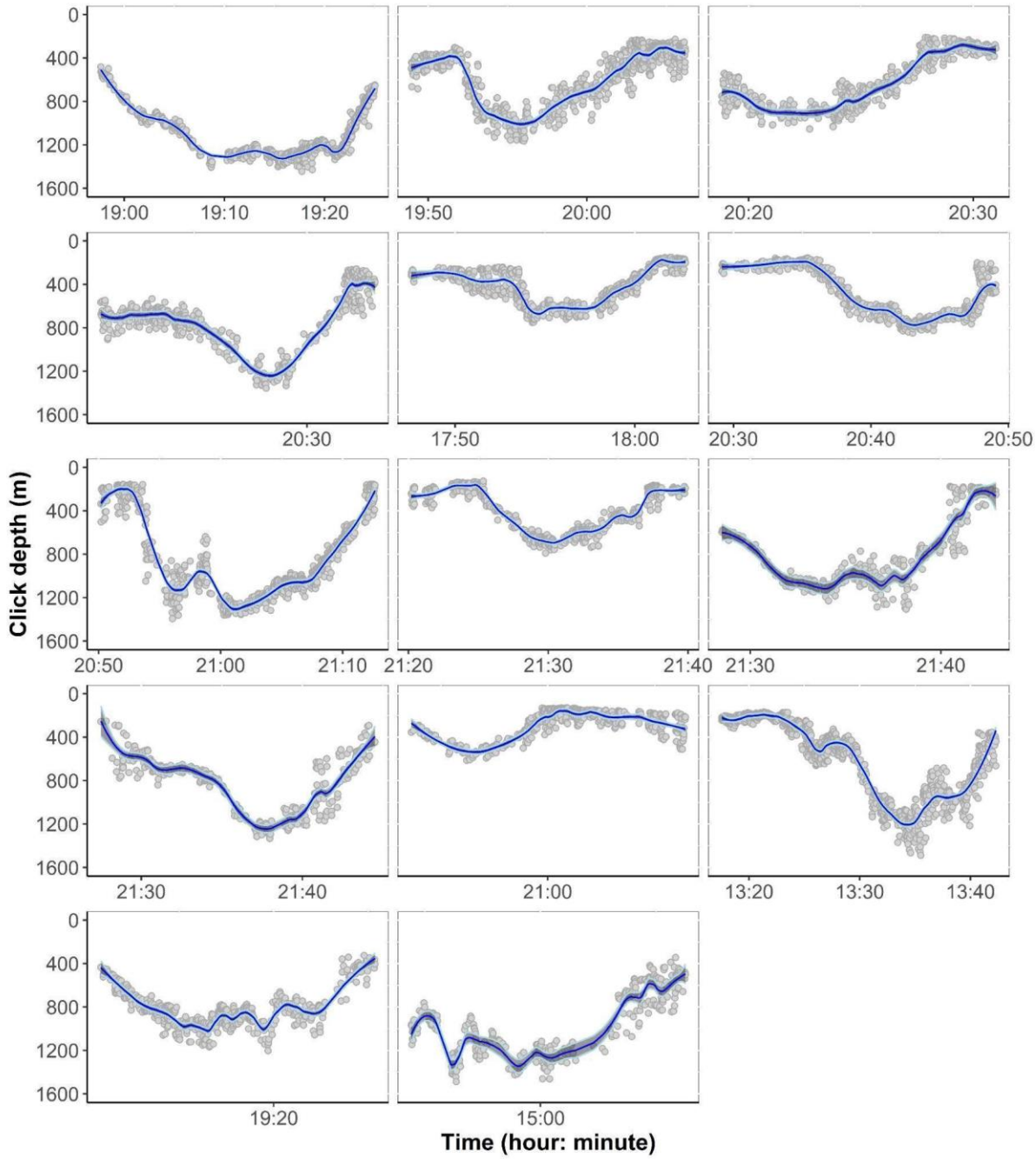

Figure 6-7. Acoustic dive profiles of 14 dives
Grey points represent the estimated depth of each click. We applied a LOESS smoothing (span = 0.2) using the statistical software R (v. 4.2.1; R Core Team 2021) to the data, where the fitted curves are dark blue lines and their 99% confidence intervals are light blue lines.

An example of one smoothed acoustic dive profile overlaid on a visualization of the EK60 data is in **Figure 6-8**. Above 500 m is predominately classified as code 1 (blue) indicating the presence of gas-bearing animals. Between 500-600 m is classified as code 3 (yellow) suggesting availability of non-gas bearing fish or squid.

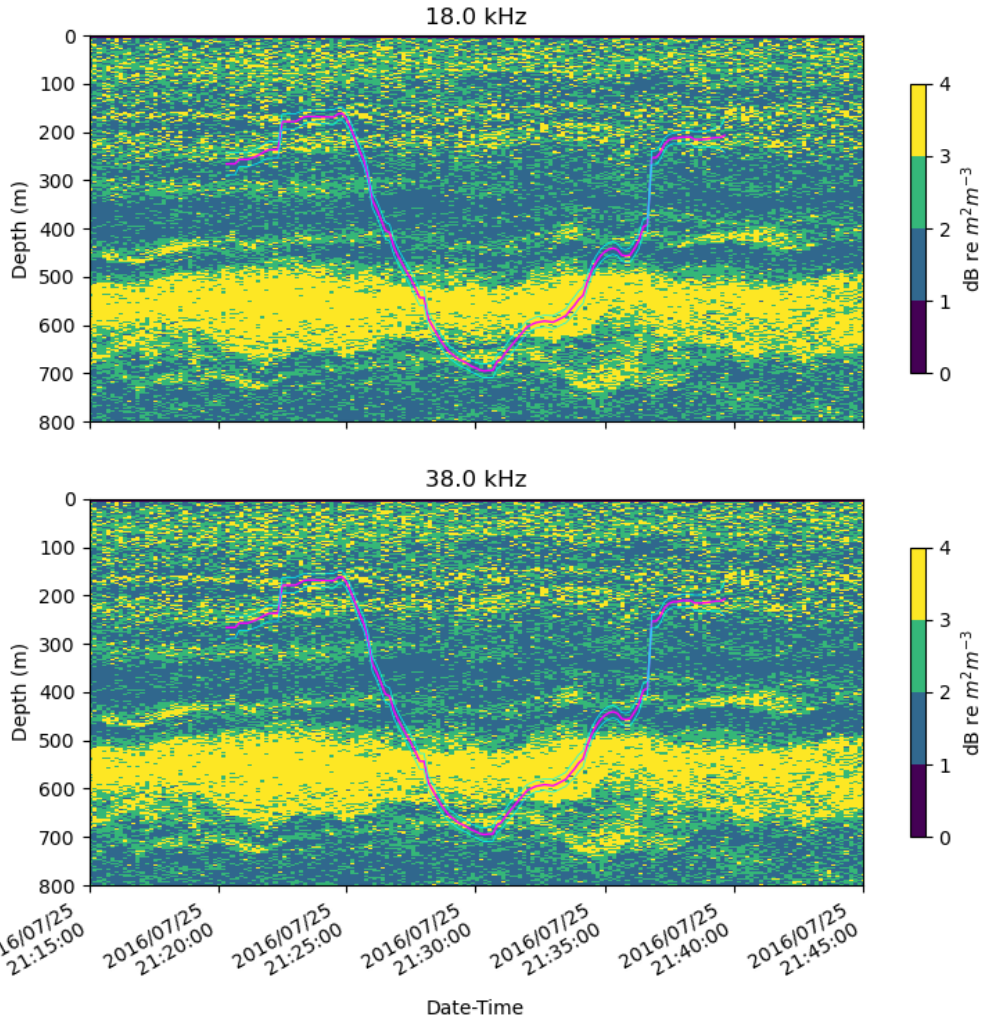

Figure 6-8. 18 and 38 kHz *Sv* relationships and dive profiles
Color denotes classification scheme, not backscatter amplitude. Code 1 is blue, code 2 is green and code 3 is yellow. The LOESS smoothed dive profile is the magenta line and its ±99% confidence interval are the cyan lines.

The localized section of this dive is 19.5 minutes in duration. We selected the active acoustic echogram cells corresponding to the LOESS-smoothed dive profile ± 99% confidence interval throughout the full dive. Summing the amount of time per code for this dive resulted in 7.7 min (39%) in code 1, 6.4 min (33%) in code 2, and 5.4 min (28%) in code 3. We binned the sperm whale's dive into 200 m intervals and calculated the amount of time per code (**Figure 6-9**). In total, the localized portion of the dive included 3.1 min at 0-200 m, 6.4 min at 200-400 m, 6.1 min at 400-600 m, and 3.9min at 600-800 m. The whale spent the greatest amount of time at 200-400 m in code 1 (17%) and at 400-600 m in code 3 (14%).

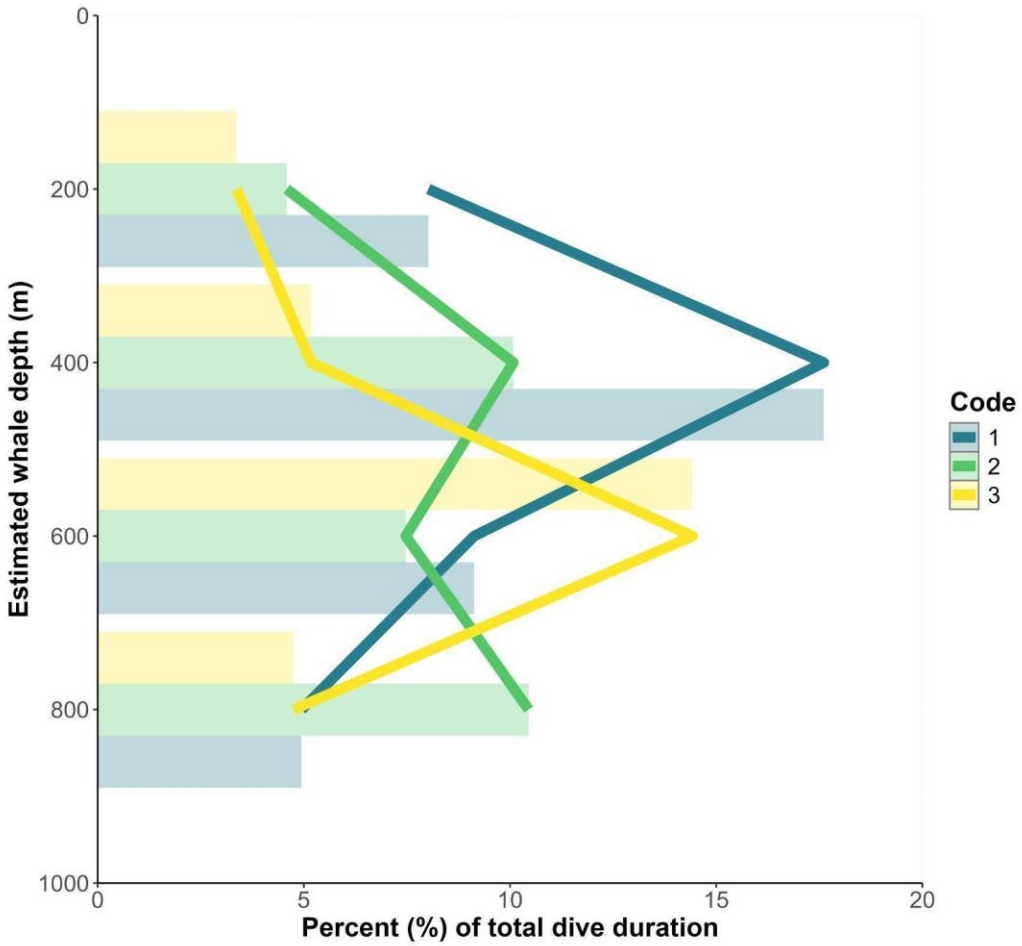

Figure 6-9. Percent (%) of total dive duration the whale spent at 200 m depth intervals per code

While the total time was highest at 200-400 m and in code 1, this section of the dive included part of the descent and ascent when the sperm whale may not have been actively foraging. Based on what is known about sperm whale dive and foraging behavior, it is possible the whale was targeting and actively foraging in the prey layer between 500 - 700 m, containing non-gas bearing fish or squid. This aligns with the peak in time spent in code 3 (non-gas bearing fish or squid) at the 400-600 m depth interval (**Figure 6-9**).

Our immediate next steps involve finalizing the methodology and summarizing the findings from all analyzed acoustic dive profiles. A key part of the project is comparing the active acoustic results with data from the survey's fish trawls. This comparison will enhance our understanding of prey layers and help us complete the classification system for the acoustic data. We will also perform additional analysis to determine the probable foraging phase for each acoustic dive profile and calculate and interpret the amount of time each sperm whale spends within different prey layers. Ultimately, we are working toward developing a scientific publication based on this methodological approach.

6.7 Understanding the Effects of Echosounders on Beaked Whales

Beaked whales have been observed to react to human-made sounds. Studies by McCarthy et al. (2011) and DeRuiter et al. (2013) demonstrated that exposure to mid-frequency active sonar pulses caused

beaked whales to change their orientation and travel directly away from the sound source. Furthermore, Cholewiak et al. (2017) found that beaked whales were rarely detected on towed hydrophone arrays when an EK60 echosounder was active. To gain a better understanding of this behavior, this section presents the results from collecting additional towed hydrophone array data, both with and without the EK60, during line transect visual surveys (detailed in Section 4.2.3), as well as the findings from dedicated experiments.

6.7.1 Methods

During NEFSC shipboard surveys in the summers of 2013, 2016, and 2021 we collected acoustic data from towed hydrophone arrays during visual line transect abundance surveys (see Section 4.2.3 for details). These were the same data that we used in the abundance estimates of vocalizing beaked whales (Section 4.10).

During the HB2102 shipboard abundance survey we conducted a designed experiment to explore the behavior of beaked whales in response to EK60 active acoustics. The experiment involved surveying three cloverleaf pattern track lines with the EK60 in active mode over three bottom mounted passive acoustics recorders (AMARs) deployed by the Department of Fisheries and Oceans Canada in the Fundian Channel, off of Georges Bank, and within Corsair Canyon (**Figure 6-10**). The depths of these recorders were at similar depths that beaked whales forage at; thus, they serve as a proxy for what the sound exposure would be for a beaked whale. Each cloverleaf's radius was 4 km. The bottom mounted recorders were duty-cycled such that two recorders recorded 6 min every 15 min, and one recorded 6 min every 30 min (NEFSC and SEFSC 2025).

Additionally, during HB2102, we conducted opportunistic playback experiments using just the 18-kHz signal of the EK60 to incoming beaked whale signals on the towed hydrophone array. This occurred around the 2000 m contour at the base of Hydrographer Canyon (**Figure 6-10**). Using PAMGuard's Bearing-Time display, the technician monitored for incoming beaked whale clicks. Upon receiving at least one minute of nearly continuous clicking, the acoustic technician signaled to the survey technician to switch the EK60 into active mode for at least one minute. We only used the 18 kHz ping for the playback experiments, we switched all other frequencies to passive mode. During the playback, the acoustic technician logged beaked whale click activity and coordinated with the ship's crew to stay within a 1.5

km slant range of the echolocating animal.

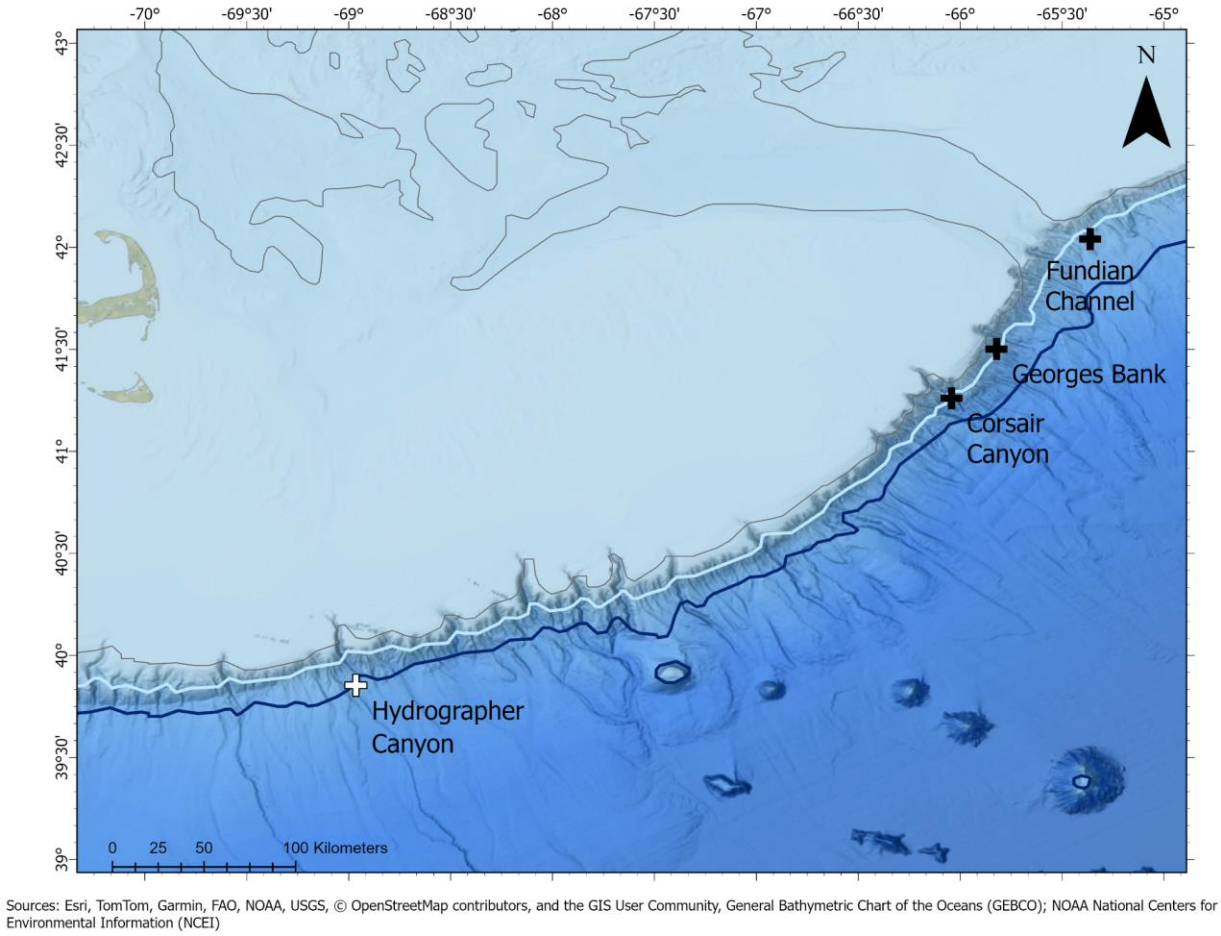

Figure 6-10. Locations of where in situ experiments were done with the EK60 during HB2102
Black crosses represent the locations where we conducted the AMARs clover-leaf passes. White cross represents the location where we conducted real-time playbacks of the EK60 to beaked whales.

For the bottom mounted acoustic recorders, we generated long-term spectral averages and manually reviewed them using the software Triton (Wiggins and Hildebrand 2007) within the program Matlab (MathWorks, Inc.) for the presence of EK60 pings. We determined the presence/absence of a ping within a one-minute time bin. We then used the GPS track of the survey vessel to calculate the true horizontal range of the EK60 and the slant range for every minute of recording. We created a matched filter detector within Matlab to detect each EK60 ping at each operating frequency to determine the received level at a given range. We then estimated the maximum sound pressure levels of each frequency of the EK60 per minute and binned per detection slant range using custom Matlab scripts.

We assessed the presence of beaked whales across the bottom mounted recorders at the daily scale throughout the full deployment to get an overall sense of beaked whale usage at the study sites. In addition, we assessed the beaked whale presence at a minute level for the three-day period around the time we completed the cloverleaves. We then analyzed the beaked whale clicks following the methods in Baumann-Pickering et al. (2013) and Stanistreet et al. (2017).

6.7.2 Results and Discussion

6.7.2.1 Line Transect Surveys

From the beaked whale passive acoustic events collected during the line transect surveys during the three shipboard abundance surveys, we identified a total of 411 beaked whale events, with the most events coming from the HB1603 survey (n= 207, **Table 6-4**). Most passive acoustic events were of goose-beaked whales (n= 297 events), then True's beaked whale (n= 157 events), with few detections of Sowerby's and Gervais' beaked whales (n= 14 and 8 events, respectively). Neither Blainville's beaked whale nor northern bottlenose whale clicks were found in these datasets.

Consistent with prior research (Cholewiak et al., 2017), the majority of beaked whale detections occurred with echosounders in passive mode (n = 472), as opposed to active mode (n = 42). Goose-beaked whales were the most frequently observed beaked whale species when the echosounder was active. Notably, we did not detect Gervais' and True's beaked whales when the EK60 echosounder was in active mode (**Table 6-4**).

Similarly, when the EK60 was in active mode, we did not detect beaked whale acoustic presence along seamount chains across all three years. Beaked whales are known to inhabit seamounts, which provide potential upwelling and nutrients in typically nutrient-poor abyssal plains (Broadus et al., 2025; Baumann-Pickering et al., 2016; Morato et al., 2016). We visually observed beaked whales along seamounts, yet our hydrophones did not detect them when the echosounder was active. We hypothesize that this is because whales alter their foraging behavior, possibly changing their orientation away from our hydrophones, when they detect an echosounder. This hypothesis is supported by McCarthy et al. (2011) and DeRuiter et al. (2013), who showed that beaked whales changed orientation and traveled directly away from a source when exposed to mid-frequency active sonar pulses. In contrast, Hazen et al. (2011) and Varghese et al. (2021) found no change in foraging effort when examining the effect of echosounder use on beaked whales; however, these studies did not include observations from tagged individuals. Therefore, fine-scale behavioral information, such as changes in animal heading, still needs to be determined.

Table 6-4. Beaked whale events detected by the towed hydrophone array deployments, by year
Each year was a northeast shipboard abundance survey. "Active" and "Passive" represent the alternating states of the EK60.

Species	2013 Active	2013 Passive	2016 Active	2016 Passive	2021 Active	2021 Passive
Goose-beaked	9	115	19	101	11	42
True's	0	48	0	67	0	42
Gervais'	0	4	0	4	0	0
True's / Gervais'	0	18	1	9	1	9
Sowerby's	0	1	0	6	1	6
Subtotals	**9**	**186**	**20**	**187**	**13**	**99**
% Presence with echosounder in active mode	5%		10%		12%	

6.7.2.2 Designed Experiment

We recorded EK60 frequencies up to 120 kHz on the bottom mounted recorders, with the 18 kHz transmit pulse being the most dominant source. The maximum slant range of the 18 kHz frequency was 6.2 km off of Fundian Channel (**Figure 6-11**). We detected all frequencies up to a maximum slant range of 1.7 km. Received levels of the 18 kHz pulse on the bottom mounted recorders ranged from 101 dB to 171 dB, with a median received level of 129 dB (**Figure 6-11**).

We detected three beaked whale species at each of the bottom mounted recorder sites: goose-beaked whales, True's/Gervais' beaked whales, and Sowerby's beaked whales. We most commonly detected Sowerby's at each site, with over 84% of days present (**Table 6-5**). The least present was True's/Gervais' at the Fundian Channel (59% of days). In the three days surrounding the cloverleaf passes, only the Georges Bank site had beaked whale presence immediately before and after the cloverleaf pass, and only of Sowerby's beaked whales (**Figure 6-12**). No pattern or response could be assessed for Sowerby's besides the fact that we detected an echolocation just prior to the start of the EK60 transmission, as well as during the transmission. Actual duration of exposure cannot be assessed due to the duty-cycling of the recorders, and instead should be noted as at least a portion of a foraging dive could contain exposure to the ship's echosounders.

During the course of the HB2102 survey, only one beaked whale encounter lasted long enough to conduct a playback trial of the 18 kHz pulse. On that encounter we detected True's beaked whale clicks on June 30, 2021 at 16:01 UTC at an initial slant range of 2.2 km. The ship stayed within 1.5 km of the detected clicks, and the closest point of approach was a slant range of around 1.2 km. This could mean the detected animal was directly under the ship or at most 1.13 km away if assuming a click depth of 0.4 km. The 18 kHz pulse started transmitting at 16:17 UTC in the midst of active clicking. Within one minute of the transmission, we recorded no clicks on the towed array. We then switched the 18 kHz ping back into passive mode at 16:20 UTC, for a total exposure duration of 2.37 min. We detected clicks from the whale two minutes after cessation of the 18 kHz ping and continued until 16:26 UTC, for a total vocal phase of 25 min. True's beaked whale vocal phases are generally around 19 min (NEFSC 2019, DeAngelis et al. 2025); thus, we presume that this animal completed one foraging dive, with a pause or orientation away from the vessel during the 18 kHz ping transmission.

The detection function of each beaked whale species for passive acoustic data collected from the towed hydrophone array on these abundance surveys (see Section 4.10) showed a horizontal effective strip half width of ~2 km (**Table 4-27**). This corresponds to received levels within the first three range bins in **Figure 6-11**. We received pulse levels in the 18, 38, and 70 kHz frequency bands ranging from 91 to 171 dB. From the one encounter with True's beaked whale with the towed array data, the whale could have been exposed to these received levels. Beaked whales have been shown to exhibit an avoidance response and cessation of foraging to active sonar pings at close ranges at estimated received levels between 89 and 127 dB (DeRuiter et al. 2013, Falcone et al. 2017). A population of goose-beaked whales within the Southern California Antisubmarine Warfare Range did not show a reduction in foraging during 12 kHz multibeam echosounder use (Varghese et al. 2020) while Cholewiak et al. (2017) and Trickey et al. (2022) showed a reduction in beaked whale acoustic presence with shipboard echosounders devices. It may be that beaked whales continue foraging while echosounders are actively transmitting, but orient themselves away from the sound source, and thus reduce their probability of being detected with single sensors. This could be why the towed array does not detect beaked whales when the EK60 is actively emitting pulses, and why Varghese et al. (2020) still detected beaked whales across the navy range. However, the Varghese et al. (2020) study was in an area of high naval activity, whereas Cholewiak et al. (2017) and Trickey et al. (2022) were in areas of acoustically "naive" populations. We need more work to understanding the nuances of beaked whale responses to shipboard echosounders.

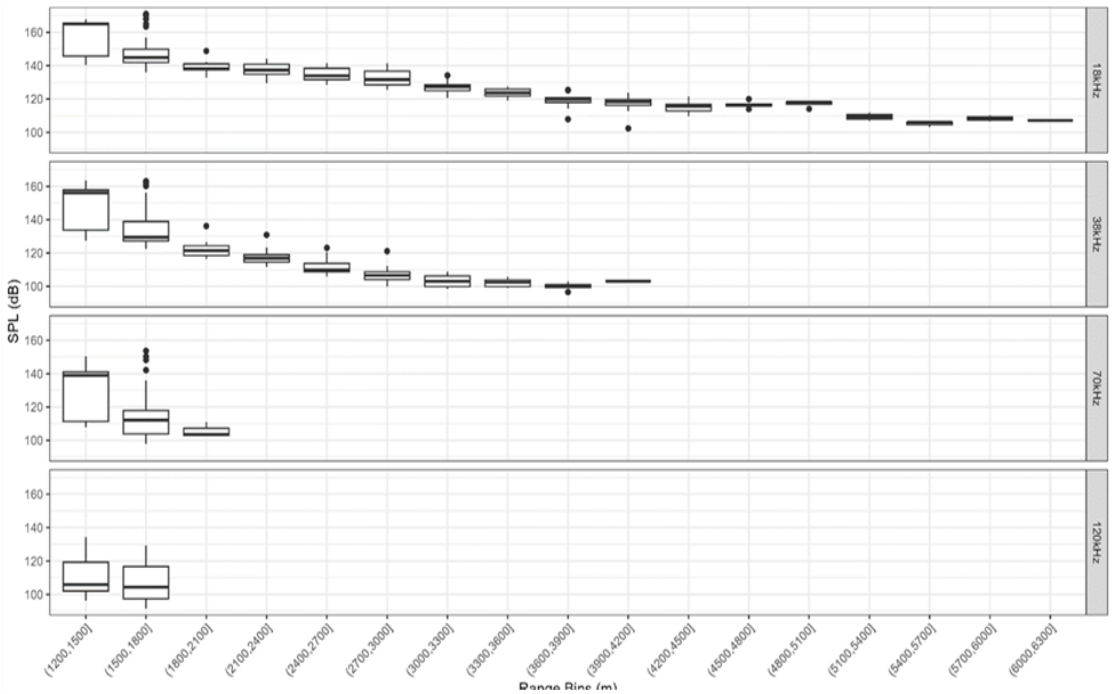

Figure 6-11. Boxplots of the maximum sound pressure level per minute for EK60 frequencies

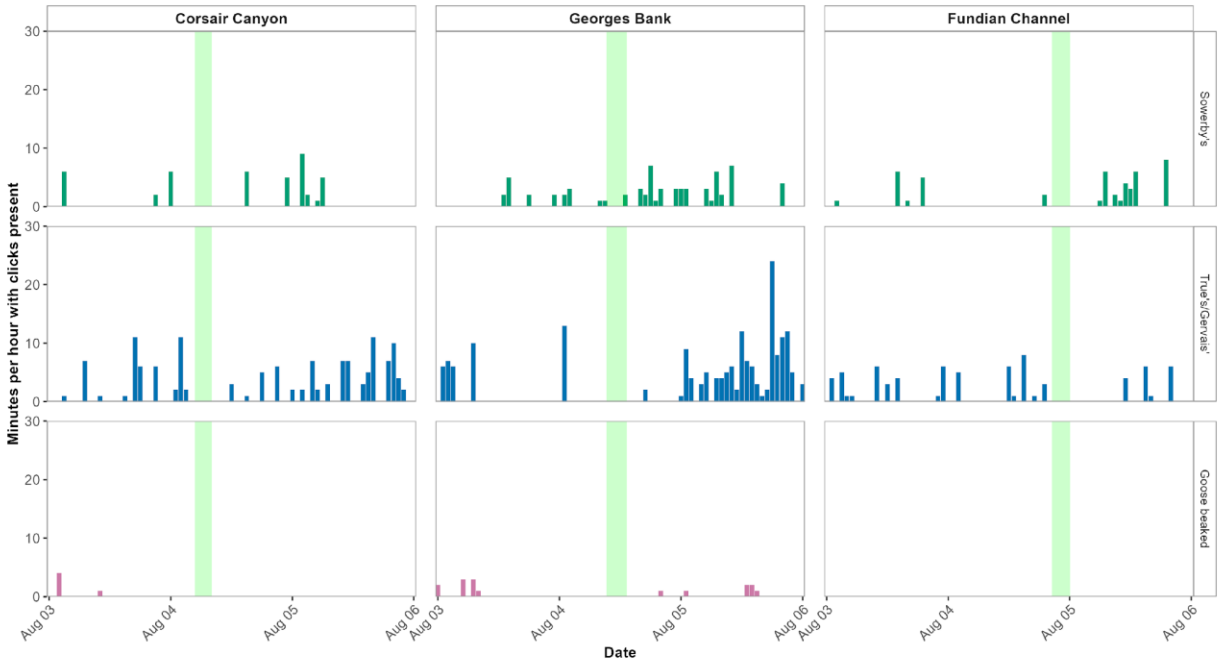

Figure 6-12. Minutes per hour with presence of beaked whales by species and location
During the three days surrounding the cloverleaf passes (green timeframe).

Table 6-5. Percent of days each beaked whale species was present, by species and location

Deployments were almost one year in duration (September 2020 - August 2021)Site	% Days Present Sowerby's beaked whale	% Days Present True's/Gervais' beaked whale	% Days Present Goose-beaked whale
Georges Bank	98	77	90
Corsair Canyon	89	89	73
Fundian Channel	84	59	72

6.8 Acknowledgements

Thank you to Taiki Sakai for his technical expertise, for writing the R functions to automate the dive depth detection method, and for integrating sperm whale inter-pulse-interval estimation into the dive depth method. Thank you to Amanda Holdman for streamlining and helping to present the dive depth detection method at the 2024 Detection, Classification, Localization, and Density Estimation workshop. Thank you to Ernst F Hollings scholars Alexandra Redford, Madison Medina, Abigail Fritz, and Nicholas Hayes for their assistance in analyzing the data for sperm whales, beaked whales, and delphinids. Thank you to our colleagues Michael Adams, Jinshan Xu, and Joy Stanistreet at the Department of Fisheries and Oceans Canada for their collaboration and efforts to measure the propagation range of the EK60.

6.9 References Cited

Barile C, Berrow S, O'Brien J. 2024. Click-click, who's there? Acoustically derived estimates of sperm whale size distribution off western Ireland. Front Mar Sci.10. https://doi.org/10.3389/fmars.2023.1264783

Barlow J, Taylor BL. 2005. Estimates of sperm whale abundance in the northeastern temperate Pacific from a combined acoustic and visual survey. Mar Mam Sci. 21(3):429–445.

Baumann-Pickering S, McDonald MA, Simonis AE, Solsona Berga A, Merkens KPB, Oleson EM, Roch MA, Wiggins SM, Rankin S, Yack TM, Hildebrand JA. 2013. Species-specific beaked whale echolocation signals. J Acoust Soc Am. 134(3):2293–2301. https://doi.org/10.1121/1.4817832

Beslin WAM, Whitehead H, Gero S. 2018. Automatic acoustic estimation of sperm whale size distributions achieved through machine recognition of on-axis clicks. J Acoust Soc Am. 144(6):3485–3495. https://doi.org/10.1121/1.5082291

Best PB. 1979. Social organization insperm whales, *Physeter macrocephalus*. In: Winn HE, Olla BL, editors. Behavior of Marine Animals: Current Perspectives in Research. Boston, MA: Springer US; p. 227–289. https://doi.org/10.1007/978-1-4684-2985-5_7

Caruso F, Sciacca V, Bellia G, Domenico ED, Larosa G, Papale E, Pellegrino C, Pulvirenti S, Riccobene G, Simeone F, et al. 2015. Size distribution of sperm whales acoustically identified during long term deep-sea monitoring in the Ionian Sea. PLOS ONE. 10(12):e0144503. https://doi.org/10.1371/journal.pone.0144503

Cholewiak D, DeAngelis AI, Palka D, Corkeron PJ, Van Parijs SM. 2017. Beaked whales demonstrate a marked acoustic response to the use of shipboard echosounders. R Soc Open Sci. 4(12):170940. https://doi.org/10.1098/rsos.170940

DeAngelis AI, Valtierra R, Van Parijs SM, Cholewiak D. 2017. Using multipath reflections to obtain dive depths of beaked whales from a towed hydrophone array. J Acoust Soc Am. 142(2):1078. https://doi.org/10.1121/1.4998709

DeAngelis AI, Westell A, Baumann-Pickering S, Bell J, Cholewiak D, Corkeron PJ, Soldevilla MS, Solsona-Berga A, Trickey JS, Parijs SMV. 2025. Habitat utilization by beaked whales in the western North Atlantic Ocean using passive acoustics. Mar Eco Prog Ser. 754:137–153. https://doi.org/10.3354/meps14771

DeRuiter SL, Southall BL, Calambokidis J, Zimmer WMX, Sadykova D, Falcone EA, Friedlaender AS, Joseph JE, Moretti D, Schorr GS, et al. 2013. First direct measurements of behavioural responses by Cuvier's beaked whales to mid-frequency active sonar. Biol Let. 9(4):20130223. https://doi.org/10.1098/rsbl.2013.0223

Fais A, Johnson M, Wilson M, Aguilar Soto N, Madsen PT. 2016. Sperm whale predator-prey interactions involve chasing and buzzing, but no acoustic stunning. Sci Rep. 6(1):28562. https://doi.org/10.1038/srep28562

Fais A, Soto NA, Johnson M, Pérez-González C, Miller PJO, Madsen PT. 2015. Sperm whale echolocation behaviour reveals a directed, prior-based search strategy informed by prey distribution. Behav Ecol Sociobiol.:1–12. https://doi.org/10.1007/s00265-015-1877-1

Falcone EA, Schorr GS, Watwood SL, DeRuiter SL, Zerbini AN, Andrews RD, Morrissey RP, Moretti DJ. 2017. Diving behaviour of Cuvier's beaked whales exposed to two types of military sonar. R Soc Open Sci. 4(8):170629. https://doi.org/10.1098/rsos.170629

Ferrari M, Trinh M, Sarano F, Sarano V, Giraudet P, Preud'homme A, Heuzey R, Glotin H. 2024. Age and interpulse interval relation from newborn to adult sperm whale (*Physeter macrocephalus*) off Mauritius. Sci Rep. 14(1):18474. https://doi.org/10.1038/s41598-024-51194-5

Fisher FH, Simmons VP. 1977. Sound absorption in sea water. J Acoust Soc Am. 62(3):558–564. https://doi.org/10.1121/1.381574

Gillespie D, Gordon J, McHugh R, McLaren D, Mellinger D, Redmond P. 2008. PAMGUARD: Semiautomated, open source software for real-time acoustic detection and localization of cetaceans. Proc Inst Acous. 30(5). https://pubs.aip.org/asa/jasa/article/125/4_Supplement/2547/698127/PAMGUARD-Semiautomated-open-source-software-for

Gordon JCD. 1991. Evaluation of a method for determining the length of sperm whales (*Physeter catodon*) from their vocalizations. J Zool. 224(2):301–314. https://doi.org/10.1111/j.1469-7998.1991.tb04807.x

Griffin DR, Webster FA, Michael CR. 1960. The echolocation of flying insects by bats. Anim Beh. 8(3):141–154. https://doi.org/10.1016/0003-3472(60)90022-1

Growcott A, Miller B, Sirguey P, Slooten E, Dawson S. 2011. Measuring body length of male sperm whales from their clicks: The relationship between inter-pulse intervals and photogrammetrically measured lengths. J Acoust Soc Am. 130(1):568–573. https://doi.org/10.1121/1.3578455

Guerra M, Hickmott L, van der Hoop J, Rayment W, Leunissen E, Slooten E, Moore M. 2017. Diverse foraging strategies by a marine top predator: Sperm whales exploit pelagic and demersal habitats in the Kaikōura submarine canyon. Deep Sea Research Part I: Oceanographic Research Papers. 128:98–108. https://doi.org/10.1016/j.dsr.2017.08.012

Kates Varghese H, Lowell K, Miksis-Olds J, DiMarzio N, Moretti D, Mayer L. 2021. Spatial analysis of beaked whale foraging during Two 12 kHz multibeam echosoundersurveys. Front Mar Sci. 8. https://doi.org/10.3389/fmars.2021.654184

Madsen P, Wahlberg M, Møhl B. 2002. Male sperm whale (*Physeter macrocephalus*) acoustics in a high-latitude habitat: implications for echolocation and communication. Behav Ecol Sociobiol. 53(1):31–41. https://doi.org/10.1007/s00265-002-0548-1

Møhl B, Wahlberg M, Madsen PT, Heerfordt A, Lund A. 2003. The monopulsed nature of sperm whale clicks. J Acoust Soc Am. 114(2):1143–1154. https://doi.org/10.1121/1.1586258

Norris KS, Harvey GW. 1972. A Theory for the Function of the Spermaceti Organ of the Sperm Whale (*Physeter Catodon L.*). In: Anim Orientation Navigation SP-262; p. 397–417. https://ntrs.nasa.gov/citations/19720017437

Northeast Fisheries Science Center, Southeast Fisheries Science Center. 2019. 2018 Annual Report of a Comprehensive Assessment of Marine Mammal, Marine Turtle, and Seabird Abundance and Spatial Distribution in U.S. waters of the Western North Atlantic Ocean – AMAPPS II. https://repository.library.noaa.gov/view/noaa/22040

Northeast Fisheries Science Center, Southeast Fisheries Science Center. 2025. 2024 Annual Report of a Comprehensive Assessment of Marine Mammal, Marine Turtle, and Seabird Abundance and Spatial Distribution in U.S. waters of the Western North Atlantic Ocean – AMAPPS III.

Orphanides CD, Jech JM, Palka DL, Collie J. 2023. Relating marine mammal distribution to water column prey structure derived from echosounding. Mar Ecol Prog Ser. 711:101–119. https://doi.org/10.3354/meps14290

Palka D, Wicker J, Martinez A, Garrison L, Reid J, Soldevilla M, DeAngelis A, Wallace J, Broughton E, Walsh H, et al. 2022. 2021 Annual Report of a Comprehensive Assessment of Marine Mammal, Marine Turtle, and Seabird Abundance and Spatial Distribution in U.S. waters of the Western North Atlantic Ocean – AMAPPS III. https://doi.org/10.25923/jazw-5467

Rice D. 1989. Sperm whale (*Physeter macrocephalus* Linnaeus 1785. In: Handbook of Marine Mammals. S. Ridgeway and R. Harrison (London).

Sakai T. 2024. PAMpal: Load and Process Passive Acoustic Data. R Package version 1.2. https://CRAN.R-project.org/package=PAMpal

Solsona-Berga A, Posdaljian N, Hildebrand JA, Baumann-Pickering S. 2022. Echolocation repetition rate as a proxy to monitor population structure and dynamics of sperm whales. Rem Sens Ecol Cons. 8(6):827–840. https://doi.org/10.1002/rse2.278

Stanistreet JE, Nowacek DP, Baumann-Pickering S, Bell JT, Cholewiak DM, Hildebrand JA, Hodge LEW, Moors-Murphy HB, Van Parijs SM, Read AJ. 2017. Using passive acoustic monitoring to

document the distribution of beaked whale species in the western North Atlantic Ocean. Can J Fish Aquat Sci. 74(12):2098–2109. https://doi.org/10.1139/cjfas-2016-0503

Teloni V, Mark JP, Patrick MJO, Peter MT. 2008. Shallow food for deep divers: Dynamic foraging behavior of male sperm whales in a high latitude habitat. J Exp Mar Biol Ecol. 354(1):119–131. https://doi.org/10.1016/j.jembe.2007.10.010

Trickey JS, Cárdenas-Hinojosa G, Rojas-Bracho L, Schorr GS, Rone BK, Hidalgo-Pla E, Rice A, Baumann-Pickering S. 2022. Ultrasonic antifouling devices negatively impact Cuvier's beaked whales near Guadalupe Island, México. Commun Biol. 5(1):1005. https://doi.org/10.1038/s42003-022-03959-9

Watwood SL, Miller PJO, Johnson M, Madsen PT, Tyack PL. 2006. Deep-diving foraging behaviour of sperm whales (*Physeter macrocephalus*). J Anim Ecol. 75(3):814–825. https://doi.org/10.1111/j.1365-2656.2006.01101.x

Weilgart L, Whitehead H. 2011. Distinctive vocalizations from mature sperm whales (*Physeter macrocephalus*). Can J Zool. 66(9):1931–1937. https://doi.org/10.1139/z88-282

Westell A, Rowell TJ, Posdaljian N, Solsona-Berga A, Van Parijs SM, DeAngelis AI. 2025. Acoustic presence and demographics of sperm whales (*Physeter macrocephalus*) off southern New England and near a U.S. offshore wind energy area. ICES J Mar Sci. 82(4):fsae012. https://doi.org/10.1093/icesjms/fsae012

Westell A, Sakai T, Holdman A. 2024. Introduction to the Dive Depth Detection method. Detection, Classification, Localization, and Density Estimation Workshop, 03 June 2024.

Westell A, Sakai T, Valtierra R, Van Parijs SM, Cholewiak D, DeAngelis A. 2022. Sperm whale acoustic abundance and dive behaviour in the western North Atlantic. Sci Rep. 12(1):16821. https://doi.org/10.1038/s41598-022-20868-3

Whitehead H. 2003. Sperm whales: social evolution in the ocean. University of Chicago Press.

Wiggins SM, Hildebrand JA. 2007. High-frequency Acoustic Recording Package (HARP) for broad-band, long-term marine mammal monitoring. In: 2007 Symposium on Underwater Technology and Workshop on Scientific Use of Submarine Cables and Related Technologies. Institute of Electrical and Electronics Engineers, Tokyo, Japan; p. 551–557. https://doi.org/10.1109/UT.2007.3707607 Sea Turtle Research

7 Sea Turtle Ecology Research

Primary authors: Kate Choate, Larisa Avens, Chris Sasso, Samir Patel, Heather Haas, Debra Palka

A growing concern surrounds the impact of human activities on sea turtles. To assess these impacts a comprehensive understanding of the current distribution, habitat usage, and life history of the turtles is essential, particularly how these factors intersect with the changing environment and human activities. Furthermore, it is important to predict the turtles' future changes in their dynamic ecosystem. This necessitates not only historical and current data on animal locations but also an understanding of the underlying reasons for their presence and behaviors.

To grasp the ecology of sea turtles within their complex ecosystem, the Atlantic Marine Assessment Program for Protected Species (AMAPPS) Turtle Ecology team, in collaboration with its partners, are using animal-borne tags employed on leatherback (*Dermochelys coriacea*) and loggerhead (*Caretta caretta*) sea turtles. The data from the tags allow us to monitor the sea turtle's spatiotemporal distribution and water-column usage and behavior. Since we had to bring the turtles onboard a ship to tag them, we also had the opportunity for collaborators to collect biological and life history characteristics, ranging from morphometric measurements to blood biochemistry. These activities address the following AMAPPS objectives (all are outlined in Section 2.2):

3) Conduct tagging studies of protected species to develop corrections for availability bias in the abundance survey data and to investigate behavior and ecology of species in areas of interest;
4) Collect additional data on life-history and ecology, including habitat use, residence time, frequency of use, and behavior;
5) Identify currently used, viable technologies and explore alternative platforms and technologies to improve population assessment studies, if necessary.
6) Assess the population size of surveyed species at regional scales; and develop models and associated tools to translate these survey data into seasonal, spatially explicit density estimates incorporating habitat characteristics.

This chapter details the data collected during AMAPPS III (Sections 7.1 and 7.2) fieldwork and the subsequent analyses. We present new information regarding sea turtle blood biochemical profiles, gas embolism risks, and trophic positions (Section 7.3). Additionally, we report on shifts in spatiotemporal location distributions (Section 7.4) and dive patterns (Section 7.5). We also used these dive patterns to estimate availability bias, which allowed us to correct at-surface abundance estimates from visual line transect surveys to achieve an unbiased abundance estimate for turtles throughout the water column (Chapter 4). Finally, this chapter examines spatiotemporal interactions of turtles with the sea scallop fishery and wind energy areas (Section 7.6).

7.1 Fieldwork FY19 - FY25

During FY19 - FY25 (Oct 2018 - Sep 2025), the AMAPPS Turtle Ecology team and collaborators completed 15 leatherback fieldwork trips (**Table 7-1**) and 13 loggerhead fieldwork trips (**Table 7-2**) with the goal to learn more about the distribution, dive patterns, life history and ecology of the turtles. We used small boats to capture the turtles (**Figure 7-1**). Then we applied 52 suction cups (**Figure 7-2**) and 81 satellite tags to leatherback turtles (**Table 7-1**) and 155 satellite tags (**Figures 7-3 - 7-5**) to loggerheads (**Table 7-2**). Across several field efforts, we also collected water samples for eDNA extraction in the vicinity of known turtle locations (**Tables 7-1 and 7-2**).

In addition, we tagged two Kemp's ridley turtles (1 in March 2023 and 1 in March 2025) on loggerhead turtle tagging cruises. During tagging trips, additional data collected from tagged turtles typically included standard morphometric measurements, tissue sampling, and PIT and flipper tag applications.

Table 7-1. Leatherback tagging trips during FY19 - FY25

Trip	Tag Type/ eDNA collected	Platform	Date	Location	Number of Tags Deployed
2019.05.DC.SE	satellite and suction cup	R/V *Selkie*, *Takacat*, spotter plane	May 2019	Off Beaufort, North Carolina	13
2019.08.DC.SE	satellite	R/V *Selkie*, *Takacat*, spotter plane	Aug 2019	Cape Cod Bay	9
2019.09.DC.SE	suction cup camera	R/V *Selkie*	Sep - Oct 2019	Off Massachusetts	19
2020.09.DC.SE	suction cup camera	R/V *Selkie*, spotter plane	Sep - Oct 2020	Off Massachusetts	11
2021.05.DC.JU	satellite	R/V *Julius*, R/V *Selkie*	May 2021	Off North Carolina	2
2021.08.DC.WJ	satellite/ eDNA	M/V *Warren Jr*, *Little Gray Boat*, R/V *Selkie* and *Takacat*	Aug - Sep 2021	Nantucket Sound, Vineyard Sound, Cape Cod Bay, South of Nantucket	1
2022.04.DC.CO	satellite	R/V *Coriacea*, NOAA Twin Otter 56	Apr - May 2022	Destin, FL	0
2022.05.DC.JU	satellite	R/V *Julius*	May 2022	Beaufort, NC	10
2022.08.DC.WJ	satellite/ eDNA	M/V *Warren Jr*, R/V *Coriacea*, *Takacat*	Aug - Sep 2022	South of Nantucket (one no DC day in Nantucket Sound)	12
2023.05.DC.JU	satellite	R/V *Julius*	May 2023	North Carolina	4
2023.08.DC.SI	satellite/ eDNA	M/V *Scarlet Isabella*	Aug 2023	South of Nantucket	17
2023.09.DC.CO (BOEM Sound Project)	suction cup/ eDNA	R/V *Coriacea*, F/V *Small Stuff*	Sep - Oct 2023	Nantucket Sound	13
2024.08.DC.CO	satellite	R/V *Coriacea*, R/V *Selkie*, *Takacat*, Twin Otter 46	Aug - Sep 2024	South, East of Nantucket	0
2025.05.DC.SE	satellite	R/V *Selkie*	May 2025	off North Carolina	13

Trip	Tag Type/ eDNA collected	Platform	Date	Location	Number of Tags Deployed
2025.09.DC.CO	satellite/ eDNA	*R/V Coriacea, R/V Selkie*, Takacat, spotter plane	Sep 2025	Nantucket Sound (no DC), South and East of Nantucket	9

Table 7-2. Loggerhead tagging trips during FY19 - FY25

Trip	Tag Type/ eDNA collected	Platform	Date	Location	Number of Tags Deployed
2019.06.CC.KA	satellite	F/V *Kathy Ann*	Jun 2019	Delmarva region of Mid-Atlantic Bight	10
2021.02.CC.SA	satellite	F/V *Salvation*	Feb - Mar 2021	Off North Carolina	9
2021.05.CC.KA	satellite /eDNA	F/V *Kathy Ann*	May 2021	Mid-Atlantic Bight	22
2022.05.CC.KA	satellite	F/V *Kathy Ann*	May 2022	Mid-Atlantic Bight	2
2022.06.CC.KA	satellite/ eDNA	F/V *Kathy Ann*	Jun 2022	Mid-Atlantic Bight	13
2023.03.CC.SA	satellite/ eDNA	F/V *Salvation*	Mar 2023	off North Carolina	9
2023.06.CC.KA	satellite/ eDNA	F/V *Kathy Ann*	Jun 2023	Mid-Atlantic Bight	15
2024.03.CC.SA	satellite	F/V *Salvation*	Mar 2024	off North Carolina	8
2024.06.CC.KA	satellite/ eDNA	F/V *Kathy Ann*	Jun 2024	Mid-Atlantic Bight	23
2024.07.CC.KA	satellite/ eDNA	F/V *Kathy Ann*	Jul 2024	Mid-Atlantic Bight	10
2025.03.CC.SA	satellite	F/V *Salvation*	Mar 2025	off North Carolina	20
2025.06.CC.KA	satellite	F/V *Kathy Ann*	Jun 2025	Mid-Atlantic Bight	10
2025.07.CC.KA	satellite	F/V Kathy Ann	July 2025	Mid-Atlantic Bight	4

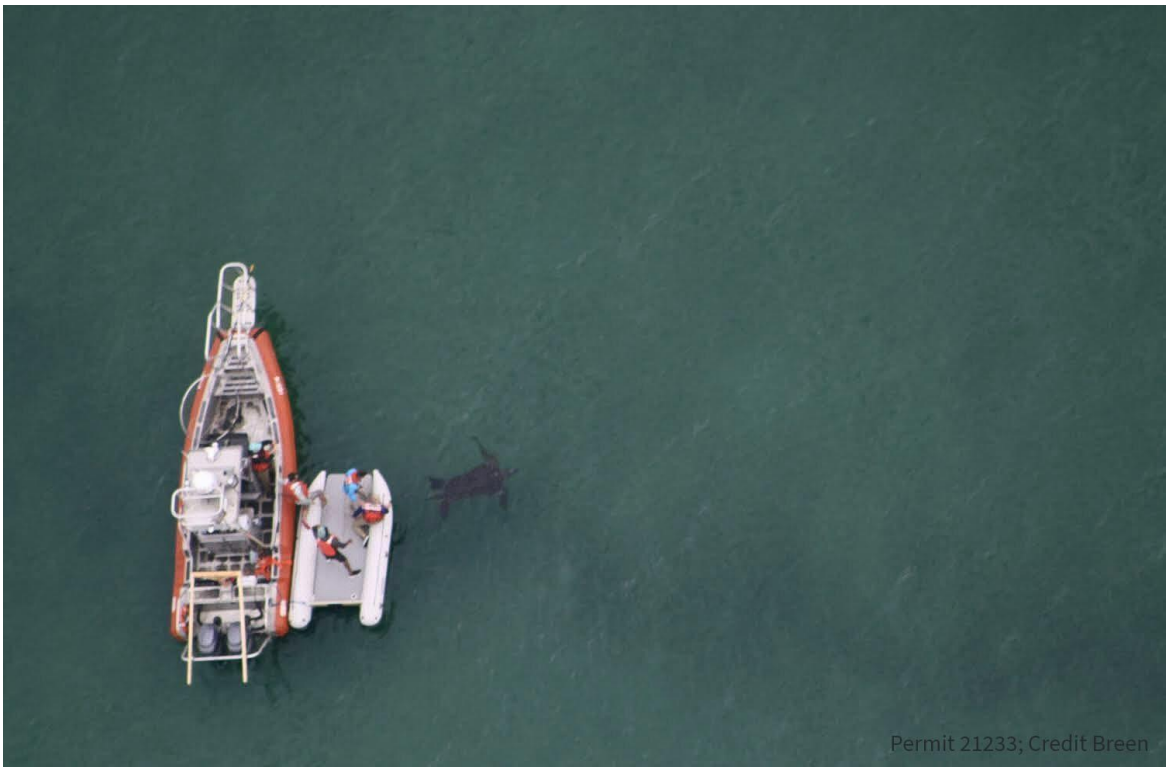

Figure 7-1. Aerial view of R/V Selkie and Takacat in Cape Cod Bay with a leatherback sea turtle
The turtle is swimming away after release in August 2019 off Massachusetts (NMFS Permit No. 21233).

Figure 7-2. Leatherback sea turtle surfaces in Nantucket Sound with a suction cup camera tag
Photo taken September 2023 off of Massachusetts (NMFS Permit No. 22218).

Figure 7-3. Scientific crew with a satellite tagged loggerhead sea turtle aboard the F/V Kathy Ann
Crew are (left to right) Michael Torselli, Kate Choate, Samir Patel, Allison Myers, YiWynn Chan, and Nathan Shivers. Photo taken June 2024 in the Mid-Atlantic Bight (NMFS Permit No. 23639).

Figure 7-4. Loggerhead sea turtle positioned for release
Photo taken March 2025 aboard the F/V Salvation off North Carolina (NMFS Permit No. 23639).

Figure 7-5. Loggerhead with satellite tag being lowered for release from F/V Kathy Ann
Photo taken June 2025 in the Mid-Atlantic Bight (NMFS Permit No. 23639; Credit NEFSC/Choate).

7.2 Database

We store all the tag and biological data in an Oracle database maintained at the Northeast Fisheries Science Center (NEFSC) in Woods Hole, MA. During AMAPPS III we expanded our Oracle database significantly to now contain 50 tables and 16 views (**Tables 7-3 - 7-5**). We are continuously striving to improve the efficiency of our data querying.

Argos and the satellite tag manufacturer report all of the data collected by the turtle satellite tags to NEFSC. We also upload a subset of that data (location data and other data associated with some of the published papers listed below) to the National Centers for Environmental Information (NCEI) data repository, where it is publicly available.

Table 7-3. Description and Size of Tables in the Turtle Ecology Oracle Database

Table name	Table description	Number of rows	Number of columns
OBSERVER_BASE	Data from turtles sampled from the Northeast Fisheries Observer Program	79	24
RESULTS_BHB	Lab results of Beta-hydroxybutyrate (mg/dL) in plasma samples	136	7
RESULTS_BLOOD_HEALTH	Blood health results from blood panel products issued by various labs, as well as results from iStat cartridges and other analyses conducted in the field	719	114
RESULTS_CORTICOSTERONE	Lab results of corticosterone (stress hormone) levels in plasma samples	59	10
RESULTS_STABLE_ISOTOPES	Lab results of stable isotope levels in plasma and red blood cell samples	880	17
RESULTS_TESTOSTERONE	Lab results of testosterone levels in plasma samples	391	23
SAMPLE_TRACKING	Inventory for used and available samples that are taken through the Sea Turtle Ecology Program, but also include incidental take samples	9,032	11
STSSN_COMP_ANALYSES	Cold stun turtles with complementary analyses (heavy metal, microbiome, gastrointestinal)	43	4
SC_VIDEO_LOG	Log from leatherback video annotations used in Rogers et al (2024)	23,631	7
SIA_LOCATIONS	Location data for cold-stun sea turtles included in Logan et al (2025) manuscript (in progress)	7,298	8
TE_DATASHEETS	Storage of capture and bloodwork datasheets for turtles captured within the Turtle Ecology Program	204	3
TE_HYRES_BASE	Metadata related to each turtle that has been tagged with a Hi-Res (high-resolution) tag	53	33
TE_MISC_BASE	Metadata related to each turtle that has been sampled as part of a Gear Research cruise, Ecosystem Survey Branch cruise, or is associated with NEAMAP or BiOp	15	55
TE_PTT_BASE	Metadata related to each turtle that has been captured, sampled, and/or tagged within the Turtle Ecology program	571	103
TE_TAXON	The relational definitions of the NESPP4 codes denoting species per the Northeast Fisheries Observer Program manual.	7	4

Table name	Table description	Number of rows	Number of columns
TE_VEMCO_DETECT	Information on detections of VEMCO tags we have deployed	191	12
TE_VEMCO_TAGS	Tag parameters and other tag specifications for tags we have purchased from VEMCO	44	45
TURTLE_STORM	Includes information on the distance between turtles at the tag position (from SMRU_DIAG and SMRU_GPS) and spatio-temporally relevant tropical storms and hurricanes. These data were calculated by J. Hatch in March 2017 and were used in Crowe et al (2020)	250,008	14
ULTRA_LOW	Serves as a map for where to find sample boxes within the UltraLow freezer, as well as information regarding if boxes are full or not	82	5
VAQS_REHAB_BASE	Movebank data from Virginia Aquarium tags	53	7
SMRU_CTD	Conductivity, Temperature and Depth data from tags	51,587	32
SMRU_DEPLOYMENTS	Details of each tag deployment (e.g. Species, Time/Date, Location, Tag Configuration)	293	33
SMRU_DEPTH_USAGE_HISTOGRAM	The proportion of each summary period (typically 6 hours) spent in each pre-defined depth bin.	157,859	51
SMRU_DIAG	Argos locations, along with other diagnostic information provided by Argos	538,573	28
SMRU_DIVE	Select diving behavior profiles (depth, speed, time)	280,217	53
SMRU_GPS	GPS locations recorded by tags	263,055	25
SMRU_HAULOUT	Records intervals when tags were not immersed for relatively long periods	50,845	18
SMRU_HAULOUT_ORIG	Detailed data on haulouts (see SMRU_HAULOUT)	52,491	9
SMRU_HIST_BINDEFS	Depth bin definitions used by SMRU_DEPTH_USAGE_HISTOGRAM	294	24
SMRU_SUMMARY	Summary statistics of dive and haulout behaviors	160,382	51
SMRU_TAG_INFO	Diagnostic information about tag status	812,927	53
SMRU_UPLINK	Raw data received in each satellite uplink transmission	1,742,207	15
WICO_ALL	All undecoded messages received from Argos for Wildlife Computer tags	485,211	62
WICO_ARCHIVE	Detailed recorded data that is only available if the tag is recovered	687,950	17

Table name	Table description	Number of rows	Number of columns
WICO_ARGOS	Satellite transmission data about each pass of an Argos satellite over a tag	272,732	20
WICO_BEHAVIOR	Records of diving behavior (depth, time, shape, dwell times)	1,055,311	29
WICO_CORRUPT	Argos messages that were rejected due to interference	234,575	44
WICO_DIVE_PDT	Depth and Temperature profiles for the deepest dives that occurred during a histogram summary period	101,253	15
WICO_FAST_GPS	Locations generated from GPS “snapshots” and a Wildlife Computer solver application	37,117	99
WICO_HISTOS	Histogram data including Time at Depth (TAD), Time at Temperature (TAT), Percent Timelines, and Twenty Minute Timelines.	251,715	53
WICO_LOCATIONS	Argos location records	318,659	18
WICO_MINMAXDEPTH	Min and max depths experienced by the tag	131,140	14
WICO_PDTS	Profiles of depth versus temperature	63,348	101
WICO_RAW_ARGOS	Raw Argos transmissions, with satellite pass information	543,722	56
WICO_RTC	Record of corrections made to tag real time clocks	524	6
WICO_SERIES	Subsample of Archive information, with more limited accuracy	1,121,461	15
WICO_SERIES_RANGE	Companion to SERIES, minimum and maximum values observed for depth and temperature and provides summarized activity data	23,429	22
WICO_SST	Estimated sea surface temperatures	59,652	11
WICO_STATUS	Tag status information	64,586	53
WICO_SUMMARY	High level information about a tag’s deployment	203	23

Table 7-4. Description and Size of Views in the Turtle Ecology Oracle Database

View name	View description	Constituent tables
BASE_UTC	TE_PTT_BASE information with times available in UTC and reused tags incorporated	TE_PTT_BASE TE_DATASHEETS
SAMPLE_COUNTS_STSSN_AVAIL	Counts of samples available from the Sea Turtle Stranding and Salvage Network	STSSN SAMPLE_TRACKING
SAMPLE_COUNTS_STSSN_USED	Counts of samples that have been used from STSSN	STSSN SAMPLE_TRACKING
SAMPLE_COUNTS_TE_AVAIL	Counts of available samples that were acquired in tagging	BASE_UTC SAMPLE_TRACKING
SAMPLE_COUNTS_TE_USED	Counts of used samples that were acquired in tagging	SAMPLE_TRACKING BASE_UTC
TE_ALL_SAMPLE_COUNTS	Counts of all samples	SAMPLE_TRACKING BASE_UTC
TE_CTD	SMRU_CTD adjusted for UTC	SMRU_CTD BASE_UTC
TE_DEPLOYMENTS	SMRU_DEPLOYMENTS adjusted for UTC	SMRU_DEPLOYMENTS BASE_UTC
TE_DEPTH_USAGE_HISTOGRAM	SMRU_DEPTH_USAGE_HISTOGRAM adjusted for UTC	SMRU_DEPTH_USAGE_HISTOGRAM BASE_UTC
TE_DIAG	SMRU_DIAG adjusted for UTC	SMRU_DIAG BASE_UTC
TE_DIVE	SMRU_DIVE adjusted for UTC	SMRU_DIVE BASE_UTC
TE_GPS	SMRU_GPS adjusted for GPS	SMRU_GPS BASE_UTC
TE_HAULOUT	SMRU_HAULOUT adjusted for UTC	SMRU_HAULOUT BASE_UTC
TE_SUMMARY	SMRU_SUMMARY adjusted for UTC	SMRU_SUMMARY BASE_UTC
TE_TAG_INFO	SMRU_TAG_INFO adjusted for UTC	SMRU_TAG_INFO BASE_UTC
TE_UPLINK	SMRU_UPLINK adjusted for UTC	SMRU_UPLINK BASE_UTC

Table 7-5. Oracle database records added during FY19 - FY25

Topic	Number in Database
Individual Turtles	789
Tissue Samples	4,311
Turtle Locations	199,540
Turtle Dive Records	641,335

7.3 Biological Analyses

During AMAPPS III the Turtle Ecology team advanced the analysis of biological samples gathered during fieldwork (**Table 7-6**). While collaborators, using external funding, performed the majority of the analyses, their work directly supported AMAPPS objectives or utilized tissues from turtles tagged for AMAPPS-related goals.

Table 7-6.Tissue samples analyzed during FY19 - FY25

Type of Analysis	Number of Samples Run
Blood analyses (blood chemistry, testosterone, corticosterone, and beta-hydroxybutyrate)	922
Stable isotope analyses	880

7.3.1 Blood Biochemistry

Yang et al. (2018) established baseline blood biochemistry and hematology profiles for healthy loggerhead turtles by analyzing blood samples collected in 2011, 2012, 2013, and 2016 (**Table 7-7**). They found significant differences in several blood variables between migratory and resident turtles, where some blood characteristics were related to water temperature. This research is crucial for comprehending the health and physiological state of healthy turtles that we can then compare to turtles impacted by anthropogenic or environmental disturbances, such as fisheries bycatch and climate change.

Blood biochemistry and haematology of migrating loggerhead turtles (*Caretta caretta*) in the Northwest Atlantic: reference intervals and intra-population comparisons by Yang et al. (2018). https://academic.oup.com/conphys/article/7/1/coy079/5308459

> ABSTRACT: *"We documented blood biochemistry and haematology of healthy loggerhead turtles (Caretta caretta) in the Northwest (NW) Atlantic in order to establish clinical reference intervals (RIs) for this threatened population. Blood samples were analysed from migratory loggerheads captured off the Mid-Atlantic coast of the USA in 2011, 2012, 2013 and 2016 as part of a long-term research program. Blood variables were determined using a point-of-care analyser, and a veterinary diagnostic laboratory service. We calculated 95% RIs with associated 90% confidence intervals (CIs) for each blood variable. We compared results obtained from our study of migratory loggerheads with published data for similarly sized loggerheads resident at a seasonal temperate latitude foraging area. Significant differences in several blood variables between migratory and resident turtles provided insight on energetic and health status during different*

behavioural states. Temperature was significantly correlated with several blood variables: lactate, pCO_2, sodium, haemoglobin and lactate dehydrogenase. Our assessment of blood chemistry in healthy loggerhead turtles in the NW Atlantic provides a baseline for clinical comparisons with turtles impacted by anthropogenic and environmental threats, and highlights the importance of identifying unique aspects of biochemical and haematological profiles for sea turtles at the intra-population level."

Table 7-7. Summary of sampling methodology by year for loggerhead turtles
Sampling methodology is characterized by capture date, key physical attributes and clinical blood analysers used for assessment. SCL_NT and Temperature (T) are presented as Median ± SD. Reproduced from Yang et al. (2018).

Year	n	Capture Dates	SCL_NT (cm)	T (cloacal, C)	n CG4+	n CG8+	n CHEM8+	n IDEXX	n HCT Tubes
2011	25	Jun 2-6	72.8 ± 7.3	21.6 ± 1.8	25	0	0	25	24
2012	28	May 31 - Jun 3	76.2 ± 8.6	19.9 ± 0.9	27	28	0	28	28
2013	15	May 21-23	72.9 ± 12.2	17.4 ± 1.9	10	15	0	15	12
2016	13	May 17-20	74.1 ± 10.0*	13.7 ± 1.3	13	0	12	0	0
TOTAL	**81**		**73.7 ± 9.2**	**19.6 ± 3.1**	**75**	**43**	**12**	**68**	**64**

*n = 12

7.3.2 Gas Embolism

Air-breathing marine diving vertebrates, such as sea turtles, naturally mitigate the risk of gas embolisms. However, gas embolisms can develop when an animal makes an abnormally rapid ascent after diving, such as when incidentally caught in fishing gear (Fahlman et al., 2017) or disturbed by acoustic sources like mid-frequency sonar (Tal et al., 2015). Severe cases of gas embolism have even resulted in immediate or delayed mortality over several days (Parga et al., 2020). Thus, understanding this physiological response contributes to a more comprehensive assessment of threats to sea turtle health.

Robinson et al. (2021) built a baseline model to estimate the risk of gas embolism formation in sea turtles (**Table 7-8**). They used the model to estimate the partial pressures of N_2, O_2 and CO_2 in various body compartments for a diving turtle, as affected by two key influencing factors: percent body-fat and cardiac output.

The model's output indicated that N_2 accumulated more quickly in the central circulation than in fat (**Figure 7-6**). Consequently, the partial pressure of N_2 in the central circulation tended to reflect ambient pressure, while fat N_2 partial pressure was more influenced by dive profiles over several hours to days (**Figure 7-7**).

A Baseline Model For Estimating the Risk of Gas Embolism in Sea Turtles During Routine Dives
by Robinson et al. (2021) https://doi.org/10.3389/fphys.2021.678555

ABSTRACT: *"Sea turtles, like other air-breathing diving vertebrates, commonly experience significant gas embolism (GE) when incidentally caught at depth in fishing gear and brought to the surface. To better understand why sea turtles develop GE, we built a mathematical model to estimate partial pressures of N_2 (PN_2), O_2 (PO_2), and CO_2 (PCO_2) in the major body-compartments of diving loggerheads (Caretta caretta), leatherbacks (Dermochelys coriacea), and green turtles (Chelonia mydas). This model was adapted from a published model for estimating gas dynamics in marine mammals and penguins. To parameterize the sea turtle model, we used values gleaned from previously published literature and 22 necropsies. Next, we applied this model to data collected from free-*

roaming individuals of the three study species. Finally, we varied body-condition and cardiac output within the model to see how these factors affected the risk of GE. Our model suggests that cardiac output likely plays a significant role in the modulation of GE, especially in the deeper diving leatherback turtles. This baseline model also indicates that even during routine diving behavior, sea turtles are at high risk of GE. This likely means that turtles have additional behavioral, anatomical, and/or physiologic adaptations that serve to reduce the probability of GE but were not incorporated in this model. Identifying these adaptations and incorporating them into future iterations of this model will further reveal the factors driving GE in sea turtles."

Table 7-8. Estimated model variables

Estimates are for mass-specific total lung capacity (TLC, ml • kg^{-1}), O_2 stores (ml • kg^{-1}) of the lung (l-O_2), blood (b-O_2), and muscle (m-O_2), hemoglobin concentration ([Hb], g • dl^{-1}), packed cell volume (PCV, %), myoglobin concentration ([Mb], g Mb • kg^{-1} muscle). Reproduced from Robinson et al. (2021).

Species	TLC	l-O_2	b-O_2	m-O_2	[Hb]	PVC	[Mb]	P50
Loggerhead	(113.6 body mass$^{0.923}$)* body mass^{-1}	16.4	7.84	3.93	0.088	30	2.9*	25
Leatherback	64	9.25	13.8	4.5	0.156	39	4.9	40
Green	115	16.6	8.72	3.93	0.098	29	2.9	47

*No data so assumed equal to another species

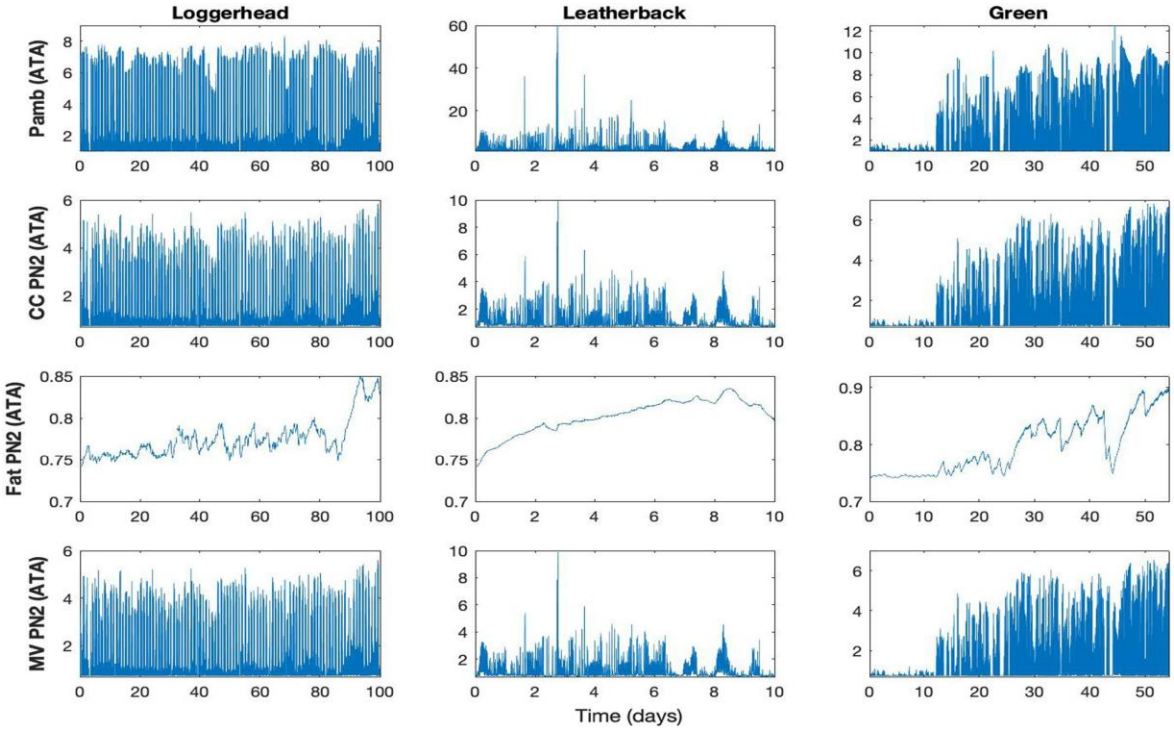

Figure 7-6. Model results for gas embolism control model

Graphs show ambient pressure (Pamb, ATA), and tissue gas tension (PN2) for central circulation (CC), fat, and mixed venous blood (MV) in a single loggerhead (Turtle ID 14293), leatherback (Turtle ID 10A1059a), and green sea turtles (Turtle ID 37800, Table 7-6). Data are shown for 100, 10, and 55 days for loggerhead, leatherback, and green turtles, respectively. The Pamb was used to generate the model output for the various tissues and the difference in tissue PN2 between CC (fast tissue) and fat (slow tissue), with the PN2 in MV being the composite of all tissues and their relative blood flow. Reproduced from Robinson et al. (2021).

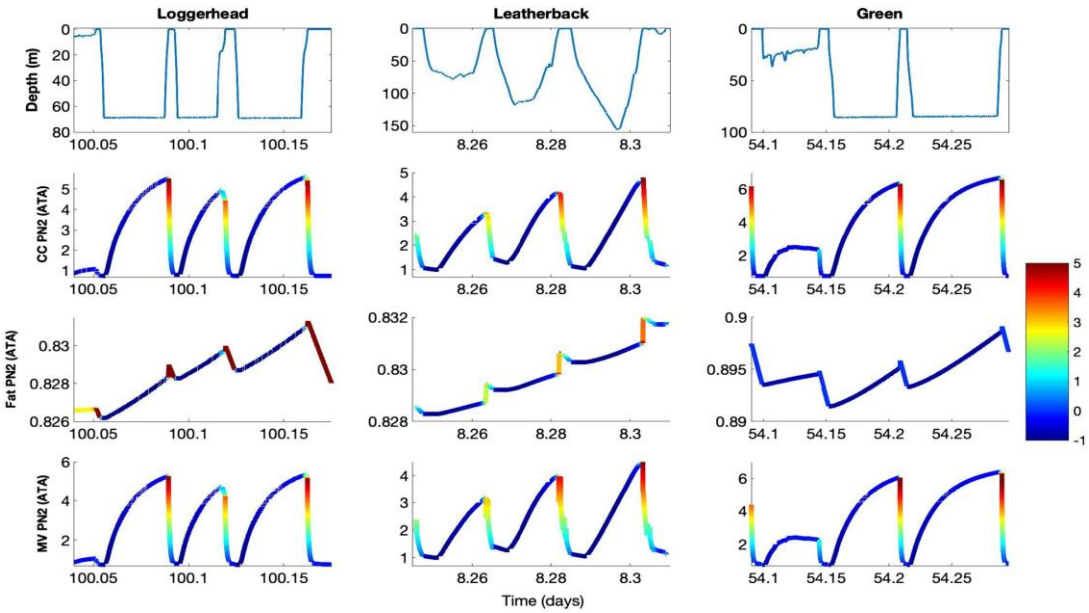

Figure 7-7. Additional model results for gas embolism control model
Graphs show depth (m), and tissue gas tension (PN_2) in central circulation (CC), fat, and mixed venous blood (MV) in loggerhead (Turtle ID 14293), leatherback (Turtle ID 10A1059a), and green sea turtles (Turtle ID 37800, Table 7-6). The data presented are a subset of those in Figure 7-10 to show specific dive patterns and blood and tissue PN_2 levels. The theoretical supersaturation [(mixed venous PN_2 – ambient pressure) • ambient pressure^{-1}, in ATA] for each of the tissues and the mixed venous blood are shown in color. The color bar shows the level of supersaturation, where negative values (blue) indicate N_2 uptake and positive values indicates the whole body, or mixed venous PN_2, exceeds the ambient pressure, i.e., risk of Gas Emboli formation (GE) and pathology (GEP). Thus, increasing value, i.e., yellow to red, indicates increasing risk of GEP. The results show increasing risk of GEP during ascent and how ascent rate or how sudden stops during ascent reduces risk, e.g., ascent from second dive in loggerhead or leatherback turtles. Reproduced from Robinson et al. (2021).

7.3.3 Trophic Position

Logan et al. (in review) utilized stable isotope analyses on juvenile Kemp's ridley, loggerhead, and green sea turtles that stranded in southern New England to understand their foraging preferences, habitat use, and trophic positions prior to stranding. The preliminary results showed similar trophic position estimates across the species, with green and loggerheads having the lowest overlap, and indicated that turtle size was the main predictor of intraspecific stable isotope variation, consistent with ontogenetic trophic position increases and shifts from oceanic to nearshore habitats.

7.4 Distribution Patterns using Tag Data

AMAPPS III revealed new insights into the shifting distribution of tagged loggerhead and leatherback sea turtles. These changes are linked to both short-term and long-term environmental variations.

7.4.1 Loggerhead Shifts Due to Short-Term Extreme Environmental Changes

Crowe et al. (2020) documented loggerhead turtle behavioral shifts in response to hurricane Irene that passed over the turtles. Most of the turtles moved northward during the hurricane (**Figure 7-8a**). After the storm, eight turtles relocated south, moving between 7.3 and 135.0 km from their usual foraging areas. The remaining ten turtles exhibited longer dives compared to pre-storm observations (**Figure 7-8b**).

Riders on the storm: loggerhead sea turtles detect and respond to a major hurricane in the Northwest Atlantic Ocean by Crowe et al. **(2020)** **https://doi.org/10.1186/s40462-020-00218-6**

ABSTRACT:

"Background

Extreme weather events, including hurricanes, have considerable biological, ecological, and anthropogenic impacts. Hurricane Irene caused substantial economic damage when it hit the Mid-Atlantic Bight (MAB) off of the eastern United States in August of 2011. The MAB is highly stratified during the summer when a strong thermocline separates warm, surface water from deep, cold water, and this oceanographic phenomenon makes modeling hurricane strength difficult. Loggerhead sea turtles (Caretta caretta) forage in the MAB primarily during the stratified season and their dive behavior to the bottom allows them to experience the oceanographic conditions of the entire water column.

Methods

In this study, we analyzed the movements and dive behavior of juvenile and adult-sized loggerhead sea turtles (n = 18) that were foraging in the MAB as Hurricane Irene moved through the region. The satellite tags deployed on these turtles transmitted location data and dive behavior as well as sea surface temperature (SST) and temperature-depth profiles during this time.

Results

Behavioral and environmental shifts were observed during and after the hurricane compared to conditions before the storm. During the hurricane, most of the turtles (n = 15) moved north of their pre-storm foraging grounds. Following the storm, some turtles left their established foraging sites (n = 8) moving south by 7.3–135.0 km, and for the others that remained (n = 10), 12% of the observed dives were longer (0.54–1.11 h) than dives observed before the storm. The in situ data collected by the turtle-borne tags captured the cooling of the SST (Mean difference = 4.47°C) and the deepening of the thermocline relative to the pre-storm conditions.

Conclusions

Some of the loggerhead behavior observed relative to a passing hurricane differed from the regular pattern of seasonal movement expected for turtles that forage in the MAB. These data documented the shifts in sea turtle behavior and distribution during an ecosystem-level perturbation and the recorded in situ data demonstrated that loggerheads observe environmental changes to the entire water column, including during extreme weather events."

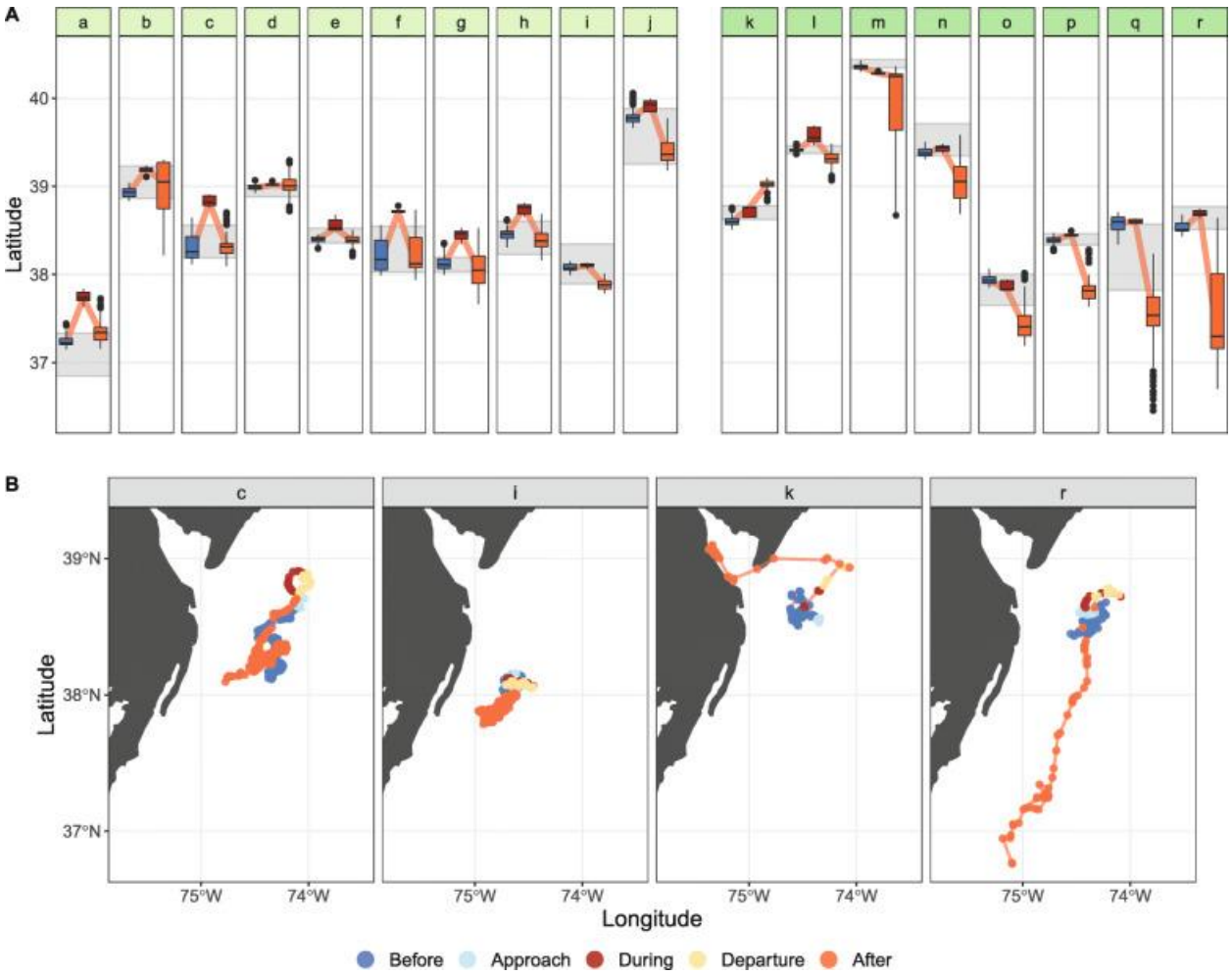

Figure 7-8. Movements of tagged turtles Before, During, and After the passing of Hurricane Irene
A. Latitudinal movements of individual tagged loggerhead turtles during each phase: For each of these phases, the colored box represents the interquartile range (25th to 75th percentile), the horizontal black line within the colored box represents the median value, the upper and lower whiskers represent values that fall within 1.5x the interquartile range, and the black dots represent the outlying points. The grey shaded area for each turtle represents its foraging range which spanned between the 5th and 95th percentile of the latitudinal extent for the time period three to six weeks prior to T0. Turtles a – j (light green) remained in their foraging range as the interquartile range within the After phase overlapped with their foraging range, while turtles k – r (darker green) left their foraging grounds after the hurricane passed. The light red line connects the medians between each phase to highlight the overall movement pattern.
B Example turtle movements in all phases: Animal c was one of the turtles that revisited their foraging grounds after moving north in the During and Departure phases; Animal i did not leave its pre-storm foraging area in the During phase, but did move a bit south in the After phase; Animal k did not return to its foraging ground, and instead was the only animal in this study that moved inshore; Animal r was one of the animals that did not return to its foraging ground, and instead went south by almost 2° of latitude in the After phase. Reproduced from Crowe et al. (2020).

7.4.2 Loggerhead Shifts Due to Long-Term Environmental Changes

Patel et al. (2021) used a high-resolution global climate model to forecast future conditions over the next 80 years, where the future atmospheric carbon dioxide doubled and sea surface temperature increased (**Figure 7-9**). Using the current relationship between sea surface temperature and locations of tagged loggerheads, they projected future northward distribution shifts in the sea turtle thermal habitat over the next 80 years (**Figure 7-10**). The largest changes were during the fall and spring (**Figure 7-11**).

Projected shifts in loggerhead sea turtle habitat in the Northwest Atlantic Ocean due to climate change by Patel et al. (2021) https://doi.org/10.1038/s41598-021-88290-9

ABSTRACT: *"It is well established that sea turtles are vulnerable to atmospheric and oceanographic shifts associated with climate change. However, few studies have formally projected how their seasonal marine habitat may shift in response to warming ocean temperatures. Here we used a high-resolution global climate model and a large satellite tagging dataset to project changes in the future distribution of suitable thermal habitat for loggerheads along the northeastern continental shelf of the United States. Between 2009 and 2018, we deployed 196 satellite tags on loggerheads within the Middle Atlantic Bight (MAB) of the Northwest Atlantic continental shelf region, a seasonal foraging area. Tag location data combined with depth and remotely sensed sea surface temperature (SST) were used to characterize the species' current thermal range in the MAB. The best-fitting model indicated that the habitat envelope for tagged loggerheads consisted of SST ranging from 11.0° to 29.7 °C and depths between 0 and 105.0 m. The calculated core bathythermal range consisted of SSTs between 15.0° and 28.0 °C and depths between 8.0 and 92.0 m, with the highest probability of presence occurred in regions with SST between 17.7° and 25.3 °C and at depths between 26.1 and 74.2 m. This model was then forced by a high-resolution global climate model under a doubling of atmospheric CO2 to project loggerhead probability of presence over the next 80 years. Our results suggest that loggerhead thermal habitat and seasonal duration will likely increase in northern regions of the NW Atlantic shelf. This change in spatiotemporal range for sea turtles in a region of high anthropogenic use may prompt adjustments to the localized protected species conservation measures."*

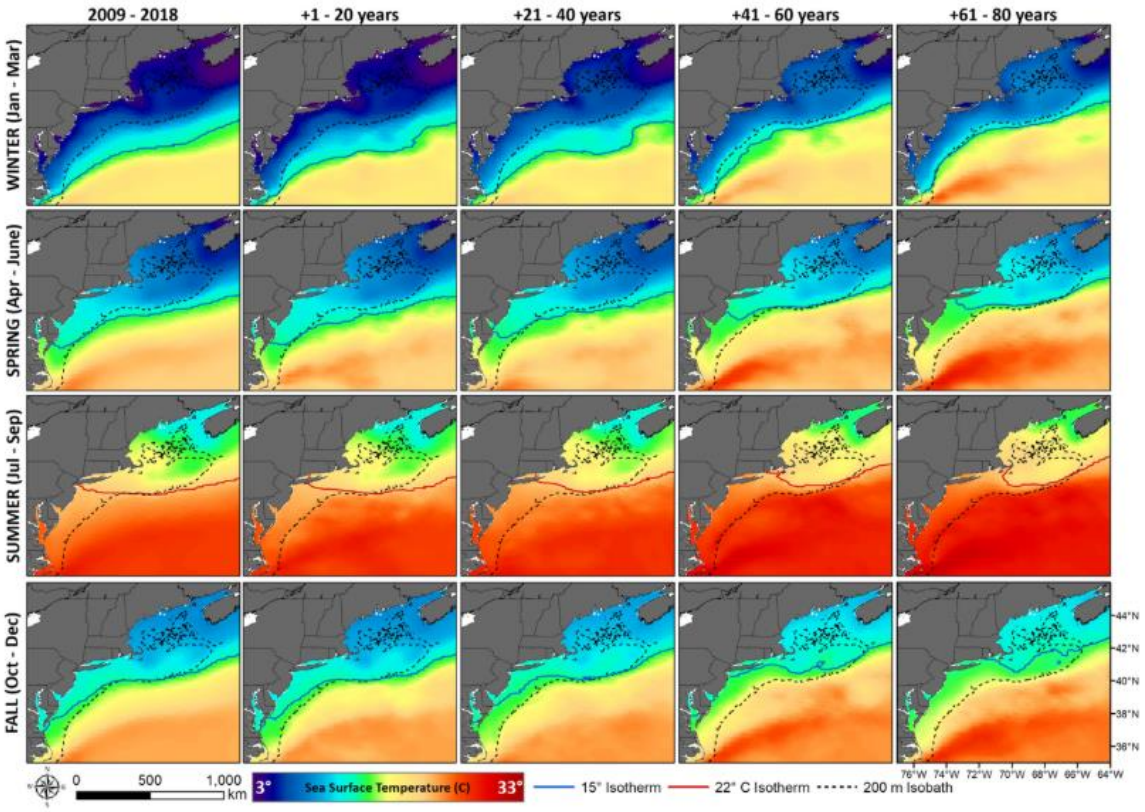

Figure 7-9. Seasonal maps of historical and projected sea surface temperature
In the northwest Atlantic, the north- and shore-ward movement of the Gulf Stream is expected to increase warming within shelf waters. Maps prepared with ArcMap 10.8, www.esri.com. Reproduced from Patel et al. (2021).

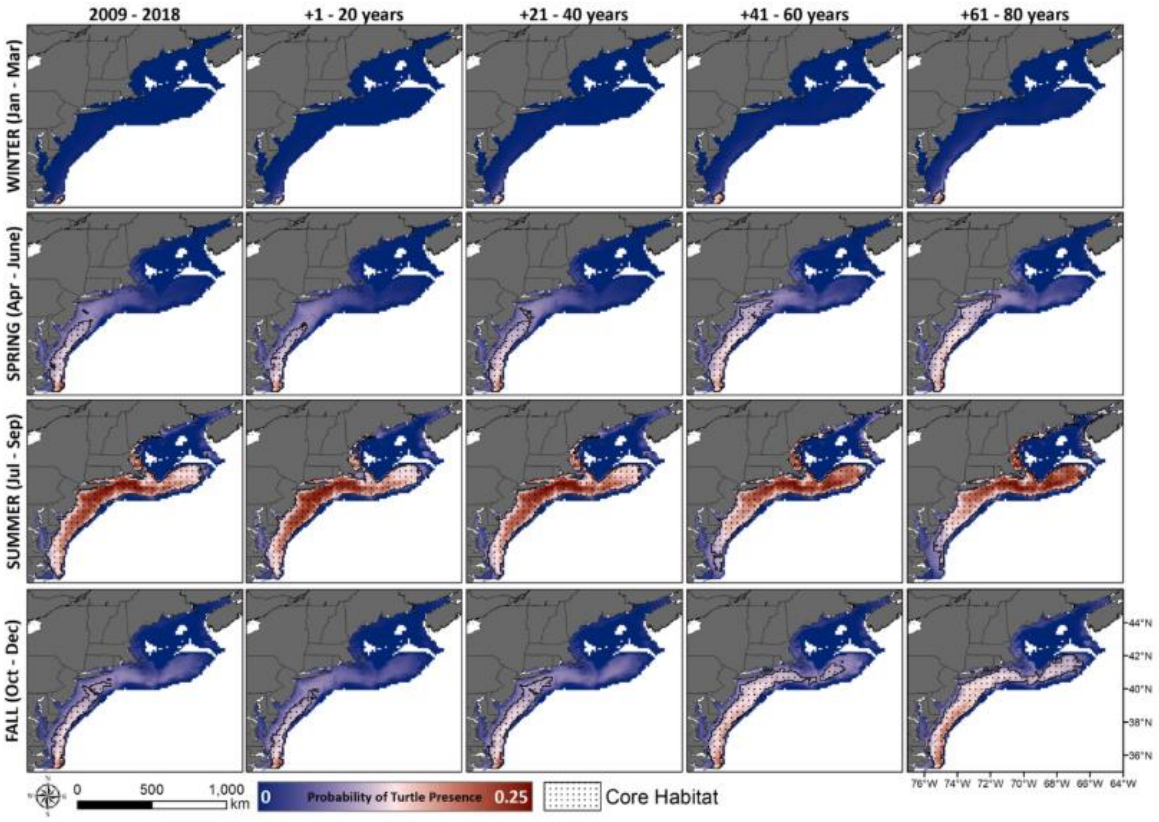

Figure 7-10. Seasonal maps of probability of loggerhead turtle presence and their core habitat
Relationship based on observed and projected sea surface temperatures (SST) using the CM2.6 model. Color ramp indicates the probability of presence based on SST and depth. Maps prepared with ArcMap 10.8, www.esri.com. Reproduced from Patel et al. (2021).

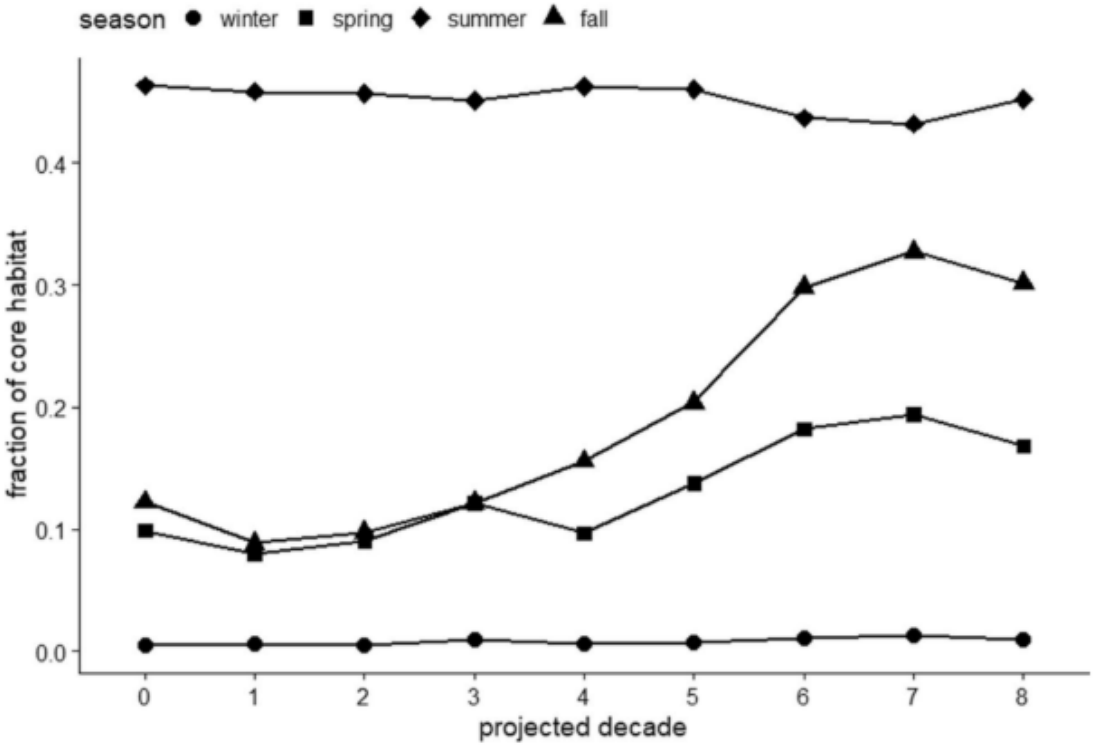

Figure 7-11. Change in fraction of the Northwestern Atlantic shelf region identified as core habitat For loggerheads across the projected 80 years binned by decade. Spring and fall are projected to have the largest change. Decade '0' refers to the observed data. Reproduced from Patel et al. (2021).

7.4.3 Leatherback Foraging Distribution Patterns

Rider et al. (2024a) used hidden Markov models on tag-borne leatherback data to differentiate between foraging (searching) and transiting behaviors. This data, collected from turtles tagged off Massachusetts (**Figure 7-12a**) and North Carolina (**Figure 7-12b**), included both location and time-depth dive patterns. An unexpected finding was that these leatherbacks foraged in the South and Mid-Atlantic Bights during the summer (**Figure 7-12c**).

Where the leatherbacks roam: movement behavior analyses reveal novel foraging locations along the Northwest Atlantic shelf by Rider et al. (2024a) https://doi.org/10.3389/fmars.2024.1325139

> ABSTRACT: "*Leatherback sea turtles (Dermochelys coriacea) migrate along the east coast of the United States, traversing the South and Mid-Atlantic Bights (SAB and MAB) while traveling to and from well-known northern foraging areas off Southern New England (SNE) and Nova Scotia. However, there is limited information on leatherback movement behavior in these regions. To identify leatherback movement patterns, we fit hidden Markov models (HMMs) to satellite transmitter data from 52 leatherbacks tagged between 2017 and 2022 off the coasts of Massachusetts and North Carolina to estimate locations of area restricted searching (ARS) and transient behaviors. Depth-temperature profiles were then paired to locations associated with ARS behavior to understand the vertical use of the water column. We observed leatherbacks displaying ARS behavior in SNE as expected, but also in the MAB and SAB. The HMM results indicated that leatherbacks were primarily foraging in SNE between Nantucket and Long Island Sound and depth-temperature plots from ARS behavior on Nantucket Shoals implied turtles foraging*

throughout the entire water column. In the MAB, ARS behavior was concentrated between Cape Hatteras, North Carolina, and the mouth of Delaware Bay during the summer. Turtles were closely associated with a well-defined thermocline, but still appeared to dive to deeper cooler waters, which may be a sign of thermoregulatory behavior. There was evidence of foraging in the SAB along the coast as well as along the continental shelf edge. The ARS behavior we documented within the MAB and SAB is the first published empirical evidence that both areas may be important foraging grounds. Our results lay a path for future research to understand how leatherbacks use these areas and the potential anthropogenic threats encountered while moving through these regions."

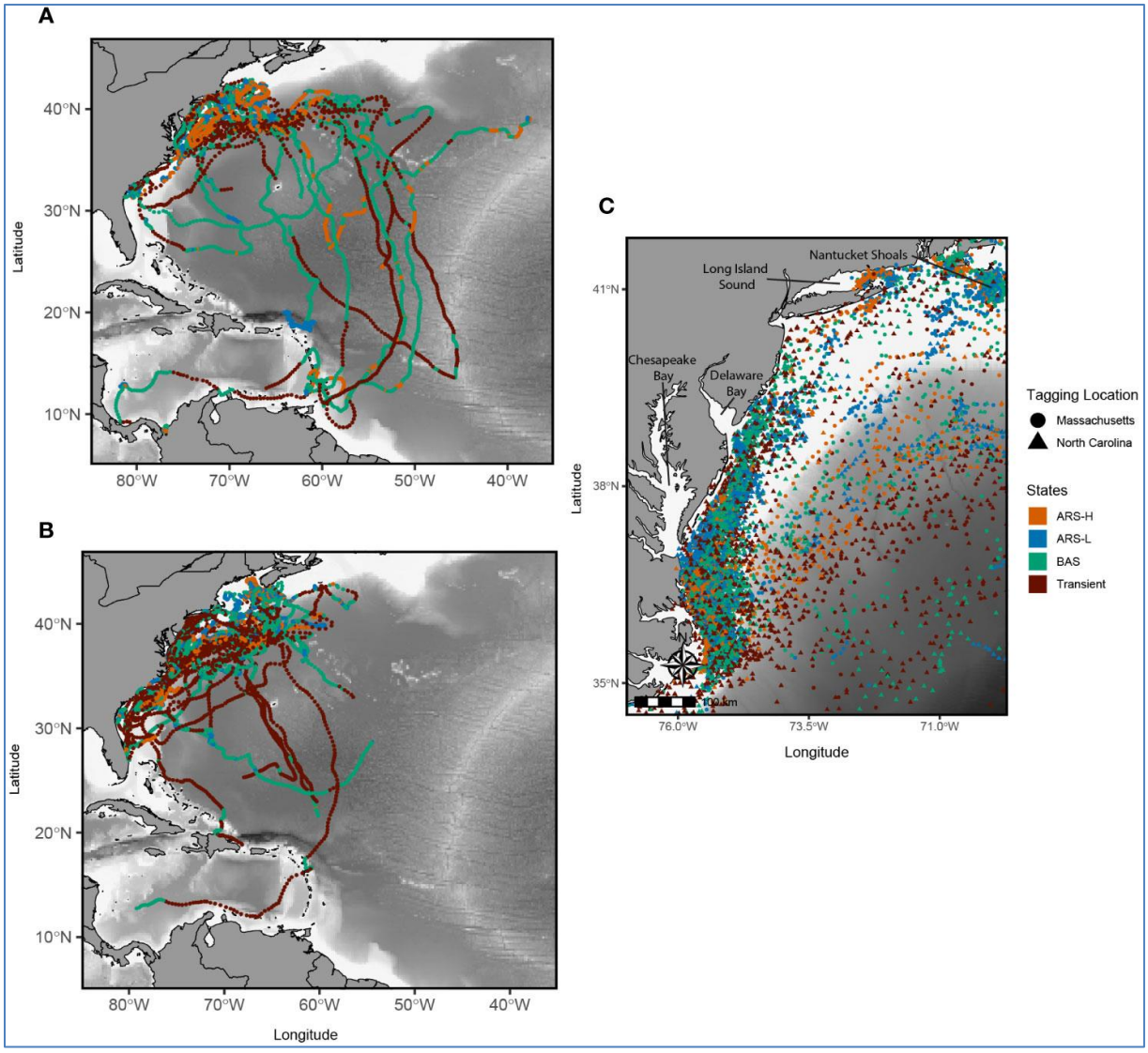

Figure 7-12. Reconstructed satellite tracks of leatherback turtles
Animals were tagged off Massachusetts in the summer **(A)** and off North Carolina in the spring **(B)** between 2017 and 2022. Locations recorded along the Mid Atlantic Bight and Southern New England are in the black box in **(A)** and enlarged in **(C)** Colors correspond to the latent states predicted by the hidden Markov model: Area restricted search with high dive intensity (ARS-H), area restricted search with low dive intensity (ARS-L), broad area search (BAS), and transient. Reproduced from Rider et al. (2024).

7.5 Dive Patterns

As detailed in Section 4.2, an availability bias correction factor is necessary to adjust at-surface abundance estimates derived from visual line-transect surveys. This adjustment accounts for sub-surface animals missed by observers, providing an unbiased estimate of a species' total abundance throughout the water column. For loggerhead and leatherback turtles, we determined this correction factor using satellite time-depth tag data, detailed below.

7.5.1 Loggerhead Turtles

To estimate average dive and surface durations, Hatch et al. (2022) used spatiotemporal regression models employing a stochastic partial differential equation approach (**Figure 7-13**).This study used the model to predict these dive durations as a monthly average for 20x20 km grid cells across the study area. We then used these gridded spatiotemporal data to calculate monthly availability bias correction factors for each grid cell. Then we applied these factors to the corresponding at-surface abundance estimate to determine the abundance of animals throughout the water column (Section 4.3).

Estimating the complex patterns of survey availability for loggerhead turtles by Hatch et al. (2022) https://doi.org/10.1002/jwmg.2220

ABSTRACT: *"Successful management strategies are important for conservation and allow accurate surveying and monitoring of populations for presence, abundance, and trend. This becomes challenging for cryptic, low-density species, and for animals that have complicated life histories where not every stage of the life cycle can be surveyed effectively. We used information from animal-borne data loggers to characterize the dive-surfacing behavior of cryptic loggerhead turtles (Caretta caretta) in the northwest Atlantic from 2009–2018. Our data covered a large geographic area off the east coast of North America, and allowed us to present estimates for and variation in 3 metrics that can be used to assess availability bias affecting visual surveys: average dive duration, average surface duration, and the proportion of time at the surface. We used a stochastic partial differential equation approach to construct spatiotemporal regression models for the availability bias metrics. Model predictions showed pronounced individual, spatial, and spatiotemporal (seasonal) variation among the 245 turtles. Overall, we estimated an average dive duration of 14.5 ± 1.36 minutes (SE), an average surface duration of 15.1 ± 2.77 minutes, and an average proportion of time at the surface of 0.50 (95% CI = 0.41–0.59). We made predictions of the 3 availability bias metrics on a 20-km × 20-km grid and further used predictions to explore seasonal variations. Our results contribute new insights into loggerhead turtle behavior and provide information that enables survey counts to be translated into more accurate abundance estimates."*

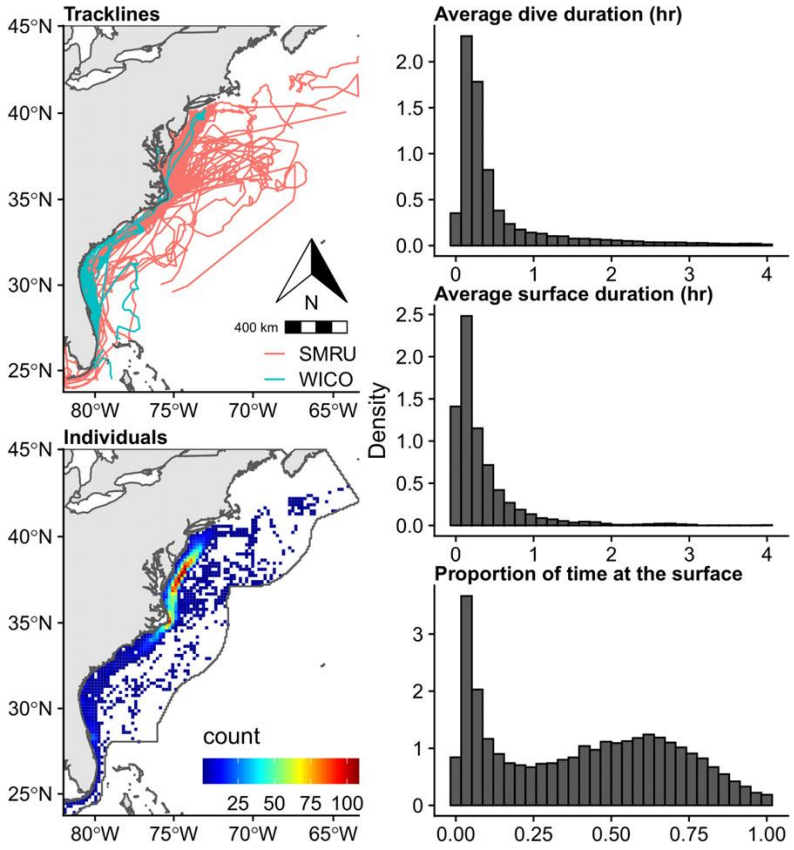

Figure 7-13. Loggerhead turtle input data and results of Hatch et al. (2022)
Track lines of the 245 loggerhead turtles tagged with satellite relay data loggers (SMRU = Sea Mammal Research Unit, WICO = Wildlife Computers), 2009–2018, within the study area off the east coast of North America (black outline), number of satellite-tagged individuals summarized over the prediction grid with a cell size of 20 km × 20 km, and histograms of average dive (~3% of values were >4 and are not shown) or surface duration (~1% of values were >4 and are not shown) and proportion of time at the surface across individuals. Reproduced from Hatch et al. (2022).

7.5.2 Leatherback Turtles

We used data from leatherback turtles equipped with satellite and suction cup tags in the AMAPPS study area in three projects to investigate the dive patterns of these turtles.

Rider et al. (2022) estimated average monthly percent time at the surface for leatherback turtles, which we tagged during 2017 - 2020 in the AMAPPS study area (**Figure 7-14**). We then used these monthly averages to derive availability bias correction factors for leatherback turtles, which we applied to the corresponding at-surface abundance estimates, as detailed in Chapter 4.

Using the dive data collected from the tagged leatherbacks, Rider et al. (2024b) found that as sea surface temperature increased the leatherbacks in the northeastern Gulf of America and Mid-Atlantic Bight increased their surface duration and decreased their dive duration to make deeper dives to cooler subsurface waters, while the opposite trend was observed in leatherbacks off the southern New England area (**Figure 7-15**).

Rogers et al. (2024) monitored the behavior of leatherback turtles using simultaneous recordings of a high-resolution suction cup camera and satellite tags (**Table 7-9**) to conclude that the mean percent time at the surface as calculated by the satellite tags was the most reliable metric to use to calculate the availability bias correction factor (**Figure 7-16**).

Surface Availability Metrics of Leatherback Turtles (*Dermochelys coriacea*) Tagged off North Carolina and Massachusetts, United States by Rider et al. (2022) https://doi.org/10.25923/82c1-4a85

ABSTRACT: *"Understanding the physical and biological characteristics associated with protected species occurrence and distribution is critical for the proper management of the protected species, especially as it faces increasing natural and anthropogenic impacts. The Atlantic Marine Assessment Program for Protected Species (AMAPPS) is a comprehensive, multi-agency research program with overarching goals to 1) assess the abundance, distribution, ecology, and behavior of marine mammals, sea turtles, and seabirds throughout the U.S. Atlantic shelf region, and 2) evaluate these data within an ecosystem context where the results are accessible to managers, scientists, and the public. This preliminary document provides simple summary statistics from the partially completed project to address immediate needs of U.S. federal agencies, following the precedent set in NEFSC (2011), while the longer-term AMAPPS III goals of more sophisticated data analysis and collection are pursued."*

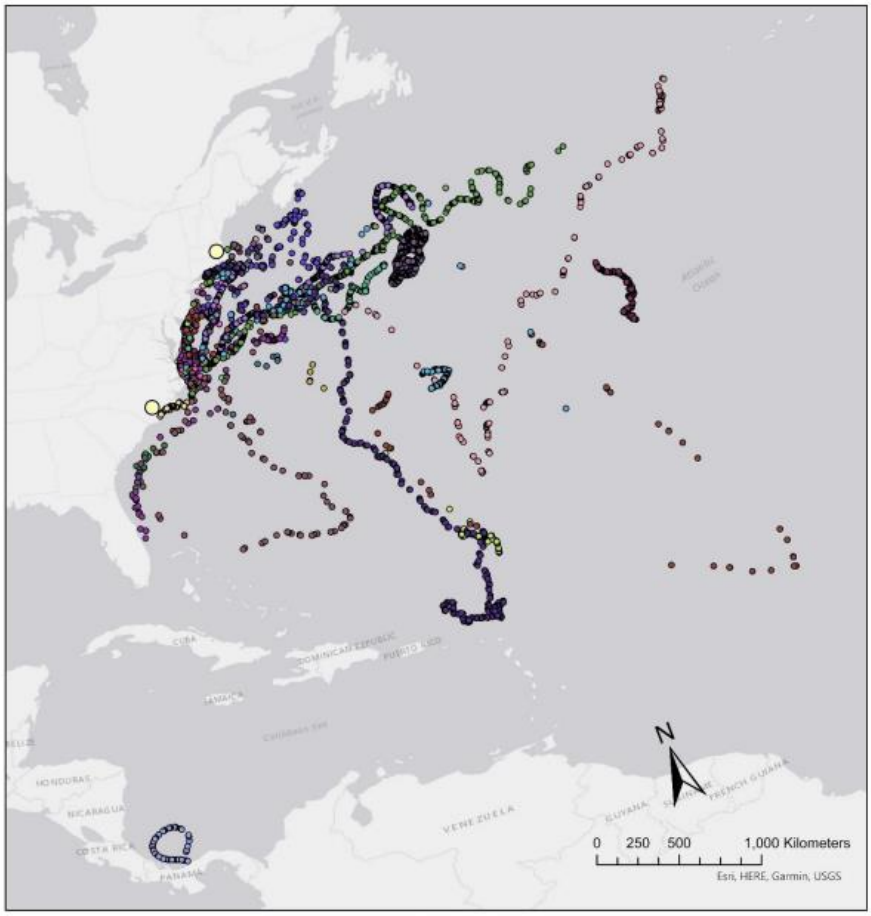

Figure 7-14. Tagged leatherback turtle locations from 2017-2020
Each color represents a single individual. Yellow points represent the two locations where turtles were tagged (i.e., North Carolina and Massachusetts). Reproduced from Rider et al. (2022).

Regional variation in leatherback dive behavior in the northwest Atlantic by Rider et al. (2024b)
https://doi.org/10.3354/esr01365

ABSTRACT: *"Understanding the movement patterns and behaviors of a migratory species across all stages of migration is critical to informing successful conservation management strategies. While the movement patterns of northwestern Atlantic leatherbacks* Dermochelys coriacea *have been widely studied, there is still a need to understand area-specific behaviors. We collected and analyzed dive data from 52 satellite-tagged leatherbacks that inhabited documented or proposed foraging areas: the northeastern Gulf of Mexico (NEGOM), the Mid-Atlantic Bight (MAB), and southern New England (SNE). We fit generalized linear mixed models (GLMMs) to these data to determine area-specific dive metrics and their relationship to several environmental variables. The most notable result from the GLMMs revealed area-specific relationships between dive behavior and sea surface temperature (SST). As SST increased, leatherbacks in the NEGOM and MAB were observed to increase their surface duration and decrease dive duration, while the opposite trend was observed off SNE. Additionally, leatherbacks in the NEGOM performed more deep dives to cooler waters with rising SSTs. Our results suggest that leatherbacks in the NEGOM are performing thermoregulatory dive behavior that may reduce time available for feeding, potentially inhibiting foraging success relative to the MAB and SNE. These findings offer a deeper comprehension of leatherback movement ecology in each area, provide critical information needed for population assessments and management, and highlight areas of conservation concern in a warming climate."*

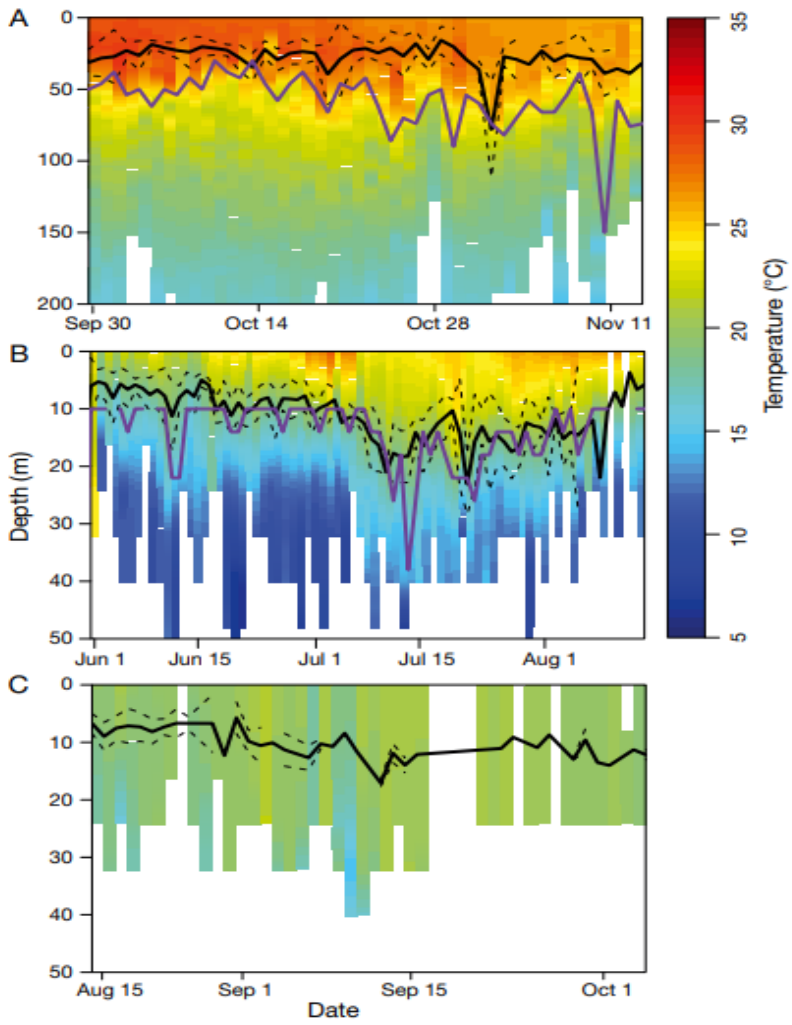

Figure 7-15. Average depth–temperature profiles derived from leatherback locations
Locations are within (A) the northeastern Gulf of Mexico (NEGOM), (B) the Mid-Atlantic Bight (MAB), and (C) the southern New England (SNE) foraging areas. Solid black lines represent the mean depth of turtles, while dashed lines represent SD. The purple line is the estimated depth of the thermocline. There is no estimated depth of the thermocline in SNE due to the high amount of vertical mixing of the water column. Each plot represents one foraging season: 2019 for the NEGOM and MAB and 2018 for SNE. Plots were created using the R package RchivalTag (Bauer 2021). Reproduced from Rider et al. (2024).

Investigating leatherback surface behavior using a novel tag design and machine learning by Rogers et al. (2024). https://doi.org/10.1016/j.jembe.2024.152012

ABSTRACT: *"Understanding the surfacing behavior of marine wildlife is an important component for improving abundance estimates derived from visual surveys. We monitored the behavior of 18 leatherback sea turtles (Dermochelys coriacea) in coastal habitats off Massachusetts, USA, using a high-resolution camera and satellite tag package (HiCAS - High Resolution Camera and Satellite) that we assembled from commercially available components which work independently. We used nine data streams derived from the multiple sensors and a video camera to explore four different depth thresholds defining surface zones. We compared classification of video images by a human to classification of those images by a machine learning algorithm. We calculated four metrics to describe*

surface behavior for each of the nine data streams. The mean percent time at the surface was the only behavior metric that changed systematically as data streams were used to assess different visible depth thresholds, increasing as the depth threshold increased. Other behavior metrics (mean surface duration, mean dive duration and number of surfacing events per hour) were less similar across data streams, making them unreliable for estimating surface availability. This study highlights the need for sustained data collection to better inform the availability bias estimates used to calculate abundance from visual observations."

Table 7-9. Definitions of the data streams we used to describe leatherback surface behavior
The size of the depth threshold increases from the top to the bottom of the table. The name of each data stream is a concatenation of the Depth Threshold, Sensor Type (HV = human classified video, MV = machine classified video, WD = wet/dry sensor, PR = pressure sensor), and Inst (Instrument; C = camera and S = satellite data logger). For example, 0.0-HV-C is the name of the data stream described in the first row of the table. Reproduced from Rogers et al. (2024).

Depth Threshold (m)	Sensor Type	Instrument	Criteria for Defining Surfacing Events
0.0	HV	C	Human classified video with sky visible in frame
0.0	MV	C	Machine classified video with supervised ML mode
0.0	WD	S	Wet/Dry sensor data >80
0.5	PR	C	Zero offset corrected depth data < 0.5m
0.5	PR	S	Zero offset corrected depth data < 0.5m
2.0	PR	C	Zero offset corrected depth data < 0.5m
2.0	PR	S	Zero offset corrected depth data < 0.5m
4.0	PR	C	Zero offset corrected depth data < 0.5m
4.0	PR	S	Zero offset corrected depth data < 0.5m

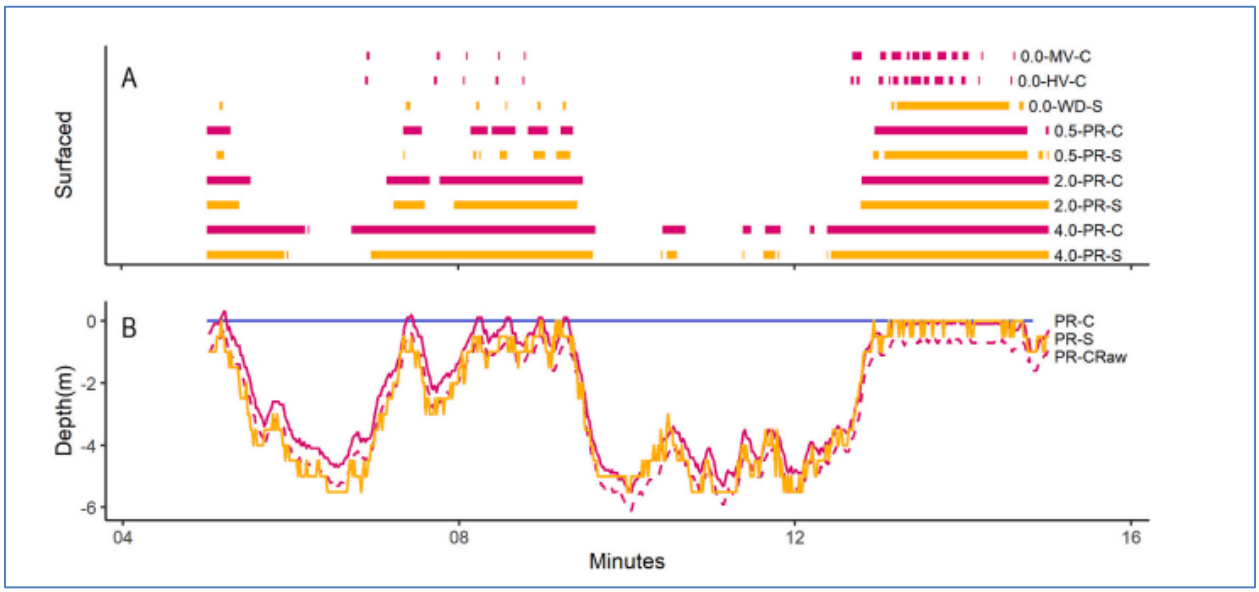

Figure 7-16. Turtle Q Dive Trace
To show detail, only a subset of the deployment is shown (from 4 to 16 min). Panel A shows the 9 data streams that have been classified into surface and non-surface behavior. The markings indicate when the turtle was at the surface or the indicated near-surface depth, and the absence of markings indicate when the turtle was at or below the threshold depth. Descriptions of the variables are shown in Table 7-7. We did not further synchronize the time between the video and pressure sensors data streams as the offset does not affect our main focus (mean percent time as the surface). Panel B shows the corresponding depth readings. The solid orange line shows depth data from the satellite data logger (PR-S) and the solid magenta line shows corrected depth data from the camera (PR-C). The dashed magenta line shows uncorrected depth data from the camera (PR-CRaw). The horizontal light blue line marks the surface of the water (zero depth). The need for camera depth data correction can be seen, as without it, the turtle never appears to rise to the surface. Values from the camera tag are shown in magenta, values from the satellite data logger are in orange. (For interpretation of the references to colour in this figure legend, the reader is referred to the web version of this article.) Reproduced from Rogers et al. (2024).

7.6 Overlapping with Human Activities

We used data from satellite tags on sea turtles in two publications to analyze their distributions, environmental predictors, and overlap with human activities.

Hatch et al. (2023) evaluated the spatiotemporal overlap between loggerhead turtles and the U.S. Atlantic sea scallop fishery as a proxy for encounter risk (**Figure 7-17**). They concluded that in this case the simple overlap metric was not a meaningful predictor of documented bycatch events.

Evaluating simple measures of spatial-temporal overlap as a proxy for encounter risk between a protected species and commercial fishery by Hatch et al. (2023).
https://doi.org/10.3389/fcosc.2023.1118418

> ABSTRACT: "*Spatial and temporal assessments of overlap are becoming increasingly popular as indicators of encounter risk. The overlap in distributions between protected species and commercial fishing effort is of interest for reducing bycatch. We explored overlap between the U.S. Atlantic sea scallop fishery and loggerhead turtles (Caretta caretta) using 2 metrics, and we assessed the ability of one of those metrics to track estimated fishery interactions over time. Moderate overlap occurred between June - September; mild overlap in the spring (May) and fall (October - November); and relatively little overlap from December to April. Qualitatively, there appeared to be some*

correspondence between the overlap values averaged across months for each calendar year and published annual loggerhead interaction estimates with fisheries, but the predictive performance of the overlap metric was low. When data on the relative distributions of commercial fishing effort and protected species are available, simple measures of spatial and temporal overlap can provide a quick and cost-effective way to identify when and where bycatch is likely to occur. In this case study, however, overlap was limited in helping to understand the relative susceptibility of protected species to commercial fishing (i.e., magnitude of interactions). We therefore caution against using overlap as a meaningful predictor of absolute risk unless there is direct evidence to suggest a relationship."

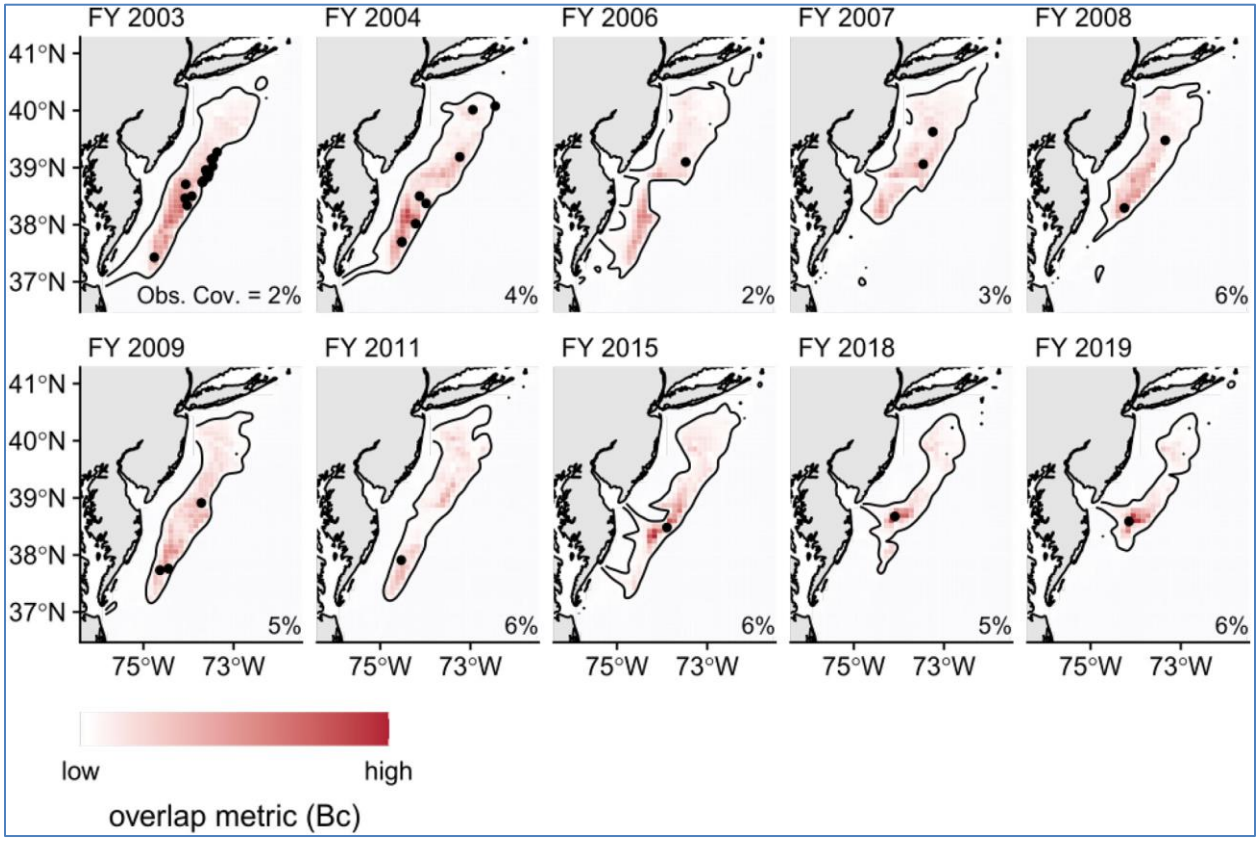

Figure 7-17. Maps of averaged overlap values across fishing years
Maps are by fishing year (FY) for years where observed interactions occurred. Superimposed, as black dots, are the corresponding observed interaction locations between loggerhead turtles and the U.S. Atlantic sea scallop fishery. The black, contour line corresponds to the lowest value of the averaged overlap metric associated with an observed location of loggerhead turtle interaction across all years. The observer coverage (Obs. Cov.) for the corresponding calendar year is listed in the lower, right-hand corner of the maps and was extracted from Murray (2011); Murray (2015); Murray (2021). Reproduced from Hatch et al. (2023).

Rider et al. (in review) found a significant overlap between the core habitat of leatherback turtles and offshore wind areas in the Mid-Atlantic Bight and Southern New England, especially during late summer. Their research involved developing core habitat models based on location data from satellite-tagged leatherbacks, correlated with various static and dynamic environmental factors.

Distribution models reveal important coastal habitats for endangered leatherback sea turtles by Rider et al. (in review)

ABSTRACT: "*This research aims to understand leatherback sea turtle distributions, their environmental predictors, and their overlap with offshore wind energy areas along the U.S. Atlantic Outer Continental Shelf. Satellite transmitters were affixed to 74 leatherbacks off the coasts of North Carolina and Massachusetts between 2017 and 2023. Location data from these transmitters were implemented in boosted regression tree models to predict leatherback distributions in relation to a suite of static and dynamic environmental covariates. We used the model predictions to categorize core habitat and determine its overlaps with active wind energy leases.The study found a higher probability of leatherbacks in the Mid-Atlantic Bight (MAB) and Southern New England (SNE) during late summer, with notable overlap between core habitat and offshore wind areas in these regions.*"

We used many resources and collaborations to address AMAPPS goals. **Table 7-10** lists our published manuscripts during FY19-FY25 and explains how they each support one or more AMAPPS goals including sea turtle distribution, behavior, population and availability, environmental factors, and BOEM-related activities.

Table 7-10. Published manuscripts during FY19-FY25 and how they relate to AMAPPS III goals

Manuscript	Distribution	Behavior	Population/ Availability	Environmental Factors	BOEM-related activities
Yang et al. 2019				✔	
Crowe et al. 2020	✔	✔		✔	
Patel et al. 2021	✔			✔	
Robinson et al. 2021				✔	✔
Hatch et al. 2022		✔	✔	✔	
Rider et al. 2022	✔		✔		
Hatch et al. 2023	✔				✔
Rider et al. 2024a (Leatherbacks roam)	✔	✔			
Rider et al. 2024b (Regional variation)		✔	✔	✔	
Rogers et al. 2024		✔	✔		

7.7 Acknowledgements

We used the NOAA Fisheries version of Google's Gemini to draft initial statements in this chapter about the relationships between our publications and AMAPPS priorities, and then the coauthors revised and incorporated some of that information into this final report.

We thank Leah Crowe, Josh Hatch, Annie Gorgone, Blake Price, Eric Matzen, Emily Christiansen, Mike Judge, Craig Harms, Matthew Godfrey, Michele Sims, Lisa Conger, Lucy McWilliams, and Sasha Milsky for their expertise in fieldwork, sample collection, and veterinary support. We also thank Camirin Braun, Nima Farchadi, Laura McDonnell, Elizabeth Babcock, Martin Grossell, Neil Hammerschlag, and Maria Estevanez for their analytical advice and manuscript reviews.

We appreciate the logistical support provided by Mass Audubon's Wellfleet Bay Wildlife Sanctuary, the UC Davis Stable Isotope Facility, and the crews, pilots, and observers associated with Anthem Commercial Air Services (Val Diers), NOAA Aircraft Operations Center, as well as the staff associated with the vessels M/V Warren Jr., M/V Scarlett Isabella, F/V Salvation, F/V Kathy Ann, R/V Julius, R/V Coriacea, and R/V Selkie.

Permits & Approvals: Animal studies were approved by the NOAA Fisheries Institutional Animal Care and Use Committee and conducted under Endangered Species Act (ESA) permits (21233, 18526, 22218, 17225, 23639) issued to the NMFS Southeast Fisheries Science Center, NMFS Northeast Fisheries Science Center, or Coonamessett Farm Foundation.

This work was funded by the U.S. Dept. of the Interior/BOEM (Agreements M14PG00005, M10PG00075, M19PG00007) and NOAA/NMFS (NEFSC, SEFSC, and the Protected Species Toolbox Initiative). Additional support was provided by the U.S. Navy, NOAA NCCOS, the Scallop Industry Sea Scallop Research Set Aside (RSA) Program, the Leatherback Trust, the NOAA Saltonstall-Kennedy Grant Program, the Massachusetts Environmental Trust, and the New Jersey Offshore Wind Research & Monitoring Initiative.

7.8 References Cited

Bauer RK. 2021. RchivalTag: analyzing and interactive visualization of archival tagging data. R package version 0.1.5. https: //CRAN.R-project.org/package=RchivalTag

Crowe LM, Hatch JM, Patel SH, Smolowitz RJ, Haas HL. 2020. Riders on the storm: Loggerhead sea turtles detect and respond to a major hurricane in the Northwest Atlantic Ocean. Mov Ecol. 8(32). https://movementecologyjournal.biomedcentral.com/articles/10.1186/s40462-020-00218-6

Fahlman A, Crespo Picazo J-L, Sterba-Boatwright B, Stacy BA, Garcia-Parraga D. 2017. Defining risk variables causing gas embolism in loggerhead sea turtles (*Caretta caretta*) caught in trawls and gillnets. Sci. Rep. 7:2739. doi: 10.1038/s41598-017-02819-5.

Hatch JM, Haas HL, Sasso CR, Patel SH, Smolowitz RJ. 2022. Estimating the complex patterns of survey availability for loggerhead turtles. J Wildl Manage. 86(4):e22208. https://doi.org/10.1002/jwmg.22208.

Hatch JM, Murray K, Patel S, Smolowitz R, Haas HH. 2022. Evaluating simple measures of spatial-temporal overlap as a proxy for encounter risk between a protected species and commercial fishery. Front Conserv Sci. 4. https://doi.org/10.3389/fcosc.2023.1118418.

Logan J, Dourdeville K, Choate K, Nielsen J, Patel SH, Prescott R, Haas HL. (in review) Niche overlap and trophic position estimates of multiple sea turtle species cold-stunned in the northwest Atlantic. Submitted for publication.

Murray KT. 2011. Interactions between sea turtles and dredge gear in the U.S. sea scallop (*Placopecten magellanicus*) fishery 2001-2008. Fisheries Res. 107, 137–146. 10.1016/j.fishres.2010.10.017

Murray KT. 2015. Estimated loggerhead (*Caretta caretta*) interactions in the mid-Atlantic scallop dredge fishery 2009-2014. Northeast Fish Sci. Cent Ref Doc. 15, 15–20. http://doi.org/10.7289/V5GT5K5W

Murray KT. 2021. Estimated loggerhead (*Caretta caretta*) interaction in the mid-Atlantic sea scallop dredge fishery 2015- 2019. NOAA Tech Memo NMFS-NE-270 18, 13. https://doi.org/10.25923/apw2-wh54.

[NEFSC] Northeast Fisheries Science Center. 2011. Preliminary summer 2010 regional abundance estimate of loggerhead turtles (*Caretta caretta*) in northwestern Atlantic Ocean continental shelf waters. U.S. Dept Commer Northeast Fish Sci Cent Ref Doc. 11-03; 33 p. Accessible at: https://repository.library.noaa.gov/view/noaa/3879.

Patel S, Winton MV, Hatch JM, Haas HL, Saba VS, Fay G, Smolowitz RJ. 2021. Projected shifts in loggerhead sea turtle habitat in the Northwest Atlantic Ocean due to climate change. Sci. Rep. 11:8850 https://doi.org/10.1038/s41598-021-88290-9.

Parga ML, Crespo-Picazo JL, Monteiro D, García-Párraga D, Hernandez JA, Swimmer Y, et al. 2020. On-board study of gas embolism in marine turtles caught in bottom trawl fisheries in the Atlantic Ocean. Sci Rep 10:5561. https://doi.org/10.1038/s41598-020-62355-7.

Rider M, Haas H, Sasso C. 2022.Surface availability metrics of leatherback turtles (*Dermochelys coriacea*) tagged off North Carolina and Massachusetts, United States. NOAA technical memorandum NMFS-NE 286. https://doi.org/10.25923/82c1-4a85

Rider MJ, Avens L, Haas HL, Hatch JM, Patel SH, Sasso CR. 2024a. Where the leatherbacks roam: movement behavior analyses reveal novel foraging locations along the Northwest Atlantic shelf. Front. Mar. Sci. 11:1325139. https://doi.org/10.3389/fmars.2024.1325139

Rider MJ, Avens L, Haas HL, Harms CA, Patel SH, Snodgrass D, Sasso CR. 2024b. Regional variation in leatherback dive behavior in the northwest Atlantic. Endang Species Res. 55:169–185. https://doi.org/10.3354/esr01365.

Rider MJ, Avens L, Haas HL, Patel SH, Sasso, C.R. (in review). Distribution models reveal important coastal habitats for endangered leatherback sea turtles.

Robinson NJ, García-Párraga D, Stacy BA, Costidis AM, Blanco GS, Clyde-Brockway CE, Haas HL, Harms CA, Patel SH, Stacy NI, Fahlman A. 2021. A baseline model for estimating the risk of gas embolism in sea turtles during routine dives. Front Physiol. 2021 Sep 1;12:678555. https://doi.org/10.3389/fphys.2021.678555.

Rogers R, Choate K, Crowe LM, Hatch J, James M, Matzen E, Patel S, Sasso C, Siemann L, Haas HL. 2024. Investigating leatherback surface behavior using a novel tag design and machine learning. J Exp Mar Bio and Ecol. 576:152012. https://doi.org/10.1016/j.jembe.2024.152012.

Tal D, Shachar-Bener H, Hershkovitz D, Arieli Y, Shupak A. 2015. Evidence for the initiation of decompression sickness by exposure to intense underwater sound. J. Neurophysiol. 114, 1521–1529. https://doi.org/10.1152/jn.00466.2015.

Yang T, Haas HL, Patel S, Smolowitz R, James MC, Williard AS. 2018. Blood biochemistry and haematology of migrating loggerhead turtles (*Caretta caretta*) in the Northwest Atlantic: reference

intervals and intra-population comparisons. Conserv Physiol 7(1): coy079, https://doi.org/10.1093/conphys/coy079.

8 Seabird Research

Primary authors: Harvey Walsh, Elizabeth Josephson

8.1 Introduction

The Oceanography Branch of the Northeast Fisheries Science Center (NEFSC) conducts Ecosystem Monitoring (EcoMon) surveys to gather extensive data on the Northeast Atlantic U.S. Shelf. These cruises occur seasonally, aiming to track seasonal to decadal shifts in ecosystem conditions by sampling the full shelf. During these surveys, we collect oceanographic and plankton samples, with a focus on the chemical, physical, and biological properties of the water column. Since 2017, EcoMon research cruises have also incorporated comprehensive visual surveys of seabirds, marine mammals, turtles, large pelagic fish, and marine debris under the Atlantic Marine Assessment Program for Protected Species (AMAPPS). This initiative expands upon existing AMAPPS projects that have previously collected seabird visual survey data on other AMAPPS shipboard cruises.

The concurrent collection of seabird and marine mammal data alongside other biotic and abiotic data enhances our understanding of species' spatiotemporal distributions and their relationships with other trophic levels within the evolving marine ecosystem. Furthermore, we shared the seabird data from AMAPPS projects with other researchers, supporting modeling efforts to map seabird distribution (Winship et al. 2018) and investigate habitat usage (Veit et al. 2015; White and Veit 2020).

In this chapter, we describe the distribution of seabird data collected during 2019 to 2025, which addresses the following AMAPPS objectives (all objectives are listed in Section 2.2):

> 1) Collect broad-scale data over multiple years on the seasonal distribution and abundance of marine mammals (cetaceans and pinnipeds), marine turtles, and seabirds using fixed passive acoustic monitoring and direct aerial and shipboard surveys of coastal U.S. Atlantic Ocean waters;
> 2) Collect similar data at finer scales at several sites of interest to BOEM, NOAA, and partners using visual and acoustic survey techniques.

8.2 Methods

We based the data collection protocol on a standardized 300 m strip transect methodology, like that used by various agencies in North America and Europe (Tasker 1984; Anon 2011; Ballance 2011) including previous AMAPPS and Bureau of Ocean Energy Management (BOEM) surveys. Observers collected data on all seabirds within a 300 m strip on one side of the ship’s track line. Observers searched from the bow to 90° to either the port or the starboard side, depending on which side had the best viewing conditions. Observers conducted surveys on the flying bridge of the ship, whenever possible. They collected data in sea states up to a Beaufort 7, in light rain, fog, and when ship speeds were between 8 and 12 knots (below 8 knots, the data becomes questionable to use for abundance estimates).

Observers used the SeaScribe program (BRI 2020) for data entry until 2023. Beginning in 2022, observers began testing SeaLog (ABR, Inc.). Both applications draw GPS coordinates, as well as time from a GPS device, so each observation receives data on the latitude-longitude position, time stamp, and ship's course. The standard data collected for observations included species identification, distance between the ship and the animal, number of individuals, association, behavior, flight direction, flight height, and if possible or applicable, age, sex, and plumage status. The primary duties of each application

were not to collect data on other marine megafauna, however, observers also recorded other species that were both inside and outside of the 300 m strip survey zone.

During surveys, the on-effort observer utilized binoculars (10x42) to scan within the survey strip. When there were two observers onboard, they alternated two-hour shifts, with a person on-effort collecting data and the other off-effort (not collecting data). If an animal proved elusive, observers used a pair of 20x60 Zeiss imaged-stabilized binoculars to attain positive identifications. To aid in approximating distance observers used custom-made range finders based on height above water and the observers' personal body measurement (Heinemann 1981).

We summarized all bird sighting data to the lowest taxonomic identification level (henceforth referred to as species) made during each cruise conducted during 2017 to 2025. We calculated the percent frequency of sighting occurrence from all cruises for each species for the Ecosystem Monitoring regions of the Northeast U.S. Shelf. For cruises conducted during 2017 to 2025, we also plotted sightings distribution maps of species classified to the following levels: Alcids, Gannet and Boobies, Gulls, Loons, Petrels, Shearwaters, Skuas, and Storm-petrels. Common and scientific names of seabirds are in Appendix A, **Table A-2**.

8.3 Results

8.3.1 Percent Frequency of Occurrence

We collected seabird visual survey data on 42 Northeast Fisheries Science Center (NEFSC) surveys during 2017 to 2025. This entailed 707 observing days on AMAPPS shipboard abundance surveys, Oceanography Branch EcoMon cruises, North Atlantic right whale surveys, and other opportunistic surveys conducted by NEFSC (**Table 8-1**).

Counts of birds within the survey zone totaled 184,261 on NEFSC surveys since 2017. We counted over 260 sea and land bird species on cruises from 2017 to 2025. Seabird percent frequency of abundance was calculated for the northeast U.S. shelf and the Slope Sea, the regions with the greatest spatial and seasonal coverage.

Overall, Shearwaters and Storm-petrels totaled 46% frequency of occurrence of seabird sightings on the northeast U.S. shelf (**Table 8-2**). During the winter, Northern Gannet had the highest percent frequency of occurrence. Spring sightings were dominated by Red Phalarope. In the summer and fall, Great Shearwater had the highest percent frequency of occurrence.

In the Slope Sea, Shearwaters and Storm-petrels totaled over 75 percent frequency of occurrence of seabird sightings (**Table 8-3**). During the winter, Dovekie had the highest percent frequency of occurrence. Spring sightings were dominated by Sooty Shearwater and Red Phalarope. Wilson's Storm-petrel had the highest percent frequency of occurrence in the summer. In the fall, Wilson's Storm-petrel, Great Shearwater and Cory's Shearwater were dominant.

Table 8-1. Spatiotemporal information on each seabird cruise during 2017 - 2025

Cruise[1]	Type	Year	Start Day	End Day	Num of Days	Min Latitude	Max Latitude	Min Longitude	Max Longitude
GU1701	EcoMon	2017	16-May	6-Jun	21	35.6	43.6	-75.8	-65.5
GU1702	EcoMon	2017	10-Jun	22-Jun	12	30	41.2	-80.2	-68.5
GU1706	EcoMon	2017	31-Oct	9-Nov	9	36.8	42.5	-76.1	-66.2
HRS1701	NARW	2017	9-Sep	17-Sep	8	39.1	40.3	-72.5	-67.2
GU1803	EcoMon	2018	21-Jul	18-Aug	28	39.5	41.9	-70.5	-64.6
GU1804	EcoMon	2018	22-Aug	30-Aug	8	36.7	41.7	-75.7	-67.5
GU18TN	Transit	2018	11-Jul	16-Jul	5	24.4	40	-81.3	-72
GU18TS	Transit	2018	2-Sep	8-Sep	6	24.3	37	-87.2	-75.4
HB1803	EcoMon	2018	23-May	4-Jun	12	38.3	43.9	-74.8	-65.4
HB18TN	Transit	2018	1-Aug	6-Aug	5	23.8	39.7	-80	-72.1
HB5065	NARW	2018	1-Aug	6-Aug	5	23.8	39.7	-80	-72.1
HRS1801	NARW	2018	1-Nov	12-Nov	11	35.9	41	-76.2	-69.8
GU1902	EcoMon	2019	15-Aug	29-Aug	14	36.8	43.4	-76.3	-65.4
GU1905	EcoMon	2019	15-Oct	30-Oct	15	36	42.1	-75.8	-66.2
HB1902	EcoMon	2019	24-May	5-Jun	12	38.1	44	-75.1	-65.5
HRS1910	NARW	2019	18-Aug	27-Aug	9	39.5	41	-70.1	-66.3
RB1904	ECOA	2019	13-May	24-May	11	39.5	40.5	-71.3	-70.7
TN0368	URI	2019	6-Jul	17-Jul	11	39.2	40.5	-71.5	-70.2
GU2102	EcoMon	2021	14-May	26-May	12	38.5	43.8	-74.7	-65.7
GU2103	AMAPPS	2021	13-Jun	4-Sep	83	24.3	39.1	-86.8	-71
HB2102	EcoMon	2021	17-Jun	21-Aug	65	36.6	42.4	-74.8	-64.2
PC2104	EcoMon	2021	6-Aug	18-Aug	12	38.8	44.2	-74.4	-65.6
PC2106	EcoMon	2021	16-Oct	25-Oct	9	36	42.9	-75.6	-68.4
RB2203	ECOA	2022	6-Aug	22-Sep	47	27.3	45.1	-81	-58.3
HB2204	EcoMon	2022	1-Jun	16-Jun	15	37.4	44.5	-75	-65.5
PC2205	EcoMon	2022	1-Nov	9-Nov	8	40	43.3	-71.8	-65.5
GM2301	BOEM	2023	29-Nov	29-Nov	1	41.4	41.4	-70.9	-70.8
GU2301	AMAPPS	2023	7-Feb	22-Apr	74	28.9	38.5	-79.2	-70.8
HB2302	EcoMon	2023	9-Jun	27-Jun	18	35.8	44.5	-75.7	-65.5
HB2303	EcoMon	2023	8-Aug	24-Aug	16	35.7	44.4	-75.7	-65.4
PC2305	EcoMon	2023	27-Oct	13-Nov	17	35.6	44.5	-75.1	-65.9
GM2401-1	BOEM	2024	9-Jan	9-Jan	1	41	41.2	-71.1	-71
GM2401-2	BOEM	2024	13-Mar	14-Mar	1	40.7	41	-70.4	-70.2
GM2402	BOEM	2024	16-Apr	18-Apr	2	40.6	41.5	-71.2	-69.7
HB2403	EcoMon	2024	26-May	13-Jun	18	38.1	43.7	-74.7	-65.4
HB2406	EcoMon	2024	12-Aug	22-Aug	10	40	44.5	-72.3	-65.5
PC2406	EcoMon	2024	27-Oct	12-Nov	16	36	41.1	-75.9	-69.6
HB2503	EcoMon	2025	27-May	5-Jun	9	38	43.2	-74.2	-67.7

First two or three letters in cruise name indicates the vessel: GU=NOAA ship *Gordon Gunter*; HRS= R/V *Hugh R. Sharp*; HB=NOAA ship *Henry B. Bigelow*; RB=NOAA ship *Robert Brown*; TN= R/V *Thomas G. Thompson*; PC=NOAA ship *Pisces*

Table 8-2. Percent frequency of occurrence of all seabirds 2017 – 2025 on Northeast U.S. shelf
Common and scientific names of seabirds are in Appendix A.

Common Name	Total	Winter	Spring	Summer	Fall
Great Shearwater	22.482	0.012	3.766	31.325	22.296
Wilson's Storm-petrel	16.303	0	11.039	26.256	0.707
Sooty Shearwater	6.945	0	11.852	9.023	0.054
Red Phalarope	6.662	0	22.876	0.729	10.799
Northern Gannet	6.287	54.628	2.2600	0.673	8.342
Herring Gull	5.503	13.559	9.041	2.446	7.840
Unidentified Large Gull	3.735	0	0.024	6.871	0.004
Cory's Shearwater	3.512	0	0.341	4.708	4.144
Great Black-backed Gull	2.511	7.822	1.802	2.023	2.63

Common Name	Total	Winter	Spring	Summer	Fall
Northern Fulmar	2.277	0.037	4.618	1.926	2.012
Leach's Storm-petrel	2.267	0	3.512	3.055	0.027
Double-crested Cormorant	2.165	0	0.814	0.471	8.172
Unidentified Phalarope	1.955	0.123	0.585	1.511	4.735
Bonaparte's Gull	1.908	6.019	0.01	0.002	6.902
Unidentified Storm-petrel	1.509	0	0.078	2.744	0.027
White-winged Scoter	1.149	0.037	2.733	0	3.128
Long-tailed Duck	1.130	0.049	6.537	0	0.019
Common Tern	1.065	0	3.722	0.784	0
Manx Shearwater	0.874	4.242	0.234	0.28	1.811
Dovekie	0.727	8.974	0.151	0.04	0.309
Unidentified Scoter	0.716	0	3.074	0	0.869
Black Scoter	0.697	0.012	0	0.002	3.209
Red-necked Phalarope	0.595	0	0.731	0.864	0.004
Unidentified Tern	0.595	0.012	2.869	0.168	0.046
Black-legged Kittiwake	0.552	0.454	0	0.008	2.387
Laughing Gull	0.536	0.025	1.120	0.246	0.962
Common Loon	0.414	0.674	1.047	0.055	0.730

Table 8-3. Percent frequency of occurrence of all seabirds 2017 - 2025 on the Slope Sea
Region is offshore of the northeast U.S. shelf. Common and scientific names of seabirds are in Appendix A.

Common Name	Total	Winter	Spring	Summer	Fall
Wilson's Storm-petrel	34.391	0	3.130	40.93	13.021
Great Shearwater	18.656	0	1.832	21.939	10.723
Cory's Shearwater	16.937	0	0.763	19.747	13.191
Leach's Storm-petrel	5.443	0	2.29	6.299	2.638
Dovekie	3.381	53.200	0.763	0	0
Audubon's Shearwater	3.038	0	0.458	3.557	1.787
Herring Gull	1.787	14.264	7.252	0.254	4.000
Sooty Shearwater	1.449	0	19.924	0.219	0.17
Unidentified Shearwater	1.449	0	0.229	1.749	0.085
Red Phalarope	1.41	0.540	19.924	0.083	0.851
Bonaparte's Gull	1.289	13.030	6.260	0	1.362
Unidentified Phalarope	1.212	0.463	16.260	0	2.723
Band-rumped Storm-petrel	0.956	0	0	1.123	0.681
Black-legged Kittiwake	0.889	10.871	0.687	0	2.894
Black-capped Petrel	0.729	0	0.687	0.567	3.915
Northern Gannet	0.666	2.082	0.687	0.071	7.660
Unidentified Storm-petrel	0.541	0	3.130	0.390	0.426
Atlantic Puffin	0.439	2.390	2.366	0.165	0.085
Pomarine Jaeger	0.377	0	0.153	0.065	5.532

8.3.2 Species Distribution Maps

Alcids: Eight species of Alcids were sighted on NEFSC cruises from 2017 to 2025 (**Figure 8-1**). Atlantic Puffin, Dovekie, Razorbill were the most frequently sighted species.

Gannet and Boobies: Five species of Gannets and three species of Boobies were sighted on NEFSC cruises from 2017 to 2025 (**Figure 8-2**). Northern Gannet and Double-crested Cormorant were the most frequently observed Gannets and Brown Booby and Masked Booby were the most frequently observed Boobies.

Gulls: Ten species of Gulls were sighted on NEFSC cruises from 2017 to 2025 (**Figure 8-3**). Herring Gull, Great Black-backed Gull, Laughing Gull, Bonaparte's Gull were the most frequently sighted.

Loons: Three species of Loons were sighted on NEFSC cruises from 2017 to 2025 (**Figure 8-4**). Common Loon and Red-throated Loon were the most abundant.

Shearwaters: Several species of Shearwaters were sighted on NEFSC cruises from 2017 to 2025 (**Figure 8-5**). Greater Shearwater, Cory's Shearwater, Sooty Shearwater, Audubon's Shearwater, Manx Shearwater were the most frequently sighted.

Skuas: Seven species of Skuas were sighted on NEFSC cruises from 2017 to 2025 (**Figure 8-6**). Pomarine Jaeger, South Polar Skua, and Parasitic Jaeger were the most frequently sighted.

Storm-petrels: Seven species of Storm-petrels were sighted on NEFSC cruises from 2017 to 2025 (**Figure 8-7**). Wilson's Storm-petrel, Leach's Storm-petrel, and Band-rumped Storm-petrel were the most frequently sighted.

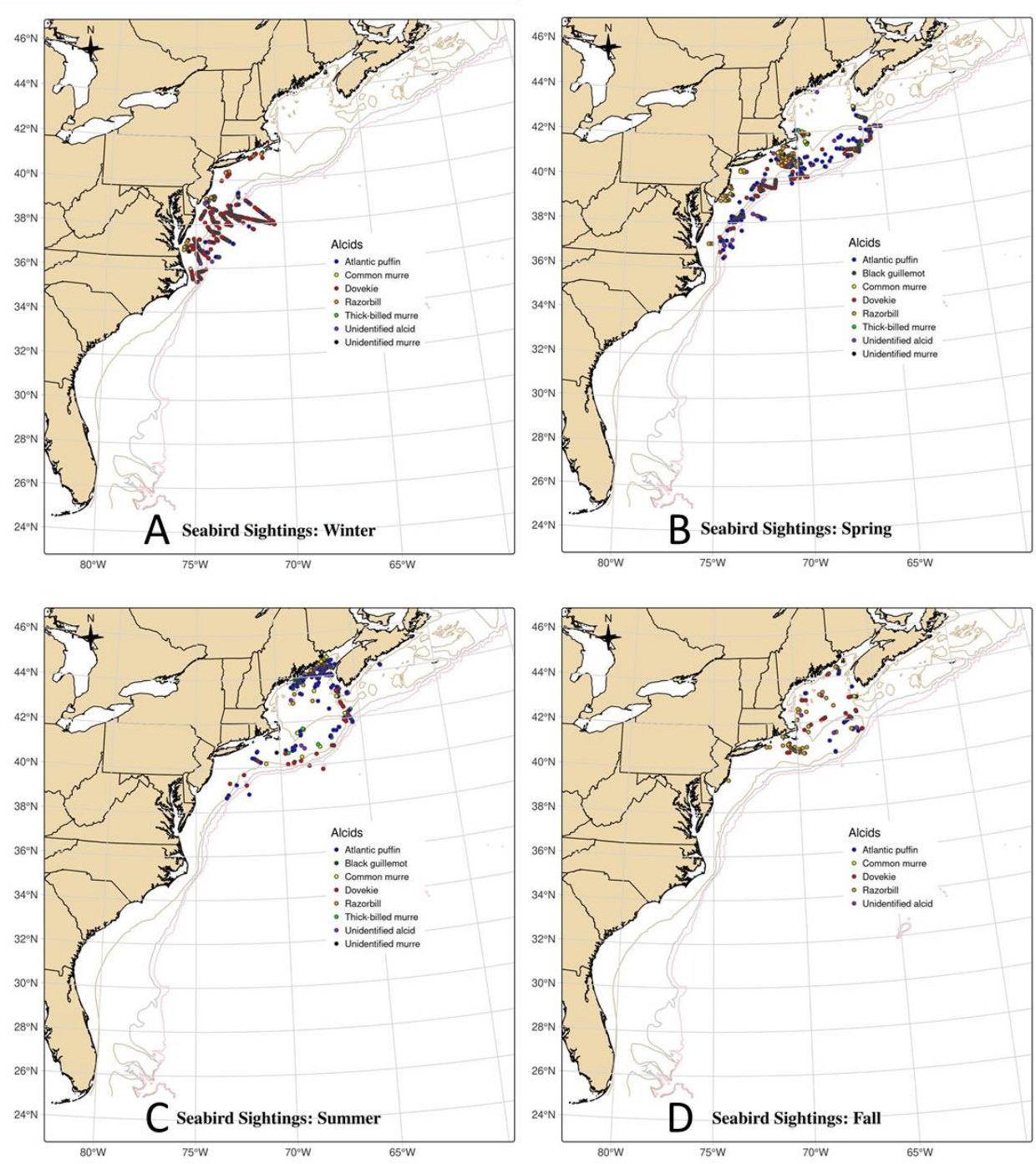

Figure 8-1. Alcids sighted seasonally on NEFSC cruises from 2017 – 2025
A: winter; B: spring; C: summer; D: fall. Common and scientific names of seabirds are in Appendix A.

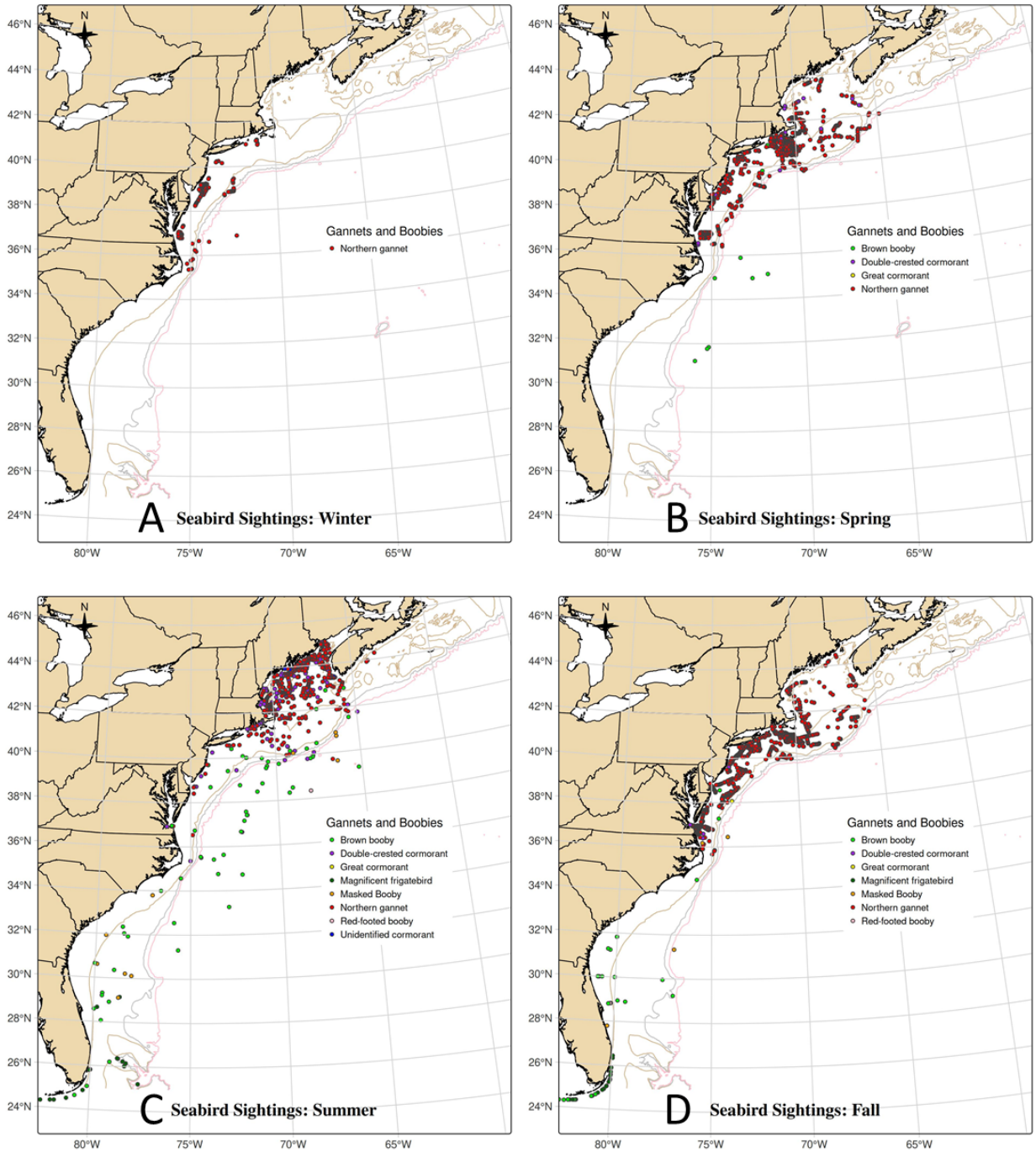

Figure 8-2. Gannets and Boobies sighted seasonally on NEFSC cruises from 2017 - 2025
A: winter; B: spring; C: summer; D: fall. Common and scientific names of seabirds are in Appendix A.

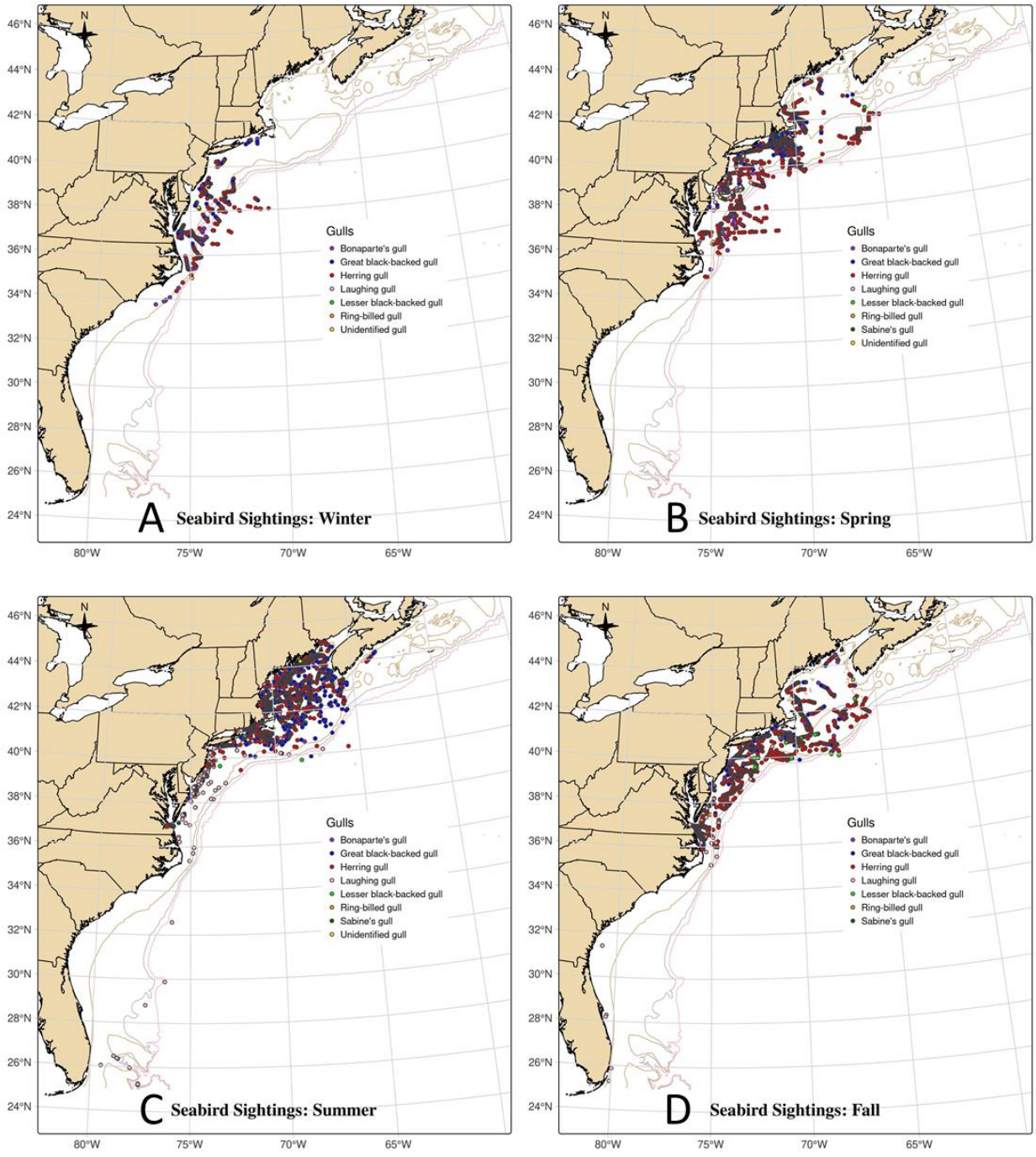

Figure 8-3. Gulls sighted seasonally on NEFSC cruises from 2017 - 2025
A: winter; B: spring; C: summer; D: fall. Common and scientific names of seabirds are in Appendix A.

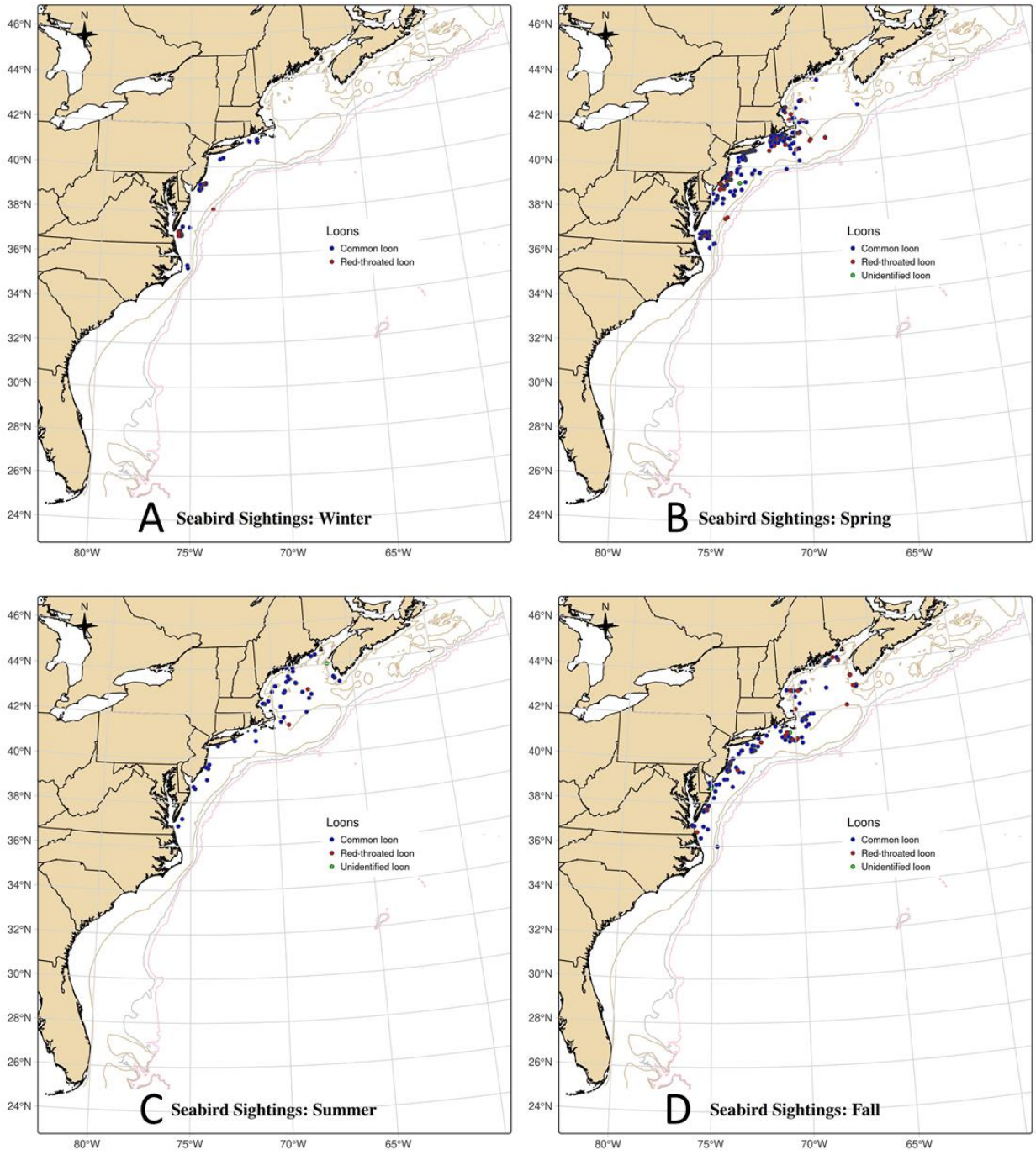

Figure 8-4. Loons sighted on NEFSC cruises from 2017 - 2025
A: winter; B: spring; C: summer; D: fall. Common and scientific names of seabirds are in Appendix A.

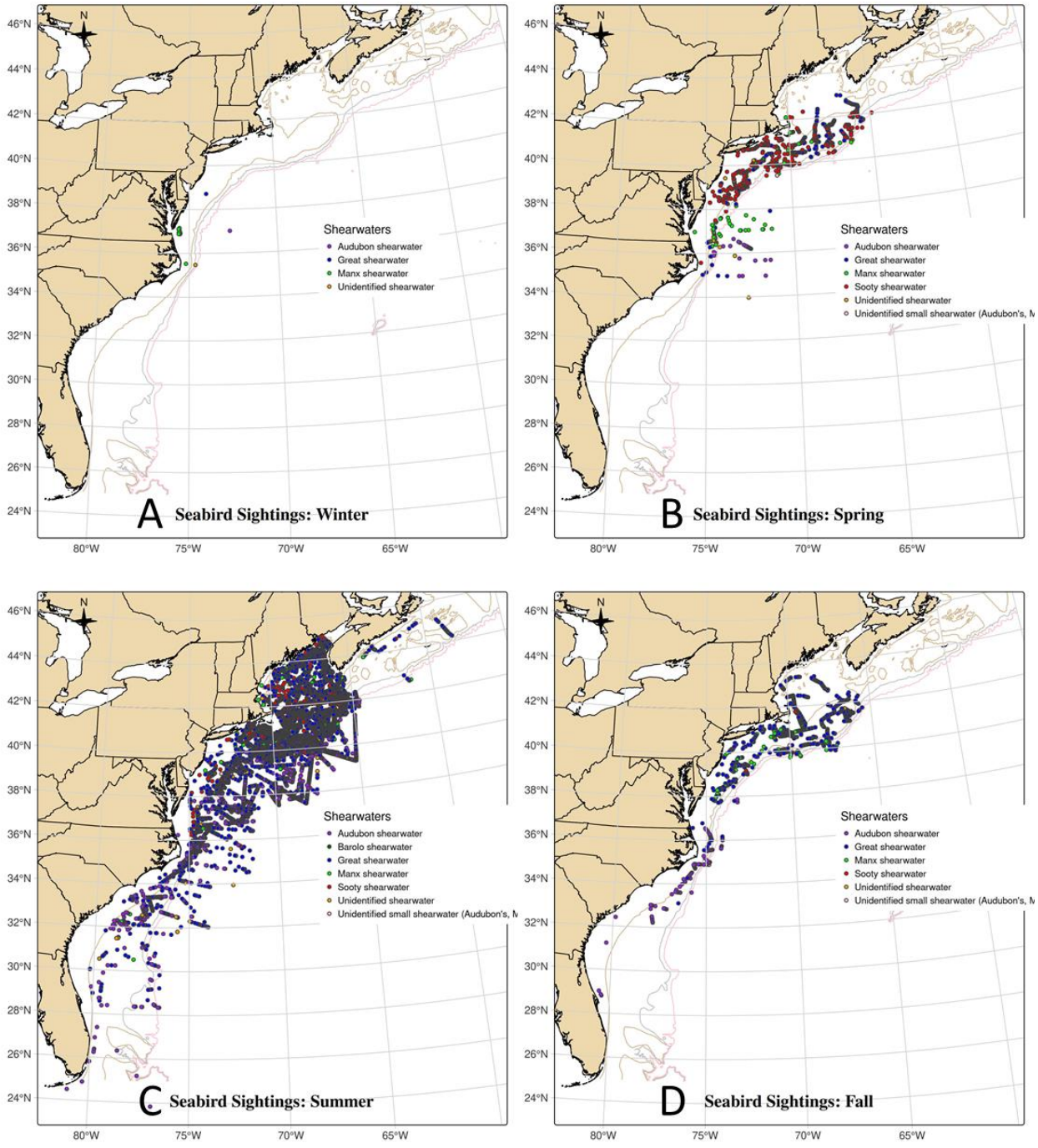

Figure 8-5. Shearwaters sighted seasonally on NEFSC cruises from 2017 - 2025
A: winter; B: spring; C: summer; D: fall. Common and scientific names of seabirds are in Appendix A.

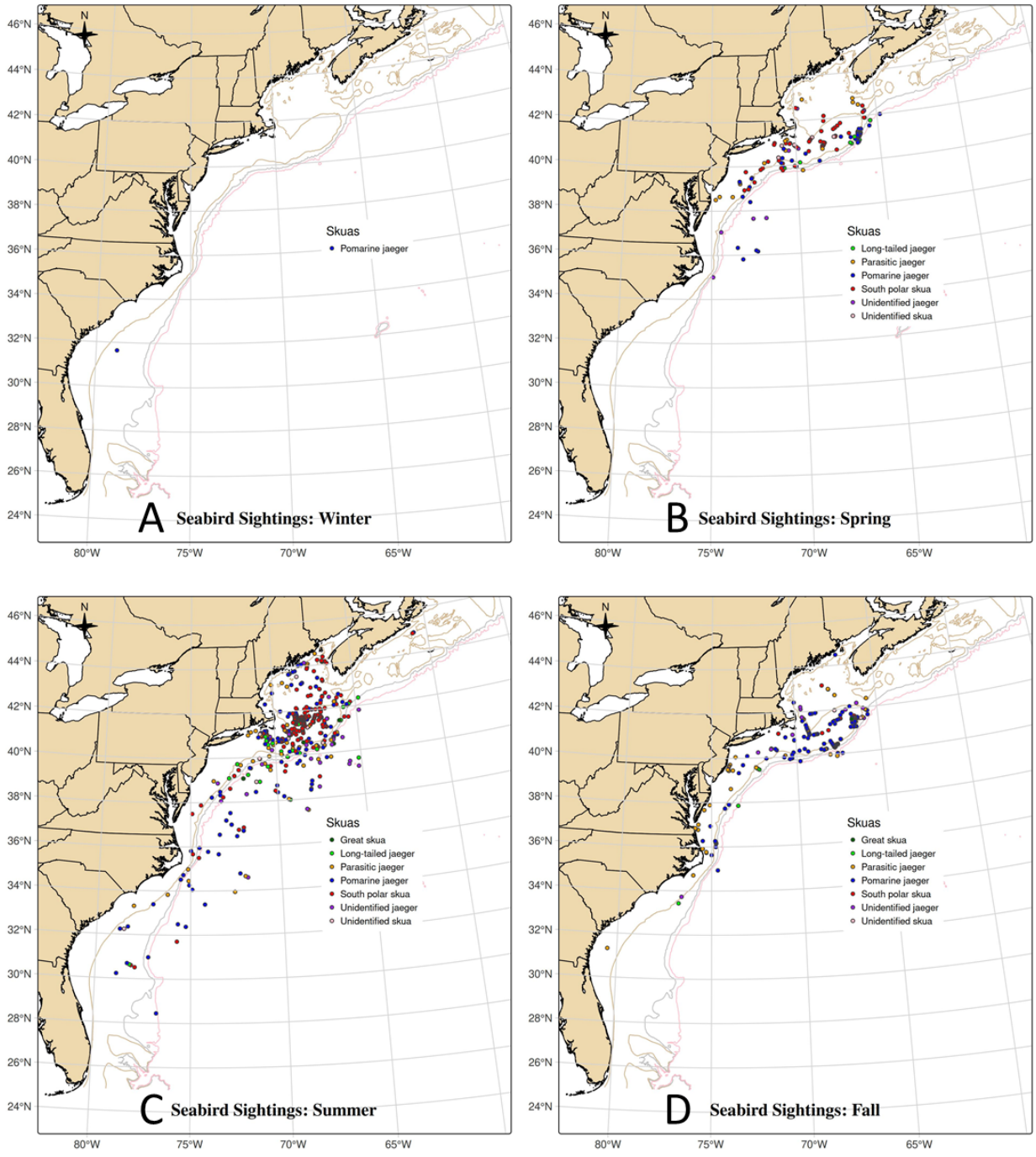

Figure 8-6. Skuas sighted seasonally on NEFSC cruises from 2017 - 2025
A: winter; B: spring; C: summer; D: fall. Common and scientific names of seabirds are in Appendix A.

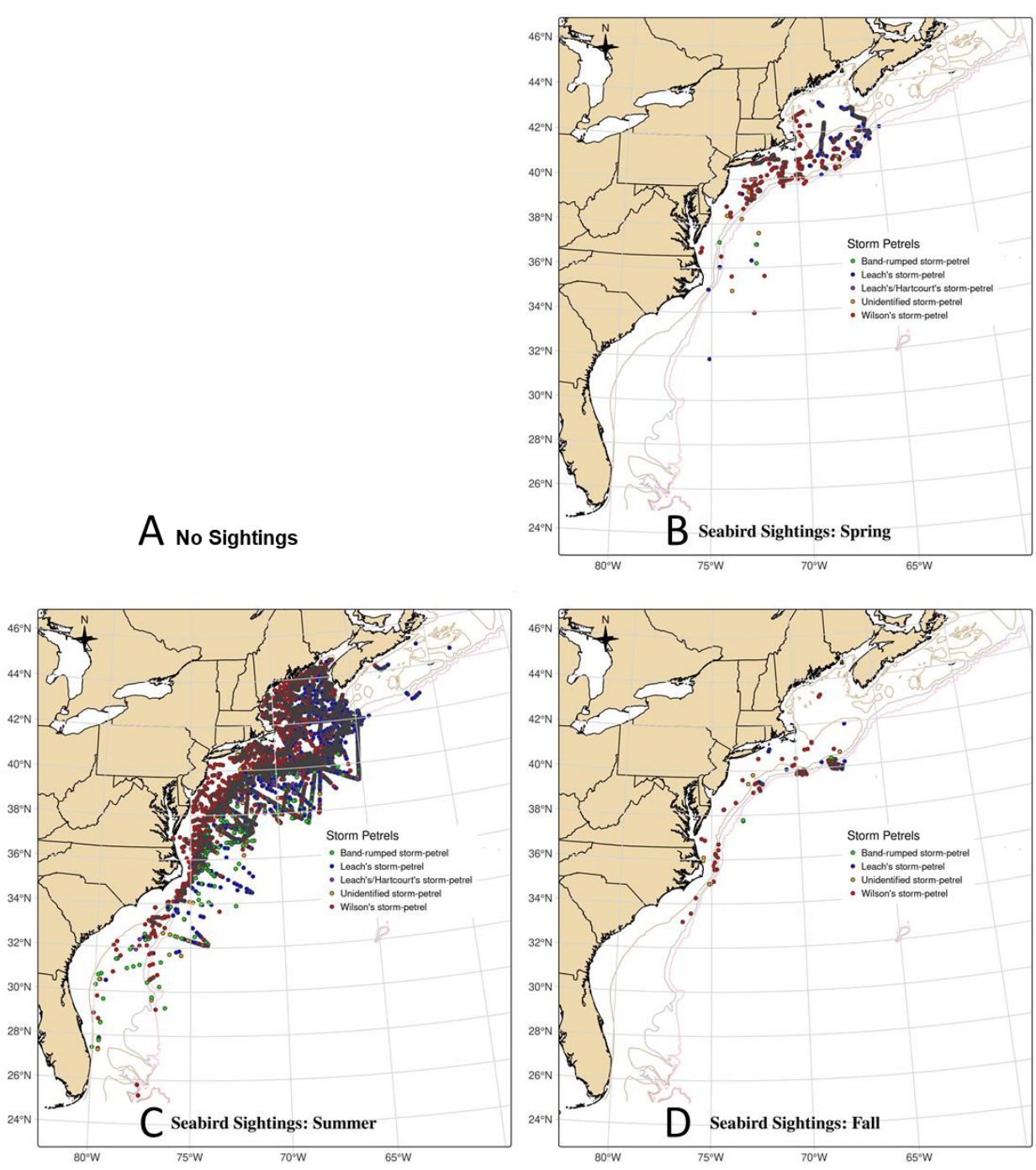

Figure 8-7. Storm-petrels sighted seasonally on NEFSC cruises from 2017 - 2025
A: winter; B: spring; C: summer; D: fall. Common and scientific names of seabirds are in Appendix A.

8.4 Acknowledgments

We would like to thank the officers and crews of all the vessels we worked on: NOAA ships *Gordon Gunter*, *Henry B. Bigelow*, *Pisces*, *Robert H. Brown*, *Gloria Michelle*, R/V *Hugh R. Sharp*, R/V *Thomas G. Thompson*.

8.5 References Cited

Anonymous. 2011. Seabird Survey Instruction Protocol. Seabird distribution and abundance, Summer 2011. NOAA RV Henry B. Bigelow. Northeast Fisheries Science Center.

Ballance L. Seabird Survey Instruction Manual, PICEAS 2011. Ecosystems Studies Program Southwest Fisheries Science Center, La Jolla, California.

Biodiversity Research Institute (BRI). SeaScribe. SeaScribe – a modern offshore survey data collection tool. [accessed 2020 Oct 5]. https://briwildlife.org/seascribe/

Drew G, Swingley C, Schoen S. 2023. SeaLog User Manual, v2.2. [accessed 2023 June 8]. https://sealog.abrinc.com/installers/SeaLog_User_Manual_v2.2.pdf

Heinemann D. 1981. A Range Finder for Pelagic Bird Censusing. J Wildl Manage. 98(2):489–493. https://doi.org/10.2307/3807930

Tasker M, Jones P, Dixon T, Blake B. 2024. Counting Seabirds at Sea from Ships: a Review of Methods Employed and a Suggestion for a Standardized Approach. The Auk. 101(3). https://digitalcommons.usf.edu/auk/vol101/iss3/16

Veit RR, Goyert HF, White TP, Martin M-C, Manne LL, Gilbert A. 2015. Pelagic Seabirds off the East Coast of the United States 2008-2013. U.S. Dept. of the Interior, Bureau of Ocean Energy Management, Office of Renewable Energy Programs, Sterling, VA. https://espis.boem.gov/final%20reports/5467.pdf

White TP, Veit RR. 2020. Spatial ecology of long-tailed ducks and white-winged scoters wintering on Nantucket Shoals. Ecosphere. 11(1):e03002. https://doi.org/10.1002/ecs2.3002

Winship A, Kinlan B, White T, Leirness J, Christiansen. 2018. Modeling At-Sea Density of Marine Birds to Support Atlantic Marine Renewable Energy Planning. NCCOS IAA MOA-2013-046-8696, BOEM OCS Study 2018-010, and NCCOS BOEM IAA M13PG00005. https://espis.boem.gov/final%20reports/BOEM_2018-010.pdf

9 Ecosystem Research

Primary authors: Harvey Walsh, Elizabeth Josephson, Debra Palka

9.1 Introduction

In chapters 4, 5 and 7 to gain insight into what influenced the patterns of distribution and abundance of protected species (marine mammals, sea turtles, and sea birds) we investigated what physical and biological characteristics were associated with the protected species. Such insight could potentially allow the discrimination between changes in protected species populations that are due to natural environmental variability versus anthropogenic impacts. In addition, such insights could improve population assessments by incorporating ecosystem aspects into single or multiple species population assessments, as has been the trend in fish population assessments (Jurado-Molina et al. 2005; Möllmann et al. 2014).

In this chapter, we address aspects of three of the objectives of the Atlantic Marine Assessment Program for Protected Species (AMAPPS), where the complete list of objectives is in Chapter 2:

> 5) Identify currently used viable technologies and explore alternative platforms and technologies to improve population assessment studies, if necessary;
>
> 6) Assess the population size of surveyed species at regional scales; and develop models and associated tools to translate these survey data into seasonal, spatially explicit density estimates incorporating habitat characteristics; and
>
> 7) Collect opportunistic plankton sampling off the northeast U.S. Shelf and Slope Sea,

AMAPPS research focused on protected species inhabiting both continental shelf waters and offshore regions, including the shelf (to 200 m depth), mesopelagic (to 1000 m) and the bathypelagic (to 4000 m). While the continental shelf is a hub for human activities like fishing (Amoroso et al. 2018) and wind energy development (BOEM 2020), and a site for extensive scientific research by federal, state, private, and university organizations (e.g., NEFSC, Northeast Area Monitoring and Assessment Program, Woods Hole Oceanographic Institution, Rutgers), many protected species also rely on offshore habitats. To fully understand the protected species' distribution, abundance, and habitat needs, information on these off-shelf waters is crucial. AMAPPS shipboard cruises provided valuable opportunities to explore these environments, allowing for sampling in diverse areas such as canyons, oceanic waters, warm-core rings, and along the shelf/slope front.

This chapter focuses on the physical and biological ecosystem data we collected during AMAPPS III shipboard surveys. We used some of the biological ecosystem data collected during the AMAPPS NEFSC surveys with distributional patterns of protected species, as demonstrated in the exploratory study in Section 6.6. Additionally, in this chapter we highlighted several studies conducted by collaborators who utilized hydrographic data collected from AMAPPS shipboard surveys. For information on physical and biological ecosystem data collected during the 2010-2015 AMAPPS I NEFSC surveys, refer to Palka et al. (2017). Details from the 2016-2019 AMAPPS II NEFSC surveys are in Palka et al. (2021).

9.2 Methods

In support of the AMAPPS objectives, we collected active acoustic, oceanographic, and biological (e.g., plankton, fish, and cephalopods) ecosystem data. We collected active acoustic multi-frequency echosounder data continuously in active and passive modes to provide spatially comprehensive information on the vertical and areal distributions of biomass (see **Figure 4-1** for distribution of active

and passive mode data collection). We collected physical oceanographic data using conductivity, temperature, and depth (CTD) casts that were in conjunction with plankton sampling casts along the visual transect lines to provide depth delimited oceanographic conditions in the study area. We sampled plankton and mesopelagic communities using a 61cm bongo net along the visual transect lines daily at dawn, noon, and dusk. During daylight hours the depth of important cetacean food sources that are phototrophic, such as euphausiids and myctophiids, precludes easy sampling. For this reason, we collected additional biological samples during the night when visual transects could not be conducted but we could sample the mesopelagic species because they migrated closer to the surface. These biological samples helped verify the species composition of the acoustic backscatter data and increased the spatial coverage of the lower trophic level categorization. Since nets can damage delicate gelatinous zooplankton and we cannot sample these plankton types quantitatively in nets, instead we deployed an imaging system to capture species and distribution information on gelatinous zooplankton, in addition to the nightly net sampling.

Descriptions and images of the following sampling methods are in Palka et al. (2021) and Section 10.6 of this report: EK60 active acoustics, visual plankton recorder, bongo net, frame-net, and a CTD.

9.3 Results

During AMAPPS III (2020 – 2025) we conducted three offshore shipboard cruises where we collected 825 samples for CTDs, bongos, visual plankton recorders and frame-nets (**Table 9-1**).

9.3.1 Plankton Data

We identified the plankton in the samples from cruises conducted in 2021 and 2023 (HB2102 and GU2301) to the lowest possible taxon for both zooplankton and ichhthyoplankton and then stored these data in the NEFSC Plankton Oracle database. We are currently processing the plankton samples from 2025 (PC2501).

Plankton samples from the AMAPPS cruises have extended the range of plankton sampling conducted by the Oceanography Branch to include the area of the Northwest Atlantic extending from New England to the mid-Atlantic Bight between the shelf slope and the Gulf Stream providing additional coverage in under sampled areas of the standard Ecosystem Monitoring plankton surveys. Data from 2021 and 2023 showed that concentrations (number of individuals per 100 m^{-3}) of zooplankton and ichthyoplankton are higher on the shelf than in the Slope Sea (**Figure 9-1 A-B**). Results from PC2501 (**Figure 9-1C**) will add to our understanding of these differences as well as differences among taxon collected in the different habitats and will be reported in the AMAPPS 2025 annual report.

Table 9-1. Number of sampling tows conducted by cruise during AMAPPS III (2020 - 2025)

Cruise[1]	CTD	Bongo (333um)	Bongo (150um)	Visual Plankton Recorder	Frame-Net
HB2102	36	180	180	33	47
GU2301	97	97	0	0	0
PC2501	85	85	85	0	0
TOTAL	**218**	**262**	**265**	**33**	**47**

[1] HB2102 on the NOAA ship *Henry B. Bigelow* in 2021. GU2301 on the NOAA ship *Gordon Gunter* in 2023. PC2501 on the NOAA ship *Pisces* in 2025, which is during the AMAPPS III time period however it was funded with Navy AMAPPS IV funds.

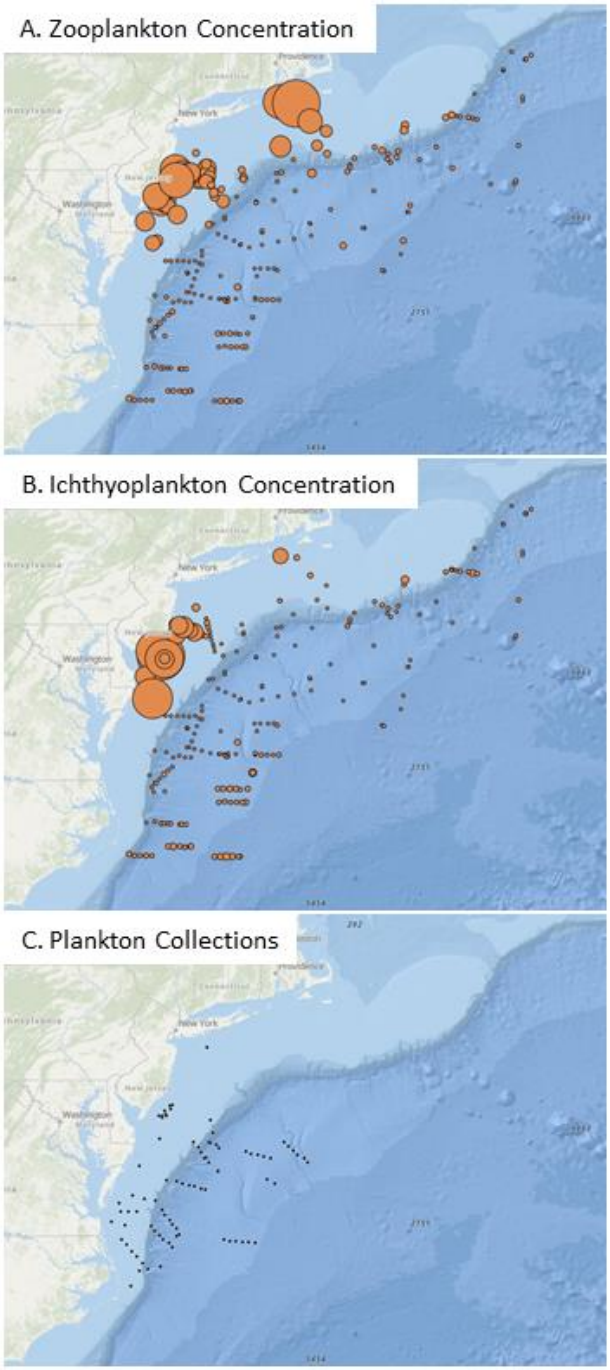

Figure 9-1. Locations and magnitude of plankton collected during 2021-2025 cruises
A. Zooplankton concentrations from samples collected on HB2102 and GU2301. **B.** Ichthyoplankton concentrations from samples collected on HB2102 and GU2301. **For A and B**: the larger the size of the circle the larger the contraction. **C.** Locations of the plankton sampling stations during PC2501.

We unexpectedly discovered larval Atlantic bluefin tuna (*Thunnus thynnus*) in routine plankton samples collected during summer offshore AMAPPS cetacean abundance shipboard surveys. This discovery suggested a previously unrecognized major spawning ground for the species in the Slope Sea off the U.S. Atlantic coastline (Richardson et al. 2016a, b).

Subsequent sample collections from AMAPPS III and other cruises have further supported the identification of the Slope Sea as a significant Atlantic bluefin tuna spawning area (Herandez et al. 2021). Genetic analysis indicates that the Atlantic bluefin tuna spawning in the Slope Sea appear to be a mix of the eastern and western populations—two weakly differentiated but demographically connected ancestral populations that interbreed there. Moreover, genetic signatures of introgression from albacore (*Thunnus alalunga*) have also been identified in the Atlantic bluefin tuna genome (Diaz-Arce et al. 2024).

Support for the Slope Sea as a major spawning ground for Atlantic bluefin tuna: evidence from larval abundance, growth rates, and particle-tracking simulations by Hernandez et al. (2021). https://doi.org/10.1139/cjfas-2020-0444

> *ABSTRACT: "Atlantic bluefin tuna (*Thunnus thynnus*) are commercially and ecologically valuable, but management is complicated by their highly migratory lifestyle. Recent collections of bluefin tuna larvae in the Slope Sea off northeastern United States have opened questions about how this region contributes to population dynamics. We analyzed larvae collected in the Slope Sea and the Gulf of Mexico in 2016 to estimate larval abundance and growth rates and used a high-resolution regional ocean circulation model to estimate spawning locations and larval transport. We did not detect a regional difference in growth rates, but found that Slope Sea larvae were larger than Gulf of Mexico larvae prior to exogenous feeding. Slope Sea larvae generally backtracked to locations north of Cape Hatteras and would have been retained within the Slope Sea until the early juvenile stage. Overall, our results provide supporting evidence that the Slope Sea is a major spawning ground that is likely to be important for population dynamics. Further study of larvae and spawning adults in the region should be prioritized to support management decisions."*

Unidirectional trans-Atlantic gene flow and a mixed spawning area shape the genetic connectivity of Atlantic bluefin tuna by Diaz-Arce et al. (2024) https://doi.org/10.1111/mec.17188

> *ABSTRACT: "The commercially important Atlantic bluefin tuna (*Thunnus thynnus*), a large migratory fish, has experienced notable recovery aided by accurate resource assessment and effective fisheries management efforts. Traditionally, this species has been perceived as consisting of eastern and western populations, spawning respectively in the Mediterranean Sea and the Gulf of Mexico, with mixing occurring throughout the Atlantic. However, recent studies have challenged this assumption by revealing weak genetic differentiation and identifying a previously unknown spawning ground in the Slope Sea used by Atlantic bluefin tuna of uncertain origin. To further understand the current and past population structure and connectivity of Atlantic bluefin tuna, we have assembled a unique dataset including thousands of genome-wide single-nucleotide polymorphisms (SNPs) from 500 larvae, young of the year and spawning adult samples covering the three spawning grounds and including individuals of other* Thunnus *species. Our analyses support two weakly differentiated but demographically connected ancestral populations that interbreed in the Slope Sea. Moreover, we also identified signatures of introgression from albacore (*Thunnus alalunga*) into the Atlantic bluefin tuna genome, exhibiting varied frequencies across spawning areas, indicating strong gene flow from the Mediterranean Sea towards the Slope Sea. We hypothesize that the observed genetic differentiation may*

be attributed to increased gene flow caused by a recent intensification of westward migration by the eastern population, which could have implications for the genetic diversity and conservation of western populations. Future conservation efforts should consider these findings to address potential genetic homogenization in the species."

9.3.2 Midwater Trawl Data

Except for the ITS.DEEP 2025 shipboard survey (Section 5.2), we did not collect new midwater trawl catch data during AMAPPS III. We will provide more information on the 2025 survey data in the AMAPPS 2025 Annual Report.

However, during AMAPPS III we processed and audited data for taxonomic consistency and swimbladder type, integrated trawl paths with active acoustic data, and used the catch information to inform prey distribution and composition for deep-diving whales, such as sperm whales (Section 6.6).

We audited midwater trawl catch data from AMAPPS surveys in 2014, 2015, and 2016, and ITS.DEEP cruises in 2018, 2019, and 2022. Also, we examined for taxonomic consistency and swimbladder presence/absence and type (physostomous, physoclistous, or lipid-filled). We obtained swimbladder types via a literature search completed by M. Jech and the NOAA Central Library (Shinn 2021). We processed trawl catches in 2018 and 2019 on board. Then Joel Llopiz and colleagues at the Woods Hole Oceanographic Institution (WHOI) flash froze the samples. Subsequently, we analyzed these specimens for diet, age, maturity, sex, and taxonomic identification using genetic methods. We also compared the genetic identifications among all cruises to generate a consistent taxonomic list of midwater trawl catches.

We merged trawl catch and active acoustic data (e.g., **Figure 9-2**) to develop and improve classification of the acoustic data to taxonomic levels that are biologically and ecologically meaningful. For example, we would like to estimate densities and biomass of the prey that top predators, such as cetaceans, tuna, and sharks are feeding on. Section 6.6 provides details of a specific investigation into sperm whale foraging. We used the extracted multifrequency volume backscatter (Sv dB re m^2 m^{-3}) data to develop classification algorithms using conventional methods (e.g., "dB differencing" or comparison of frequency responses) or more advanced analytical methods such as machine learning techniques. As an example, we coded the frequency response of the Sv data extracted from the trawl haul and investigated cetacean foraging.

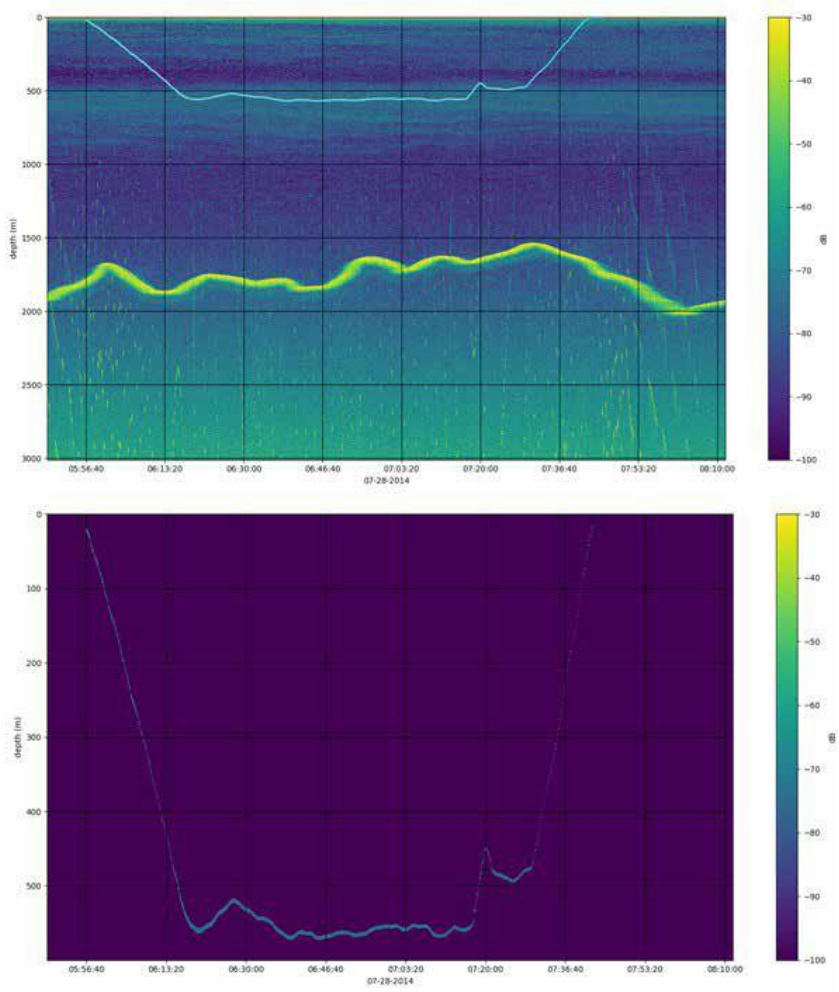

Figure 9-2. Echogram of 38-kHz Volume backscatter data (Sv) data
Data collected on 28 July 2014 from 0548 to 0805 GMT on the HB201403 cruise (upper panel). The midwater trawl haul profile is denoted by the cyan lines. The lower panel shows the Sv data that correspond to the midwater trawl haul.

Samples collected from AMAPPS shipboard cruises, among other cruises, contributed to the finding in Govindaragan et al. (2023) who compare results from eDNA analysis with traditional net sampling, and that found eDNA and net samples often resulted in different species identifications, where eDNA samples often detected more species than traditional net methods.

Assessing mesopelagic fish diversity and diel vertical migration with environmental DNA by Govindarajan et al. 2023. https://doi.org/10.3389/fmars.2023.1219993

> *ABSTRACT: "Mesopelagic fishes are an important component of the world's oceans in terms of their abundance, biomass, and ecosystem function. These fishes are important contributors to the biological carbon pump via their feeding and behaviors, whereby they facilitate the transfer of carbon from shallow waters to the deep sea. Several species undertake diel vertical migration, feeding in shallower waters at night and moving to deeper waters during the day. This process actively expedites the downward flux of carbon. However, carbon budgets and climate models require accurate information regarding the depth distributions and migration patterns of these fishes, and environmental DNA (eDNA)*

analyses can provide this information. Here, we utilize eDNA approaches, generating taxonomically-informative COI and 12S reference barcodes for 80 species of mesopelagic fishes, which can be used for species-level identification of eDNA sequences. Using these, along with a publicly available barcodes database, we compare results from eDNA analysis with traditional net sampling, and explore the ability of eDNA techniques to detect diel vertical migration in fishes from samples collected in Northwest Atlantic Slope Water. We found that eDNA and net samples often resulted in different species identifications, demonstrating that eDNA can detect species that would otherwise be missed with traditional methods. In our eDNA samples, we also detected more species (12) in our shallowest depth category (0 - 100 m) from night samples than from day samples (3). This is consistent with increased diversity in shallow waters at night due to diel vertical migration. Based on the variability observed in sample duplicates, we suggest that future mesopelagic eDNA studies incorporate larger sample volumes and scaled-up sampling efforts. We also note the potential applications of eDNA analysis in addressing ecological questions related to predator-prey relationships, identification of foraging hotspots, and carbon flow through the ocean's midwaters."

9.4 References Cited

Díaz-Arce N, Gagnaire P-A, Richardson DE, Walter III JF, Arnaud-Haond S, Fromentin J-M, Brophy D, Lutcavage M, Addis P, Alemany F, et al. 2024. Unidirectional trans-Atlantic gene flow and a mixed spawning area shape the genetic connectivity of Atlantic bluefin tuna. Mol Ecol. 33(1):e17188. https://doi.org/10.1111/mec.17188

Govindarajan AF, Llopiz JK, Caiger PE, Jech JM, Lavery AC, McMonagle H, Wiebe PH, Zhang W (Gordon). 2023. Assessing mesopelagic fish diversity and diel vertical migration with environmental DNA. Front Mar Sci. 10. https://doi.org/10.3389/fmars.2023.1219993

Hernández CM, Richardson DE, Rypina II, Chen K, Marancik KE, Shulzitski K, Llopiz JK. 2022. Support for the Slope Sea as a major spawning ground for Atlantic bluefin tuna: evidence from larval abundance, growth rates, and particle-tracking simulations. Can J Fish Aquat Sci. 79(5):814–824. https://doi.org/10.1139/cjfas-2020-0444

Palka D, Aichinger Dias L, Broughton E, Chavez-Rosales S, Cholewiak D, Davis G, DeAngelis A, Garrison L, Haas H, Hatch J, et al. 2021. Atlantic Marine Assessment Program for Protected Species: FY15-FY19. OCS Study BOEM 2021-051. https://repository.library.noaa.gov/view/noaa/47287

Richardson DE, Marancik KE, Guyon JR, Lutcavage ME, Galuardi B, Lam CH, Walsh HJ, Wildes S, Yates DA, and Hare JA. 2016a. Discovery of a spawning ground reveals diverse migration strategies in Atlantic bluefin tuna (*Thunnus thynnus*). Proc. Natl. Acad. Sci. U.S.A. 113(12):3299- 3304.

Richardson DE, Marancik KE, Guyon JR, Lutcavage ME, Galuardi B, Lam CH, Walsh HJ, Wildes S, Yates DA, Hare JA. 2016b. Reply to Safina and Walter et al.: Multiple lines of evidence for size-structured spawning migrations in western Atlantic bluefin tuna. Proc. Natl. Acad. Sci. U.S.A. 113 (30):E4262-4263.

Shinn H. 2021. Swimbladders in Mesopelagic Fishes: Bibliography. NCRL subject guide 2021-06. https://repository.library.noaa.gov/pdfjs/web/viewer.html?file=/view/noaa/30728/noaa_30728_DS1.pdf

10 Databases and Data Sharing

The Atlantic Marine Assessment Program for Protected Species (AMAPPS) I-III was a multi-year, collaborative effort by several agencies conducted from 2010 to 2025. This initiative successfully collected extensive data in pursuit of its seven objectives, which are detailed further in Chapter 2. This current chapter is dedicated to the datasets specifically gathered by the Northeast Fisheries Science Center (NEFSC) and Southeast Fisheries Science Center (SEFSC) during the AMAPPS I-III period (2010 – 2025).

The data collected under AMAPPS (**Table 10-1**) included:

- **Visual Sightings Data:** Shipboard and aerial observations of marine mammals, sea turtles, and seabirds.
- **Telemetry Data:** Information from animal-borne tags placed on sea turtles.
- **Passive Acoustic Detections:** Recordings of cetaceans and fish species.
- **Environmental Data:** Information from satellites, ocean models, and physical oceanographic data collected from animal-borne tags on turtles, shipboard computers, and CTD sampling devices.
- **Biological Data:** Samples obtained from shipboard sampling devices, eDNA, biopsy samples, and biological samples from tagged turtles.

Shipboard abundance surveys were instrumental in collecting multiple data types simultaneously, enabling continuous collection of oceanographic and acoustic data that complemented visual observations. Similarly, cruises dedicated to tagging turtles provided a variety of data, including biological and life history characteristics—ranging from morphometric measurements to blood biochemistry—which enhanced the tag data on location, time-at-depth, and sometimes water temperature.

You can find additional details on each survey in individual cruise reports found in the AMAPPS annual reports.

Table 10-1. Overall summary of data collection during AMAPPS I, II and III

Trip Identifier/Project[1]	Year	Description	Agency and Partners[2]	Visual MM Observation	Visual Seabird Observation	Passive Acoustics Towed Array	Archival PA Recorder Deployment	Sonobuoy Deployment	EK-60	Bongos	CTD/XBT	Trawl	VPR	Tag Deployment	Blood/Tissue Sampling	Photo-Id	UAS deployment	eDNA collection
TONE10SUM	2010	summer aerial survey	NEFSC	X														
TOSE10SUM	2010	summer aerial survey	SEFSC	X														
SEFSC Turtle Tagging	2010	loggerhead capture and tagging	SEFSC											X	X			
NEFSC Turtle Tagging	2010	loggerhead capture and tagging	NEFSC, CFF											X	X			
TONE11SUM	2011	summer aerial survey	NEFSC	X										X	X			
TONE11WIN	2011	winter aerial survey	NEFSC	X														
TOSE11SUM	2011	summer aerial survey	SEFSC	X														
TOSE11WIN	2011	winter aerial survey	SEFSC	X														
HB1103	2011	shipboard abundance survey	NEFSC	X	X	X			X	X	X		X					
GU1102	2011	shipboard abundance survey	SEFSC	X	X	X			X		X				X			
NEFSC Turtle Tagging	2011	loggerhead capture and tagging	NEFSC, CFF											X	X			
Canadian Loggerhead Tagging	2011	Canadian Grand Banks loggerhead tagging	NEFSC, DFO											X				
Harbor Seal Survey	2011	pupping season aerial	NEFSC	X										X	X			

Trip Identifier/Project[1]	Year	Description	Agency and Partners[2]	Visual MM Observation	Visual Seabird Observation	Passive Acoustics Towed Array	Archival PA Recorder Deployment	Sonobuoy Deployment	EK-60	Bongos	CTD/XBT	Trawl	VPR	Tag Deployment	Blood/Tissue Sampling	Photo-Id	UAS deployment	eDNA collection
		survey of Maine coast																
TONE12FAL	2012	fall aerial survey	NEFSC	X														
TONE12SPR	2012	spring aerial survey	NEFSC	X														
Harbor Seal Survey	2012	pupping season aerial survey of Maine coast	NEFSC	X										X	X			
TOSE12FAL	2012	fall aerial survey	SEFSC	X														
TOSE12SPR	2012	spring aerial survey	SEFSC	X														
TOSE13WIN	2013	winter aerial survey	SEFSC	X														
HB1303	2013	shipboard abundance survey	NEFSC	X					X	X	X		X					
GU1304	2013	shipboard abundance survey	SEFSC	X	X	X			X		X				X			
Gray Seal Captures	2013	adult gray seal captures	NEFSC, IFAW, WHOI, Duke, DFO											X	X			
NEFSC Turtle Tagging	2013	loggerhead capture and tagging	NEFSC, CFF					X						X	X			
HB1403	2014	shipboard habitat survey	NEFSC	X	X	X	X		X	X	X	X	X					
TOSE14SPR	2014	spring aerial survey	SEFSC	X														

Trip Identifier/Project[1]	Year	Description	Agency and Partners[2]	Visual MM Observation	Visual Seabird Observation	Passive Acoustics Towed Array	Archival PA Recorder Deployment	Sonobuoy Deployment	EK-60	Bongos	CTD/XBT	Trawl	VPR	Tag Deployment	Blood/Tissue Sampling	Photo-Id	UAS deployment	eDNA collection
TONE14SPR	2014	spring aerial survey	NEFSC	X														
TONE14WIN	2014	winter aerial survey	NEFSC	X														
HB1503-1	2015	sei whale survey	NEFSC	X	X	X		X	X		X	X				X		
HB1503-2	2015	turtle tagging	NEFSC	X					X	X	X		X	X	X		X	
Gray seal pup captures	2015	gray seal pup capture	NEFSC, MIT, etc.											X	X			
TOSE15WIN	2015	winter aerial survey	SEFSC	X														
TONE16FAL	2016	fall aerial survey	NEFSC	X														
TOSE16FAL	2016	fall aerial survey	SEFSC	X														
TOSE16SUM	2016	summer aerial survey	SEFSC	X														
TONE16SUM	2016	summer aerial survey	NEFSC	X														
HB1603	2016	shipboard abundance survey	NEFSC	X	X				X	X	X	X	X					
GU1605	2016	shipboard abundance survey	SEFSC	X		X		X	X		X				X			
TONE17SPR	2017	spring aerial survey	NEFSC	X														
TONE17WIN	2017	winter aerial survey	NEFSC	X														
TOSE17FAL	2017	fall aerial survey	SEFSC	X														
TOSE17SPR	2017	spring aerial survey	SEFSC	X														

Trip Identifier/Project[1]	Year	Description	Agency and Partners[2]	Visual MM Observation	Visual Seabird Observation	Passive Acoustics Towed Array	Archival PA Recorder Deployment	Sonobuoy Deployment	EK-60	Bongos	CTD/XBT	Trawl	VPR	Tag Deployment	Blood/Tissue Sampling	Photo-Id	UAS deployment	eDNA collection
EN2017	2017	marine mammal distribution	NEFSC	X					X		X							
GU1701	2017	Ecosystem monitoring	NEFSC	X	X				X	X	X							
GU1702	2017	Ecosystem monitoring	NEFSC	X	X				X	X	X							
GU1706	2017	Ecosystem monitoring	NEFSC	X	X				X	X	X							
HB1704	2017	cetacean and turtle survey	NEFSC	X			X		X	X	X		X	X	X			
HRS1701	2017	beaked whale survey	NEFSC	X	X	X												X
EN1801	2018	marine mammal distribution	NEFSC	X						X	X		X					
GU1803	2018	shipboard shelfbreak ecology	NEFSC	X						X	X							X
GU1804	2018	Ecosystem monitoring	NEFSC	X	X				X	X	X							
HB1803	2018	Ecosystem monitoring	NEFSC	X	X				X	X	X							
GU1902	2019	Ecosystem monitoring	NEFSC	X	X				X	X	X							
GU1905	2019	Ecosystem monitoring	NEFSC	X	X				X	X	X							
HB1902	2019	Ecosystem monitoring	NEFSC	X	X				X	X	X							
TONE19SPR	2019	spring aerial survey	NEFSC	X														
TOSE19SPR	2019	spring aerial survey	SEFSC	X														

Trip Identifier/Project[1]	Year	Description	Agency and Partners[2]	Visual MM Observation	Visual Seabird Observation	Passive Acoustics Towed Array	Archival PA Recorder Deployment	Sonobuoy Deployment	EK-60	Bongos	CTD/XBT	Trawl	VPR	Tag Deployment	Blood/Tissue Sampling	Photo-Id	UAS deployment	eDNA collection
EN2019	2019	marine mammal distribution	NEFSC	X					X	X	X	X	X					
HRS1910	2019	beaked whale survey	NEFSC	X														X
RB1904	2019	Ecosystem monitoring	NEFSC	X	X				X	X	X							
TN0368	2019	Ecosystem monitoring	NEFSC	X	X				X	X	X							
TONE19FAL	2019	fall aerial survey	NEFSC	X														
TOSE19WIN	2019/ 2020	winter aerial survey	SEFSC	X														
HB2005	2020	ecosystem monitoring	NEFSC	X														
GU2102	2021	Ecosystem monitoring	NEFSC	X	X				X	X	X							
GU2103	2021	shipboard abundance survey	SEFSC	X							X							
HB2102	2021	shipboard abundance survey	NEFSC	X	X	X			X	X	X		X			X		
PC2104	2021	Ecosystem monitoring	NEFSC	X	X				X	X	X							
PC2106	2021	Ecosystem monitoring	NEFSC	X	X				X	X	X							
TONE21SPR	2021	spring aerial survey	NEFSC	X														
TONE21SUM	2021	summer aerial survey	NEFSC	X														
TOSE21SUM	2021	summer aerial survey	SEFSC	X														

Trip Identifier/Project[1]	Year	Description	Agency and Partners[2]	Visual MM Observation	Visual Seabird Observation	Passive Acoustics Towed Array	Archival PA Recorder Deployment	Sonobuoy Deployment	EK-60	Bongos	CTD/XBT	Trawl	VPR	Tag Deployment	Blood/Tissue Sampling	Photo-Id	UAS deployment	eDNA collection
RB2203	2022	Ecosystem monitoring	NEFSC	X	X				X	X	X							
HB2204	2022	Ecosystem monitoring	NEFSC	X	X				X	X	X							
PC2205	2022	Ecosystem monitoring	NEFSC	X	X				X	X	X							
GU2301	2023	shipboard abundance survey	SEFSC	X	X				X	X	X							
HB2302	2023	Ecosystem monitoring	NEFSC	X	X				X	X	X							
HB2303	2023	Ecosystem monitoring	NEFSC	X	X				X	X	X							
PC2305	2023	Ecosystem monitoring	NEFSC	X	X				X	X	X							
TOSE23SPR	2023	spring aerial survey	SEFSC	X														
TONE23SPR	2023	spring aerial survey	NEFSC	X														
GM2401-1	2024	Ecosystem monitoring	NEFSC	X	X				X	X	X							
GM2401-2	2024	Ecosystem monitoring	NEFSC	X	X				X	X	X							
GM2402	2024	Ecosystem monitoring	NEFSC	X	X				X	X	X							
HB2403	2024	Ecosystem monitoring	NEFSC	X	X				X	X	X							
HB2406	2024	Ecosystem monitoring	NEFSC	X	X				X	X	X							
PC2406	2024	Ecosystem monitoring	NEFSC	X	X	X			X	X	X							
PC2501	2025	shipboard abundance survey	NEFSC	X	X	X			X	X	X					X		

Trip Identifier/Project[1]	Year	Description	Agency and Partners[2]	Visual MM Observation	Visual Seabird Observation	Passive Acoustics Towed Array	Archival PA Recorder Deployment	Sonobuoy Deployment	EK-60	Bongos	CTD/XBT	Trawl	VPR	Tag Deployment	Blood/Tissue Sampling	Photo-Id	UAS deployment	eDNA collection
HB2502	2025	Beaked whale	NEFSC	X	X	X			X	X	X	X					X	X
HB2503	2025	Ecosystem monitoring	NEFSC	X	X				X	X	X							

[1]First 2 letters of trip identifier indicated the ship or plane. EN = R/V Endeavor; HB = NOAA ship *Henry B. Bigelow*; GU = NOAA ship *Gordon Gunter*; HRS = R/V *Hugh R. Sharp; PC*=R/V *Pisces, GM=R/V Gloria Michelle*; TO = NOAA's Twin Otter aircraft. For the aerial surveys, the 3rd and 4th digits indicate the lead center: NE = Northeast Fisheries Science Center; SE = Southeast Fisheries Science Center; the 5th and 6th digits indicates the year; and the last 3 digits indicate the season the survey was conducted in: FAL = fall; SPR = spring; SUM = summer; WIN = winter. For the shipboard surveys, the 2nd and 3rd digits indicate the year, and the last 2 digits indicate the cruise number within the year, except for the Endeavor cruises which have the last 4 digits as the year.

[2] CFF = Coonamessett Farm Foundation; DFO = Department of Fisheries and Oceans Canada; Duke = Duke University, NC; IFAW = International Fund for Animal Welfare; MIT = Massachusetts Institute of Technology; NEFSC = Northeast Fisheries Science Center; SEFSC = Southeast Fisheries Science Center; WHOI = Woods Hole Oceanographic Institution.

10.1 Visual Data (Seabirds, Marine Mammals and Sea Turtles)

Primary authors: Elizabeth Josephson, Laura Aichinger Dias and Debra Palka.

10.1.1 Provenance

The NEFSC and the SEFSC conducted shipboard and aerial surveys following standard line-transect survey methods (Hiby and Hammond 1989; Buckland et al. 2004). Surveys used the "independent observer" data collection approach with distance sampling analysis methods to estimate detection probabilities for observed marine mammal groups (Laake and Borchers 2004; Garrison et al. 2011). During the shipboard abundance surveys (**Table 10-1**), two teams, each with two marine mammal observers using "big-eye" binoculars (25 × 150) positioned on port and starboard sides of the flying bridge and bridge deck, worked isolated from each other to avoid cueing the other team to the presence of marine mammals. Data recorders maintained independent communication with both teams and recorded data on sightings by each team. In addition, usually there was also a seabird observer independently focusing on detecting and recording birds while conducting a strip transect survey. Seabird observations operated simultaneously with the marine mammal teams throughout most of the shipboard surveys. Data recorders entered data on a custom-developed program, such as VisSurv and SeaScribe. Specific data fields collected by the NEFSC and the SEFSC differed slightly but for most sightings they included group size, bearing and distance to the sighting, presence of calves, behavior, and the factor that cued the observer to the sighting (blow, splash, etc.). We automatically recorded time and position when the sighting was entered or new effort information was entered. Observers scored environmental conditions such as Beaufort sea state, cloud cover, swell height and direction, visibility, and precipitation at a minimum of every 30 mins or when conditions changed. Observers changed positions every 30 mins.

During the ecosystem monitoring surveys (**Table 10-1**), there was only a single team focusing on seabirds, marine mammals, and sea turtles conducting a strip transect survey while recording the data in a program like SeaScribe.

Similarly, during aerial surveys two independent teams with two observers and one data recorded each, in addition to two pilots, conducted the aerial surveys. All surveys used a DeHavilland Twin Otter DHC-6 flying at 183 m (600 ft) above the water surface at about 200 km/h (100 kts). The forward team consisted of two observers stationed in bubble windows on each side (left and right) of the plane and one data recorder. The back team (aft) consisted of two observers, one stationed in a rear right side bubble window and one in a belly window (looking straight down), along with one recorder. The NEFSC collected data using the data entry program VOR and the SEFSC used an aerial survey version of VisSurv (as described for the ship surveys).

Observer teams on both ships and planes were "on-effort" when actively scanning the water for cetaceans, sea birds or sea turtles and the ship was steadily cruising on a trackline or the plane flying at survey altitude and speed. We classified sightings seen by off-duty observers, other crewmembers or during other operations as "off-effort". We conducted the aerial surveys over the continental shelf and shelfbreak out to about the 200 or 2000 m depth contour, depending on the location. Shipboard surveys were generally in the deeper offshore waters, deeper than 100 m (**Figure 10-1**). We surveyed about 290,000 km of track lines in the shipboard and aerial surveys (**Table 10-2**).

For detailed descriptions of survey methods for each cruise, please refer to cruise reports in the AMAPPS annual reports and Chapters 4 to 9 in this document.

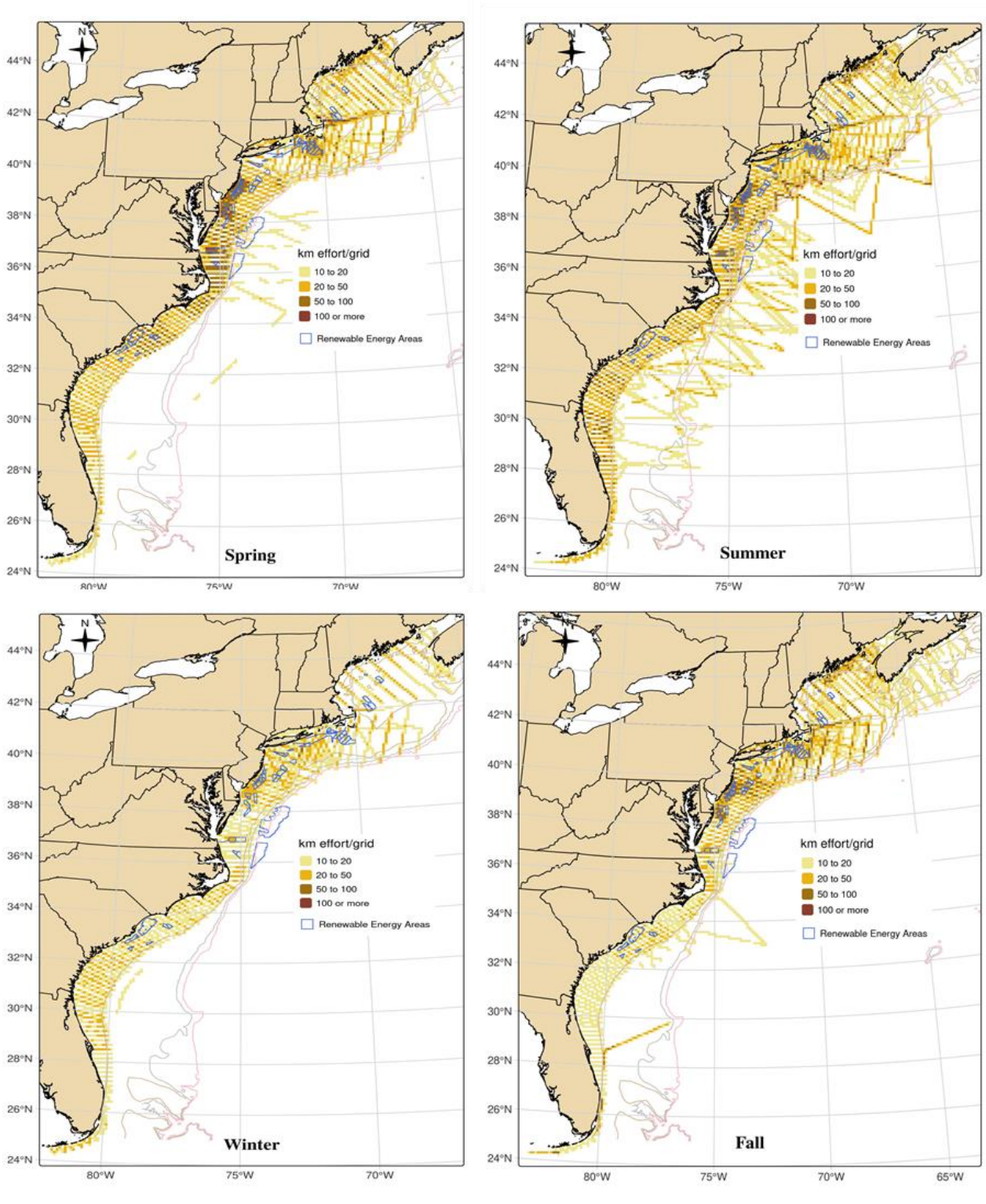

Figure 10-1. Visual effort by grid cell and season for all AMAPPS I, II and III surveys
Spring is March to May; summer is June to August; fall is September to November; and winter is December to February. Grid cells are 10 km x 10 km.

Table 10-2. Aerial and shipboard survey effort by season, 2010 to 2023

Season	Aerial On-effort Track line Length (km)	Shipboard On-effort Track line Length (km)
Spring (March - May)	70,528	8,485
Summer (June - August)	71,449	41,276
Fall (September - November)	58,076	2,629
Winter (December - February)	35,850	590
TOTAL	235,903	52,980

10.1.1.1 NEFSC Shipboard Surveys

During 2010 to 2025, the NEFSC completed over 50 shipboard surveys that collected line-transect sightings data under the AMAPPS programs (**Table 10-3**). These included six dedicated abundance surveys with two-independent team data collection. The remaining surveys included some with specific taxa focus or other types of surveys during which a visual observer collected data opportunistically. Note, the Navy AMAPPS IV funded the 2025 shipboard abundance survey, while AMAPPS III funded the rest of the 2025 shipboard surveys.

Table 10-3. Summary of NEFSC shipboard surveys conducted during 2010 to 2025

Trip Identifier	Year	Purpose	Start Date	End Date	Days with Sighting Effort	Number of Visual Teams	Visual Survey On-Effort (km)	Mammal Sighting Records[1]	Turtle Sighting Records[1]	Bird Sighting Records
HB1103	2011	abundance survey	2-Jun	1-Aug	40	2	4,973	2,543	25	1,135
HB1303	2013	abundance survey	2-Jul	18-Aug	38	2	5,021	2,119	74	2,207
GU1402	2014	abundance survey	12-Mar	27-Apr	33	2	4,014	998	3	2,493
HB1403	2014	beaked whale survey	25-Jul	30-Jul	5	2	740	221	2	336
HB1502	2015	ecosystem monitoring	20-May	2-Jun	14	1	NA[2]	155	4	0
HB1503-1	2015	sei whale survey	10-Jun	19-Jun	8	2	1,228	704	2	937
HB1503-2	2015	turtle tagging	24-Jun	1-Jul	6	1	NA[2]	86	13	0
HB1603	2016	abundance survey	28-Jun	24-Aug	45	2	5,203	5,097	58	2,031
EN2017	2017	marine mammal distribution	14-Apr	19-Apr	6	1	58	61	0	0
GU1701	2017	ecosystem monitoring	16-May	6-Jun	18	1	2,923	91	22	1,773
GU1702	2017	ecosystem monitoring	10-Jun	22-Jun	13	1	1,856	37	2	1,177
GU1706	2017	ecosystem monitoring	31-Oct	9-Nov	10	1	1,083	21	1	861
HB1704	2017	cetacean and turtle survey	7-Jul	18-Jul	12	1	NA[2]	168	10	0
HRS1701	2017	beaked whale survey	8-Sep	17-Sep	10	1	NA[2]	244	0	255
EN2018	2018	marine mammal distribution	3-Apr	8-Apr	4	1	NA[2]	3	0	0

Trip Identifier	Year	Purpose	Start Date	End Date	Days with Sighting Effort	Number of Visual Teams	Visual Survey On-Effort (km)	Mammal Sighting Records[1]	Turtle Sighting Records[1]	Bird Sighting Records
HS1801	2018	ecosystem monitoring	1-Nov	12-Nov	10	1	1,099	16	3	1,282
HB1803	2018	ecosystem monitoring	23-May	4-Jun	13	1	2,214	54	1	1,516
GU18TN	2018	NOAA ship transit	11-Jul	16-Jul	6	1	1,213	10	2	371
GU1803	2018	beaked whale survey	21-Jul	1-Aug	13	1	NA[2]	758	0	522
HB18TN	2018	NOAA ship transit	1-Aug	6-Aug	6	1	1,213	51	0	485
GU1804	2018	ecosystem monitoring	22-Aug	30-Aug	9	1	1,537	28	18	636
GU18TS	2018	NOAA ship transit	2-Sep	9-Sep	8	1	1,216	21	10	327
EN2019	2019	marine mammal distribution	18-Apr	23-Apr	5	1	NA[2]	3	0	0
HB1902	2019	ecosystem monitoring	24-May	5-Jun	13	1	2,614	144	4	1,510
GU1902	2019	ecosystem monitoring	15-Aug	29-Aug	14	1	2,334	50	7	1,364
GU1905	2019	ecosystem monitoring	15-Oct	30-Oct	14	1	1,675	40	11	1,100
HRS1910	2019	beaked whale survey	18-Aug	27-Aug	8	1	580	8	1	441
RB1904	2019	ecosystem monitoring	13-May	24-May	11	1	2,422	20	0	202
TN368	2019	ecosystem monitoring	6-Jul	17-Jul	12	1	814	3	0	155
GU2103	2021	ecosystem monitoring	14-May	26-May	12	1	1,350	3	10	1,331
HB2102	2021	abundance survey	17-Jun	20-Aug	42	2	5,870	1,246	39	2,068
PC2104	2021	ecosystem monitoring	6-Aug	18-Aug	13	1	697	63	0	1,116
PC2106	2021	ecosystem monitoring	16-Oct	25-Oct	10	1	774	33	3	554
HB2204	2022	ecosystem monitoring	1-Jun	16-Jun	15	1	2,377	117	6	1,475
ECOA2022	2022	ecosystem monitoring	6-Aug	22-Sep	39	1	3,699	85	2	846
PC2205	2022	ecosystem monitoring	1-Nov	9-Nov	9	1	1,353	57	0	950
HB2302	2023	ecosystem monitoring	9-Jun	27-Jun	19	1	3,599	171	10	1,987
HB2303	2023	ecosystem monitoring	8-Aug	24-Aug	17	1	2,009	52	10	529

Trip Identifier	Year	Purpose	Start Date	End Date	Days with Sighting Effort	Number of Visual Teams	Visual Survey On-Effort (km)	Mammal Sighting Records[1]	Turtle Sighting Records[1]	Bird Sighting Records
PC2305	2023	ecosystem monitoring	27-Oct	13-Nov	17	1	1,782	74	0	939
GM2301	2023	ecosystem monitoring	29-Nov	29-Nov	1	1	6	0	0	4
GM2401-1	2024	ecosystem monitoring	9-Jan	9-Jan	1	1	38	5	0	25
GM2401-2	2024	ecosystem monitoring	13-Mar	14-Mar	2	1	98	5	0	86
GM2402	2024	ecosystem monitoring	16-Apr	18-Apr	3	1	185	5	0	122
HB2403	2024	ecosystem monitoring	26-May	13-Jun	14	1	2,692	142	7	1,142
HB2406	2024	ecosystem monitoring	12-Aug	22-Aug	11	1	1,983	94	0	808
PC2406	2024	ecosystem monitoring	27-Oct	12-Nov	11	1	1,201	34	2	798
PC2501	2025	abundance survey	6-Jan	15-Feb	27	1	3,513	22	0	1,653
HB2503	2025	ecosystem monitoring	27-May	5-Jun	10	1	1,272	65	0	506
HB2504	2025	beaked whale survey	4-Jul	17-Jul	13	1	1,326	13	0	346
PC2502	2025	ecosystem monitoring	16-Jul	22-Jul	7	1	734	13	0	114
PC2503	2025	ecosystem monitoring	1-Aug	14-Aug	14	1	1,905	145	3	1,687
Subtotal – AMAPPS I	2010 – 2014				116		14,748	5,881	104	6,171
Subtotal – AMAPPS II	2015 – 2019				284		31,282	7,870	169	169,945
Subtotal – AMAPPS III	2020-2025				307	23	38,463	2,444	92	19,086
GRAND TOTAL	2010 – 2025				707	23	84,493	16,195	365	195,202

[1] Mammal and turtle sighting counts include duplicates and resightings.
[2] Not applicable (NA) because these cruises did not conduct standardized line transect searching protocols since the goals of these surveys required *ad hoc* searching procedures.

10.1.1.2 NEFSC Aerial Surveys

NEFSC completed 16 aerial surveys under the AMAPPS program during 2010 to 2025 (**Table 10-4**). We completed spring surveys in 2012, 2014, 2017, 2019, and 2023, summer surveys in 2010, 2011, and 2016 and 2021, fall surveys in 2012, 2016, and 2019, and winter surveys in 2011, 2014, 2017, and 2025. The 2010 and 2011 NEFSC summer aerial surveys used the single team "circle-back" data collection and analysis methods to estimate perception bias and the probability of detecting a group on the track line (Hiby and Lovell 1989; Hiby 1999). All other surveys used the two-independent team procedures.

During AMAPPS III, on 43 survey days, we flew over 24,000 km of on-effort track lines and detected 1,985 marine mammal and 414 sea turtle unique sightings seen by one or both teams during on- and off-effort times (**Table 10-4**). Note, the Navy AMAPPS IV funded the 2025 aerial survey.

Table 10-4. Summary of NEFSC aerial abundance surveys during 2010 to 2025
All flights conducted on the NOAA Twin Otters (TO). Spring is March to May; summer is June to August; fall is September to November; and winter is December to February.

Trip Identifier	Year	Description	Start Date	End Date	Days with Sighting Effort	Visual Survey On-Effort (km)	Mammal Sighting Records*	Turtle Sighting Records*
TONE10SUM	2010	summer	17-Aug	26-Sep	16	9,206	449	87
TONE11SUM	2011	summer	8-Aug	26-Aug	11	6,481	386	85
TONE11WIN	2011	winter	28-Jan	15-Mar	8	4,550	303	2
TONE12FAL	2012	fall	17-Oct	19-Nov	11	7,134	354	62
TONE12SPR	2012	spring	28-Mar	3-May	10	6,793	500	0
TONE14SPR	2014	spring	22-Feb	25-Mar	12	4,904	182	0
TONE14WIN	2014	winter	5-Dec	14-Jan	14	5,671	107	3
TONE16FAL	2016	fall	17-Oct	17-Nov	11	6,995	647	23
TONE16SUM	2016	summer	15-Aug	26-Sep	17	11,782	713	676
TONE17SPR	2017	spring	10-Jun	9-Jul	10	9,479	976	270
TONE17WIN	2017	winter	23-Nov	3-Jan	10	7,738	648	11
TONE19FAL	2019	fall	15-Oct	23-Nov	14	7,771	736	13
TONE19SPR	2019	spring	5-Apr	13-May	16	10,392	1,280	2
TONE21SUM	2021	summer	01-Aug	14-Sep	17	11,465	903	285
TONE23SPR	2023	spring	20-Apr	27-May	15	7,889	840	4
TONE25WIN	2025	winter	15-Jan	23-Feb	11	4,964	242	125
Subtotal – AMAPPS I	2010 – 2014				82	44,729	2,281	239
Subtotal – AMAPPS II	2015 – 2019				78	54,157	5,000	995
Subtotal- AMAPPS III	2020- 2025				43	24,318	1,985	414
GRAND TOTAL	2010 – 2025				203	123,204	9,266	1,648

* Mammal and turtle sighting counts include duplicates and resightings.

10.1.1.3 SEFSC Shipboard Surveys

During 2010 to 2024, the SEFSC completed five shipboard line-transect surveys under the AMAPPS program (**Table 10-5**). During all surveys, we used the two-independent team procedures, where observers focused primarily on recording marine mammals, which took precedence over turtles.

During AMAPPS III, the SEFSC conducted 80 on-effort days resulting in 10,987 km of on-effort track lines, 1,089 marine mammal, 11 sea turtle, and 3,166 bird unique sightings seen by one or both teams during on- and off-effort times.

Table 10-5. Summary of SEFSC shipboard abundance surveys during 2010 to 2024

Trip Identifier	Year	Purpose	Start Date	End Date	Days with Sighting Effort	Visual Survey On-Effort (km)	Mammal Sighting Records	Turtle Sighting Records	Bird Sighting Records
GU1102	2011	abundance survey	19-Jun	1-Aug	35	5,210	331	21	1,135
GU1304	2013	abundance survey	16-Jul	15-Sep	42	6,209	561	174	1,374
GU1605	2016	abundance survey	1-Jul	24-Aug	44	5,968	544	2	0[1]
GU2103	2021	abundance survey	13-Jun	04-Sep	37	5,926	643	4	2,744
GU2301	2023	abundance survey	04-Feb	27-Apr	43	5,061	445	7	422
Subtotal-AMAPPS I	2010 – 2014				77	11,419	892	195	2,509
Subtotal-AMAPPS II	2015 – 2019				44	5,968	544	2	0[1]
Subtotal-AMAPPS III	2020-2025				80	10,987	1,089	11	3,166
GRAND TOTAL	2010 – 2025				201	28,374	2,524	208	5,675

[1]no seabird survey conducted

10.1.1.4 SEFSC Aerial Surveys

During 2010 to 2025, the SEFSC completed 16 aerial line-transect surveys under AMAPPS, across all seasons (**Table 10-6**). During all surveys, we used the two-independent team procedures.

During AMAPPS III, the SEFSC conducted 37 on-effort days resulting in 15,516 km of on-effort track lines, 2,059 marine mammal and 1,379 sea turtle unique sightings seen by one or both teams during on- and off-effort times.

Table 10-6. Summary of SEFSC aerial abundance surveys during 2010 to 2024
All flights conducted on the NOAA Twin Otters (TO). Spring is March to May; summer is June to August; fall is September to November; and winter is December to February.

Trip Identifier	Year	Description	Start Date	End Date	Days with Sighting Effort	Visual Survey On-Effort (km)	Mammal Sighting Records	Turtle Sighting Records
TOSE10SUM	2010	summer	24-Jul	11-Aug	14	8,072	181	1,411
TOSE11SUM	2011	summer	6-Jul	29-Jul	15	8,765	199	1,426
TOSE11WIN	2011	winter	7-Feb	13-Mar	11	4,892	159	793
TOSE12FAL	2012	fall	11-Sep	20-Oct	22	11,818	241	1,722
TOSE12SPR	2012	spring	3-Apr	21-May	22	11,670	290	1,353
TOSE13WIN	2013	winter	15-Feb	23-Mar	16	7,402	197	139
TOSE14SPR	2014	spring	24-Mar	28-Apr	13	7,815	152	495
TOSE15WIN	2015	winter	23-Jan	3-Mar	13	6,314	133	573
TOSE16SUM	2016	summer	23-Nov	31-Dec	10	11,406	183	1,516
TOSE16FAL	2016	fall	3-Jul	9-Aug	21	5,893	114	87
TOSE17FAL	2017	fall	18-Oct	20-Nov	17	7,507	132	561
TOSE17SPR	2017	spring	17-Apr	20-May	17	9,703	241	839
TOSE19SPR	2019	spring	18-May	24-Jun	18	9,713	260	1,304
TOSE19WIN	2019/ 2020	winter	7-Dec	24-Jan	14	6,108	127	495
TOSE21SUM	2021	summer	17-Jun	31-Jul	22	9,003	210	1086
TOSE23SPR	2023	spring	01-Mar	14-Apr	15	6,513	196	561
Subtotal-AMAPPS I	2010 – 2014				113	60,434	1,419	7,339
Subtotal-AMAPPS II	2015 – 2019				110	56,644	1,190	5,375
Subtotal-AMAPPS II	2020-2025				37	15,516	2,059	1,379
GRAND TOTAL	2010 – 2025				260	132,594	4,668	14,093

10.1.2 Processing

10.1.2.1 Quality control checks

We subjected both shipboard and aerial data to rigorous quality control. First, the data entry program has initial data value checking, such as allowing the entry of only a pre-specified range of acceptable values for some variables or using drop down choices for other variables. Observers note mistakes in an Error Log. At the end of each field day, data managers made corrections based on the Error Log notes and checked the data to identify fields inadvertently left blank or out of range. We also checked to make sure the data were internally consistent. Examples include:

- at any time, each observer is only assigned to one position on one team and the location of sightings correctly reflect these positions;
- the total number of animals in the group should be greater than the number of calves recorded for that group;
- the on-effort segments, as defined by the times entered by the record, corresponded to straight and uninterrupted segments of track lines, as defined by the GPS file that independently recorded the time and location of the ship or plane, and this was consistent for both teams;
- all sightings not detected on an on-effort track line were categorized as off-effort sightings; and

- the species identification of a group detected by both teams is the same for both teams.

10.1.2.2 Duplicate Resolution

During the two-independent team sighting surveys, only one team detects some groups of animals, while both teams detect other groups of animals. We determined the animal groups that both teams detected (termed a duplicate sighting) by investigating the times and locations of the sightings. This determination was done in real-time and during the data quality checking stage.

Since the plane was traveling fast, the amount of time an animal group is available to either team was short. Consequently, most groups that we confidently defined as a duplicate (termed a "definite" duplicate) we recorded within a few seconds of each other (less than about 3 sec), on the same side of the plane, and at about the same angle of declination (less than 10° difference). We defined the angle of declination as the angle between the line straight down from the plane to the line between the plane and the geometric center of the group. However, due to measurement error in the angle or a slow response to record a group, we defined a "possible" duplicate as a group detected by both teams within 6 secs and within 20° of each other. In the case of larger groups (greater than 5 animals), it was feasible that observers took their angle of declination measurements at different locations within the spatial region covered by the group, thus we used the criteria of a possible duplicate for a definite duplicate of a large group. We took special care when determining duplicates for recorded groups close to the track line (within 5°). This is because it was feasible that an observer sitting on one side of the plane can see all or part of a group when viewing through the large bubble windows, where the geometric group was actually on the other side of the plane yet close to the track line or on both sides of the trackline.

We used the same concepts to identify duplicates from the shipboard data, but it was more complicated because the ship was traveling slowly (9-11 knots) and the window of opportunity to detect a group of animals using high-powered binoculars (25 x 150) is in the range of 10 to 15 min. In some cases, we identified duplicates in real-time while on the ship, where an independent person talked with both teams (while still maintaining no communication between the teams) assimilated all the information and made a decision on whether the group was a duplicate or not. In other cases, we identified duplicates after field data collection, by matching up the tracks of detected groups from both teams using the time, location, and swim direction recorded at the initial location and at subsequent "follow-up" locations of the same group that either or both teams recorded.

During SEFSC ship surveys, we identified duplicate groups in real-time by an independent data recorder communicated separately with observers in both teams and made a decision. We based the determination usually on the location of the sighting (usually detections less than one nmi from each other), animal behavior, and species or taxa group identification. We conducted these surveys in passing mode, i.e., the ship maintained its course and speed along the trackline and did not approach the group (closing mode). Each observer entered group sizes independently without group discussion. During aerial surveys, if only one team detected a marine mammal sighting, that team waited until the sighting was aft of the airplane to ask the pilots to depart from the trackline to circle the sightings to verify species and count group sizes. Therefore, for example, if only the forward team detected a sighting, the data recorder marked this group as detected by the forward team and "missed" by the aft team. The recorder entered a common and single group size for sightings seen by both teams. We treated sea turtle sightings differently. We recorded sea turtles independently by each team. We then identified duplicate sea turtle sightings after the survey during the data quality checking stage. We based the determination upon time (sightings less than 15 sec of each other), location (same side of the aircraft), position relative to the trackline (angles measured by both teams are ± 15° apart) and number of animals (must be equal).

During NEFSC ship surveys, we identified duplicate groups after the completed survey day. We developed an R script that plotted the locations of initial and subsequent "follow-up" recordings of a sighting as made by each team at the time of each detection and then also at the time progressed by matching up the predicted tracks of detected groups from both teams using the time, location, and swim direction recorded at the initial location and at subsequent "follow-up" locations of the same group.

10.1.2.3 Derived Fields

We stored several parameters important for data analysis within the Oracle datasets as derived fields. We calculated some derived fields by using stored Oracle functions and others we calculated externally before data upload. Examples of derived fields include the spatial point geometry field that we calculated from the latitude and longitude entries for each sighting and a spatial line geometry field we added after creating line segments (see below). We converted the shipboard binocular reticle values recorded by observers into linear distances based on the height of the ship's platform and type of binocular. We calculated perpendicular distances from the radial distance and bearing values entered by observers for shipboard sightings, and from the survey altitude and angle of declination of the aerial sightings. In addition, we created some derived fields to accommodate and standardize differences in data collection over the years and between regions.

10.1.2.4 Segmentation

We convert raw effort tables to summarized tables that compress data to short straight-line segments with a start and end position. If there was a speed or course change recorded, change in environmental conditions recorded by observers, rotation of observers, or any break in effort status, we created a new line segment. We considered as off-effort times when maneuvering between tracklines, transits to and from tracklines, circling over sightings during aerial surveys, and closing on sightings during ship surveys.

10.1.2.5 Oracle Upload

We developed R scripts to process and upload data to Oracle data tables housed on NEFSC servers.

10.1.2.6 Gridding

In preparation for their use in density-habitat models, we associated all sightings and visual survey effort data with a custom-developed 10 km x 10 km grid, in oblique Mercator projection, that encompassed the Atlantic study area. In addition, to facilitate matching to temporally explicit covariates such as satellite-derived ocean color products, we associated all sighting and visual effort data with an 8-day temporal segment.

10.1.2.7 Preparation for Distance Analysis

In preparation for use in analysis using the distance software package (Thomas et al. 2009), we processed the sightings and visual effort data to present the on-effort survey distance for each spatial stratum by 8-day segment. We aggregated the data such that each sighting had a record for each sighting team, with information on whether that team sighted or did not sight that animal group. All grids with effort were associated with environmental sighting conditions as recorded by observers, as well as static and non-static environmental covariates.

10.1.3 Presentation

10.1.3.1 Cruise Reports

Detailed cruise reports are included in AMAPPS annual reports. A full list of publications and presentations produced using these data during AMAPPS I is in Palka et al. (2017), those produced during AMAPPS II is in Palka et al. (2021) and those produced during AMAPPS III is listed in Table 3-2 in this document.

10.1.3.2 Submissions to Online Websites

As part of the Ocean Biodiversity Information System (OBIS), researchers from Duke University developed OBIS-SEAMAP (Ocean Biodiversity Information System - Spatial Ecological Analysis of Megavertebrate Populations). This interactive online archive provides spatially and temporally organized data on marine megafauna, including marine mammals and sea turtles. Contributors worldwide share their distributional data through this platform (Halpin et al. 2009).

We contributed data collected during AMAPPS shipboard and aerial surveys to OBIS-SEAMAP. These data primarily comprise of on-effort sightings of marine mammals and sea turtles, recorded by the flying bridge team during ship surveys, the forward team during aerial surveys, or by both teams combined during integrated ship and aerial surveys. The sighting data are accompanied by corresponding on-effort trackline information.

We submitted seabird data regularly to managers of the Atlantic Offshore Seabird Dataset Catalog. These data went into the Avian Knowledge Network and iPac tools and contributed to such publications as "Modeling at-sea density of marine birds to support Atlantic marine renewable energy planning" by Winship et al. (2018). We also archived the raw data with the National Centers for Environmental Information (NCEI; this dataset) and in the Global Biodiversity Information Facility.

At NCEI we also developed an AMAPPS Collection (NOAA et al. 2024) that is intended to host all vessel and aerial abundance survey datasets going back to 2010. Currently, the 2021 (GU2103) and 2023 (GU2301) Gunter cruises are available (Palka et al. 2024, Palka et al. 2025). We are preparing submissions of the Northeast Fisheries Science Centers vessel data and additional Southeast Fisheries Science Center data, which are not yet available publicly. Furthermore, environmental data associated with the AMAPPS surveys, such as scientific echosounder (EK - Water Column Sonar Data Viewer) and surface underway measurements like sea surface temperature and salinity, are also at NCEI (e.g.: EK and underway measurements for vessel survey GU2103).

We contributed the AMAPPS marine mammal, seabird and sea turtle data to develop a multi-dataset NOAA NCCOS model that is publicly available on the Northeast Regional Ocean Council and MARCO Mid-Atlantic Ocean data portals as maps.

We also archived and documented the NEFSC and SEFSC visual sighting data through the InPort metadata library. NEFSC has the AMAPPS survey data set available as one entry and SEFSC has an archive node for AMAPPS aerial surveys (SEFSC AMAPPS).

10.1.3.3 Other Reports and Publications

The sightings data and associated abundance estimates and density-habitat models are important components of marine mammal stock assessment reports. A full list of publications produced during AMAPPS I (FY10 - FY14) is in Palka et al. (2017), during AMAPPS II (FY15 - FY18) is in Palka et al. (2021), and those produced during AMAPPS III (FY19 - FY25) is in **Table 3-2** of this report.

10.1.3.4 Model Viewer

Outputs from density-habitat models generated from data collected under AMAPPS I and II are on the AMAPPS Marine Mammal Model Viewer website. Density-habitat models generated using data from AMAPPS I - III are presented in Chapter 4 and Appendices B-E in this document; in addition, they will be in a public gitHub site.

10.2 Environmental Covariate Data

Primary authors: Kimberly Hyde, Samuel Chavez-Rosales and Elizabeth Josephson

10.2.1 Provenance

We compiled different types of environmental covariate data to use as candidates in density surface models that modeled the relationships between a species density (and number of groups detected) and environmental habitat descriptors, as described in Section 4.2.2.

10.2.1.1 Static Covariates

Several static covariates were candidates for the density-habitat models, including depth, slope, distance from shore, and distance from various isobaths. We obtained bathymetric depth from the ETOPO 11 Arc-Minute Global Relief Model (Amante and Eakin 2009). We obtained the nearest distance from the coastline to the center point of each grid from the National Aeronautics and Space Administration (NASA) 0.04° OceanColorWeb dataset).

10.2.1.2 Satellite-derived Covariates

We acquired daily level 3 mapped (4 km resolution, sinusoidally projected) satellite ocean color data from the European Space Agency's Ocean Colour Climate Change Initiative (OC-CCI; version 6.0) (Sathyendranath et al., 2019, Sathyendranath et al, 2023) and GlobColour Project (Maritorena et al., 2010). Additional sea surface temperature (SST) data sources include the 4 km nighttime NOAA Advanced Very High Resolution Radiometer (AVHRR) Pathfinder (Casey et al. 2010; Saha et al. 2018) and the daily 1 km Group for High Resolution Sea Surface Temperature (GHRSST) Multiscale Ultrahigh Resolution (MUR, version 4.1) Level 4 (Chin, Vazquez-Cuervo, and Armstrong 2017; Project 2015) data. Earlier iterations of the AMAPPS model (Palka et al. 2017; 2021) included ocean color and SST data from the Moderate Resolution Imaging Spectroradiometer (MODIS) (NASA Ocean Biology Processing Group 2017) on the Aqua and Terra (SST only) satellites obtained from the NASA Ocean Biology Processing Group. We transitioned to the new ocean color and SST datasets in 2023 due to data degradation from the MODIS Aqua sensor.

10.2.1.3 Ocean Data Assimilation Covariates

Ocean data assimilation products that we used included bottom temperature, mixed layer depth, salinity, and sea surface height. These products were the result of integrated output from ocean modeling, *in situ* observations, and remotely sensed images of environmental variables.

One reason for using products from ocean data assimilations is that they overcome limitations of ocean models in terms of resolution and ability to accurately reflect phenomena of surface and subsurface flows (Chassignet et al. 2009). Ocean data assimilations incorporate modeling and data assimilation techniques to produce high resolution near real-time global ocean prediction systems. One such system is the U.S.

Navy nowcast/forecast system that uses the 1/12 HYbrid Coordinate Ocean Model (HYCOM) and the 3-dimensional multivariate optimum interpolation Navy Coupled Ocean Data Assimilation technique. Distributions of hindcasts from the global U.S. Navy HYCOM + Navy Coupled Ocean Data Assimilation prediction system are available through the HYCOM consortium at https://www.hycom.org/. To date, they provide 11 fields that include surface water flux, mixed layer depth, mixed layer thickness, surface heat flux, sea surface height, surface salinity trend, surface temperature trend, salinity, potential temperature, u-velocity, and v-velocity.

The HYCOM Consortium provided access to near real-time global ocean predictions based on the HYCOM and Navy Coupled Ocean Data Assimilation technique. Outputs from the near real-time global ocean prediction system were converted to a native Mercator-curvilinear HYCOM horizontal grid with a 1/12 equatorial resolution, which consisted of a Mercator projection from 78°S to 47°N and a bipolar patch north of 47°N. The HYCOM Data Service provided access to modeled outputs using NetCDF files through a subsetting service, allowing for a user-specified bounding box.

10.2.1.4 Distance from the Gulf Stream

We calculated the distances between the centers of the spatiotemporal strata to the north and south Gulf Stream wall locations on a corresponding date by using ArcGis. The Gulf Stream location data were available from the Naval Oceanographic Office's website. The location of the Gulf Stream is based on the maximum surface temperature change over 10 nm from detailed analyses of Infra-Red satellites, bathythermographs, and drifting buoy data. The reported positions are accurate to within 11 nm.

10.2.1.5 North Atlantic Oscillation Index

We did not use the North Atlantic Oscillation daily index as a potential covariate in the density-habitat models developed in Chapter 4 and Appendices B-D of this document, although it was considered for the AMAPPS II models. The NOAA Climate Prediction Center provided the North Atlantic Oscillation daily index, which reflected monthly North Atlantic Oscillation patterns. Each daily value was standardized by the standard deviation of the monthly North Atlantic Oscillation index from 1950 to 2020, interpolated to the specific day. The calculation of this daily teleconnection index followed the Rotated Principal Component Analysis method described by Barnston and Livezey (1987), which identified primary teleconnection patterns across all months and enabled the construction of a time series for these patterns.

10.2.2 Processing

10.2.2.1 Static Covariates

Static covariates used in this document are listed in **Table 4-2**. We computed slope from the depth raster using the R 'terrain' package. We then resampled the depth, slope, and distance from shore rasters using bilinear or nearest neighbor methods with the R function "spatial_sync_raster" from the spatial.tools R package to align to the extent, projection, and resolution of the AMAPPS study grid.

10.2.2.2 Satellite-derived Covariates

Satellite-derived covariates used in this document are listed in **Table 4-2**. The global OC-CCI, GlobColour, AVHRR (SST) and MUR (SST) data were mapped to the same sinusoidal map projection and subset to the U.S. east coast region (SW longitude=82.5° W, SW latitude=22.5° N, NE longitude=51.5° W, NE latitude=48.5° N). The L3 OC-CCI products merge data from multiple ocean color sensors (SeaWiFS, MODIS Aqua, MERIS, VIIRS, Sentinel 3A and 3B OLCI) and include chlorophyll a (CHL). The CHL blended algorithm weighs the outputs of the best-performing chlorophyll

algorithms based on the water types present, which improves performance in nearshore water compared to open-ocean algorithms. The L3 GlobColour products use data from the same ocean color sensors as the OC-CCI. GlobClolour data include photosynthetic available radiation (PAR), particulate inorganic carbon (PIC), and particulate organic carbon (POC) products.

We detected oceanic fronts for SST and the natural log of the chlorophyll *a* (due to the log-normal distribution of chlorophyll) using the Belkin and O'Reilly (2009) algorithm, and a contextual median filter to isolate noise while preserving edges in the daily Level 3 binned files. We computed the gradient vector using IDL's CONVOL function using two 3 x 3 convolution kernels. We used the width and height of each pixel to compute the gradient magnitude per km in the X (G_x) and Y (G_y) directions. We estimated net primary production as a function of chlorophyll *a*, photosynthetically available radiation and the photosynthetic efficiency by using a variation of the Vertically Generalized Production - Eppley Model (Behrenfeld and Falkowski 1997). In the Vertically Generalized Production - Eppley Model version, we replaced the original temperature-dependent function to estimate the chlorophyll-specific photosynthetic efficiency with the exponential "Eppley" function as modified by Morel (1991). For more details see NEFSC (2020). Prior to being input into the Vertically Generalized Production - Eppley Model, we temporally interpolated and smoothed the daily chlorophyll *a* data to increase the data coverage and better match data collected from different sensors and different times. Because cloud cover did not affect the daily photosynthetic available radiation data and the MUR SST data was a blended/gap free data product, we did not interpolate these products. Daily data at each pixel location are linearly interpolated based on days in the time series using interpx.pro. Prior to interpolation, the CHL data are log-transformed to account for the log-normal distribution of chlorophyll *a* data (Campbell, 1995). The time series are processed in one-year chunks, with each yearly series including 60 days from the previous year and 60 days from the following year to improve the interpolation at the beginning and end of the year. Following interpolation, the data are smoothed with a tri-cube filter (width=7) using IDL's CONVOL program. In order to avoid over interpolating data when there were several days of missing data in the time series, the interpolated data were removed and replaced with blank data if the window of interpolation spanned more than seven days.

For chlorophyll *a*, particulate inorganic carbon, particulate organic carbon, photosynthetic available radiation, and gradient magnitude, we calculated statistics, including the arithmetic mean, geometric mean, standard deviation, and coefficient of variation at daily (8-day running means) intervals.

If values of an environmental variable within the AMAPPS study area were missing, we used a hierarchical spatial-temporal interpolation approach to replace missing values. This approach first filled in a missing value using the calculated mean from the nearest-neighbor cells from the same time that contained the non-missing data. Then, if that was not sufficient, we calculated the missing value from the mean value of the spatial cell of interest for the 8-day time period before and after. This process provided enough information of the seasonal tendency, without compromising the overall quality of the data.

10.2.2.3 Ocean Data Assimilation Covariates

The AMAPPS prediction grid extends beyond 47°N and continues into the HYCOM bipolar patch. This made it difficult to synchronize HYCOM data to the AMAPPS projection north of 47°N, and as such, we used 47°N as an upper bound to retrieve HYCOM data. To date, no AMAPPS survey effort extended beyond 47°N, which suggests that this is a reasonable cutoff. We spatially synchronized HYCOM data to the AMAPPS prediction grid by using the following process:

1) We downloaded HYCOM data for each day from 2010 to 2023 using a bounding box defined by North = 47°N; South = 22°N; East = 320°E; and West = 277°E.
2) We spatially synchronized the HYCOM data to the AMAPPS grid by re-projecting into the AMAPPS projection, and then re-sampling to the AMAPPS resolution using bilinear interpolation.

3) We created 8-day composites from the synced HYCOM data.
4) We wrote rasters to CDF files.

The variables we downloaded included: ocean mixed layer depth (m), ocean mixed layer thickness, bottom temperature (°C) and surface salinity (psu).

The mixed layer depth is the depth (in m) at which the density changes from the surface by 0.03 kg/m^3. We defined the bottom temperature as the temperature (in °C) of the deepest HYCOM z-level.

The Mixed Layer Thickness is the depth where the density difference compared to a reference level is 0.01kg/m^3.

10.2.3 Presentation

We used these covariates as candidate predictor variables in the density surfacing models described in Chapter 4. Covariates in AMAPPS I and II are downloadable from the NEFSC Inport metadata library, while covariates used in Chapter 4 of this document are being uploaded.

A full list of publications and presentations produced using these data during AMAPPS I is in Palka et al. (2017), those produced during AMAPPS II is in Palka et al. (2021) and those produced during AMAPPS III is listed in **Table 3-2** of this document.

10.3 Telemetry Data

Primary authors: Heather Haas and Christopher Sasso

10.3.1 Provenance

During 2010 to 2025, NMFS worked collaboratively with many partners to deploy hundreds of animal-borne data loggers and transmitters on loggerhead turtles (*Caretta caretta*) and leatherback turtles (*Dermochelys coriacea*). The types of tags deployed vary by taxa. We deployed 362 long-term satellite tags on loggerhead turtles and 99 on leatherback turtles (**Table 10-7**). Across the full suite of tags, we collected information on animal location and behavior, wet/dry status, depth, and water temperature (**Table 10-8**). Chapter 7 provides further information on the turtle tagged animal tracking and data collection since 2010.

Table 10-7. Number of satellite tags deployed on loggerhead and leatherback turtles, by year
Tallies include shared tags.

Year	Loggerhead	Leatherback
2010	14	0
2011	26	0
2012	32	0
2013	20	0
2014	20	0
2015	11	0
2016	22	0
2017	25	1
2018	37	8
2019	10	22
2020	0	0
2021	29	3

Year	Loggerhead	Leatherback
2022	15	22
2023	24	21
2024	43	0
2025	34	22
TOTAL	362	99

Table 10-8. Summary of data in Turtle Ecology Oracle database between 2010 and 2025
We deployed most tags as part of a collaboration, where AMAPPS did not financially support many of the tags.

Topic	Number in Database
Individual Turtles	1,404
Number of long-term satellite tags	537
Tissue Samples	9,032
Turtle Locations	1,157,404
Turtle Dive Records	753,139

10.3.2 Processing

We routinely uploaded animal behavior data from satellite-relay data loggers into an NEFSC-maintained Oracle database (**Table 10-8**). We then merged these telemetry-based behavior data with deployment data into Oracle Views where some basic quality control filtering also occurred. For selected research topics, additional data processing (including interpolation) also occurred.

10.3.3 Presentation

Results from the sea turtle telemetry data are available publicly via publications and datasets. A full list of publications and presentations produced using these data during AMAPPS I is in Palka et al. (2017), those produced during AMAPPS II is in Palka et al. (2021) and those produced during AMAPPS III is listed in **Table 3-2** in this document.

Publicly available datasets include:

- Estimated monthly distributions of tagged loggerheads from Winton et al. (2018)
- Temperature and depth data from tagged loggerheads from Patel et al. (2018)
- Location, dive, and temperature-depth data from Crowe et al. (2020)
- Sea turtle location data from satellite tags in the Northwest Atlantic Ocean from 2009 to 2024 (submitted to NCEI)

The first three datasets are accessible from the Turtle Ecology program's NOAA webpage: https://www.fisheries.noaa.gov/new-england-mid-atlantic/endangered-species-conservation/sea-turtle-ecology-and-population-dynamics.

10.4 Passive Acoustic Data

Primary authors: Annamaria DeAngelis, Elizabeth Josephson and Melissa Soldevilla

10.4.1 Provenance

10.4.1.1 NEFSC Towed Hydrophone Array Data

During 2010 to 2025, the NEFSC AMAPPS program completed 12 shipboard surveys that collected data from towed hydrophone arrays (**Table 10-9**). These included 6 dedicated abundance surveys; the remaining surveys focused on studies of specific taxa. During AMAPPS III, two surveys collected acoustic data on 48 days during about 7,000 km of track lines. In addition, in 2025 PC2501 collected towed hydrophone array data in an abundance survey funded by the Navy AMAPPS IV.

The passive acoustic team deployed a towed hydrophone array approximately 300 m behind the vessel, in water depths greater than 100 m. We used two different arrays that were of the same build. These contained three HTI-96-Min hydrophones (High Tech Inc.) within an oil-filled endline section and an internal depth sensor (Keller America, PA7FLE). When the internal depth sensor malfunctioned due to air bubbles present in this section, we relied on an external Sensus Ultra depth sensor (ReefNet Inc.) to collect array depth information that we extracted after deployment. We typically collected hydrophone array data for 12 to 24h/day on the abundance surveys and focal taxa surveys, depending on survey needs and design. The passive acoustic team recorded data and monitored the array using PAMGuard. PAMGuard is an open-source software program for real-time acoustic monitoring and post-processing applications, developed by Doug Gillespie (Gillespie et al. 2008).

Table 10-9. Summary of towed hydrophone array data from NEFSC shipboard surveys
Acoustic survey effort often differed from visual survey effort because the acoustic monitoring can continue during night and inclement weather.

Trip Identifier	Year	Purpose	Start Date	End Date	Days with Acoustic Effort	Acoustic Survey Effort (km)
HB1103	2011	abundance survey	2-Jun	1-Aug	40	~ 5,580
HB1303	2013	abundance survey	2-Jul	18-Aug	33	~ 5,940
GU1402	2014	abundance survey	12-Mar	27-Apr	16	~ 2,610
HB1403	2014	beaked whale survey	25-Jul	30-Jul	4	~ 800
HB1503-1	2015	sei whale survey	10-Jun	19-Jun	7	~ 540
HB1503-2	2015	turtle tagging	24-Jun	1-Jul	3	332
HB1603	2016	abundance survey	28-Jun	24-Aug	40	5,354
HRS1701	2017	beaked whale survey	8-Sep	17-Sep	9	2,053
GU1803	2018	beaked whale survey	21-Jul	1-Aug	23	4,470
HRS1910	2019	beaked whale survey	17-Aug	28-Aug	9	1,050
HB2102	2021	abundance survey	17-Jun	20-Aug	36	5,396
HB2504	2025	beaked whale survey	7-Jul	17-Jul	12	1,600
Subtotal-AMAPPS I	2010 – 2014				93	~ 14,930
Subtotal-AMAPPS II	2015 – 2019				91	~ 13,799
Subtotal-AMAPPS III	2020 – 2025				48	6,996
GRAND TOTAL	2010 – 2025				232	~ 35,725

10.4.1.2 SEFSC Towed Hydrophone Array Data

During 2010 to 2025, the SEFSC AMAPPS program completed 5 shipboard abundance surveys that collected data from towed hydrophone arrays. During AMAPPS II, these surveys collected acoustic data on 39 days during over 5,000 km of track lines (**Table 10-10**). During AMAPPS III, these surveys collected acoustic data on 43 days during about 4,440 km of track lines (**Table 10-10**).

Table 10-10. Summary of towed hydrophone array data from SEFSC shipboard surveys
Acoustic survey effort often differed from visual survey effort because the acoustic monitoring can continue during night and inclement weather.

Cruise/Project	Year	Purpose	Start Date	End Date	Days with acoustic effort	Acoustic Survey Effort (Km)
GU1102	2011	abundance survey	21-Jun	2-Aug	33	4,275
GU1304	2013	abundance survey	16-Jul	15-Sep	37	1,900
GU1605	2016	abundance survey	1-Jul	24-Aug	39	5,381
GU2103	2021	abundance survey	12-Jun	31-Aug	33	~3400
GU2301	2023	abundance survey	23-Jan	28-Apr	10	~1040
Subtotal-AMAPPS I	2010 – 2014				70	6,175
Subtotal-AMAPPS II	2015 – 2019				39	5,381
Subtotal - AMAPPS III	2020 – 2025				43	~4,440
GRAND TOTAL	2010 – 2025				109	15,996

10.4.1.3 Bottom-mounted Recorder Data

During AMAPPS III (2019-2025), AMAPPS did not fund deployment of bottom-mounted recorders. During 2015 to 2019, the NEFSC worked with collaborators at Scripps Institution of Oceanography and Cornell University to deploy bottom-mounted archival acoustic recorders along the continental shelf and on the shelfbreak (**Table 10-11**). We collected continuous passive acoustic recordings (10 Hz to 100 kHz) from High-Frequency Acoustic Recording Packages (HARPs; Wiggins and Hildebrand 2007) at eight sites along the North American east coast during April 2015 to June 2019. These sites were at varying depths, ranging from about 800 m to 1100 m. HARPs recorded continuously at a sampling rate of 200 kHz and lasted typically for up to a year. In contrast, we deployed multiple marine autonomous recording units (MARUs, Clark et al. 2010) in five lines spanning the continental shelf, from south of Nantucket, MA to Brunswick, GA. MARUs recorded continuously at a sampling rate of 2 kHz for up to six months. We recovered and redeployed recording units multiple times, with the goal of maintaining continuous sampling for three years.

Table 10-11. Summary of bottom-mounted recorders deployed under AMAPPS I and II
HARP deployments involved a single recorder at a single site. MARU deployments involved multiple recorders (numbers in parentheses) spanning the continental shelf; thus, we provided a representative latitude, longitude, and date range. Note, individual recording units may have recorded for less than the date range specified.

Recorder Type	Site Name; Location	Recording Date Range	Latitude (N)	Longitude (W)
HARP	WAT_HZ; Heezen Canyon	Jun 2015 - Mar 2016 Apr 2016 - Jun 2017	41.0619	-66.3515

Recorder Type	Site Name; Location	Recording Date Range	Latitude (N)	Longitude (W)
		Jul 2017 - Jan 2018 Jun 2018 - May 2019		
HARP	WAT_OC; Oceanographer Canyon	Apr 2015 - Feb 2016 Apr 2016 - May 2017 Jul 2017 - May 2019	40.2633	-67.9862
HARP	WAT_NC; Nantucket Canyon	Apr 2015 - Sep 2015 Apr 2016 - May 2017 Jul 2017 - Apr 2018 Jun 2018 - Jun 2019	39.8325	-69.9821
HARP	WAT_BC; Babylon Canyon	Apr 2016 - May 2019	39.1911	-72.2287
HARP	WAT_WC; Wilmington Canyon	Apr 2016 - May 2019	38.3742	-73.3707
HARP	WAT_GS; Gulf Stream	Apr 2016 - Jun 2019	33.6656	-76.0014
HARP	WAT_BP; Blake Plateau	Apr 2016 - May 2019	32.1060	-77.0943
HARP	WAT_BS; Blake Spur	Apr 2016 - Jun 2019	30.5838	-77.3907
Deep-HARP	WAT_BR	Jul 2018 - Aug 2018	40.0328	-67.9884
MARU (4-7 recorders)	Nantucket, MA	Dec 2015 - Feb 2018 Dec 2018 - Jun 2019	41.2499	-70.3895
MARU (1-5 recorders)	Cape Hatteras, NC	Oct 2015 - Jul 2018	35.4012	-75.4010
MARU (1-5 recorders)	Cape Fear, NC	Nov 2015 - Feb 2018 Nov 2018 - Jun 2019	34.3674	-77.4878
MARU (1-7 recorders)	Charleston, SC	Nov 2015 - Jan 2018	32.8781	-79.4803
MARU (3-8 recorders)	Brunswick, GA	Oct 2015 - Aug 2018 Oct 2018 - May 2019	31.0079	-81.1553

10.4.1.4 Other Passive Acoustic Data (Drifting Recorders, DTAG)

During AMAPPS III (2019-2025) we did not deploy any other passive acoustic devices. From 2010 to 2019, the NEFSC and SEFSC collected passive acoustic data during shipboard surveys using drifting platforms, as detailed in **Tables 10-12**. The platforms included U.S. Navy-provided sonobuoys and Drifting Autonomous Spar Buoy Recorders (DASBRs), which were constructed by the NEFSC in collaboration with the Southwest Fisheries Science Center. Both types of platforms enabled the collection of passive acoustic monitoring data from a distance, thereby avoiding vessel noise interference. Sonobuoys transmitted data directly to the ship, while DASBRs required recovery for data download. Additionally, the NEFSC deployed a digital acoustic recording tag (DTAG) on a True's beaked whale (*Mesoplodon mirus*) to gather environmental acoustic detections and dive profile information.

Table 10-12. Summary of passive acoustic data collected using mobile or drifting platforms

Platform Type	Trip Identifier	Number of Deployments	Approximate Total Duration (hh:mm)
Sonobuoys	HB1503-1	14 (11 successful; 3 failed)	?
Sonobuoys	HB1603	30 (22 successful; 8 failed)	62:26
Sonobuoys	GU1605	30	?
DASBR	GU1803	5	155:58
DTAG	GU1803	1	?

10.4.2 Processing

10.4.2.1 Towed Hydrophone Array Data

The acoustic team used the software PAMGuard to collect and monitor the data. Real-time data processing varied depending on the goals and needs of the individual survey. Analysts recorded information such as species identification, bearing, GPS location, and correspondence with visual sightings for target species groups. We also conducted detailed post-processing data analyses, focused on addressing targeted questions for each survey. Details of these analyses are in the AMAPPS annual reports and in the manuscripts listed in Chapters 4-6.

10.4.2.2 Bottom-mounted Recorder Data

The primary goals of the bottom-mounted data collection were to document baleen whale occurrence and migratory movements. We used MARUs along the continental shelf, with a focus on North Atlantic right whales (*Eubalaena glacialis*). We used HARPs to document cetacean species occurrence and diversity along the shelfbreak, and determine the impacts of anthropogenic noise on cetacean vocal activity at specific shelf-break sites. For all datasets, we used a combination of manual review and automated acoustic detectors/classifiers to determine the occurrence of target species groups. In addition, we quantified the daily presence of anthropogenic activities such as airguns, echosounders, sonar, and vessel noise at each of the HARP sites. For many of the ongoing analyses we are working closely with collaborators at the Woods Hole Oceanographic Institution and Scripps Institution of Oceanography.

10.4.2.3 Drifting Recorder Data

We use sonobuoys during shipboard surveys to conduct acoustic point sampling for baleen whales because the towed hydrophone array used during shipboard surveys could not sufficiently capture baleen whale vocalizations. Sonobuoys transmit audio data in real-time, and we used the software packages Raven and PAMGUARD to record and analyze these data. DASBRs archive audio recordings, and are equipped with satellite GPS transmitters for real-time tracking. We used a combination of manual review and automated acoustic detectors and classifiers to determine the occurrence of target species groups.

10.4.2.4 DTAG Data

We used custom-built MATLAB scripts to identify times of the clicks made by the tagged True's beaked whale, as well as those made by members of its group. We also analyzed the accelerometer data to provide a dive profile over the course of the tag duration, complete with vocal periods. We also analyzed the other types of sounds recorded by the DTAG using the software Raven.

10.4.3 Presentation

All towed array beaked whale, sperm whale, and *Kogia* analyses collected from AMAPPS surveys spanning 2013 - 2025 are available for viewing on the Passive Acoustic Cetacean Map webpage (https://passiveacoustics.fisheries.noaa.gov/pacm/#/) hosted on the NOAA's Passive Acoustic Homepage (https://passiveacoustics.fisheries.noaa.gov/). All real-time and post-processed analyses from all AMAPPS surveys will be uploaded to Makara, the passive acoustic database. Additional work is being done to upload towed array acoustic files to NCEI's passive acoustic data archive for release to the public.

A full list of publications and presentations produced using these data during AMAPPS I is in Palka et al. (2017), those produced during AMAPPS II is in Palka et al. (2021) and those produced during AMAPPS III is listed in **Table 3-2** in this document.

10.5 Oceanographic data

Primary authors: Elizabeth Josephson, Harvey Walsh, Debra Palka and Laura Aichinger Dias

10.5.1 Provenance

10.5.1.1 Scientific Computer System Data

Shipboard sensors connected to the ship's Scientific Computer System collect constant records of *in-situ* environmental parameters including water temperature, salinity, and weather conditions (e.g., wind speed and wind direction). **Table 10-13** is an example of the suite of parameters collected on a survey.

Table 10-13. Information collected from ship Scientific Computer System recording systems

Sensor/Parameter (units)	Sensor/Parameter (units)
Date (MM/DD/YYYY)	Time (hh:mm:ss)
TSG-Conductivity (s/m)	EK60-38kHz-Depth (m)
TSG-External-Temp (ºC)	EK60-18kHz-Depth (m)
TSG-InternalTemp (ºC)	ADCP-Depth (m)
TSG-Salinity (PSU)	ME70-Depth (m)
TSG-Sound-Velocity (m/s)	ES60-50kHz-Depth (m)
MX420-Time (GMT)	Doppler-Depth (m)
MX420-COG (º)	Air-Temp (ºC)
MX420-SOG (Kts)	Barometer-2 (mbar)
MX420-Lat (DDMM.MM)	YOUNG-TWIND-Direction (º)
MX420-Lon (DDMM.MM)	YOUNG-TWIND-Speed (Kts)
Doppler-F/A-BottomSpeed (kts)	Rel-Humidity (%)
Doppler-F/A-WaterSpeed (kts)	Rad-Case-Temp (ºC)
Doppler-P/S-BottomSpeed (kts)	Rad-Dome-Temp (ºC)
Doppler-P/S-WaterSpeed (kts)	Rad-Long-Wave-Flux (W/m^2)
High-Sea Temp (ºC)	Rad-Short-Wave-Flux (W/m^2)
POSMV – Time (hhmmss)	ADCP-F/A – GroundSpeed (kts)
POSMV – Elevation (m)	ADCP-F/A – WaterSpeed (kts)
POSMV – Heading (º)	ADCP-P/S – GroundSpeed (kts)
POSMV – COG (kts)	ADCP-P/S – WaterSpeed (kts)
POSMV – SOG (kts)	Gyro (º)
POSMV – Latitude (DDMM.MM)	POSMV – Quality (1=std)
POSMV – Longitude (DDMM.MM)	POSMV – Sats (none)
POSMV – hdops (none)	

10.5.1.2 Sampling tows

In addition to the ship's Scientific Computer System to collect data on water characteristics during the AMAPPS shipboard surveys, we deployed several sampling devices. To measure water temperature at depths, we deployed Conductivity, Temperature, and Depth (CTD) profilers at least once daily on many surveys and expendable bathythermographs (XBTs) on some surveys at regular intervals along the trackline, typically at stations spaced 15 to 20 km apart (**Table 10-14**).

Table 10-14. Number of sampling tows conducted by cruise during AMAPPS I - III
Tows collected physical oceanographic water characteristics from CTD and XBTs. Other sampling tows collected biological samples (see Section 10.6).

Cruise	CTD/ XBT	Bongo (333um)	Bongo (150um)	VPR	Frame-net	Midwater Trawl	Other Types	Other Count
HB1103	111/ 44	90	90	81	0	0	-	0
GU1102	67/ 302	0	0	0	0	0	-	0
HB1303	116	89	89	30	0	12	MOCNESS	9
GU1304	27/ 227	0	0	0	0	0	-	0
HB1403	64	127	127	13	0	2	MOCNESS Beam trawl Sediment-grab	3 70 233
HB1503	63	26	26	4	0	24	Go-Pro DIDSON	16 8
GU1605	34/ 145	0	0	0	0	0	-	0
HB1603	252	113	113	0	34	35	Neuston	42
HB1704	56	16	15	26	33	0	Go-Pro	16
EN1801	21	5	5	4	0	0	-	0
GU1803	21	5	5	0	1	0	-	0
EN1901	20	5	5	4	0	0	-	0
GU2103	34	0	0	0	0	0	-	0
HB2102	36	180	180	33	47	0	-	0
GU2301	97	97	0	0	0	0	-	0
PC2501	83	83	83	0	0	0	-	0

10.5.2 Processing

Upon retrieval, technicians processed all raw CTD profile data ashore, employing standard Seabird Electronics software to generate profiles averaged over 1-decibar intervals. To ensure quality control for the CTD salinity data, we collected water samples at sea using vertical casts, usually twice daily. After each cruise, we analyzed these samples with a Guildline AutoSal laboratory salinometer. Following manufacturer guidelines, we calculated a slope correction based on the comparison between CTD-measured conductivity and salinometer results; we then applied this correction to the CTD-measured conductivity before conversion to salinity. We also scrutinized the vertical density profiles for inversions, which might be due to poor conductivity or temperature readings and/or sensor misalignment. In these cases, we assigned a flag value.

10.5.3 Presentation

We loaded the processed hydrographic CTD data into ORACLE data tables and made them publicly available via the Ecosystem Monitoring of the Northeast U.S. Continental Shelf: Plankton Dataset | NOAA Fisheries. For most NEFSC cruises involving CTD data collection, the NEFSC Oceanography Branch produced a comprehensive CTD report, which summarized and mapped surface and bottom

temperature and salinity data. Examples include the report for the 2021 HB2102 survey (Holzwarth-Davis 2023) and other cruises documented in Holzwarth-Davis (2012, 2014, 2015, 2016, 2019a, 2019b, 2020a, 2020b, 2023 2025).

Scientific Computer System data from NOAA ships are accessible through the National Centers for Environmental Information website.

SEFSC surface underway measurements like sea surface temperature and salinity, are also at NCEI (e.g., underway measurements for vessel survey GU2103).

10.6 Biological Sampling

Primary authors: Elizabeth Josephson, Laura Aichinger Dias and Michael Jech

10.6.1 Provenance

10.6.1.1 Mesopelagic and Benthic Sampling

We conducted mesopelagic and benthic sampling on AMAPPS shipboard surveys (**Figure 10-2**; **Table 10-2** and **Table 10-14**) using sampling techniques including imaging (e.g. towed Visual Plankton Recorder, GoPro, and Sonar), acoustic (e.g. echosounder), and direct sampling (e.g. bongo net, mid-water trawl, and bottom grabs).

A thorough description of the sampling methods for each device is in Chapter 10 of the AMAPPS II final report (Palka et al. 2021).

Figure 10-2. Side deck of NOAA ship *Henry Bigelow* with several biological sampling devices

10.6.1.2 eDNA Sampling

Environmental DNA (eDNA) sampling captures genetic signatures from an animal's environment rather than directly from its tissue. Thanks to advancements in DNA magnification and sequencing, detecting and identifying species is now possible even with very low densities of genetic material (Ficetola et al. 2008).

In 2017 and 2018, NEFSC conducted pilot studies, collecting eDNA samples during two shipboard surveys with the goals to 1) confirm the species identification of cryptic species, such as beaked whales, using eDNA sampling, 2) determine if eDNA samples can provide data relevant to stock structure, and 3) evaluate the effectiveness of eDNA sampling under various conditions (e.g., within an animal's fluke print after a dive, or at a distance or depth from an aggregation of animals).

We designed these surveys specifically to investigate the ecology of deep-diving cetaceans in offshore habitats (**Table 10-15**). For each eDNA sample, scientists recorded data including GPS location and time. We will provide more information on the additional eDNA samples collected on the beaked whale cruise HB2502 in the AMAPPS 2025 Annual Report.

Table 10-15. Summary of the numbers of eDNA samples per target species during 2010 and 2024

Trip Identifier	Year	Species	Number of Samples
HRS1701	2017	*Mesoplodon mirus*	9
HRS1701	2017	*Ziphius cavirostris*	5
GU1803	2018	*Mesoplodon mirus*	12
GU1803	2018	*Ziphius cavirostris*	2
GU1803	2018	*Stenella coeruleoalba*	1
GU1803	2018	Deep water CTD	3
TOTAL			32

10.6.1.3 Biopsy Sampling

Whenever possible, scientists onboard the SEFSC and NEFSC shipboard surveys collected biopsy samples from marine mammals (**Table 10-16**). Only personnel trained and authorized under marine mammal research permits conducted the biopsy sampling. From the bow of the ship, scientists used a modified 0.22 caliber dart rifle fitted with a tethered dart and custom designed biopsy heads to sample bow-riding delphinids. We also used a rigid-hulled inflatable boat deployed from the survey ship to sample larger cetaceans, like sperm whales (*Physeter macrocephalus*), baleen whales, and pilot whales (*Globicephala* sp.). We collected biopsies of the larger cetaceans by using a crossbow fitted with custom designed biopsy heads.

The biopsy heads on both sampling tools extract a small plug of tissue from the animals, usually including skin and blubber. We usually subsampled the cetacean tissues to use for various analyses (**Table 10-16**). We used the skin for stable isotopes analyses to investigate diet, and for genetic analyses to identify the species and determine population structure. We subsampled the blubber for contaminant and hormone analyses. Scientists recorded data on each biopsy attempt that included GPS location, time, date, sampler and recorder name, species, body location struck, behavioral reaction, and whether or not we obtained a sample. We collected samples located in the Gulf of Mexico during transit to and from port.

Table 10-16. Numbers of cetacean biopsy subsamples by analysis types during 2010 – 2025

Species	Animals Sampled	Skin-DMSO[1] or Ethanol (Genetics)	Skin-Frozen (Stable Isotope)	Blubber-Frozen (Contaminants Hormones)	Blubber (RNA[2] genetics)	Other	Total Sub-samples
Balaenoptera edeni	4	4	0	0	0	0	4
Balaenoptera physalus	1	2	0	0	0	0	2
Delphinus delphis	3	5	0	0	0	0	5
Globicephala sp.	6	8	4	6	0	0	18
Mesoplodon mirus	3	4	0	0	0	0	4
Physeter macrocephalus	1	2	1	2	0	4	9
Pseudorca crassidens	1	1	0	0	0	0	1
Stenella attenuata	5	5	5	6	0	0	16
Stenella clymene	1	1	1	0	1	0	3
Stenella coeruleoalba	7	7	0	0	0	0	7
Stenella frontalis	40	40	20	21	7	1	89
Stenella longirostris	3	5	1	2	0	0	8
Steno bredanensis	3	3	1	0	1	0	5
Tursiops truncatus	57	59	22	24	8	0	113
TOTAL	135	146	55	61	17	5	284

[1] DMSO = Dimethyl sulfoxide
[2] RNA = Ribonucleic acid

10.6.1.4 Sea turtle samples

As part of sea turtle satellite tagging fieldwork efforts, biological samples are taken in order to gain valuable biological and ecological information regarding the animal's health, habitat use, genetics, diet, sex, and exposure to environmental contaminants. This knowledge obtained by scientists is critical to identify long-term ecological trends, and provides a better understanding of sea turtle life history and ecology to inform our management decisions for sea turtle conservation.

Turtle biopsy sampling as conducted simultaneously with other biological sampling procedures, such as morphometrics and blood draw, when we brought a captured turtle on board the vessel (**Table 10-17**). Chapter 7 of this report provides more information on the numbers and locations of sampled turtles, and the sampling protocols we used.

Table 10-17. Summary of sea turtle biological samples collected during AMAPPS I - III
Data are tracked in the NEFSC Oracle tissue tracking database. Total samples include blood, skin, and other miscellaneous biological samples such as scutes.

Year	Total Samples	Blood Samples	Skin Samples
2010	0	0	0
2011	19	19	0
2012	224	192	32
2013	107	92	15
2014	126	103	20
2015	115	91	24
2016	222	178	44
2017	239	189	50
2018	228	158	70

Year	Total Samples	Blood Samples	Skin Samples
2019	130	104	26
2020	0	0	0
2021	237	176	61
2022	146	116	30
2023	246	196	50
2024	466	338	85
2025	388	274	76
TOTAL	2,893	2,226	583

10.6.2 Processing

10.6.2.1 Mesopelagic and Benthic Sample Processing

Chapter 9 of this document details the processing and data handling for mesopelagic and benthic samples from a variety of sampling devices.

10.6.2.2 eDNA Sample Processing

During daytime small boat operations, we collected paired water samples for eDNA testing using 1L bottles from either side of the small boat, and in the fluke print of an animal upon a dive. We maintained water samples in a cooler with frozen ice packs, and transferred them back to the ship for refrigerator storage at either midday or end of day. We also collected several water samples concurrent with deep-CTD casts. We performed the initial processing of the eDNA samples on board the vessel according to standard protocols. We filtered samples through 0.4 μM filters, and we stored them in Longmire's buffer for subsequent analyses. Qualified laboratories are conducting DNA extraction and analyses (Baker et al. 2018).

10.6.2.3 Biopsy Sample Processing

Researchers process the subsamples from the biopsy tissues in various ways according to study goals. Onboard the ships, researchers only conduct limited subsampling, preservation and storage of the samples. Qualified laboratories conducted DNA extraction and other analyses. We did not list samples associated with stranded or bycaught animals. This tally included some samples that we have now consumed in analyses and so are not available for further analyses. Although we collected the samples on an AMAPPS supported field study, collaborators conducted and funded most of the analyses of the tissue samples.

10.6.2.4 Sea turtle sample processing

Researchers gather the sea turtle samples during AMAPPS fieldwork efforts onboard the tagging vessel. Samples such as blood, skin, and scute are collected and preserved in cryovials onboard (frozen or in saline depending on sample type). We spun down the collected blood in a centrifuge, then transferred the samples to cryovials and kept frozen. Skin samples are either kept frozen or in saline cryovials. Scute samples are kept frozen in vials. After fieldwork concludes, the frozen samples are then transferred to a -80 ° Ultra Low freezer. We then coordinated with our collaborators or qualified outside laboratories and shipped the samples for various analyses, such as stable isotope or genetic analyses.

10.6.3 Presentation

A full list of publications and presentations produced using these data during AMAPPS I is in Palka et al. (2017), those produced during AMAPPS II is in Palka et al. (2021) and those produced during AMAPPS III is in **Table 3-2** in this document.

10.6.3.1 Mesopelagic and benthic sampling

We archived the mesopelagic and benthic sampling data from trawls, including deployment date, time, duration, latitude, longitude, tow depth-time profile, catch weight and numbers by taxa, and individual lengths by taxa, locally in the NEFSC trawl database and they are available publicly through the InPort portal.

All active acoustic data (EK60 and other echosounder data) are accessible through the NOAA National Centers for Environmental Information water column sonar data portal.

The Oceans and Climate Branch at the NEFSC in Woods Hole, MA maintains all hydrographic, plankton and VPR data. Hydrographic data are accessible through the Branch website and the NCEI World Ocean Database. After researchers identify and enumerate the plankton samples, the plankton data are in the Plankton Archive. Visual plankton recorder oceanographic data and images are currently available by request only.

Woods Hole Oceanographic Institution maintained all Imaging Flow Cytobot data. Metadata and images are available through the Imaging Flow Cytobot website.

10.6.3.2 eDNA sampling

We archived new genetic information in GenBank, as appropriate.

10.6.3.3 Biopsy samples

We incorporated information from biopsy sampling into several research publications and maintained an extensive archive of tissue samples for later analyses or sharing in an NEFSC Oracle database.

The genetic samples that the SEFSC collected during the AMAPPS cruises are stored at the Marine Mammal Molecular Genetics laboratory in Lafayette, LA. Scientists at this lab extracted DNA from all biopsies and then archived to extractions that are available for future research. All other samples are stored either at the Miami, FL facility or at the Pascagoula, MS laboratory.

10.6.3.4 Sea turtle biological samples

We have published information from sea turtle biological sampling during AMAPPS I - III and have maintained a sea turtle tissue tracking database in the NEFSC Turtle Ecology Oracle database. We also have an archive of tissue samples in our -80° Ultra Low freezer for future analyses.

Blood samples collected from loggerhead sea turtles in the Mid-Atlantic Bight during the 2011, 2012, 2013, and 2016 satellite tagging trips were analyzed in Yang et al. (2019) to establish clinical reference intervals for this threatened population, providing a baseline for comparisons with turtles affected by anthropogenic or environmental threats.

10.7 References Cited

Amante C, Eakins BW. 2009. ETOPO1 arc-minute global relief model : procedures, data sources and analysis. NOAA Technical Memorandum NESDIS NGDC-24. https://repository.library.noaa.gov/view/noaa/1163

Baker CS, Steel D, Nieukirk S, Klinck H. 2018. Environmental DNA (eDNA) From the Wake of the Whales: Droplet Digital PCR for Detection and Species Identification. Front Mar Sci 5. https://doi.org/10.3389/fmars.2018.00133

Balch WM, Gordon HR, Bowler BC, Drapeau DT, Booth ES. 2005. Calcium carbonate measurements in the surface global ocean based on Moderate-Resolution Imaging Spectroradiometer data. J Geophys Res Oceans. 110(C7). https://doi.org/10.1029/2004JC002560

Barnston AG, Livezey RE. 1987. Classification, Seasonality and Persistence of Low-Frequency Atmospheric Circulation Patterns. Mon Weather Rev. 115(6):1083–1126. https://doi.org/10.1175/1520-0493(1987)115%253C1083:CSAPOL%253E2.0.CO;2

Behrenfeld MJ, Falkowski PG. 1997. Photosynthetic rates derived from satellite-based chlorophyll concentration. Limn and Oceanog. 42(1):1–20. https://doi.org/10.4319/lo.1997.42.1.0001

Belkin IM, O'Reilly JE. 2009. An algorithm for oceanic front detection in chlorophyll and SST satellite imagery. J Mar Sys. 78(3):319–326. https://doi.org/10.1016/j.jmarsys.2008.11.018

Buckland ST, Anderson DR, Burnham KP, Laake JL, Borchers DL, Thomas L. 2004. Advanced Distance Sampling: Oxford University Press. https://doi.org/10.1093/oso/9780198507833.001.0001

Campbell JW. 1995. The lognormal distribution as a model for bio-optical variability in the sea. J Geophys Res Oceans. 100(C7):13237–13254. https://doi.org/10.1029/95JC00458

Chassignet EP, Hurlburt HE, Metzger EJ, Smedstad OM, Cummings JA. 2015. U.S. GODAE: Global Ocean Prediction with the HYbrid Coordinate Ocean Model (HYCOM). Oceanography. 22(2):64–75. https://doi.org/10.5670/oceanog.2009.39

Chin TM, Vazquez-Cuervo J, Armstrong EM. 2017. A multi-scale high-resolution analysis of global sea surface temperature. Rem Sens Env. 200:154–169. https://doi.org/10.1016/j.rse.2017.07.029

Clark CW, Brown MW, Corkeron P. 2010. Visual and acoustic surveys for North Atlantic right whales, *Eubalaena glacialis*, in Cape Cod Bay, Massachusetts, 2001-2005: Management implications. Mar MamSci. 26(4):837–854. https://doi.org/10.1111/j.1748-7692.2010.00376.x

Crowe L, Hatch JM, Patel S, Smolowitz RJ, Haas HL. 2020. Riders on the storm: Loggerhead sea turtles detect and respond to a major hurricane in the Northwest Atlantic Ocean. Mov Ecol. 8(32). https://movementecologyjournal.biomedcentral.com/articles/10.1186/s40462-020-00218-6

Ficetola GF, Miaud C, Pompanon F, Taberlet P. 2008. Species detection using environmental DNA from water samples. Biol Lett. 4(4):423–425. https://doi.org/10.1098/rsbl.2008.0118

Garrison L, Martinez A, Maze-Foley K. 2010. Habitat and abundance of cetaceans in Atlantic Ocean continental slope waters off the eastern USA. J Cetacean Res Manage. 11(3). https://journal.iwc.int/index.php/jcrm/article/view/606

Gillespie D, Gordon J, McHugh R, McLaren D, Mellinger D, Redmond P. 2008. PAMGUARD: Semiautomated, open source software for real-time acoustic detection and localization of cetaceans. Proc Inst Acoust. 30(5). https://pubs.aip.org/asa/jasa/article/125/4_Supplement/2547/698127/PAMGUARD-Semiautomated-open-source-software-for

Halpin PN, Read AJ, Fujioka E, Best BD, Donnelly B. 2015. OBIS-SEAMAP: The world data center for marine mammal, sea bird, and sea turtle distributions. Oceanog. 22(2):104–115. https://doi.org/10.5670/oceanog.2009.42

Hiby AR, Hammond PS. 1989. Survey techniques for estimating abundance of cetaceans. Rep Int Whal Comm. 11:47–80.

Hiby L. 1999. The objective identification of duplicate sightings in aerial survey for porpoise. In: Marine Mammal Survey and Assessment Methods. CRC Press.

Hiby L, Lovell P. 1998. Using aircraft in tandem formation to estimate abundance of harbour porpoise. Biometrics. 54(4):1280. https://doi.org/10.2307/2533658

Holzwarth-Davis, TJ. 2012. Oceanography Branch CTD data report CTD_REPORT_2011003HB https://repository.library.noaa.gov/view/noaa/24979

Holzwarth-Davis, TJ. 2014. Oceanography Branch CTD data report CTD_REPORT_2013003HB https://repository.library.noaa.gov/view/noaa/23954

Holzwarth-Davis, TJ. 2015. Oceanography Branch CTD data report CTD_REPORT_2015003HB https://doi.org/10.25923/myyk-gj25

Holzwarth-Davis, TJ. 2016. Oceanography Branch CTD data report CTD_REPORT_2014002GU https://repository.library.noaa.gov/view/noaa/23656

Holzwarth-Davis, TJ. 2019a. Oceanography Branch CTD data report CTD_REPORT_2018001EN https://doi.org/10.25923/f9q0-y231

Holzwarth-Davis, TJ. 2019b. Oceanography Branch CTD data report CTD_REPORT_2018003GU https://doi.org/10.25923/y6ea-zm53

Holzwarth-Davis, TJ. 2020a. Oceanography Branch CTD data report CTD_REPORT_2014003HB https://repository.library.noaa.gov/view/noaa/23658

Holzwarth-Davis, TJ. 2020b. Oceanography Branch CTD data report CTD_REPORT_2016003HB https://doi.org/10.25923/p6nq-4e14

Holzwarth-Davis, TJ. 2023. Oceanography Branch CTD data report CTD_REPORT_2021002HB https://doi.org/10.25923/jx96-4v91

Holzwarth-Davis, TJ. 2025. Oceanography Branch CTD data report CTD_REPORT_2025001PC https://doi.org/10.25923/rk7r-fw07

Laake JL, Borchers DL. 2004. Methods for incomplete detection at distance zero. In: Buckland ST, Andersen DR, Burnham KP, Laake JL, Thomas L, editors. Advanced distance sampling. New York: Oxford University Press; p. 108–189.

National Oceanic and Atmospheric Administration (NOAA), National Marine Fisheries Service (NMFS), NOAA Northeast Fisheries Science Center Woods Hole Laboratory, NOAA Southeast Fisheries Science Center (SEFSC). Cetacean, sea turtle, and seabird visual observations using line-transect survey methods from ships and aircraft during the Atlantic Marine Assessment Program for Protected Species (AMAPPS) surveys from 2010 to present. NOAA National Centers for Environmental Information. https://www.ncei.noaa.gov/access/metadata/landing-page/bin/iso?id=gov.noaa.nodc:AMAPPS

Northeast Fisheries Science Center. 2020. Technical Documentation, State of the Ecosystem. https://doi.org/10.25923/64pf-sc70

O'Reilly JE, Maritorena S, Mitchell BG, Siegel DA, Carder KL, Garver SA, Kahru M, McClain C. 1998. Ocean color chlorophyll algorithms for SeaWiFS. J Geophys Res Oceans. 103(C11):24937–24953. https://doi.org/10.1029/98JC02160

Palka D, Chavez-Rosales S, Josephson E, Cholewiak D, Haas H, Garrison L, Jones M, Sigourney D, Waring G, Jech M, et al. 2017. Atlantic Marine Assessment Program for Protected Species: FY10-FY14. Washington: U.S. Dept. of the Interior, Bureau of Ocean Energy Management, Atlantic OCS Region.

Palka D, Garrison L, Soldevilla M, Martinez A, Dias L, Rapucci G. 2024a. Cetacean visual observations using line-transect survey methods onboard the NOAA Ship Gordon Gunter (GU) during the Atlantic Marine Assessment Program for Protected Species (AMAPPS) in the Western North Atlantic Ocean (survey GU2103) from 2021-06-13 to 2021-09-04 (NCEI Accession 0309425).

Palka D, Garrison L, Soldevilla M, Martinez A, Dias L, Rapucci G. 2024b. Cetacean visual observations using line-transect survey methods onboard the NOAA Ship Gordon Gunter (GU) during the Atlantic Marine Assessment Program for Protected Species (AMAPPS) in the Western North Atlantic Ocean (survey GU2301) from 2023-02-04 to 2023-04-27 (NCEI Accession 0290563). https://www.ncei.noaa.gov/access/metadata/landing-page/bin/iso?id=gov.noaa.nodc:0290563

Patel SH, Barco SG, Crowe LM, Manning JP, Matzen E, Smolowitz RJ, Haas HL. 2018. Loggerhead turtles are good ocean-observers in stratified mid-latitude regions. Estuar Coast Shelf Sci. 213:128–136. https://doi.org/10.1016/j.ecss.2018.08.019

Project JPL MUR MEaSUREs. 2015. GHRSST Level 4 MUR Global Foundation Sea Surface Temperature Analysis (v4.1). Physical Oceanography Distributed Active Archive Center (PODAAC). https://podaac.jpl.nasa.gov/dataset/MUR-JPL-L4-GLOB-v4.1

Saha K, Zhao X, Zhang H, Casey K, Zhang D, Baker-Yeboah S, Kilpatrick K, Evans R, Ryan T, Relph J. 2018. AVHRR Pathfinder version 5.3 level 3 collated (L3C) global 4km sea surface temperature for 1981-2023. NOAA National Centers for Environmental Information/V52J68XX [Internet]. https://www.ncei.noaa.gov/access/metadata/landing-page/bin/iso?id=gov.noaa.nodc:AVHRR_Pathfinder-NCEI-L3C-v5.3

Maritorena S, Fanton d'Andonb OH, Mangin A, Siegel DA. 2010. "Merged Satellite Ocean Colour Data Products Using a Bio-Optical Model: Characteristics, Benefits and Issues," Remote Sensing of Environment, Vol. 114, No. 8, 2010, pp. 1791-1804. doi:10.1016/j.rse.2010.04.002

Sathyendranath S, Brewin RJW, Brockmann C, Brotas V, Calton B, Chuprin A, Cipollini P, Couto AB, Dingle J, Doerffer R, et al. 2019. An Ocean-Colour Time Series for Use in Climate Studies: The Experience of the Ocean-Colour Climate Change Initiative (OC-CCI). Sensors. 2019; 19(19):4285. https://doi.org/10.3390/s19194285

Sathyendranath S, Brewin RJW, Ciavatta S, Jackson T, Kulk G, Jönsson B, Vicente VM, Platt T. 2023. Ocean Biology Studied from Space. Surv Geophys 44, 1287–1308. https://doi.org/10.1007/s10712-023-09805-9

Thomas L, Laake J, Rexstad E, Strindberg, Marques F, Buckland S, Borchers D, Anderson D, Burnham K, Burt M, et al. 2009. Distance 6.0. Release 229 2.

Wiggins SM, Hildebrand JA. 2007. High-frequency Acoustic Recording Package (HARP) for broad-band, long-term marine mammal monitoring. In: 2007 Symposium on Underwater Technology and Workshop on Scientific Use of Submarine Cables and Related Technologies. Institute of Electrical and Electronics Engineers, Tokyo, Japan; p. 551–557. https://doi.org/10.1109/UT.2007.370760

Winship A, Kinlan B, White T, Leirness J, Christiansen. 2018. Modeling at-sea density of marine birds to support Atlantic marine renewable energy planning. NCCOS IAA MOA-2013-046-8696, BOEM OCS Study 2018-010, and NCCOS BOEM IAA M13PG00005. https://espis.boem.gov/final%20reports/BOEM_2018-010.pdf

Winton MV, Fay G, Haas HL, Arendt M, Barco S, James MC, Sasso C, Smolowitz R. 2018. Estimating the distribution and relative density of satellite-tagged loggerhead sea turtles using geostatistical mixed effects models. Mar Eco Prog Ser. 586:217–232. https://doi.org/10.3354/meps12396

Yang T, Haas HL, Patel S, Smolowitz R, James MC, Williard AS. 2019. Blood biochemistry and haematology of migrating loggerhead turtles (*Caretta caretta*) in the Northwest Atlantic: reference intervals and intra-population comparisons. Conserv Physiol. 7(1):coy079. https://doi.org/10.1093/conphys/coy079

11 Initial AMAPPS Investment in GAIA: Catalyzing a National Framework for Satellite-Based Marine Mammal Monitoring

Primary authors: Christin Khan and Kimberly Goetz

Monitoring marine mammals across their full geographic and ecological range remains a longstanding challenge for management agencies and researchers, including those engaged in offshore energy planning and environmental review. Many species occupy remote or difficult-to-access regions, traverse international boundaries, or inhabit offshore environments where vessel and aerial surveys are often constrained by cost, weather, and logistics. Very high-resolution commercial satellite imagery has emerged as a promising complementary data source, offering the ability to observe marine mammals in places that are challenging to survey using traditional platforms. Although satellite imagery obtained through existing government contracts do not provide comprehensive coverage at the desired 50 cm resolution, they enable targeted tasking in priority habitats and offer new opportunities to improve understanding of marine mammal distribution and habitat use (Khan et al. 2023).

The Geospatial Artificial Intelligence for Animals (GAIA; https://www.fisheries.noaa.gov/new-england-mid-atlantic/science-data/geospatial-artificial-intelligence-animals) initiative was established to harness these emerging capabilities. Led by the Northeast Fisheries Science Center and the Alaska Fisheries Science Center, GAIA brings together a broad network of academic, government, and private-sector collaborators and has undertaken several early exploratory efforts in satellite-based whale detection. During this exploratory period, National Oceanic and Atmospheric Administration (NOAA) collaborated with the Bureau of Ocean Energy Management, the Naval Research Laboratory, Microsoft AI for Good, and the British Antarctic Survey to evaluate whether very high-resolution satellite imagery and modern cloud computing could be combined into a scalable scientific monitoring system. These activities set the stage for GAIA's development of an operational, cloud-based platform for detecting and annotating marine mammals in satellite imagery.

Within this exploratory landscape, the Atlantic Marine Assessment Program for Protected Species (AMAPPS) provided early funding to support annotation of satellite imagery collected over bowhead whale (*Balaena mysticetus*) habitat in the Arctic. GAIA contracted with Maxar Technologies to use the GeoHIVE platform for crowdsourced annotation, but the resulting dataset contained too many false positives to support reliable model training. The high error rate stemmed largely from the use of non-expert annotators and downsampled image chips that made confident whale identification challenging. This experience clarified where annotation workflows broke down, underscored the need for improved preprocessing workflows capable of rendering whale color and shape accurately while preserving native resolution, and highlighted the importance of involving subject matter experts familiar with marine mammal identification to ensure annotation accuracy.

These insights directly informed the development of the GAIA cloud application. The early GeoHIVE effort made clear that NOAA needed a dedicated, secure, cloud-native annotation environment capable of

preserving native-resolution imagery, supporting multi-annotator workflows, and ensuring consistent quality control. It also highlighted the need for a custom preprocessing workflow to enhance visual clarity through projection and orthorectification, radiometric correction, pansharpening, and histogram stretching, all of which improve the visibility of subtle features such as whale coloration and body shape. The resulting GAIA platform, launched within NOAA Fisheries' Microsoft Azure environment, now provides automated ingestion of Maxar WorldView-2, WorldView-3, and GeoEye-1 imagery, cloud-rendered display of full-resolution Cloud Optimized GeoTIFFs, structured annotation and validation workflows, and built-in tools for resolving potential duplicate detections. This system addresses key limitations identified during the GeoHIVE campaigns and provides the foundation necessary to create high-quality training datasets across species and regions.

GAIA's first operational use case focuses on a well-studied habitat where rigorous comparison with traditional survey methods is possible. This initial project uses Maxar imagery collected over North Atlantic right whale (*Eubalaena glacialis*) habitat in Cape Cod Bay from 2020–2024, specifically targeting days when the Center for Coastal Studies aerial surveys documented whale presence. Leveraging a dataset with known whale locations allows GAIA to systematically evaluate detection performance under controlled conditions. Annotation of these satellite scenes is underway through two complementary approaches: manual expert review in ArcGIS and an "interesting points" workflow, developed in collaboration with Microsoft AI for Good, that identifies candidate features and presents them for review within the GAIA cloud application. Together, these methods support methodological testing and the creation of high-quality training data for future automation.

With this foundation in place, GAIA is expanding to support priority species across multiple NOAA Fisheries Science Centers. Upcoming projects include work at the Alaska Fisheries Science Center on Cook Inlet beluga whales (*Delphinapterus leucas*); the Pacific Islands Fisheries Science Center on Hawaiian monk seals (*Monachus schauinslandi*) and sea turtles; the Southeast Fisheries Science Center on Rice's whales (*Balaenoptera ricei*); the Southwest Fisheries Science Center on humpback (*Megaptera novaeangliae),* blue (*Balaenoptera musculus*), and gray whales (E*schrichtius robustus*); and the Northwest Fisheries Science Center on Southern Resident killer whales. (*Orcinus orca*) These five additional projects represent the next phase of GAIA's expansion, and additional species and regions are expected to follow as the system continues to mature.

The combination of an operational annotation platform, expanding multi-species training datasets, and coordinated cross-center workflows positions GAIA to move beyond the exploratory testing phase. While satellite imagery will not replace vessel or aircraft surveys, it can augment them by sampling offshore regions that are difficult to survey and providing additional spatial or temporal coverage. Over time, satellite-based data may contribute to stratified sampling frameworks in which satellite acquisitions supplement traditional survey methods, improving coverage in areas where survey effort is otherwise limited.

In this way, the initial AMAPPS investment, though limited in its direct scientific yield, played a crucial role in guiding NOAA's strategic direction. It highlighted key methodological challenges, clarified system requirements, and provided early momentum toward building GAIA as a national platform for

satellite-based marine mammal monitoring. Although GAIA remains under active development, the system already demonstrates the value of a shared cloud infrastructure for annotation, data management, and cross-center collaboration. Future work will focus on making the platform more robust, including improving concurrency handling in the backend database, implementing enhanced quality assurance tools and routine database backups, and developing new features that meet emerging user needs. Planned improvements to page loading times, workflow responsiveness, and user interface performance will further strengthen GAIA's ability to support operational annotation and long-term data stewardship. The pace and scope of these enhancements will depend on securing sustained funding to support continued system maintenance, evolution, and user support.

Khan CB, Goetz KT, Cubaynes HC, Robinson C, Murnane E, Aldrich T, Sackett M, Clarke PJ, LaRue MA, White T, et al. 2023. A Biologist's Guide to the Galaxy: Leveraging Artificial Intelligence and Very High-Resolution Satellite Imagery to Monitor Marine Mammals from Space. J. Mar. Sci. Eng. 2023, 11, 595. https://doi.org/10.3390/ jmse11030595